REDUCTION OF RADAR CROSS SECTION OF TARGETS USING PERIODIC STRIP GRATING TECHNIQUE

A THESIS SUBMITTED BY

K. A. JOSE

IN PARTIAL FULFILMENT OF THE REQUIREMENTS
FOR THE DEGREE OF

DOCTOR OF PHILOSOPHY

COCHIN UNIVERSITY OF SCIENCE AND TECHNOLOGY
FACULTY OF TECHNOLOGY
DEPARTMENT OF ELECTRONICS
COCHIN - 682 022
INDIA

JULY 1989

Dedicated

to .

those who stride for the unknown

CERTIFICATE

This is to certify that the thesis entitled "REDUCTION OF RADAR CROSS SECTION OF TARGETS USING PERIODIC STRIP GRATING TECHNIQUE" is a bona fide record of the research work carried out by Mr.K.A.Jose under my supervision in the Department of Electronics, Cochin University of Science and Technology. The results embodied in this thesis or part of it have not been presented for any other degree.

Dr.K.G.Nair
(Supervising Teacher)
Professor and Head
Department of Electronics
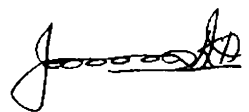Cochin University of
Science and Technology

Cochin 682 022
17 July 1989

DECLARATION

I hereby declare that the work presented in the thesis entitled "REDUCTION OF RADAR CROSS SECTION OF TARGETS USING PERIODIC STRIP GRATING TECHNIQUE" is based on the original work done by me under the supervision of Dr.K.G.Nair, in the Department of Electronics, Cochin University of Science and Technology, and that no part thereof has been presented for the award of any other degree.

Cochin 682 022

17 July 1989

K.A.JOSE.

ACKNOWLEDGEMENTS

Department of Electronics for their kind hearted co-operation. My special thanks are due to my colleague Dr.C.K.Aanandan (Lecturer, Government Brennen College, Tellicherry), for his immense help and inspiration when he was in Cochin University of Science and Technology. A special expression of gratitude is reserved to Dr.P.Mohanan for his invaluable help and kind hearted co-operation during the course of this study. Thanks are due to Dr.K.Vasudevan for his valuable suggestions during the course of this work.

I owe special debt to Mr.K.K.Narayanan, SRF of Microwave laboratory, for sincere help and co-operation. I acknowledge with thanks the help rendered by Mr.P.Venugopalan, Scientist, NPOL, Cochin, Mr.Babu Anto, Research Associate, Department of Electronics, Cochin University of Science and Technology.

All research scholars and technical personnel of the Department of Electronics were extending their co-operation and help in the preparation of this thesis in its present form. While thanking all of them for their goodwill, I should like to express my thanks particularly those in the Microwave Group of the Department of Electronics. Mr.Stephen Rodrigues, Mr.Wilson Gomez (Lecturers, Department of Physics, St.Paul's College, Kalamassery), Mr.N.K.Narayanan (Lecturer, Government Brennen College, Tellicherry), part-time research students,

CONTENTS

Chapter 1

INTRODUCTION

1

Chapter 1

INTRODUCTION

1.1 BACKGROUND

The classic experiment of Heinrich Hertz verified the theoretical prediction of Maxwell that both radio and light waves are physical phenomena governed by the same physical laws. This has started a new era of interest in interaction of electromagnetic energy with matter. The scattering of electromagnetic waves from a target is cleverly utilized in RADAR. This electronic system used to detect and locate objects under unfavourable conditions or obscuration that would render the unaided eye useless. It also provides a means for measuring precisely the range, or distance of an object and the speed of a moving object.

When an obstacle is illuminated by electromagnetic waves, energy is dispersed in all directions. The dispersed energy depends on the size, shape and composition of the obstacle and frequency and nature of the incident wave. This distribution of energy is known as 'scattering' and the obstacle as 'scatterer' or 'target'.

2

In earlier radar systems, the accuracy of detection depends on the knowledge of the targets' Radar Cross Section (RCS) levels and the scattering mechanisms. Radar can process only the information imposed on the scattering wave which characterises by the interaction of transmitted electromagnetic wave with a physical body. For this reason, it is important to know the scattering properties of all types of targets. While this fundamental objective is still required today, the recent developments in Radar technology and the processing systems have generated a corresponding change in the interest of RCS measurements. Now RCS measurements have the potential to determine the techniques to distinguish different types of targets, modifying target scattering properties and separating real targets from background clutter. The fundamental parameters like far-field, polarization, instrumentation sensitivity, and range facility requirements influence the RCS. Also the response of the radar target is dependent on operating frequency, the target orientation relative to the radar system, and the radar waveform. Polarization plays an important role in RCS characteristics.

The RCS definition distinguishes between monostatic and bistatic systems. Many radar systems co-locate the transmitter and receiver. In this case, aspect angles

relative to the target are identical for both the radar transmitter and receiver, and the corresponding RCS is referred to as 'monostatic' Radar Cross Section. When the transmitter and receiver are separately placed, the aspect angles are different and the RCS is referred to as 'bistatic' one.

1.2 BASIC THEORY - THE RADAR EQUATION

The radar range equation provides most useful relation between radar cross section and various radar system parameters. The value of RCS is determined not by direct measurement but rather by measurement of received power reflected from the target. The Radar equation for free-space propagation may be expressed [1] as,

$$P_r = \frac{P_t G_t G_r \lambda^2 \sigma}{(4\pi)^3 R^4}$$

where

P_r = received power

P_t = transmitted power

G_t, G_r = transmitting and receiving antenna gains

λ = operating wavelength

R = range from radar-to-target.

For a monostatic radar system, the above equation is expressed in more convenient form as,

$$P_r = P_t \, G^2 \lambda^2 \sigma \ / \ [(4\pi)^3 R^4]$$

Since the same antenna is used for the transmission and reception, so that, $G_t = G_r = G$.

The far field conditions required for RCS are the same as those required for antenna measurements. The power reflected or scattered by a target is the product of effective area and the incident power density. In general, that 'area' is called scattering cross section of the target. For directions back towards the radar, it is called 'back-scattering cross section' or the 'Radar Cross Section', and other directions, it is bistatic cross section. The scattering cross section is not a constant. It is an angular-dependent property of the target. The RCS definition also assumes a target in free space. It does not include multipath interaction or scattering from surrounding background. The far field RCS does not vary with changes in range.

The RCS of a target is defined in terms of area. But it is important to note that RCS has no general relationship to the physical area of the target. RCS of a target

depends on the target's geometry, its material properties, its orientation relative to the radar, the radar frequency and waveform and the incident and received polarization. These factors must be carefully specified to provide data of RCS of a target.

RCS of a target will have a wide variation, if the illuminating electromagnetic wave has got a wide range of frequencies. The low frequency scattering mechanism is the excitation of dipole moments by the incident plane wave. At high frequencies, the incident plane wave excites currents at the surface of the target and the scattering is influenced by the nature of the target.

The instrumentation for the measurement of RCS takes different forms. Simple, continuous wave (CW) radar configured from conventional microwave components and standard receivers and transmitters. Modern Network Analyzers and frequency synthesizers have greatly expanded CW radar facility. The transformation techniques like frequency to time domain available in most modern network analyzer systems further increased measurement speed, accuracy and convenience.

1.3 CURRENT AREAS OF INTEREST – RADAR CROSS SECTION REDUCTION

Nowadays, the prime focus is in deriving effective methods for targets of low RCS so as to increase survivability by reducing detectability. The increase in 'smart' detecting systems actually threatens the defence missions. The field of RCS studies is now advanced very much with the thrust and concentration on developing methods for RCS Reduction (RCSR) of targets of strategic importance. By reducing the RCS of the target, it can be made 'invisible' to radars and thus its potential use and 'survivability' are enhanced.

Four basic techniques are already existing for reducing RCS of targets. These techniques are:

a) shaping of targets

b) coating the targets with radar absorbing materials (RAM).

c) passive cancellation

d) active cancellation.

1.3.1 Shaping of targets

The aim of shaping is to orient the target surfaces and edges so as to deflect the incident energy in directions away from the radar. The sharp cuts and dihedral and tri-hedral corners are avoided in shaping technique, by bringing these intersecting surfaces in acute or obtuse angles. However this cannot be done in all viewing angles.

1.3.2 Coating the targets with e.m.wave absorbers

In radar absorbing materials (RAM), the energy is absorbed through a kind of ohmic loss in which the micro-wave energy is converted into heat energy. The imaginary part of the complex refractive index of the material accounts for the loss. At microwave frequencies, the loss is due to the finite conductivity and molecular friction experienced in attempting to follow the alternating fields. This in turn, would cause dissipation of energy within the materials. The use of RAM will cause serious problems like added weight, volume, and surface maintenance.

1.3.3 Passive cancellation

In passive cancellation, the basic concept is to introduce an echo source whose amplitude and phase can

be adjusted so as to cancel another echo source. Though this method is applicable for fixed targets, it is not possible to adopt it to moving targets.

1.3.4 Active cancellation

In active cancellation, the target must emit radiation whose amplitude and phase should cancel the reflected energy. In this case the target must sense the angle of arrival, intensity, frequency and waveform of the incident energy. Because of the practical problems associated with this, the above technique is not widely adopted.

The advantages in reduction of RCS are balanced against many disadvantages. For example, reduction in RCS at one viewing angle will enhance at another, when target surfaces are reshaped or reoriented to achieve the reduction.

The requirement of reduced echo target mainly depends on the current requirement of weapon systems. In the final system design, all possible environments like mission, design flexibility and cost are taken as inevitable conditions. The change in payload, the maintenance problem and the added weight are also playing as a penalty for the RCSR. Because of these, the passive and active cancellation

techniques are not considered as practical methods of reduction of RCS. In the present study, the main concentration is on the shaping techniques of simple targets and the work presents a technique without any sacrifice in target parameters.

1.4 MOTIVATION

The traditional way of eliminating reflections from a plane metallic plate is by making corrugations on it. Triangular, rectangular, sinusoidal and fin-shaped corrugations are mainly employed for the reduction of reflection from planar surfaces. Various corrugated surfaces in current use are shown in Fig.1.1. Using the principle of Bragg Scattering, it is possible to eliminate specular reflections from plane metallic surfaces employing corrugations.

However, the fabrication of such corrugated surfaces on a metallic plate is a tedious and time-consuming task. In the case of reduction of Instrument Landing System Interference, the corrugated structure must be numerous and wider enough to cover the whole terminal building. Fabricating corrugated surfaces of such wider areas is costly and it involves hard labour. The motivation of the present
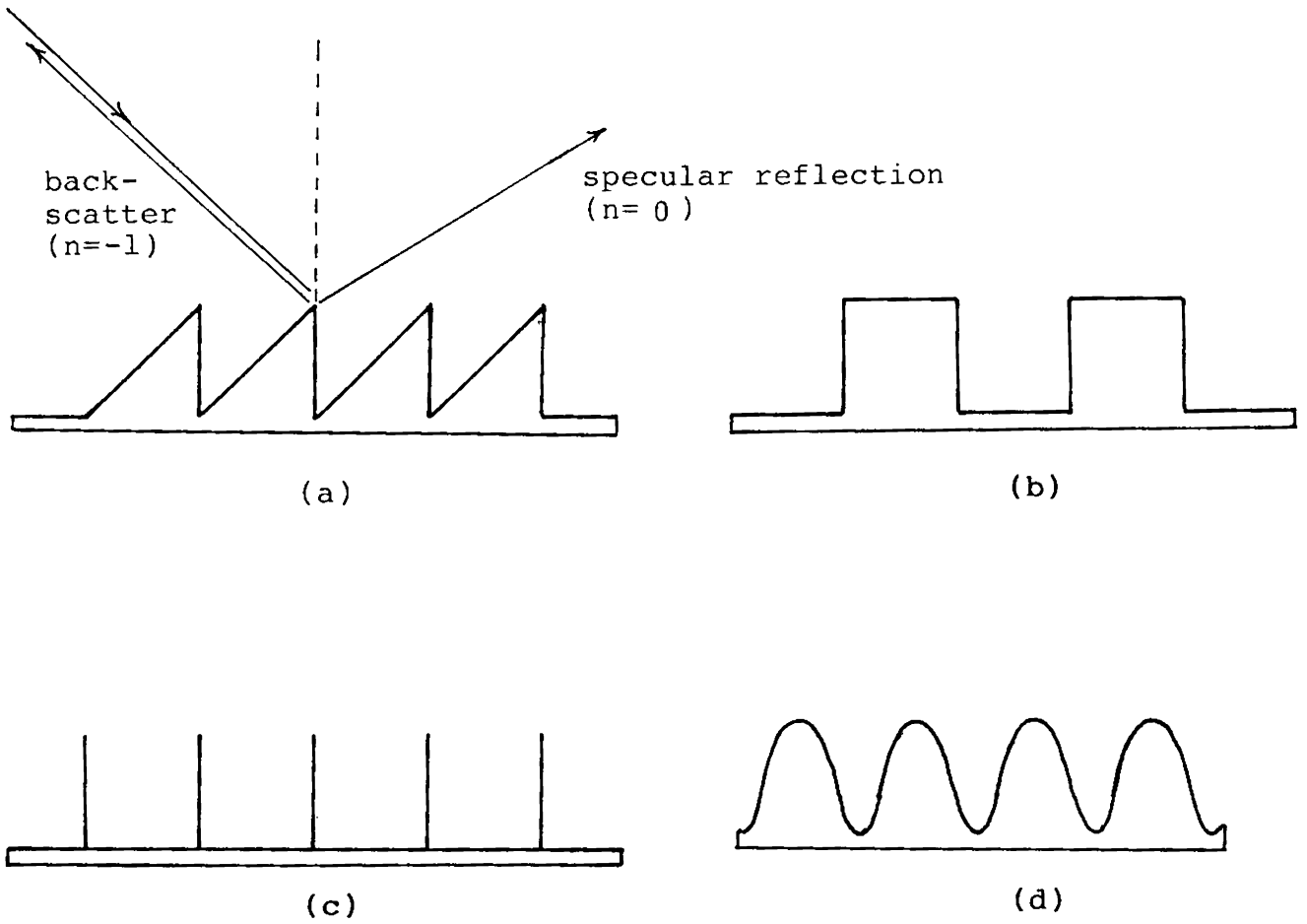
Fig. 1.1. Different corrugated metallic surfaces

(a) Triangular   (c) Fin-corrugated

(b) Rectangular   (d) Sinusoidal

work is to find an alternative system for corrugated metallic surfaces, which will have all advantages of metallic corrugations.

The periodic metallic strips of regular period on a dielectric sheet with a conducting ground plane behind it shows similar properties of a corrugated metallic plate. The effect of various parameters like thickness of the dielectric medium, grating period, variation of reflected power for normal and near-normal incidence are studied in detail.

1.5 OUTLINE OF THE WORK

1.5.1 Comparison between strip gratings and metallic corrugated surfaces

Rectangular metallic corrugations are fabricated in aluminium sheet and its scattering behaviour is compared with a periodic strip structure over a dielectric sheet with a ground plane. When the period d of the strip grating satisfies the Bragg condition

$$d = \lambda/(2 \sin \theta_i)$$

The specularly reflected power is completely eliminated

(perfectly blazed) and a non-reflecting conducting surface is obtained.

1.5.2 RCS reduction for normal and near normal incidence

In the case of metallic corrugated surface, the necessary condition for the elimination of specular reflection is $19.4° \leq \theta_i \leq 90°$. The low angle specular reflection reduction could not be achieved for an angle of incidence less than $19.4°$ in corrugated surface. But using strip grating configuration, it is possible to reduce the normal incidence and near-normal incidence specular reflection. In this case, the system would be a low back scattered strip structure. By covering the planar structure with a strip grating, it is possible to reduce its RCS to a considerable extent.

1.5.3 Advantages of the strip gratings

The shaping technique to reduce the RCS of a target is limited in many ways like aerodynamical problems in aircrafts and missiles. The corrugation technique is not possible in such systems. But the strip gratings would not offer any air resistances, because thin strips are in same plane as dielectric sheet. Another important advantage of the strip gratings is in fabrication technique. The photolithographic and etching techniques are very much helpful for the

accurate design and fabrication. The thickness of the corrugated surface (depth of corrugation) can also be reduced very much in the case of strip gratings.

Another advantage is the increase in bandwidth of effective elimination of specular reflection.

1.5.4 Scheme of the present work

The following parameters of the strip gratings are studied in detail:

1. Variation of grating period

2. Variation of the thickness of dielectric sheet

3. Single and dual periodic strip grating

4. Elimination of normal and near normal incidence specular reflection

5. Variation of frequency

The schematic figure of the work is as follows.

The review of the past work done in the field of RCS and RCS reduction is presented in chapter 2. Main emphasis is given to the reduction techniques and the strip grating systems.

The methodology adopted and the experimental techniques for the present investigation are described in chapter 3.

Chapter 4 introduces the experimental results of the investigation. Various parameters like dielectric constant, incident frequency and grating period are taken for the special consideration in the reduction of RCS of planar structures. The course mainly concentrated and devoted to the measurement of the reflected power. Efforts are made to compare the difference in reflected power from plane metallic surface and the strip gratings, which would give the level of RCS of the target.

Fifth chapter is devoted to the theoretical explanation of the experimental results. Comparison between theoretical and experimental results showed good agreement.

Final conclusions drawn from these investigations are presented in chapter 6. Advantages of the developed system is examined along with the scope of further investigation in this line.

Work done by the author in related fields are presented in Appendices I, II and III. The monitoring of

the curing conditions of a solid rocket propellant is presented in appendix I. The detection of inhomogeneities in non-metallic material using microwave Non-Destructive Testing (NDT) is possible. The position of inhomogeneity in rocket propellant is critical and appendix II is devoted to the accurate location of inhomogeneity using microwaves.

The environment of the experimental set up is most important for any kind of investigations. In the case of e.m. wave propagation studies, the most important one, viz., the Anechoic chamber is an essential facility. A new convertible microwave anechoic chamber is constructed and the design, development and evaluation is presented in appendix III.

Chapter 2

REVIEW OF THE PAST WORK IN THE FIELD

17

Chapter 2

REVIEW OF PAST WORK IN THE FIELD

2.1 INTRODUCTION

This chapter presents a chronological review of work that has already been published in the field of Radar Cross Section (RCS) and techniques developed for reduction of RCS. The chapter is mainly divided into four parts. The first part presents a review of RCS studies along with RCS measurement methods and the second part presents a review of RCS reduction techniques. The shaping technique for RCS reduction using corrugations is reviewed in part three, and the strip grating technique for the reduction of RCS is reviewed in the last part. The chapter is concluded with the presentation of the new strip grating technique for RCS reduction and this forms the major part of work reported in this thesis.

Estimation of RCS is a technique based more on science, particularly optics. The knowledge of the modes of scattering of energy incident upon a target is of greater importance in such estimation. In fact, understanding of target cross section follows from a detailed comparison of theory with experimental results. The increasing speed and

capabilities of present day computational techniques have made solutions of integral equations which are involved in such calculations, faster and efficient.

2.2 RADAR CROSS SECTION

Most of the work on RCS, reported in open literature can be found in books [1-5]. Harrison and Heinz [9] has derived a formula for the RCS of solid wire, tabular and strip chaff of finite conductivity approximating one-half wavelength or less in length.

Knop [10] analysed the RCS of a coated metal plate. Here, the thickness of the plate and that of the coating are assumed to be thin, and the size of the plate is large so that physical optics approximation could be used.

Experimental measurements have been made by Blore [11] for the nose on back-scattering RCS of ogives, cone spheres, double-backed cones, double-rounded cones and cone spheres.

Rheinstein [12] had carried out several series of rigorous numerical calculations of the backscatter cross sections of a conducting sphere with a thin lossless dielectric coating.

Hu [13] had measured the RCS of a dipole antenna in the VHF range using a 20 inch diameter sphere as a reference target. The input terminals of the dipole were shorted and they compared the experimental results with theoretical values.

The CW balanced-bridge measurement system for 35 and 70 GHz frequency band is presented by Blore et al. [14]. This system is most suited to perform sensitive measurements of small targets at short distances from the radar, usually in an indoor microwave anechoic chamber. The major limitation is the difficulty in obtaining a complete cancellation of background signal and in maintaining this cancellation.

Blacksmith et al. [15] reviewed the history of radar cross section measurements and some terms are defined along with discussions of major problems. It is pointed out that the various range geometries and measurement techniques in use today were based on the approach used to solve the basic measurement problems. They have also presented detailed discussion about the popular RCS measuring techniques like CW, pulsed, doppler, and standing-wave-ratio methods, with a review of model range problems.

The analytical techniques available for estimating the backscattering cross section of a metal target are

reviewed by Senior [16]. In this review a classification is given on the basis of wavelength to dimension of the targets. An attempt is made to interpret the results on the basis of scattering process.

Crispin and Maffett [17-18] reviewed RCS measurement methods for simple and complex shapes, with special attention being devoted to results rather than to derivations of the formulae. The discussion is limited to mainly ellipsoids, finite cones, ogives, cylinders, thin wires, and flat plates. Special emphasis is placed on an approach which could be applied to 'complex' shapes of more practical interest such as aircraft, missiles, satellites, navigational beacons, etc. Several examples are reviewed to give an idea of the nature of the results achievable with this approximation method. Since the ultimate objective is the determination of radar reflectivity properties of an object of practical interest, interpretations and comparisons of RCS data are critical. Moreover, these techniques have proved to be most effective to prescribe modification, and even design of RCS characteristics of complex shapes.

Kouyoumjian and Peters [19] have given the conditions of RCS measurement in terms of variations in the amplitude and phase of the incident field at the target. A number

of minimum range conditions are listed and discussed. Freeny [20] had presented theoretical and measured data pertaining to background levels which can be achieved with conventional target supports.

The factors which govern bistatic scattering are discussed and the relation between bistatic and monostatic scattering are presented in terms of the combined effect of individual scattering centers on the target, by Kell [21]. The concept of radiation lobe pattern of the individual scattering centers is used to define the bistatic pattern in terms of monostatic pattern and the bistatic angle.

The use of the scattering matrix leads to the formulation of radar reflectivity that is independent of radar polarisation, target range, and target rotation about the line of sight is presented by Lowenschuss [22].

Kell and Pedersen [23] have compared RCS measurements in two measurement system. One is a narrow band-CW system and the other, a short pulse system. They have presented data for one model target with low RCS.

Liepa and Senior [24] have investigated the scattering of a plane electromagnetic wave by a metallic sphere

loaded with a circumferential slot in a plane normal to the direction of incidence. The slot is assumed to be of small width and the field scattered in any direction is obtained by superposition of the field diffracted by an unloaded sphere, and the field radiated by excited slot. Numerical and experimental results of backscattering are also presented. Beckmann [25] presented the investigations on scattering by a superposition of several random process such as small plus sea plus ripple.

In 1965, a bibliography of articles on radar reflectivity and related subjects had been presented by Corriher and Pyron [26].

Alongi et al. [27] have illustrated the design of an extremely high range resolution FM/CW X-band radar and the RCS measurements. The primary design objective is to provide the capability to measure RCS of scaled models with a range resolution equal to a small fraction of the target length. Springston [28] reported a high-data rate RCS measurement system especially designed for high angular precision and direct digital recording. Particular features of this system include semiautomatic control, optical indexing of model azimuth, and the centre of gravity adjustments of the model.

Millin et al. [29] developed a method for calculating the scattering from an infinitely long cylinder of arbitrary cross section.

Ross [30] carried out an investigation of the scattering from rectangular flat plate. The simple physical optics theory provides an accurate means of predicting the near-specular values of plate cross section but fails to account for polarisation dependence. The calculations based upon the geometrical theory of diffraction show excellent agreement with measured data.

The backscattering characteristics of various types of insects found in the lower atmosphere were measured and the results are presented by Hajovsky et al. [31]. This paper presents discussion of the measuring equipment and its capability.

Van Vleck et al. [32] studied the radar response of wires and thin metallic strips as a function of their length and thickness, and of radar frequency. Macrakis [33] derived the geometrical optics approximation for the backscattering cross section per unit length of an infinite ribbon.

Monostatic RCS results for five and eleven wave-
length straight wires are presented by Miller et al. [34].
The numerical RCS values obtained from solving Pocklington's
integral equation for induced current fall within 1 dB of
experimental measurements.

Alexopoulos [35] had applied the geometrical optics
technique to obtain the reflected electric field from a per-
fectly conducting sphere coated with a special class of
spherically inhomogeneous dielectrics. The result is comp-
ared to the second order approximation which is obtained
by asymptotic theory.

Johnson et al. [36] have described a compact range
technique for measuring the gain patterns of full size micro-
wave antennas and for making radar reflectivity measurements.
The basic principle of this technique is the use of a large
collimating device to generate a uniform plane wave across
the aperture of a target or antenna without requiring the
normal far-field separation. RCS patterns, as a function
of aspect angle were measured for various size standard tar-
gets and compared with theoretically calculable RCS patterns.

Miller and Morton [37] have studied the RCS of a
metal plate with resonant slot. Yu [38] presented RCS of
a thin plate near grazing incidence with three higher order
diffraction techniques.

Rahmat-Samii and Mittra [39] have employed a new integral equation to calculate the current distribution on a rectangular plate when illuminated by a plane wave. Numerical results are also obtained for the RCS of a plate for different angles of incidence and different dimensions of the plate.

Lin et al. [40] have investigated RCS of a conducting rectangular plate, numerically and experimentally by a wire mesh model. This numerical example also included the edge-on incidence where physical optics and geometrical theory of diffraction have failed.

The development of a rapid RCS measurement technique over wide frequency bands has been presented by Weir et al. [41] in 1974. The Hewlett-Packard(HP) automatic network analyser, along with scattering-parameter measurement system has been adapted for RCS measurements. Typically the clutter, antenna cross coupling, and system errors in the absence of target are reduced to an equivalent value of -45 dBsm.

The broad side RCS of a rectangular box is presented by Tsai [42]. The solution is formed by integral equation technique. Appel-Hensen [43] had used a two-port network

and geometrical interpretation of equations involved in antenna scattering, to determine the antenna characteristics in properly designed scattering measurements.

Keen [44] had developed a numerical technique for the evaluation of the monostatic RCS of any regular shape of corner reflector consisting of three orthogonal plates.

A plain and simple, yet accurate formula to calculate the backscattered RCS of a perfectly conducting hollow, finite circular cylinder with a closed termination is proposed by Huang [45]. The radiated field from the cavity region is evaluated via, the Kirchoff approximation and the reciprocity theorem.

A solution is presented by Le Vine [46] for the monostatic RCS of dielectric disks of arbitrary shape, thickness and dielectric constant. This result is obtained by employing a Kirchoff-type approximation technique. The internal fields induce polarisation and conduction currents from which the scattered field and RCS can be computed.

Sanyal and Bhattacharyya [47] have applied the uniform asymptotic theory of diffraction (UAT) to obtain an

expression for RCS of curved plates. Comparison with experimental results show good agreement even for different small and intermediate radii of curvature of the plate.

The measurement of the RCS of a long metallic rod is reported by Rembold [48], using continuous wave Doppler radar at 60 GHz. The derived expression for RCS demonstrates good agreement with the measured data.

Bhattacharyya et al. [49] described a monostatic CW RCS measurement facility on X-band. This set up is capable of automatically measuring the CW monostatic RCS over the aspect angle ranging from 0 to ±180 for both parallel and perpendicular polarisation. The typical value of effective isolation between transmitted and received signal is of the order of 60 dB and dynamic range of 35 dB.

Radiation characteristics of 90° dihedral corner reflectors are examined in detail by Corona et al. [50], with proper choice of the measurement scanning angle, this corner reflector was conveniently used as a reference target in experimental determination of RCS. The numerical model developed using physical optics and the image method, has been improved by taking into account, the rays diffracted by the corner edges.

Yaghjian and Mc Gahan [51] predicted the broadside RCS of a perfectly conducting cube, from arbitrarily low to arbitrarily high frequencies, and compared to measured data taken for cube of side lengths ranging from 0.15 to 4 wavelengths. At low frequencies, the magnetic field integral equation was 'augmented' to eliminate its spurious homogeneous solutions and thus to produce high accuracy beyond the resonance region up through the intermediate range. At high frequencies, diffraction solution was 'enhanced' to produce high accuracy down through the intermediate frequency range into the resonance region.

Dybdal [52] has reviewed the fundamentals of RCS measurements in 1987. Measurement facilities including the present active compact range techniques, are described. The wide bandwidth electronics and digital signal processing capabilities encouraged the earlier objective of determining RCS and have extended to include the developing techniques to distinguish different types of targets and modifying the target scattering properties. Achievable accuracy and those factors that limit the accuracy of RCS measurements are discussed.

Delisle et al. [53,54] have reported analytical and experimental results on RCS of classical targets and

real projectiles such as 20 mm bullet, a M1-105 mm shell and small cylinder with films. The analytical methods used to obtain the results include geometrical and physical optics, geometrical theory of diffraction and moment methods. Welsh and Link [55] developed two theoretical models for RCS measurements of large targets consisting of multiple independent point scatters.

2.3 RADAR CROSS SECTION REDUCTION

The low RCS measurement requires careful cancellation of the background reflections. The large size of the target tends to upset the background cancellation balance obtained in the absence of the target. So, when the cross section of the target is large, the target to background cross section ratio can be made approximately large. Bachman et al. [56-58] have presented a careful analysis of low RCS measurement techniques and the important problems incurred in realizing the sensitivities for long ranges. They listed five types of RCS ranges.

Bradford [59] presented a physical optics solution for the monostatic RCS of a corrugated metallic pipe. The surface of corrugation is sinusoidal.

The RCS of a flat, coated metal plate of arbitrary shape is presented by Knop [10]. Knott [60] has analysed the RCS of a dihedral corner and showed that the double bounce mechanism dominates the Radar echo and this contribution can be reduced by a considerable extent if the electrical size of the dihedral corner sides are known. In 1973 Emerson [61] reviewed in detail the electromagnetic wave absorbers which will reduce scattering and reflection from metallic objects considerably.

The deformation of metallic flat plates into cylindrical segments and shielding of flat plates by such segments to reduce the large specular reflection-echo is presented by Knott [62]. Even though it has not reduced the mean cross section by more than 1 dB, a useful reduction in mean return was achieved when the angle subtended by the cylindrical segment was greater than the angular base interval over which the mean is taken. This reduction was achieved independent of frequency.

Kennaugh [63] had presented the variation of back-scattered RCS with common transmit receiver polarisation P by a simple geometrical construction on a Poincare sphere.

Bhattacharya and Tandon [64] have presented an asymptotic high frequency estimation of monostatic RCS of

a finite planar metallic structure coated with a lossy dielectric and compared with experiments in X-band. The expression for RCS is obtained by using a diffraction coefficient involving Maliuzhient's function. They used a continuous wave (CW) monostatic RCS measurement set up for the experimental results, and achieved a reduction of 5 dB with a single coating of epoxy resin of thickness $\lambda/20$.

Radar performances like, detection tracking and position and velocity measurement are mainly affecting the statistical properties of radar targets. In [65], Peter Swerling et al. have studied the main issues in reducing RCS data in the form of statistical models. RCS data are obtained from measurements in an indoor or outdoor range. From these data, 'empirical' RCS distributions are determined. They have given attention primarily on deriving models of the probability distribution of individual RCS samples.

Ray and Mittra [66] have suggested the reduction of RCS using strips having electrical resistance. The description is useful in scattering calculations for a wide range of incident field angles. Cuba and Rawat [67] have presented a method to control RCS by impedance loading.

2.4 RCS REDUCTION USING CORRUGATIONS

The scattering of electromagnetic waves by struct-
ures which are periodic in one dimension is of interest in
many areas. These gratings are adequately treated by simple
approximations of the boundary conditions from Maxwell's
equations. The fields of an infinite grating excited by
a monochromatic plane wave consists essentially of an infinite
set of plane waves; with 'propagating modes' which carry
energy in specific directions and 'surface waves' which are
exponentially damped normal to the plane of the grating.
The existence of these waves follows from the periodicity
of the structure and the field must be represented as a
Fourier series, and this has been the starting point of many
authors. In 1907, Rayleigh [68] first applied this proce-
dure to the 'corrugated grating'. Propagation of electro-
magnetic waves along an infinite corrugated surface whose
slots are vanishingly thin is investigated by Hurd [69] using
a method based on the calculus of residues. Twersky [70]
had expressed the field of a grating of cylinders excited
by a plane wave as a transmitted set, a reflected set, and
essentially the sum of the two inside the grating. Senior
[71] had analysed the scattering of a plane wave by a per-
fectly conducting sheet having sinusoidal corrugations.

The possibility of reducing or enhancing the RCS of metallic targets is presented by Lowrie and Peters [72]. Wirgin and Deleuil [73] have developed a rigorous electromagnetic theory of the diffraction of light by a blazed lamellar grating.

De Santo [74,75] presented the solution of an incident plane wave scattered from a surface corrugated in one dimension, and infinite number of periodic finite depth, infinitesimally thin parallel plates having soft boundary and hard boundary.

Roumiguieres et al. [76] have investigated the possibility of making perfectly conducting rectangular groove gratings perfectly blazed simultaneously in both polarisations and numerous efficiency curves are given.

Kalhor [77] has analysed diffraction of parallel polarised electromagnetic waves from corrugated, periodic, perfectly conducting surfaces by rigorous method and method based on Rayleigh hypothesis.

An exact description of scattering of an incident plane wave with TE polarisation at an interface between two dielectric media with triangular shaped teeth was presented

by Marcuse [78]. The field in the grating region is taken as a double Fourier series expansion.

Ebbeson [79] has presented the results of an analytical and numerical investigation of TM polarised plane wave scattering from an infinite, fin corrugated surface. This surface was composed of infinitely thin fins of spacing $\lambda/2 < a < \lambda$, and specular reflections from this surface can be completely converted to backscatterer in a direction opposite to the incident wave when the fin period and height are properly chosen.

Jull and Ebbeson [7] have proposed the use of corrugated surfaces to reduce the interfering reflections from buildings, in particular, instrument landing system (ILS) interference from hangers near airport runways. A numerical examination of infinite comb grating for TM polarisation is made with spacing $\lambda/2 < a < \lambda$. Model measurements at 35 GHz verified that the surface behaves exactly as predicted for infinite comb. They have also reported [80] perfect blazing of reflection grating to the $n = -1$ spectral order for both TE and TM polarisations. Simultaneous 100% blazing for both polarisations with rectangular grooves is possible for $19.5° < \theta_i < 59.4°$. Design curves for these surfaces have also been presented.

Loewen et al. [81] have investigated the diffraction efficiency behaviour of both blazed and holographic gratings. The theory of scattering by periodic metal surface has been presented by Whitman and Schwering [82], utilising the physical optics approximation to determine the current distribution in the metal surface. The solutions are determined from the condition that the field radiated by the current distribution into the lower half-space must cancel the primary plane wave in the space range.

Cheo [83] has presented numerical results for plane-wave scattering from a perfectly conducting diffraction grating with triangular groove profile. Simultaneous blazing with 100% efficiency is obtainable in a littero arrangement. The range of the angle of incidence, for which such simultaneous blazing occurs, is considerably narrower than that obtained in a rectangular groove profile.

Heath and Jull [84] have predicted the theoretical evaluation of the coefficients of the matrices, governing the scattering mode, for a plane electromagnetic wave incident on a perfectly conducting periodic surface with a rectangular groove profile. When Bragg condition is satisfied, the matrices are decomposed. They also demonstrated the elimination of specular reflection for TE, TM or both modes,

numerically and experimentally [85]. Application to radar target design is also proposed [85].

James [86] has reported the surface reactance of a corrugated plate, illuminated by a plane wave using rigorous solution. The dependence of the surface reactance on slot period, depth, width and the angle of the incident wave are discussed.

Triangular and rectangular groove surfaces which reflect only transverse electric (TE) polarisation while totally backscattering transverse magnetic (TM) polarisation are investigated by Jull et al. [87,88]. Experimental design data are also provided. Hurd and Jull [89] have investigated the scattering of a plane polarised wave from a grating composed of narrow grooves in a perfectly conducting surface.

Metal gratings of high diffraction efficiency can be effective for mm wave polarisers, frequency filters and multipliers. At lower frequencies, their use is generally limited by the physical size. A numerical study of the effect of finite size on high efficiency reflection gratings is given by Jull and Hui [90].

A low back-scatter corrugated metal surface has been designed, fabricated and tested for H-polarised transverse electromagnetic incident wave by Bhattacharyya and Tandon [91]. The problem has been formulated using scattering matrix approach and the reflection and transmission coefficients at the fin-air interface are determined using an integral equation approach, and thus the RCS is obtained. They have carried out the experimental work in an outdoor CW scattering range using analog background cancellation technique with the help of hybrid junctions.

Jull et al. [92] have examined the effect of reflection grating size on its performances. A numerical analysis of thin corrugated conducting strips with rectangular groove profile dual blazed to n = -1 spectral order shows that high efficiency gratings remain efficient as the number of grating elements reduced to four or two, provided that the incidence is not near grazing. Experimental investigations of crossed gratings of square pyramids are given by Cai et al. [93]. Yasura et al. [94] analysed the diffraction from a sinusoidal metal grating.

The widely used transversely corrugated surfaces having the same anisotropic surface impedance deserve a common name. Kildal [95] proposed to call them as "soft

surfaces" analogous to soft surfaces in acoustics. The soft and hard surfaces can be used as general design elements when constructing scatterers to obtain certain desired radiation characteristics.

2.5.1 Strip gratings

Lewis and Casey [96] have showed that the effect of increasing resistivity of the wires in a grating is to decrease the amplitude of the reflection coefficient and phase of the transmission coefficient. The sign of these changes depends upon that of similar gratings having no resistance.

The control and direction of electromagnetic waves are accomplished in general, by the use of boundary materials and structures which produce desired effects on such waves when incident on them. Groves [97] proposed an important class of boundary structure for this purpose, having alternative areas of conducting and non-conducting materials.

The solution for the problem of a plane wave incident obliquely on a parallel-wire grid, which is backed by a plane conducting surface is presented by Wait [98].

It is shown that, in certain cases, a resistive wire grid will absorb all energy of the incident wave.

Primich [99] investigated theoretical and experimental results for the reflection and transmission of uniform plane electromagnetic waves, normally incident on an ideal strip grating. The theory is based on the variational method, and the measurements were made at normal incidence in a parallel plate region operating in the 8-10 cm wavelength range.

Larsen [100] has presented a survey of literature concerning the electromagnetic properties of wire grids. It included a short description of properties and applications of wire grids along with some particular grid configurations like ferromagnetic wire grids, dielectric coated wire grids, parallel grids with parallel wires and crossed wires, and grids parallel to conducting and dielectric interfaces.

As a practical application of diffraction grating, Takada and Shinji [101] have presented a diffraction grating which was a new version of microwave passive repeator developed to improve the transmission qualities of links utilising mountain diffraction. It has special advantages in the high frequency region and in 11 GHz common carrier band,

where the construction of a large aperture flat reflector encounters difficulties and becomes uneconomical. Principles and characteristics of diffraction gratings are given with test results. Villeneuve [102] presented an approximation technique for computing transmission and reflection coefficients for plane waves propagating through stratified slabs.

Sigelmann [103] studied the surface wave modes in a dielectric slab covered by a periodically slotted conducting plane. Sampling and variational methods are used to obtain the surface-wave modes.

Neureuther and Zaki [104] presented a method for improving the accuracy of approximate numerical solutions of doubly infinite sets of simultaneous linear algebraic equations. The method is based on using prior information about the asymptotic behaviour of the solution to anticipate the dominant contributions of the terms. The advantages and disadvantages of this method are discussed for the well known problem of scattering from a planar grating.

Jacobsen [105] has described an analytical numerical and experimental investigation of a practical, two-dimensional periodically modulated slow-wave structure. The structure is a dielectric slab covered on one side by a

perfectly conducting ground plane and on the other side by perfectly conducting thin strips perpendicular to the direction of propagation.

Chen [106] has formulated the boundary value problem of an infinite array of thin plates arranged in a doubly periodic grid along any two coordinates, in a general form for an arbitrarily polarised plane wave incident from any oblique angle. Both magnitude and phase of the reflection coefficients are determined explicitly.

Green [107] has proposed integral equations for currents induced on an infinite perfectly conducting grating for a plane wave. These integral equations are approximated by matrix equations, which are readily solved for currents. From these currents the strengths of the grating modes are obtained. It is also possible to extend this technique to dielectric gratings.

Kalhor and Neureuther [108] have suggested a general numerical technique for analysing diffraction gratings of arbitrary groove shape as electromagnetic boundary-value problem. The method yields the induced surface current, from which the energies in various radiating orders can be

conveniently obtained. The accuracy and versatility of the technique are demonstrated.

A numerical solution for the problem of scattering of a plane wave by a dielectric sheet with an embedded periodic array of conducting strips was presented by Lee [109]. The primary motivation for introducing the strips is to reinforce the mechanical hardness of the sheet in certain random applications. The additional strips also improve the transmission through the composite structure.

Mittra et al. [110] have investigated two methods for solving the problem of plane wave diffraction by grating with sinusoidal profiles, one the extension of Rayleigh hypothesis and the other analytic continuation technique.

Ikuno and Yasuura [111] have presented and applied a model expansion to solve the boundary value problem of scattering from a periodic structure composed of a perfectly conducting surface.

The solution to the problem of scattering of a plane wave by an infinite periodic array of thin conductors on a dielectric slab was formulated by Montgomery [112]. Numerical results are presented with experimental data.

Kalhor and Armand [113] have presented numerical integral equation technique for the analysis of the problem of diffraction of electromagnetic waves by an infinite array of conducting cylinders. The solution of the integral equation gives the surface field over one element of the grating from which the reflected and the transmitted mode amplitudes are conveniently calculated.

Hurd and Sachdeva [114] have formed the low frequency solution of the diffraction problem of E-polarised plane wave incident on a dielectric loaded slit in a perfectly conducting plane.

Wilton and Govind [115] have demonstrated the importance of incorporating the edge behaviour into the moment method solution procedure for TM-wave scattering by a conducting strip. Various numerical schemes for treating the edge behaviour are examined for low frequencies, where an analytical solution of the quasi-static integral equation is available for comparison.

Analysis of the scattering by an infinite periodic array of microstrip disks on a dielectric sheet using Galerkin solution of vector integral equation was made by Montgomery [116]. Later, he studied [117] the solution of TE and TM

electromagnetic scattering for an infinite array of multiple parallel strips using the perturbational form of the modified residue calculus technique (MRCT). Numerical results are presented and discussed in it. The solution is found from the canonical problem of an infinite periodic array of semi-infinite parallel plates.

Kalhor [118] has analysed diffraction of electromagnetic waves by a planar array of perfectly conducting strips, by a simple numerical technique based on mode expansion and point matching. Results are compared against other numerical results available in literature. Further numerical results are presented which show usefulness of these structures as shielding grids, reflectionless metallic supports and polarisers.

By using microwave models of optical gratings, Tamir et al. [119-124] realised dielectric grating with asymmetric triangular or trapezoidal profiles that exhibit beam coupling efficiencies. The behaviour of leaky modes along microwave gratings shows that, Bragg scattering approach provides simple design criteria for blazed dielectric gratings and broad band high efficient optical beam coupling devices.

Rope and Tricoles [125] have described the beha-
viour of corrugations with their heights normal to the surface
of the sheet or tilted. The latter have heights inclined
to the sheets and these are called blazed gratings. Experi-
mental data are given for several sheets corrugated with
triangular grooves. Dielectric constant, groove spacing
and groove depth are also taken as variables.

The scattering of e.m. waves by planar arrays
of perfectly conducting strips is analysed by a simple method
based on physical optics by Kalhor [126]. The induced current
is determined using simple computation to obtain the ampli-
tudes of various propagating space harmonics.

Richmond [127] developed the theory of scattering
from a strip and that from a strip grating. The convergence
of moment method solution is found to be greatly improved
when the basic function include the edge mode. Numerical
results are presented for the reflection coefficient of the
strip grating.

Pauchard [128] has investigated the scattering
of electromagnetic plane wave by a plane grating of conducting
wires. The wires are parallel, equidistant and alternatively

continuous and discontinuous. The discontinuous wires may be considered as dipole lines. The problem is numerically solved and conducting currents are determined by means of a system of first kind integral equations which are converted to a linear equation system by moment method.

A plane electromagnetic wave is represented as a series of plane waves. The known solution of the problem of diffraction of a plane wave by a double grating is analysed by Prosvinrnin and Reznik [129]. The distribution of the transmitted field in the near zone, the shape of the radiation pattern, and the magnitude of the transmission coefficient, all depending on the parameters of the grating structure, are also considered. A method of analysis for strip gratings with more than one conducting strip per period is given by Archer [130]. The method is then applied to a periodic twin-strip grating with two unequal gaps.

Marcuvitz [131] has presented the formula for the equivalent, normalised parameters for various grid configurations. In all cases, the plane of incidence is perpendicular to the wires and solutions are determined by an integral equation method. Petit [132] presented electromagnetic theory of plane grating, in which the integral methods and differential methods are studied in greater depth.

Kalhor and Ilyas [133] have investigated the scattering of electromagnetic waves by an array of perfectly conducting rectangular cylinders embedded in a dielectric slab, by a numerical procedure based on an integral equation technique. The solution of this integral equation gives the induced surface currents on the surface of the scatterers.

Parker et al. [134-135] have reported arrays of simple rings on close packed square or triangular lattices. These are useful as frequency selective surfaces for reflector antennas. The scattering problem of surface waves by a metallic strip above a dielectric clad ground plane is treated by Hayshi and Ohro [136]. The Green's function is rigorously evaluated and the reflection and transmission coefficients of the TE and TM surface waves incident upon the thin conducting strip loaded perpendicular to the ground plane are obtained.

Hall and Mittra [137-138] have formulated solution for scattering for the case in which the conductivity is finite and a resistive boundary condition. The problem of scattering from this resistive strip grating is formulated in the spectral domain. The results presented are for a periodic array of resistive strips that are invariant in the X direction and periodic in Y. The reflection coefficients

are presented for perfectly conducting strips and strips
with resistivities upto 750 ohms/square. The finite conducti-
vity has reduced the reflection coefficient and lowered the
resonance for the structure.

Formulae for ideal and good grating systems are
given by Jeadong and Guorui [139]. Some applications of
the grating system such as $\pi/2$ and π frequency filter, pola-
risation rotators and impedance transformers are introduced
and the principle design considerations of an impedance trans-
former are discussed.

Gallagher and Brammer [140] have studied the scat-
tering of a plane wave from a periodic broken-wire grid buried
in a dielectric sheet for general angle of incidence and
for arbitrary linear polarisation. These periodic grid of
broken wires behave as a capacitative structure below reso-
nance and inductive above resonance. The measurements showed
that a transition from capacitative to inductive behaviour
is there when the frequency increases through resonance.

Cwik and Mittra [141-142] have presented a review
of techniques for the analysis of a planar periodic struct-
ure along with the outline of an iterative solution which
allows for the treatment of surfaces composed of arbitrary
geometries.

The problem of scattering of vertically polarised e.m. wave from underground cylindrical objects is determined by Kanellopoulos et al. [143] and for oblique incidence by Bogdanov and Kevanishvili [144].

Yamauchi [145] has described a new modal theory based on the orthogonal properties of the grating modes which are in general composed of almost periodic functions. The amplitude of the diffracted waves are determined and comparisons are made numerically between the diffracted efficiencies of the scattered wave for first, second, third Bragg angles. Surattesu and Petit [146] have presented a numerical study of perfectly conducting wire grating using the Hamiltonian method.

Buyukaksoy and Uzgoren [147] have studied the diffraction of plane waves by a metallic strip residing in the interface of two dielectric media, in order to clarify the secondary diffraction characteristics within the frame work of ray optics.

Kobayashi [148] has investigated the problem of diffraction by a thick strip grating with the aid of Wiener-Hopt technique. Kobayashi in [149-150], considered periodic parallel plate grating with dielectric loading, and the

problem is analysed with the same technique. The Wiener-Hopt equation is solved by decomposition procedure and then the modified residue calculus technique (MRCT) is applied to increase the accuracy of the solution.

Nishimoto and Aoki [151] analysed the scattering of e.m. waves by a semi-infinite strip grating, under the assumption that the strip is narrow relative to the wavelength.

A fast convergent integral equation solution to the scattering problem of a transverse electric or transverse magnetic (TE/TM) plane wave by a one-dimensional periodic array of thin metal strips on a dielectric substrate is described by Wu [152]. It is shown that the dielectric substrate has a strong effect on the scattering from the large spacing strip grating.

Theoretical and experimental studies of the scattering by a two-dimensional periodic array of narrow perfectly-conducting plates have been carried out by Ott et al. [153]. The scattering in resonance region is treated for normal incident plane wave.

Rao and Bhartia [154] have determined the even and odd mode impedances for the case of a structure consisting of elliptic bars located symmetrically between two infinite parallel plates.

2.5.2 Strip grating with conducting ground plane

Few results are available in literature about the scattering of e.m. waves by a strip grating with reflector. Yamsaki and Hinata [155] presented a numerical analysis for the scattering problem of an electromagnetic wave by planar grating with reflector. The capacitive grating with small gap in which the strip thickness can be neglected has been analysed in [155]. In [156] the grating with inductance and capacitive reflectors are analysed by Kitajima et al.

Moshiko and Adachi [157] have analysed the plane wave scattering or reflection from an infinite planar array consisting of loaded half-wave dipoles over a lossy half-space. When the dipoles are arranged approximately and loaded with an approximate impedance, the incident plane wave may be completely absorbed by the load impedances and the lossy half-space medium, results no reflection.

Kalhor and Ilyas [158] invesitgated the problem of electromagnetic scattering by periodic conducting cylinders

embedded in a dielectric slab backed by a plane conducting plate. Using Green's function approach, the problem of e.m. scattering from conducting cylinders located above the ground is considered by Cottis and Kannllopoulos [159] and study of scattering by multiple conducting and dielectric cylinders by El-Gamal and Shafai [160].

Kalhor [161] analysed the scattering from strips on a dielectric slab over a ground plane by mode expansion method. The fields are expanded in terms of suitable pro-pagating and evanescent modes in various regions. This method is interesting because, it is analytically simple and fast in computation.

A corrugated surface is a reactive surface which exhibits pass band-stop band characteristics with respect to the propagation of a surface wave. The pass band-stop band characteristics depend on the depth of the slots and the direction of propagation across the surface. Moreover, the longitudinal surface impedance also depends on the depth of corrugations.

It is possible to control the RCS of targets by altering the propagation properties of surface wave mode. The feasibility of this concept by use of a corrugated surface

is demonstrated in [72]. Using these surfaces it is possible to reduce or enhance the RCS of metallic targets. Bhattacharyya and Tandon [91] invented a low back-scattered corrugated surface for H-polarised wave. Such surfaces find useful practical application where the radars operating in crowded airports, to reduce the permanent echoes from terminal building and large aircraft hangers.

2.6 ORIGIN OF THE PRESENT WORK

From the above review,it can be seen that attempts have been made to reduce the RCS of a metallic target using different types of corrugations. There is considerable reduction or enhancement in RCS due to adoption of corrugations. It would be possible to reduce the reflectivity of a target by properly utilising the destructive interference phenomena in scattering from such targets. Scattering from conducting objects above a lossy medium is a problem of current interest concerning radar detection and identification of targets near the ground.

The implimentation of metallic corrugation for the reduction of RCS is a difficult and time-consuming process. No attempt has been reported about development of an alternative system to metallic corrugated surface for

RCS reduction. To overcome the technical and practical diffi-
culties encountered in the implementation of corrugated sur-
faces, a simulated corrugated surface (SCS) has been developed
in the present work. The SCS consists of thin conducting
strips on a dielectric sheet with a metallic reflector behind
it. This system behaves exactly as a metallic corrugated
surface in its scattering properties. Further, this strip
grating has several advantages over metallic corrugated sur-
faces. From the designer's point of view, the fabrication
of SCS is much more simple and easy than that of conventional
metallic corrugated surfaces.

In the present investigation, the behaviour of
the strip grating for the reduction of normal and near-normal
back-scattering is also studied in detail. The advantages
of the SCS over metallic corrugated surfaces are established
from experimental data over a wide range of frequencies.

As a part of the present work, a theory of scat-
tering from the elements of the strip grating has been deve-
loped. On the basis of this theory, the experimental results
were interpreted and a comparative analysis is made. The
observed effects of the strip grating system is thus explained
on a sound theoretical basis.

Chapter 3

METHODOLOGY AND EXPERIMENTAL SET UP

Chapter 3

METHODOLOGY AND EXPERIMENTAL SET UP

3.1 INTRODUCTION

This chapter presents the techniques adopted for the measurements and estimation of RCS parameters of the targets. Experimental set up and computation techniques employed are described in detail.

Measurement methods of Radar Cross Section (RCS) involve, three basic elements.

1. a source or radiator of electromagnetic energy

2. a target or scatterer of energy

3. a receiving antenna which measures the properties of electromagnetic field at points in space.

The electromagnetic field resulting from the source in the absence of scatterer is termed as the 'incident field'. The total field is the electromagnetic field resulting from the source current but with the presence of the scatterer.

57

The vector difference at each point between the total field and the incident field is termed as the 'scattered field'.

For the present study, the microwave source used is a sweep oscillator with a frequency band of 8.0-12.4 GHz (HP 8620). It gives levelled output power for all frequencies with a level control. Isolators, variable attenuators, waveguide detectors, directional couplers, coaxial cables and other essential components are used in the experimental set up. The dimensions of the waveguide components are such that they will support TE_{10} mode. Measuring amplifiers and X-Y/t recorders are used for analyzing and recording the received power. Movable and adjustable transmitting and receiving systems are specially designed with a turntable at the centre of an arch-shaped platform over which the transmitter or receiver or both can be precisely moved. Microwave absorbing materials are interposed so as to avoid direct coupling between transmitter and receiver. Maximum care is taken to avoid the reflections and scattering from nearby conducting surfaces.

3.2 ANECHOIC CHAMBER

The anechoic chamber is simply an enclosure lined-up with microwave absorbing material. The ordinary rectangular anechoic chamber admits, in addition to the direct ray from target to antenna, a number of single-bounce rays.

An improvement of this design is realized by making the walls of the chamber in the shape of a shallow wedge, with a rectangular silent zone or quiet zone. These are called 'tapered' anechoic chambers. Such chambers designed using ray optics principle can eliminate the single-bounce rays and it in-turn improves the performance of the quiet zone.

However, each design is devoted to specific interest of measurement and the peculiarities of the targets to be measured. Monostatic or single antenna method is preferred in tapered chambers while such chambers are of no use for measurements using bistatic techniques of RCS. As a means for achieving both advantages, a "convertible anechoic chamber" has been designed and its fabrication is completed. By minor manual adjustments, the rectangular chamber can be converted to a tapered one, depending on the type of measurement. Work carried out in the design and development of this convertible anechoic chamber is described in appendix III. This modern convertible chamber is unique in its design and it is useful for all types of antenna and RCS measurements. The target under test is mounted on a turn-table which is kept in the quiet zone of the chamber. The turn-table is controlled remotely from a control room, outside the chamber.

3.3 EXPERIMENTAL TECHNIQUES

The principle involved in RCS measurements is simple and well known. RCS is most often determined by comparison with the energy scattered by a calibration target of known cross section. Measurement methods can be broadly classified according to how the transmitted and received fields are separated. The incident and the scattered fields may be separated by

1. a difference in propagation direction (hybrid-tee, two-antenna system, SWR systems).

2. a frequency difference (Doppler and FM systems).

3. delay line (pulsed systems).

3.3.1 Difference in propagation direction

1. Hybrid junction cancellation

The continuous wave (CW) cancellation method requires only a single antenna in hybrid junction (magic-tee) system and is explained in section 3.5.1. with typical arrangement. For making this an accurate measurement, the frequency stability of the source must be accurately maintained, and the introduction of the scatterer must not substantially change the magnitude and phase of the background return.

2. Bistatic method

The waveguide magic-Tee junction can be avoided by using separate antennas for transmission and reception. The bistatic or quasimonostatic measurements can be made with such two antenna systems. An important consideration with a two antenna-system is the isolation between transmitter and the receiver, especially when cross-polarization measurements are involved.

3. SWR method

By using field probes, direct measurements of the scattered and incident fields can be made, eliminating the need for calibration targets. Small monopoles are usually used with an image plane which shields the transmission line and other necessary equipment from direct illumination.

The monopole is moved along a line between the source and target to measure the amplitudes of standing waves caused by interference between the incident field and scattered field. The reflection coefficient of the scattered field is given by [2]

$$b = \frac{\ell \omega_2 \, [\, \rho/(\ell_1 - \omega_2)\,] - [1/(\ell - \omega_1)]}{\rho + (\omega_2 / \omega_1)}$$

where ω_2 = the distance from the scatterer to a null in the total field

ω_1 = distance from the scatterer to a maximum in total field

ℓ = distance from source to scatterer

ρ = measured voltage standing wave ratio,

$$\rho = \frac{E_i + E_s}{E_i - E_s}$$

where E_i is the incident field and E_s the scattered field.

The back scattering cross section is given by

$$\sigma = 4\pi b^2$$

SWR determinations assume:

1. The probe is in the far field of both source and target.

2. The incident field polarization and scattered field polarization are parallel.

3. The probe does not perturb the field.

3.3.2 Modulation methods: Doppler method:-

Separation of incident and scattered field may also be accomplished by modulating either field at the

63

transmitter or at the target. If the target is given a component of velocity along the direction of illumination, the scattered field will be shifted in frequency and may be separated.

Fig.3.1 shows a Doppler system used in free space range. The target and calibrating object are mounted on a rotating disc. The Doppler signal being recorded during one portion of the forward motion.
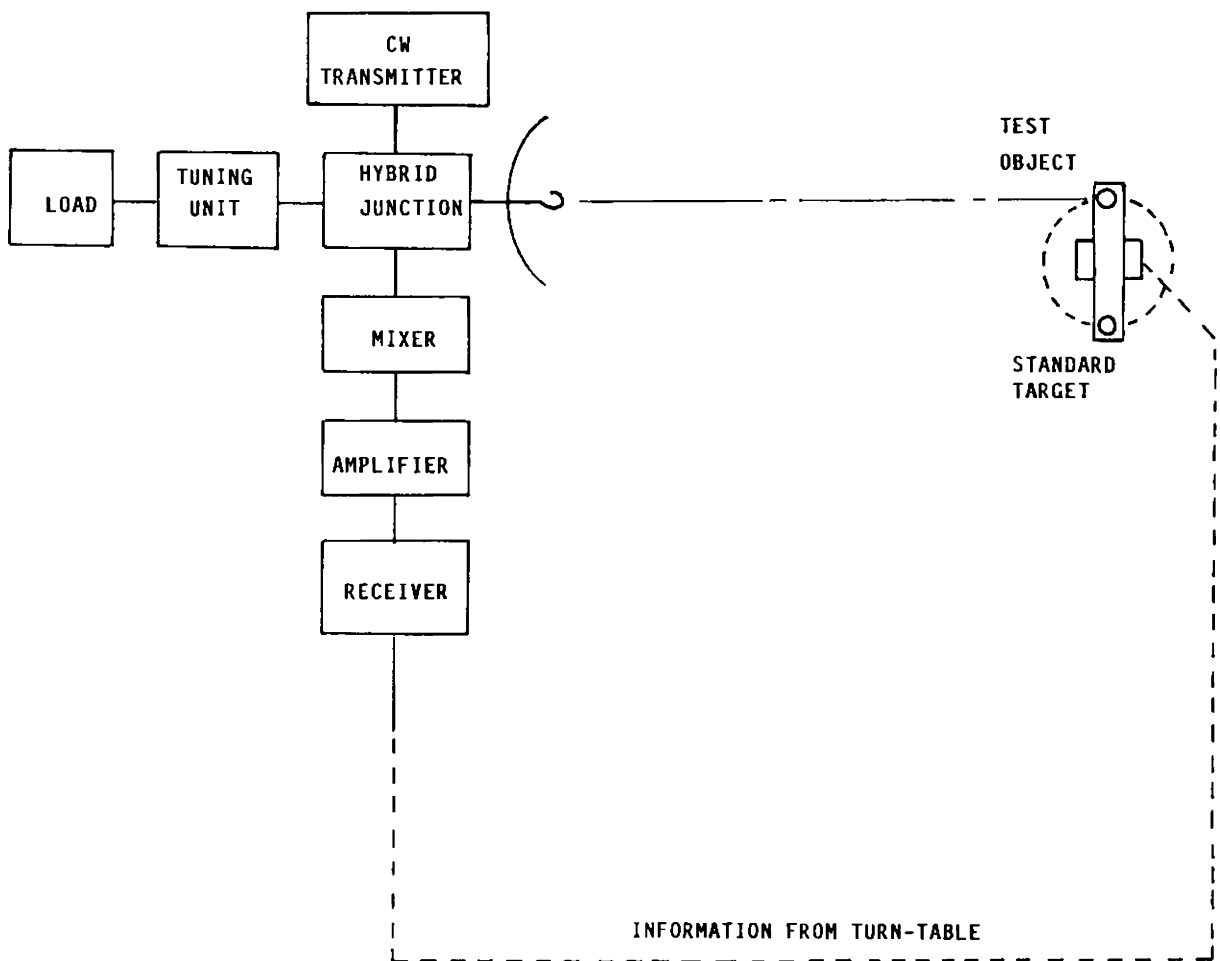
Fig. 3.1 Doppler system for measuring radar cross-sections

The attractive features of the Doppler method are amplitude stabilities are not required, high isolations are not required in the tee and irregularities in the measurement tend to cancel, since they affect both standard and model.

3.3.3 Pulse systems

The scattered field from the incident field is separated on the basis of time differences. A pulse measuring system is essentially a simplified radar adapted for measurements at short ranges.

3.4 RADAR ABSORBER MEASUREMENTS

The very important property of a radar absorber is the reflectivity of component materials. It is dependent on frequency and there are different measurement procedures to estimate the reflectivity of the absorber material. These are discussed below.

The basic objectives of the absorber measurements are (1) the performance evaluation and (2) verification of material properties (e.m. properties). These evaluations are mainly for the finished absorber panels or sheets, and the evaluation procedure must be of non-destructive type.

In this case, the simple one is the reflectivity measurement in single or swept frequency. The methods available for the reflectivity measurements are,

1. Arch method

2. RCS method

3. Waveguide method

Out of the above three methods, the first two are free space method and the waveguide method requires large waveguides of the size of the sample. In waveguide method, the materials are evaluated by recording the output of the probe, which is moved to and fro in the waveguide. With this arrangement, the measurement could only be at one frequency.

The measurement systems of electromagnetic properties of absorber materials are always closed systems. Irrespective of the thickness of the sample, the reflecting and transmitting properties of a sample is measured based on the insertion properties of the sample in a transmission line. The measurement procedures of e.m. properties of the sample are listed as follows.

1. Network analyzer

2. Time domain reflectometer

3. Slotted section interferometer

The sample in a transmission line is a discontinuity and the amplitude and phase of the reflecting signal from the sample, giving clues of the electromagnetic properties of the sample.

In time domain reflectometer, narrow pulse waveforms are transformed to the frequency domain by means of Fast Fourier Transform (FFT). Microprocessor based system analyses the waveforms, digitizes them and perform the FFT.

A load at the end of a transmission line causes reflection if the load impedance is not equal to the characteristic impedance of the line. The measurement of the standing wave patterns in front of the test sample leads to the determination of the sample properties.

In the present study of strip gratings, which can be used as a radar absorbing material, arch method is found to be most suitable.

3.5 ARCH METHOD

In arch method, the test panel is often placed in front of illuminating and receiving antennas. The arch itself is a vertical wooden framework that allows a pair of antennas to be fixed at a constant radius from the centre of the test panel, for a variety of subtended angles. Each antenna is mounted on a carriage, which can be slowly rotated, such that the carriage designed to keep the horn is pointed to the centre of the test target, no matter where the carriage is positioned (Fig.3.2). To reduce the direct coupling of energy from transmitter and receiver, it is necessary to place microwave absorbers between the two antennas.

The strip grating system with proper metallic backing plate is placed on a turn-table at the centre of the arch. While making measurements, it is ensured that the plane of the strip grating system is always perpendicular to the plane of incidence of electromagnetic energy. A plane aluminium plate of same dimension is used for the calibration of the measurements.

3.5.1 Transmitting system

As shown in Fig.3.2, the set-up needed for the measurement of reflected (n = 0 mode) and backscattered

Receiver
for specular reflection

Transmit-
receive
system

Strip grating system

Turn-table
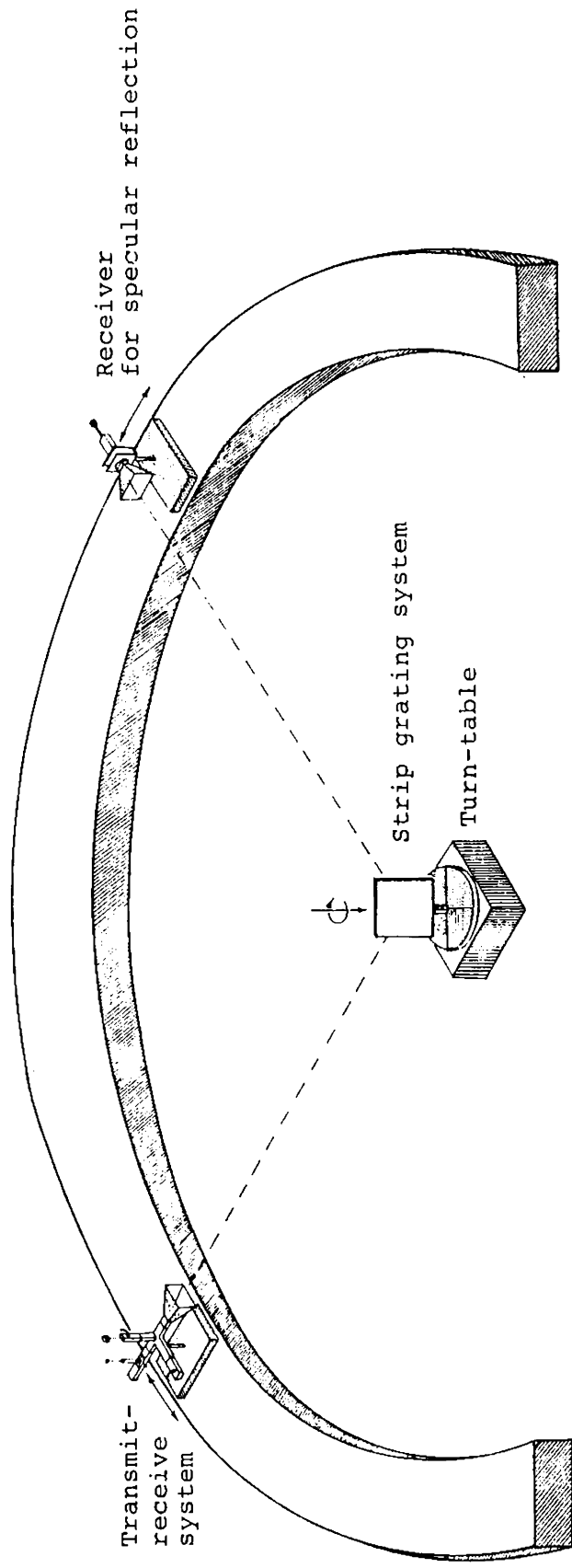
Fig. 3.2   Arch method for RCS measurements

(n = -1 mode) power is quite simple. The amplitude modulated output from a sweep oscillator (HP 8620 C, 8-12.4 GHz) is fed through precision attenuator to one of the crossed arms of the magic-Tee. Components of a typical CW system are shown in Fig.3.3.

The magic-Tee is a waveguide junction which can be represented as a four terminal network. If the four terminals are terminated in matched or balanced impedances, a signal entering any terminal will divide equally between the two adjacent terminals and be isolated effectively from the fourth. In most cases, this system have a transmitter and receiver attached to the branch arms of a waveguide magic-Tee, tuners and matched load are attached to one collinear arm and a single transmit-receive horn is attached to the other. In a perfect matched system of a completely symmetrical tee, the transmitter and the receiver would be completely isolated, the transmitter signal would divide equally between the collinear arms, and the received signal would divide evenly between the matched load and the receiver. In practice, the load is purposely mismatched slightly to reflect a small part of the signal from the load arm into the receiver arm of the tee. This signal is used to cancel unwanted background reflections. It is controlled in amplitude and phase by

adjusting the tuners. The ratio of the power remaining in the receiver arm of the tee after cancellation to the power in transmitting arm is commonly called the 'isolation' of the system. The isolation required increases as the required accuracy increases. The sensitivity of the CW system is limited by an amount of isolation that can be held between transmitter and receiver arms of the hybrid-tee. This degree of isolation is, of course, affected by several factors like frequency stability of RF source, temperature change of the hybrid-tee and mechanical stability of the the waveguide system.

3.5.2 Receiving system

The receiving system consists of a waveguide detector, from which the rectified output is given to a measuring amplifier (Type 2636 Bruel and Kjaer). This amplifier is provided with proper RF filters and it gives output in dB as well as in volts directly from the meter. The recorder output from the amplifier is given to XY/t recorder (Type HP 7047 A).

The set up for the measurement of specularly reflected power consists of a horn antenna and the waveguide detector as shown in Fig.3.7. The detected output is given to the measuring amplifier and XY/t recorder.
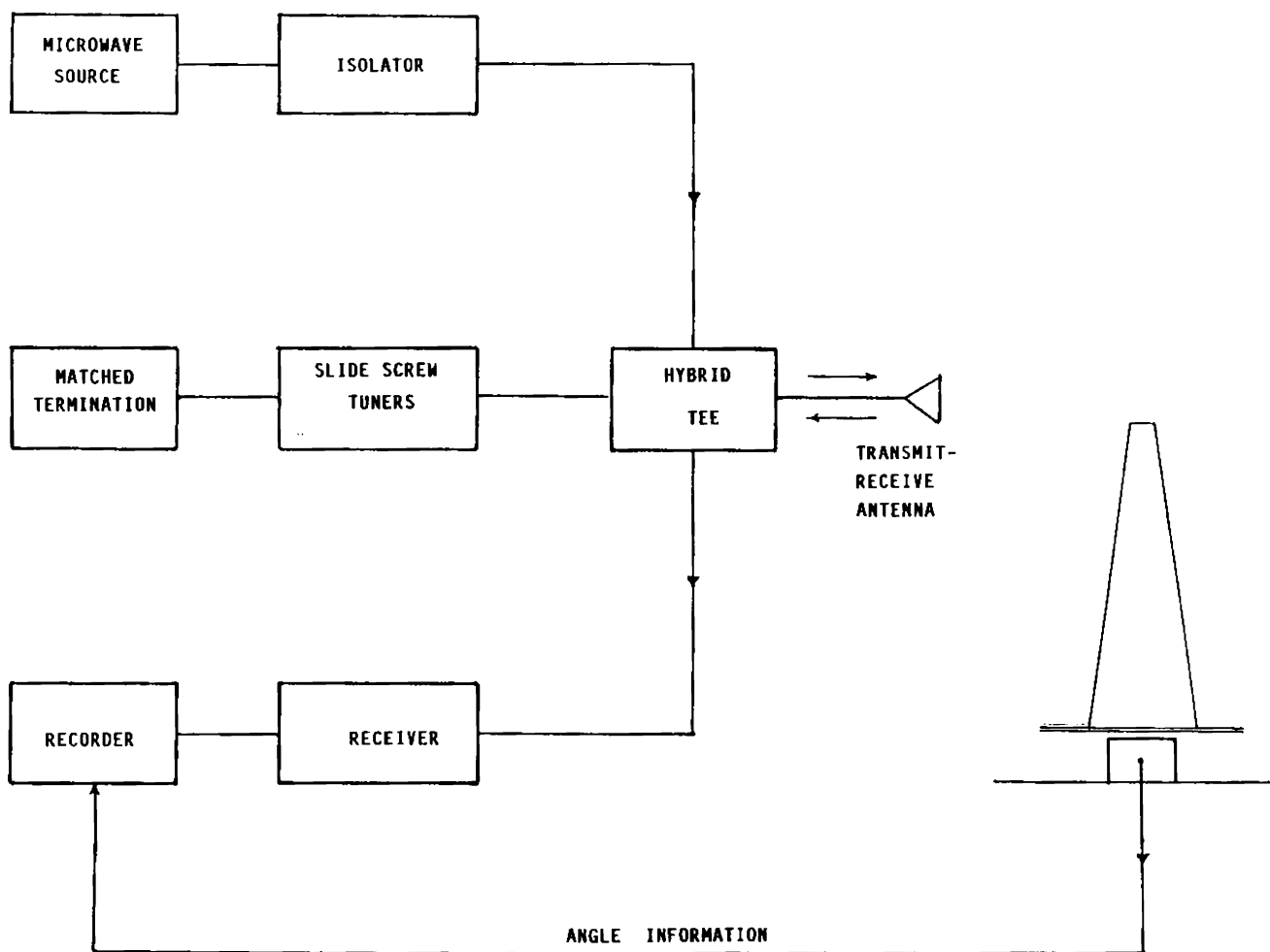
Fig. 3.3 (a). Typical continuous wave(CW) system for RCS measurements
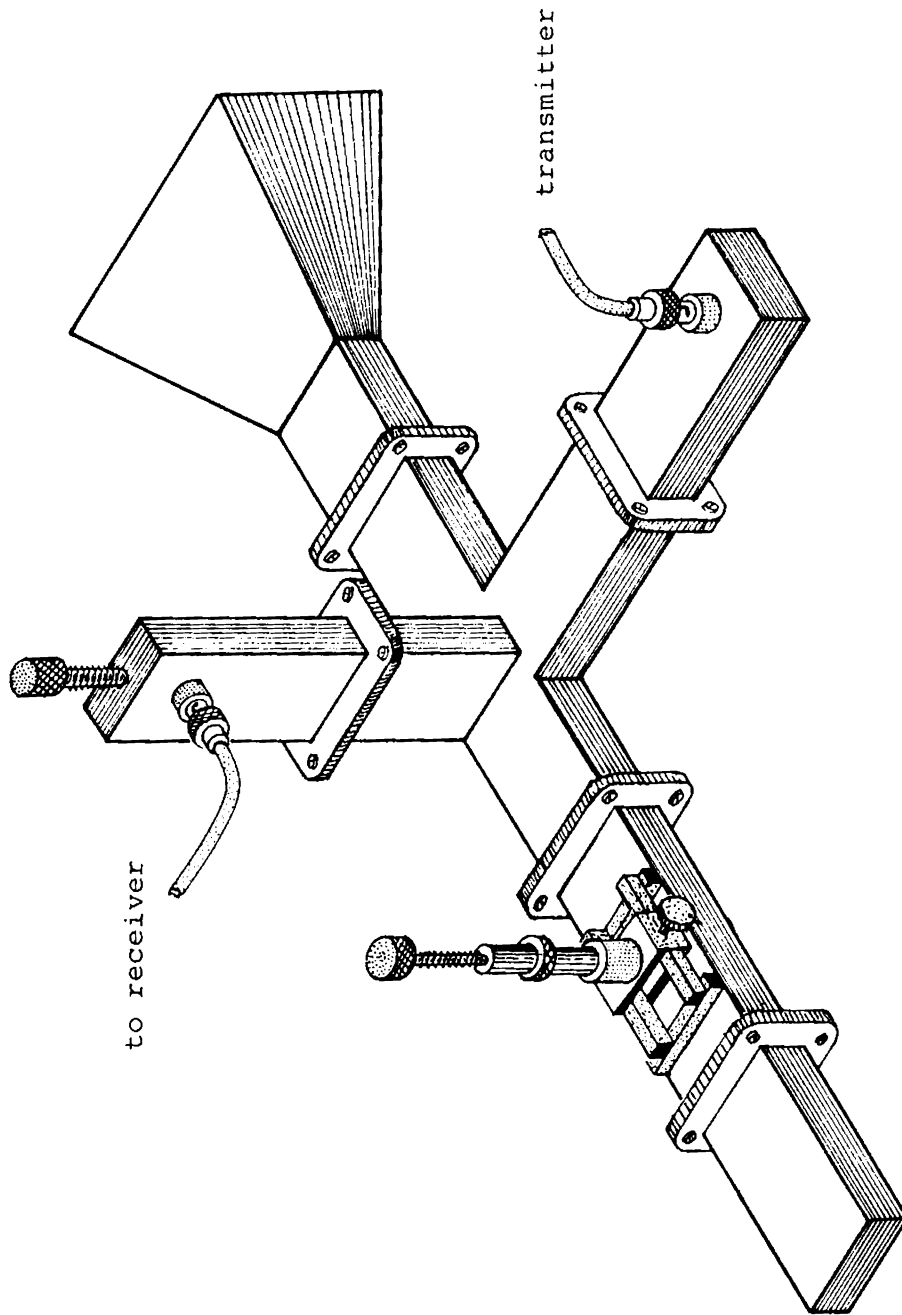
Fig. 3.3 (b) CW Cancellation technique using magic-tee.

3.6 MEASUREMENT PROCEDURE

The measurement procedure starts with the support stand (mount) in place of model. The slide screw tuner is adjusted until there is no detectable signal in the receiver arm of the hybrid-tee. That is, the field reflected from the mount and the background are cancelled. The model is then placed in position, creating an uncancelled signal in the receiver arm. This signal is recorded. The model is then replaced by a standard object, and the uncancelled signal from the standard is measured. In the present case, the standard object is a plane metallic plate of the same size as the strip grating and the reflected power from the strip grating is compared with that from the metallic plate. The strip grating system has a size 30 cm x 30 cm with 10-12 grating elements.

A graphical display of the various power levels in RCS measurement is shown in Fig.3.4.

The strip grating with a metallic reflector behind it is set for an angle of incidence θ_i, using the turn-table. The back-scattered power is measured from the receiver arm of the hybrid tee and the specularly reflected power is

Transmitted power level P_t

Maximum   RCS

Usable dynamic range

Minimum usable RCS level

Accuracy requirement
Background level

Thermal noise (components)

Receiver thermal noise

Relative power levels
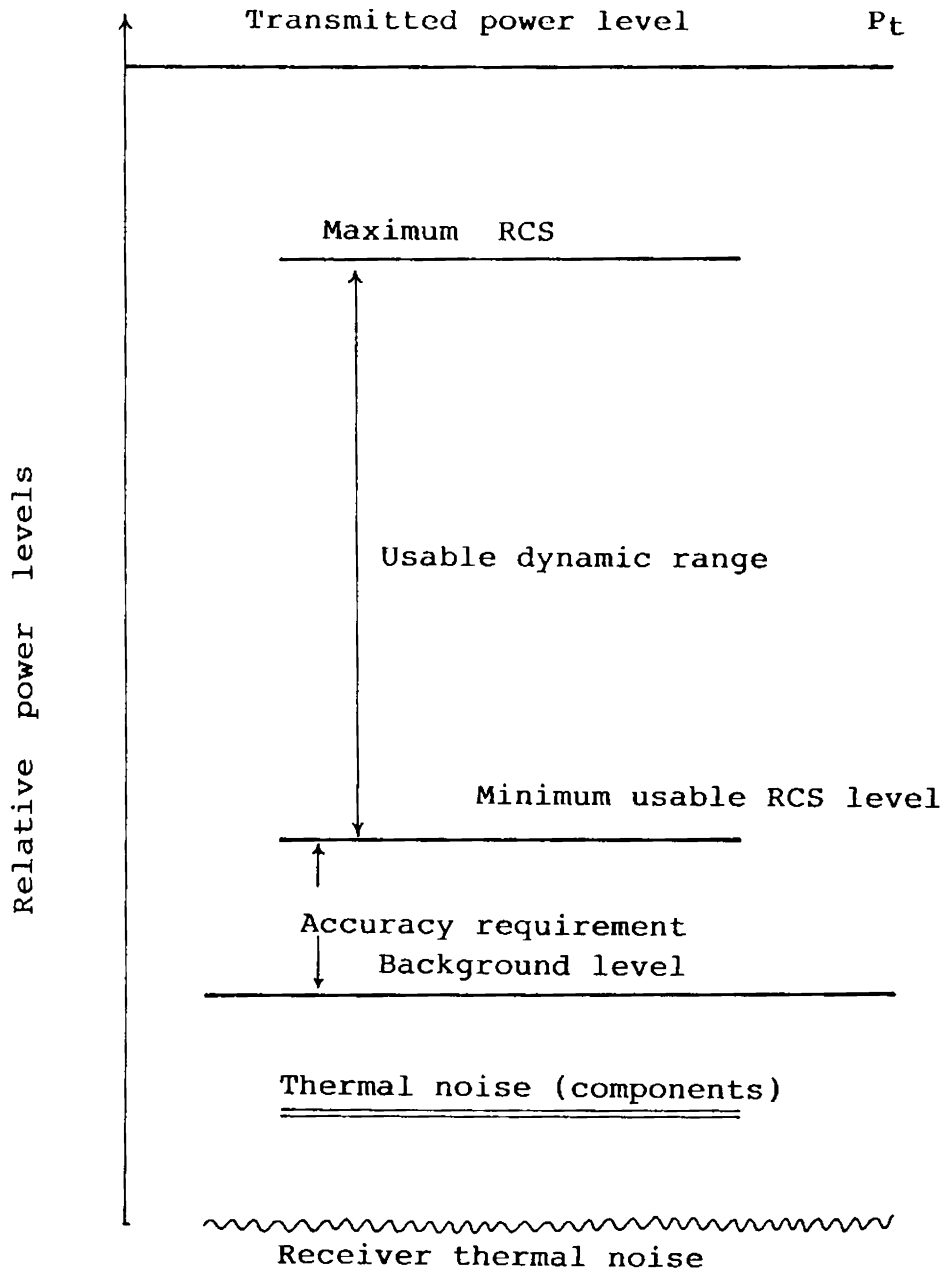
Fig. 3.4 Power levels in RCS measurements

measured by setting the other receiver for an angle of reflection, same as θ_i. Now replacing the strip grating by a plane metallic plate of same size the back-scattered and reflected power is measured. The measurements are repeated for different angles of incidence and the relative power level is plotted.

3.7 FABRICATION OF STRIP GRATING

In most of the recently developed corrugated reflectors for the elimination of specular reflection in airports and Instrument Landing Systems (ILS), the materials used are brass and aluminium. The design parameters are mainly,

1. Shape of corrugation

2. Period, d

3. Width of the grooves, a

4. Corrugation depth, h.

A corrugated surface is a reactive surface, which exhibits pass band and stop band characteristic with respect to the propagation of a surface wave. The pass band - stop band characteristics depend on the depth of the slots and the directions of propagation [72]. Further, the longitudinal

surface-impedance, that is the impedance seen by the wave travelling along the surface, also depends on the depth of corrugations h.

The following rectangular corrugated surfaces are fabricated and studied using aluminium plate of thickness 20 mm and 30 mm and dimensions of 30 cm x 30 cm.

No.	a cm	b cm	h cm	d cm	a/d
P_1	1.71	0.30	1.50	2.01	0.851
P_2	1.70	1.30	1.50	3.00	0.566
P_3	1.70	0.20	0.80	1.90	0.894
P_4	1.70	0.30	0.70	2.00	0.850

Table 3.1

3.8 STRIP GRATING SYSTEM

Thin copper strips of dimension b are fixed on a dielectric sheet of size 30 cm x 30 cm. The dimension of a and b are kept same as that of the corrugated surface as shown in Figs.3.5 and 3.6. The following strip grating systems are fabricated and studied (Table 3.2).

metallic corrugations.

strip grating system.
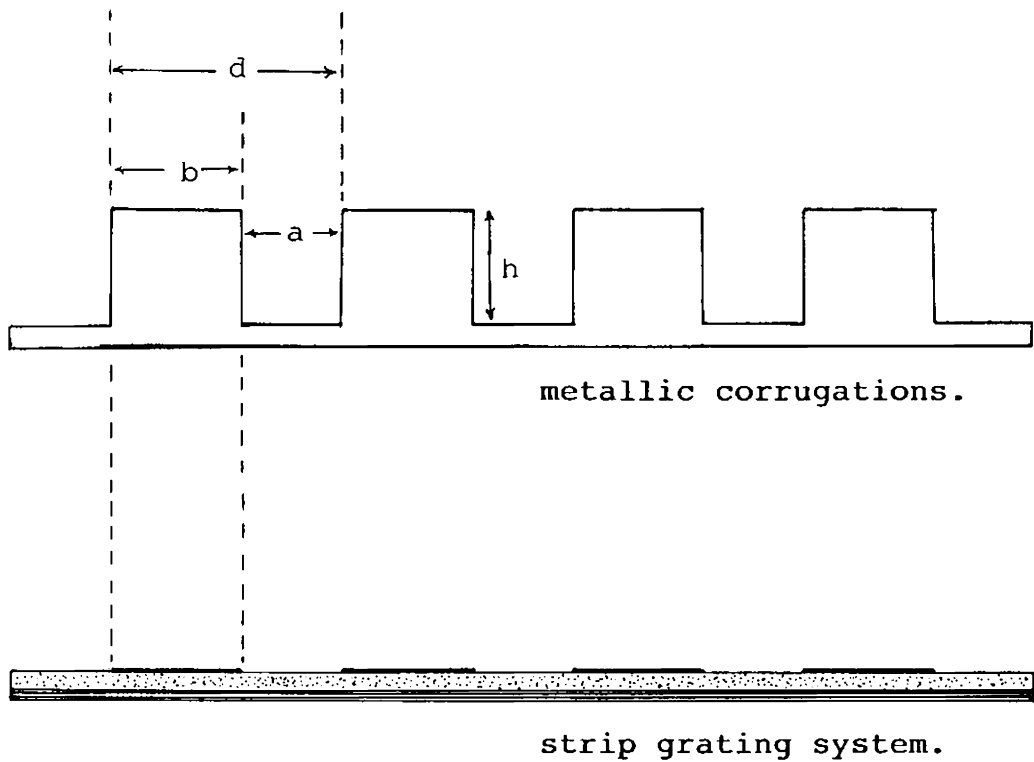
Fig. 3.5 Rectangular metallic corrugated surface and equivalent strip grating system.
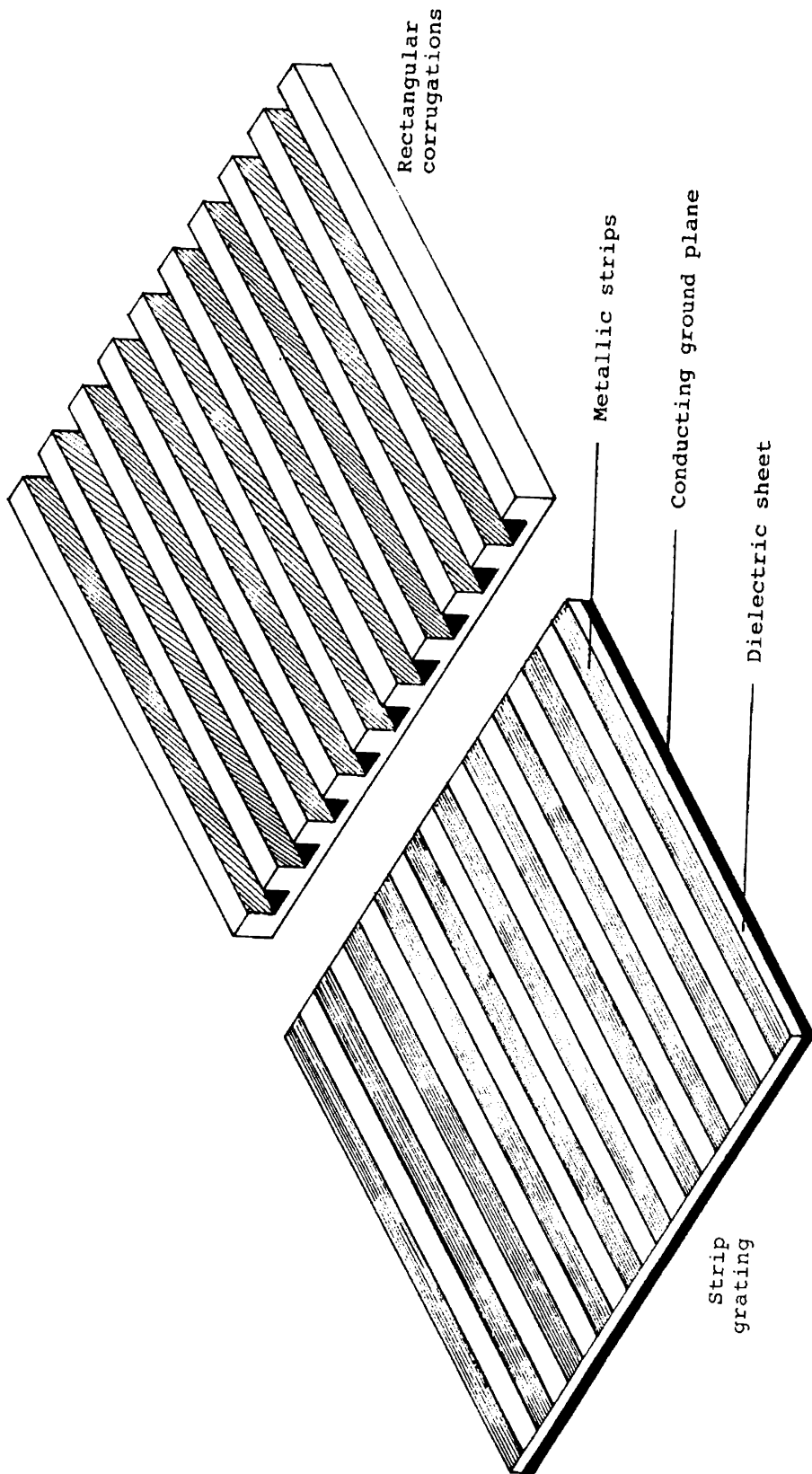
Fig. 3.6 Metallic corrugated surface and equivalent strip grating system.

No.	a cm	b cm	d cm	a/d
s_1	1.6	1.5	3.1	0.516
s_2	0.2	1.8	2.0	0.100
s_3	1.71	0.3	2.01	0.851
s_4	1.3	1.5	2.80	0.464
s_5	1.7	1.3	3.0	0.5666
s_6	3.6	0.2	3.8	0.947
s_7	1.8	0.3	2.1	0.857
s_8	2.4	1.0	3.4	0.705
s_9	1.5	1.5	3.0	0.500
s_{10}	1.4	1.4	2.8	"
s_{11}	1.2	1.2	2.4	"
s_{12}	1.0	1.0	2.0	"
s_{13}	0.8	0.8	1.6	"
s_{14}	1.8	1.8	3.6	"
s_{15}	2.0	2.0	4.0	"

Table 3.2

3.9 TRANSVERSE ELECTRIC (TE) AND TRANSVERSE MAGNETIC (TM) POLARIZATION MEASUREMENTS

The elimination of specular reflection (perfect blazing) for one spectral order can be achieved by either transverse electric (TE) polarization, in which the electric field is parallel to the grooves of a reflection grating or for transverse magnetic (TM) polarization, in which the magnetic field is parallel to the grooves.

The strip grating system is placed on a turn table. The specularly reflected power is measured using the receiver as polarization analyzer. The polarization analyzer is a receiving system in which the receiving pyramidal horn antenna can be rotated about its own axis depending on TE or TM polarization as shown in Fig.3.7. Here, one end of the waveguide which is passing through two bearings, is connected to a pyramidal horn and the other end to a crystal detector with an adjustable short. This mechanism provides an easy rotation of the receiving antenna about a horizontal axis. The whole system is attached to the receiving arm of the arch as shown in Fig.3.2.

3.10 MEASUREMENT AND RECORDING OF BACK-SCATTERED POWER

The strip grating is fixed on a turn-table placed at the centre of the arch. The turn table has a speed of

0.75 rpm. After the preliminary adjustments, the turn-table
is rotated and the back-scattered power is recorded. Instead
of strip grating, the reference target is placed in the same
position and the back-scattered power is recorded without
any change in the measurement system.

3.11   SELF-COMPLEMENTARY STRIP GRATINGS

The elimination of normal incidence reflected power
(back-scattered power) is not possible in the case of rect-
angular metallic corrugated surface. However, using self
complementary strip gratings, it is possible to eliminate the
normal and near normal incidence specular reflection. In
self-complementary strip grating the width of the strip 'b'
is equal to the spacing between the elements 'a'. The grating
period d is chosen such that the Bragg condition is satisfied
for perfect blazing.

The self-complementary strip grating with a metallic
reflector behind it also behaves as metallic corrugations
in eliminating the specular reflection in an angular range
of $19.4° < \theta_i < 90°$. The variation of the grating period 'd'
against the variation of reflected power is studied keeping
the condition a = d/2.
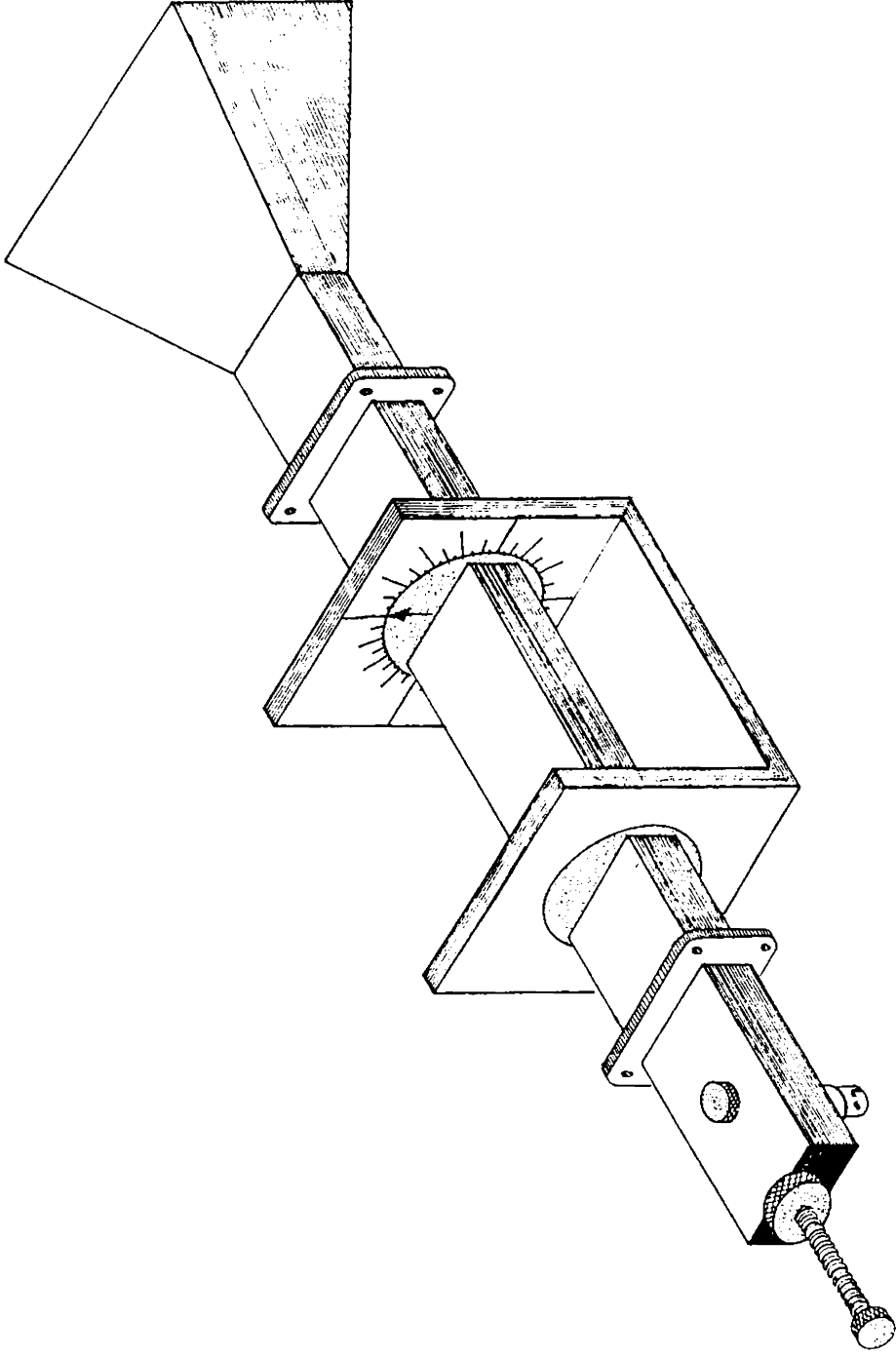
Fig. 3.7 Antenna polarization positioner.
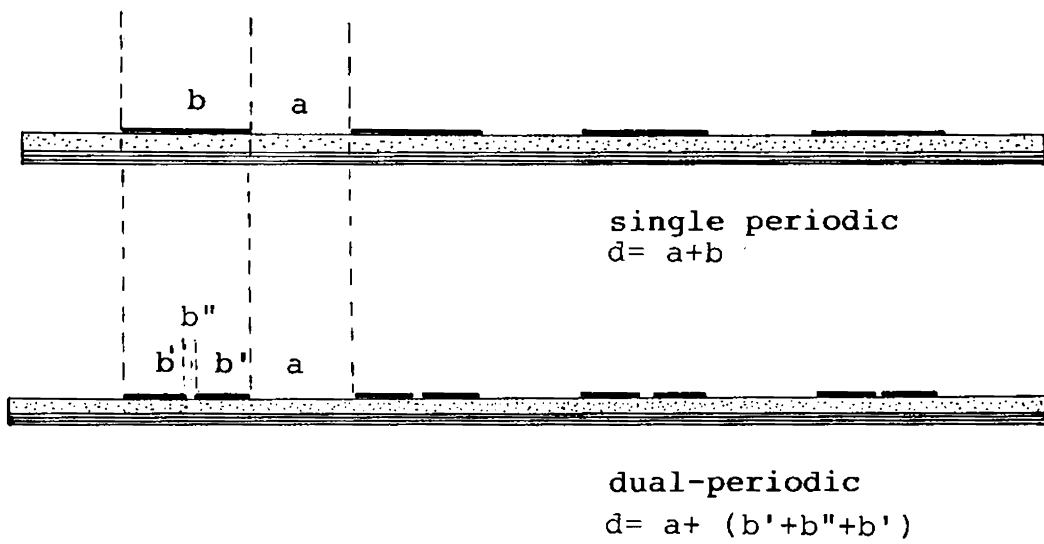
Fig.3.8 Single periodic and dual periodic strip gratings.

The variation of reflected power due to the change in dielectric thickness is also studied by changing the dielectric sheet in between the strip grating and the reflector.

3.12 MULTI ELEMENT STRIP GRATING

The minimum thickness of the dielectric sheet for the elimination of specular reflection can be further reduced by using multi-element strip gratings. The strips of width 'b' are split up such that b = b' + b" + b', keeping the spacing between the strips 'a' as constant as shown in Fig.3.8. The variation of the reflected power due to the variation of the thickness of dielectric sheet, and the variation due to the change in incident angle are studied in detail.

Chapter   4

EXPERIMENTAL   RESULTS

Chapter 4

EXPERIMENTAL RESULTS

4.1 INTRODUCTION

This chapter concentrates on the design and perform-
ance evaluation of different types of strip gratings which
possess the properties of Radar Absorbing Materials (RAM)
to reduce Radar Cross Section (RCS) to a considerable extent.
The main concentration in the performance evaluation is the
reflected RF power. Little attention is given to the actual
calculation of RCS. However, the magnitude of the reflected
power from a target, as such, gives an indication of the magni-
tude of its radar cross section.

As discussed in Chapter I, the practical graded
dielectric RAMs like Salisbury Screens and Jaumann absorbers
have many limitations. These limitations are in bandwidth,
physical thickness, weight, appropriate dielectric and mag-
netic properties and aerodynamical properties. In most cases,
the unwanted reflections can be greatly reduced by coating
or covering the reflecting surfaces with suitable absorbing
materials. The strip grating technique described in this
thesis can be used for the same purpose, with great advantages.

86

To reduce the reflections from flat metallic surfaces, in the present work, a technique has been developed using perfectly blazed strip gratings on a dielectric sheet. This technique is more successful and useful in eliminating the specular reflections from conducting surfaces for normal incidence and near normal incidence, than coating by RAM's.

A flat metallic plate is taken as RCS standard target and the performance of the corrugated metallic plate and strip grating is compared with that of the plane metallic plate. The following observations were carried out on strip grating system.

1. Comparison of the performance of reflector-backed strip gratings and the metallic corrugated plate.

2. The effect of variation of frequency.

3. The effect of variation of the thickness of dielectric medium ('h').

4. Elimination of normal incidence and near-normal incidence specular reflections.

5. Variation of back-scattered power against the variation of dielectric thickness h for normal incidence, self-complementary strip grating.

6. The effect of multi-elements (dual periodic) on specular reflection.

The variations of the back-scattered (n = -1) and reflected (n = 0) power for all these grating systems are studied for different incident angle and are summarised below.

4.2 COMPARISON OF THE BEHAVIOUR OF STRIP GRATINGS AND CORRUGATED METALLIC PLATES

Multipath interference from terminal buildings and control towers is a serious problem in Instrument Landing Systems (ILS). This type of interference is also occurring in urban TV reception. The incident microwave signal from a transmitting radar is reflected to different directions and is constantly received as an interference in receiving system. A suitable method to eliminate this interference is to dress up the building with absorbing materials. These absorbing materials are essentially a long matching network between the free space and the reflecting surfaces.

Several methods may be used to perform this translation. As discussed in Chapter I, the earliest technique, and the one still in use, is deflecting or scattering the incident energy into different directions. In this simple

technique, infinitely long wire screens or 'radar fences' which will appear as an inductive or capacitive admittance, depending on the polarisation of the incident waves, are used. Because of optimisation requirement, these screens should be wide enough to block all reflections. The impedance associated with a wire grid is that of a series RL circuit. The wire radius, spacing, and conductivity can be adjusted to provide specific impedance behaviour as a function of frequency.

Specular reflections from a conducting surface can be eliminated by corrugations of proper period and depth [7]. These corrugations can be of any shape like saw tooth, rectangular, or fin corrugations. These periodically spaced scatterer act as a grating and corrugations of period between one-half and one wavelength in a conducting surface will scatter only two spectral orders, specular reflection and diffraction in the direction of incidence or back-scatter [80]. When the period satisfies the Bragg condition required for perfect blazing, the specular reflection (n = 0 mode) is completely cancelled and the corrugated surface becomes a 100% back-scatterer (n = -1 mode). If the period is chosen for constructive interference in the direction of incidence, the specular reflection is minimised and can be eliminated

by proper choice of corrugation depth. Then it becomes a 'non-reflecting' conducting surface.

However, the fabrication of such metallic corrugations is a time-consuming and difficult task. Thin conducting strips on a dielectric sheet with a metallic reflector behind it, behaves like a corrugated structure, which produces equivalent effects of perfectly blazed rectangular grooves. It is important to note that this reflector-backed strip grating configuration avoids the laborious task of fabricating corrugations on metallic surfaces.

When a plane wave incident at an angle θ_i from the normal to a conducting periodic surface, scattering occurs at discrete angles θ_n determined from the condition for constructive interference from adjacent cells. (Fig. 4.1)

$$\sin \theta_n = \sin \theta_i + n \ \lambda/d; \ n = 0, \ \pm 1, \ \pm 2 \ldots \tag{1}$$

The condition for constructive interference in the direction of incidence is

$$kd \sin \theta_i = m\pi, \quad m = 1, 2 \ldots$$

where $k = 2\pi/\lambda$ is the free-space propagation constant and λ is the wavelength.
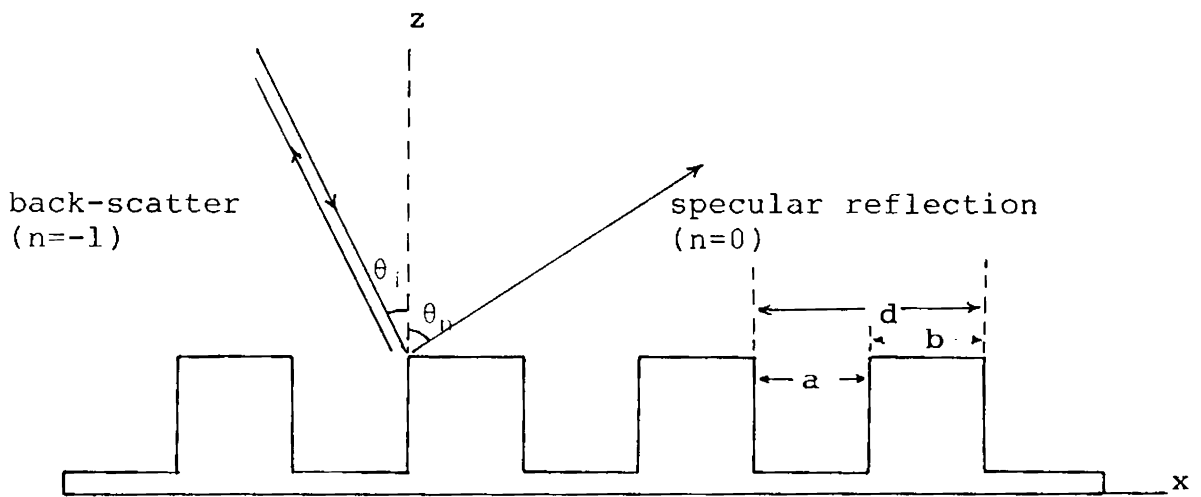
Fig. 4.1 Co-ordinates for scattering by rectangular
metallic corrugations.

When m = 1,

$$\sin \theta_i = \lambda /2d \tag{2}$$

which is often called the Bragg-condition. Combining equations (1) and (2)

$$\sin \theta_n = (n + 1/2) \lambda/d; \quad n = 0, \pm 1 ... \tag{3}$$

When period d is between $\lambda/2$ and $3\lambda/2$, the above equation provides real solutions for the specular reflection (n = 0) and back-scatterer (n = -1) $\theta_o = \theta_i$ and $\theta_{-1} = -\theta_i$. Consequently, for minimum specular reflection and maximum back-scattering, the grating period d is

$$d = \lambda /(2 \sin \theta_i) \tag{4}$$

form eqn.(3) in the angular range of $19.47° < \theta_i < 90°$.

The specularly reflected power from a reflector backed strip grating S_5 is measured for different angles of incidence, θ_i and the results are shown in Fig.4.2. Thin conducting strips of width 'b' were fixed with a separation a = 0.566d on a dielectric sheet of thickness h = 0.171λ . This profile with a plane conducting plate behind it behaves

Reflected power vs angle of Incldene

Angle of incidence,
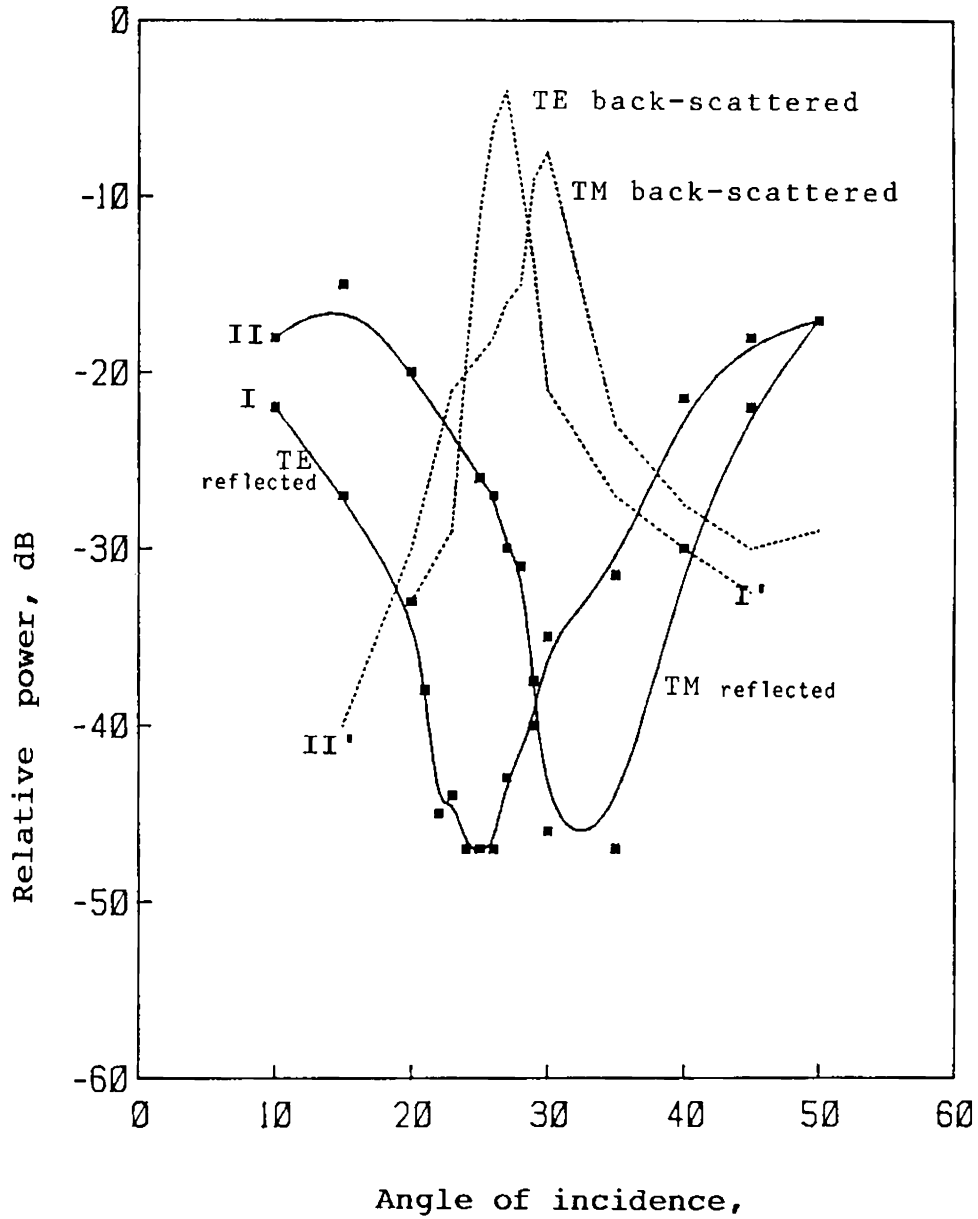
Fig. 4.2. Measured TE and TM reflected and
back-scattered power for strip grating S_5
d = 30.mm, a = 0.566 d

for I & I' , f=10.84 GHz, h=0.171λ

for II & II', f=9.84 GHz , h=0.120λ

similar to a corrugated metallic plate of same 'a' and 'd'. The specularly reflected power is minimum corresponding to maximum back-scattering is obtained when the incident angle θ_i satisfies Bragg condition. This important condition is termed as "perfect blazing".

Fig.4.3 shows the experimental results obtained for a corrugated metallic plate P_2 with a/d = 0.566; h = 1.50 cm (0.516 λ). The blazing properties are measured for both TE and TM polarisations.

The observations are repeated for gratings and corrugated plates of different period and a/d. Fig.4.4 shows the experimental results of a strip grating S_3 with dimensions a/d = 0.851 and dielectric thickness h = 0.177 λ with period d = 0.724 λ . TE – polarised reflected power is completely eliminated at an angle of incidence θ_i = 43.5°.

Fig.4.5 shows the reflected and back-scattered power for corrugated metallic plate P_1 of dimensions a/d = 0.851, corrugation depth h = 0.551λ, d = 0.724λ.

4.3 THE EFFECT OF VARIATION OF FREQUENCY

Fig.4.6 shows the frequency behaviour of the strip grating S_5 for TE and TM polarisations. Keeping the grating

Reflected power vs angle of incidence
Metallic corrugatios
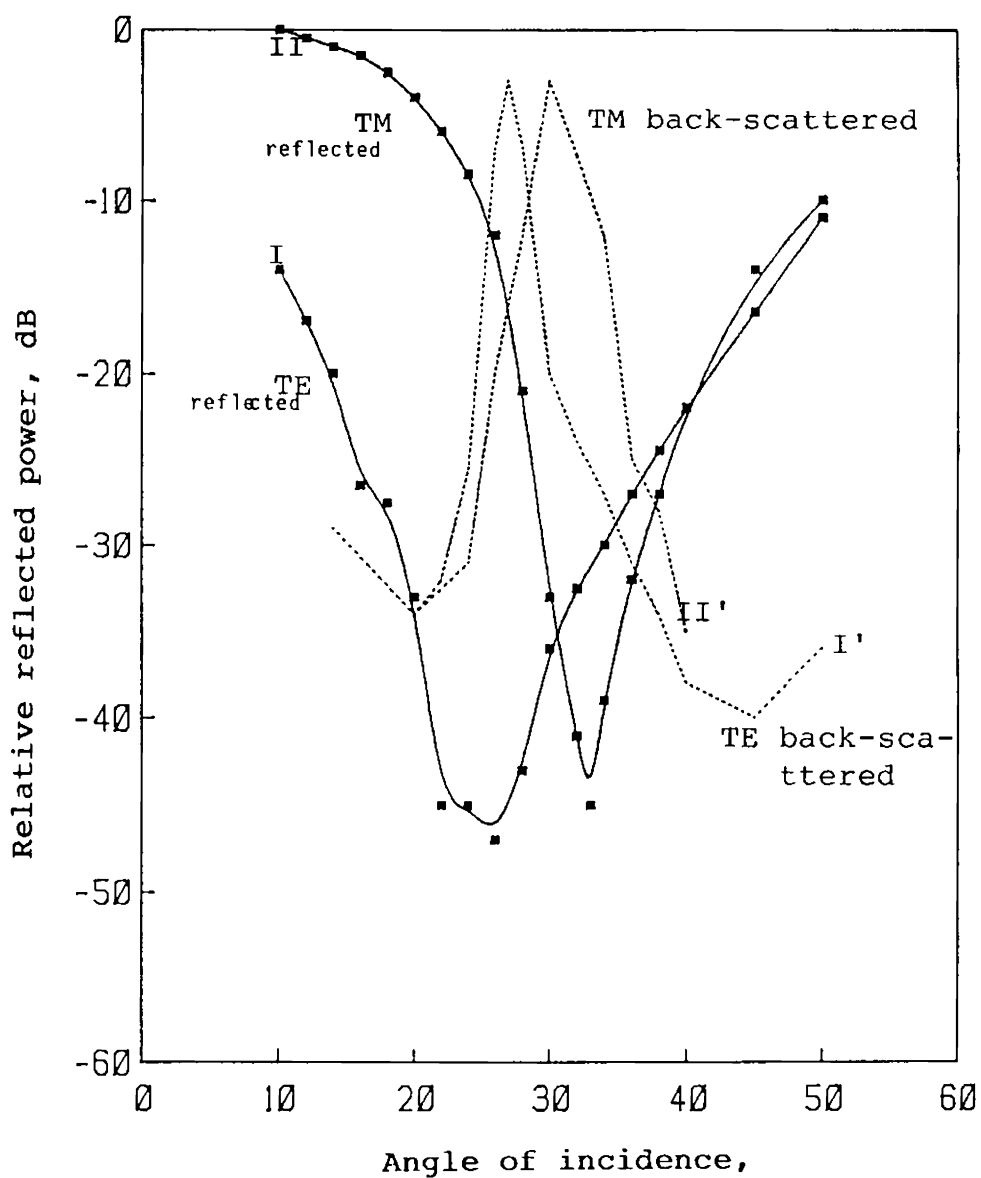
Fig.4.3 Measured   TE   and   TM   polarised
reflected and back-scattered power
for metallic corrugations,P_2

d=30mm, a=0.566 d, h=0.516λ

for I & I' f = 10.92 GHz
for II & II' f = 9.750 GHz

Reflected power vs angle of Incidence
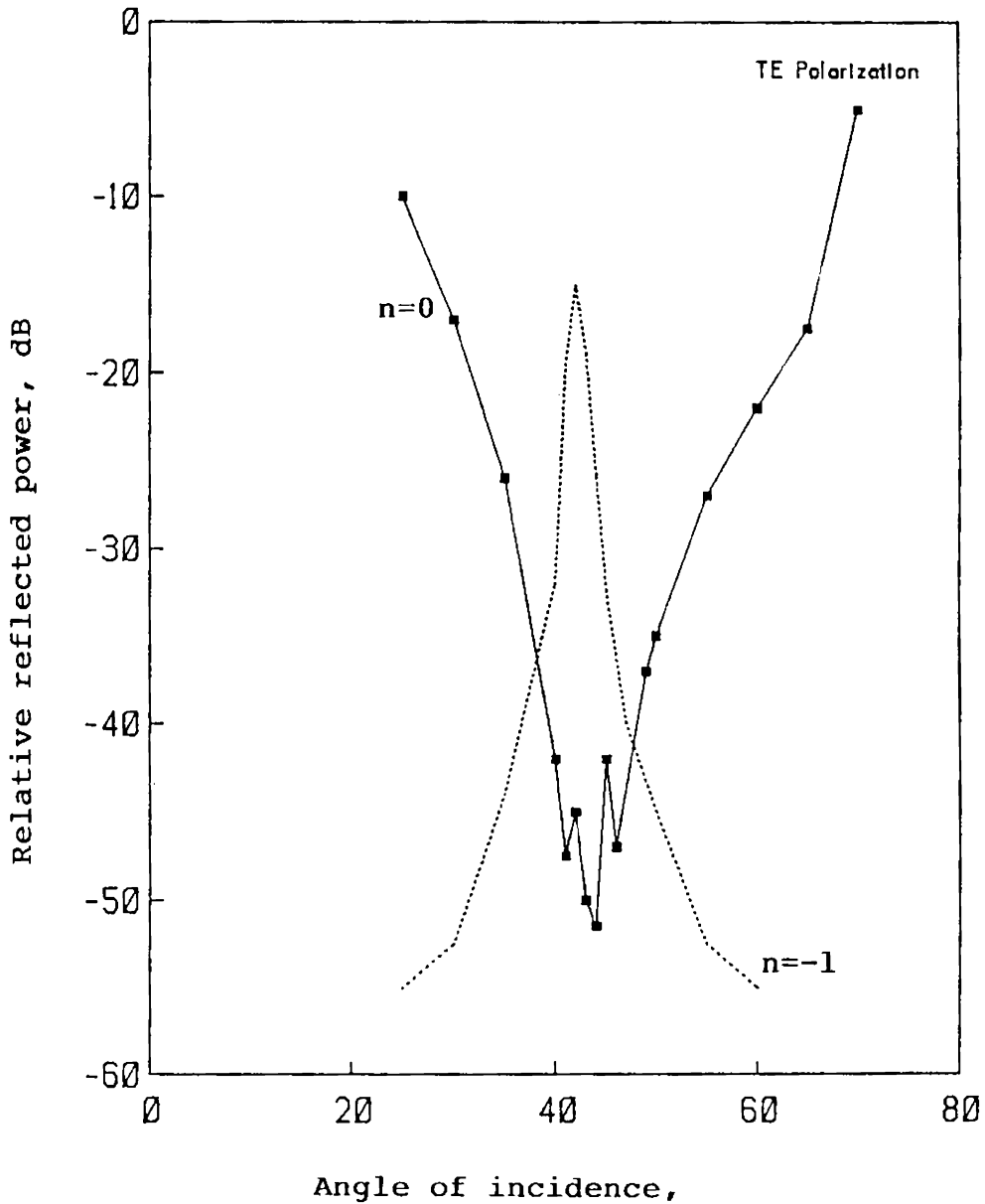
Fig. 4.4 Variation of reflected and back-
scattered power against incident
angle for strip grating S_3

a=0.851d, h=0.177 λ, f=10.651 GHz

————————— reflected power

·········· back-scattered power

Reflected power vs angle of incidence
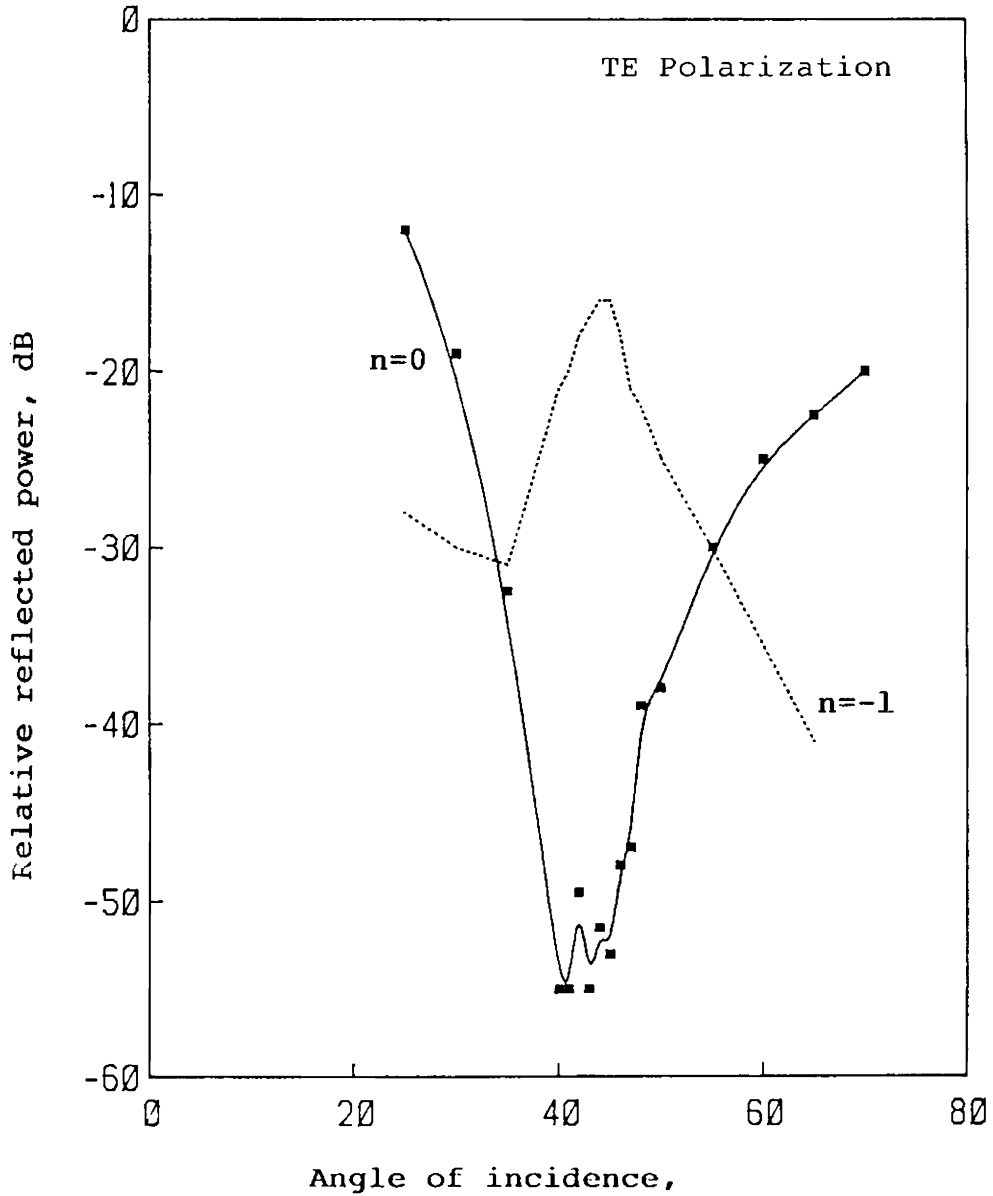
Fig. 4.5 Variation of reflected and back-scattered power against the incident angle for corrugated metallic plate, P_1

a=0.851 d, h=0.551 λ , f=10.345 GHz

———————— reflected power

.........back-scattered power

system for a fixed incident angle, the reflected as well as back-scattered power is measured for different frequencies. The angle of incidence θ_i is chosen from the Bragg condition, given by eqn.(2).

The frequency response of the corrugated metallic plate P_2 of same dimensions is taken and is shown in Fig.4.7. The bandwidth of effective elimination of specular reflection is considerably increased in the case of a strip grating system.

Fig.4.8 shows the frequency behaviour of the strip grating S_3 of dimensions a/d = 0.851, h = 0.177 λ, d = 2.01 cm.

Fig.4.9 shows the frequency behaviour of corrugated metallic plate P_1 with dimensions same as S_3.

4.4 VARIATION OF REFLECTED POWER DUE TO THE VARIATION OF DIELECTRIC THICKNESS 'h'

Metallic reflection gratings with rectangular grooves show perfectly blazing properties when the depth of corrugation satisfies the minimum condition h $\geq$ λ /4 for all θ_i, the incidence angle, which corresponds to an infinite reactance across the slot of the surface [84]. The current

T

G 21.395-969
109

Reflected power vs frequency
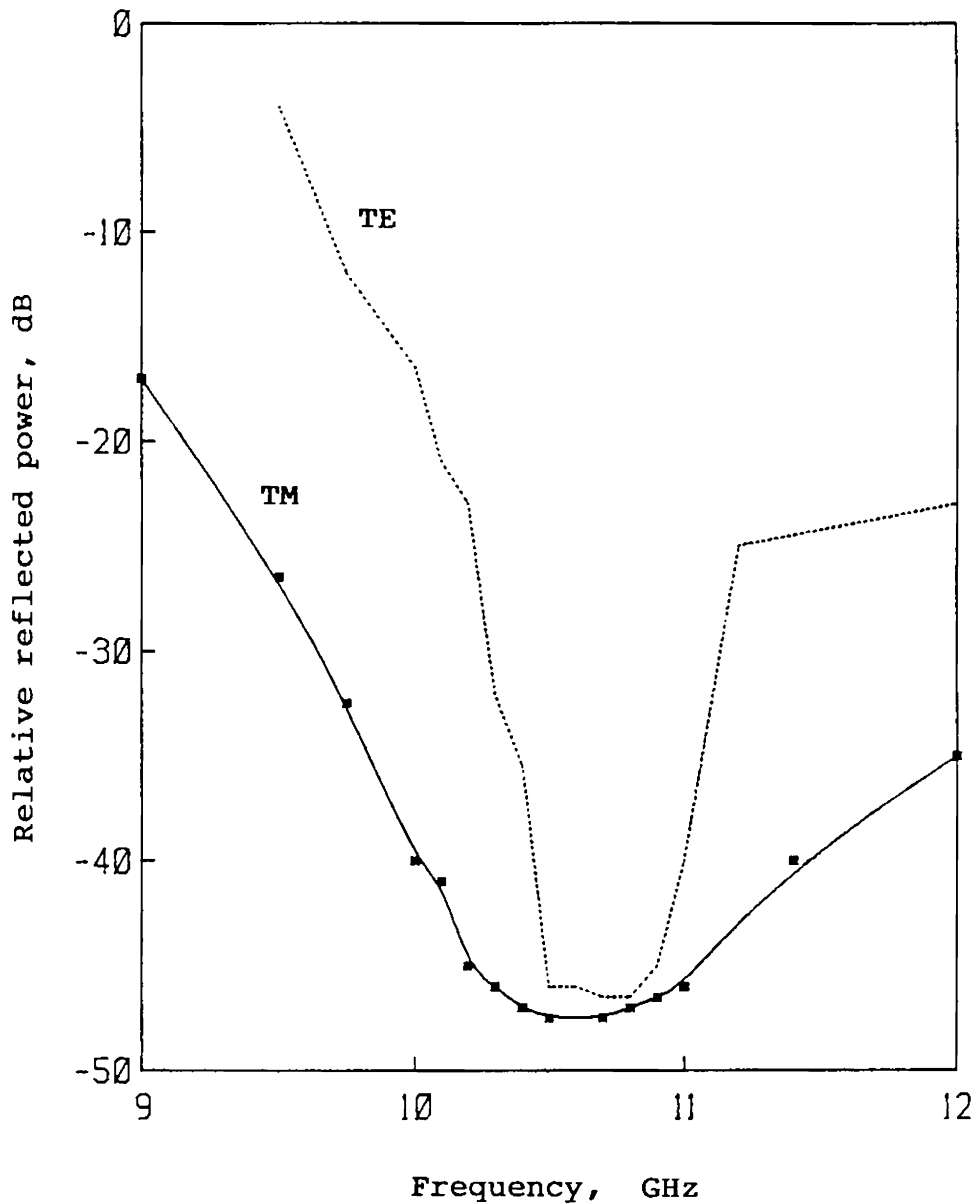
Fig. 4.6 Variation of reflected power with
frequency for strip grating S₅

d= 30mm; a = 0.566 d

............TE polarization, h=0.171 λ
———————— TM polarization, h=0.120 λ

Frequency vs reflected power
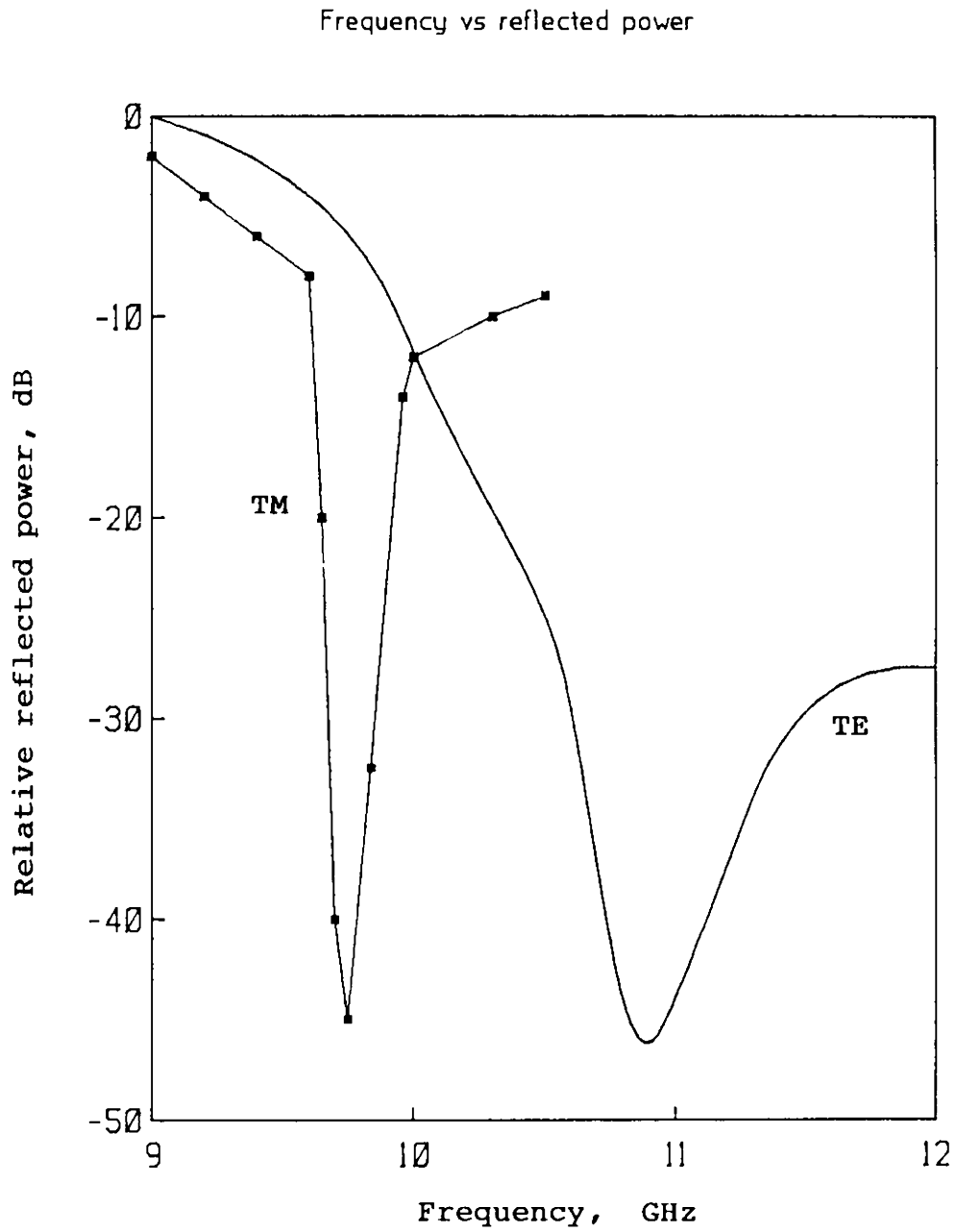
Fig. 4.7 Variation of reflected power against
frequency for metallic corrugated plate P_2

d= 30.0mm, a=0.566 d, h=0.516 λ

Frequency vs Reflected power
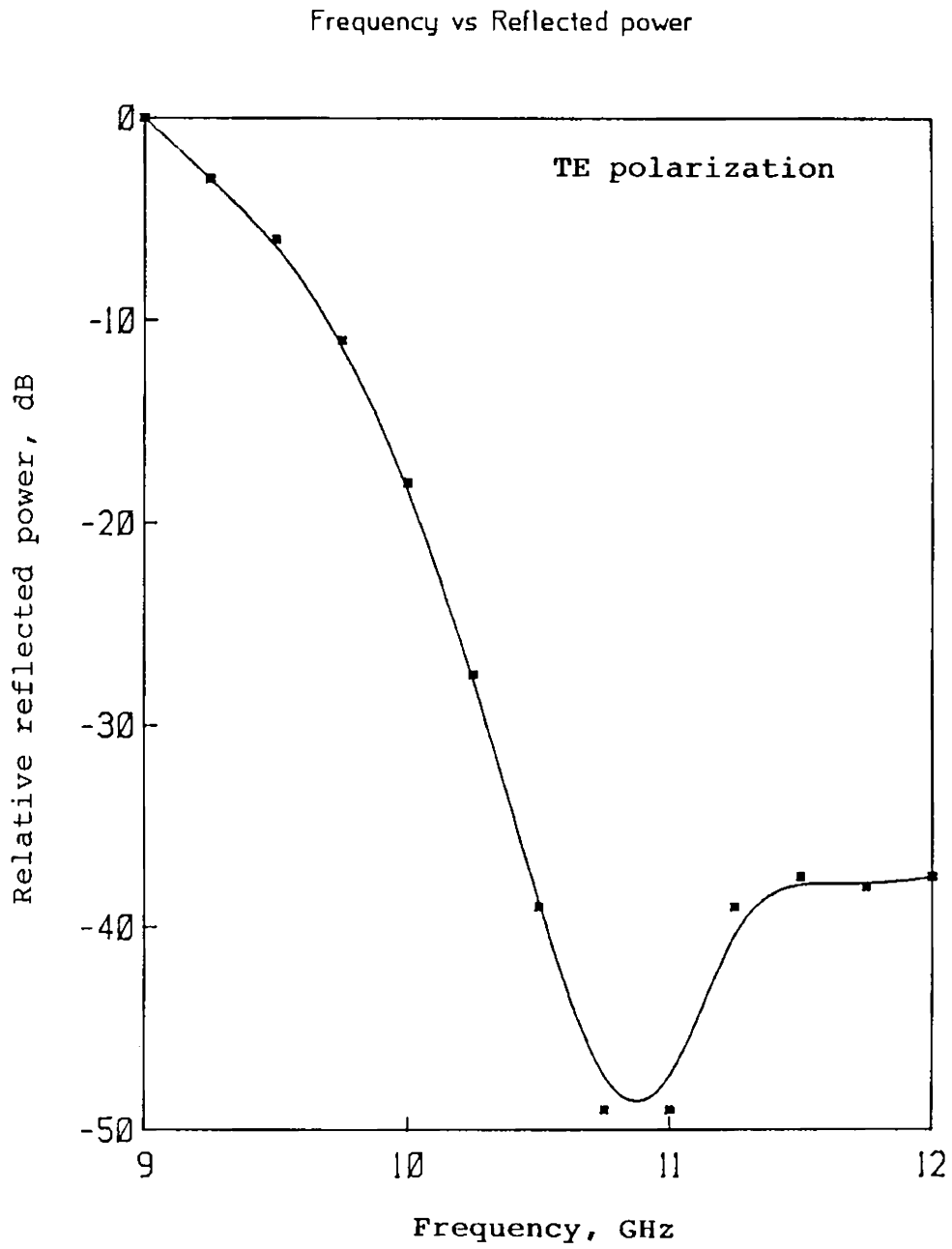
Fig. 4.8 Variation of reflected power against frequency for strip grating S_3

a=0.851d, h=0.177 λ

Frequency vs reflected power
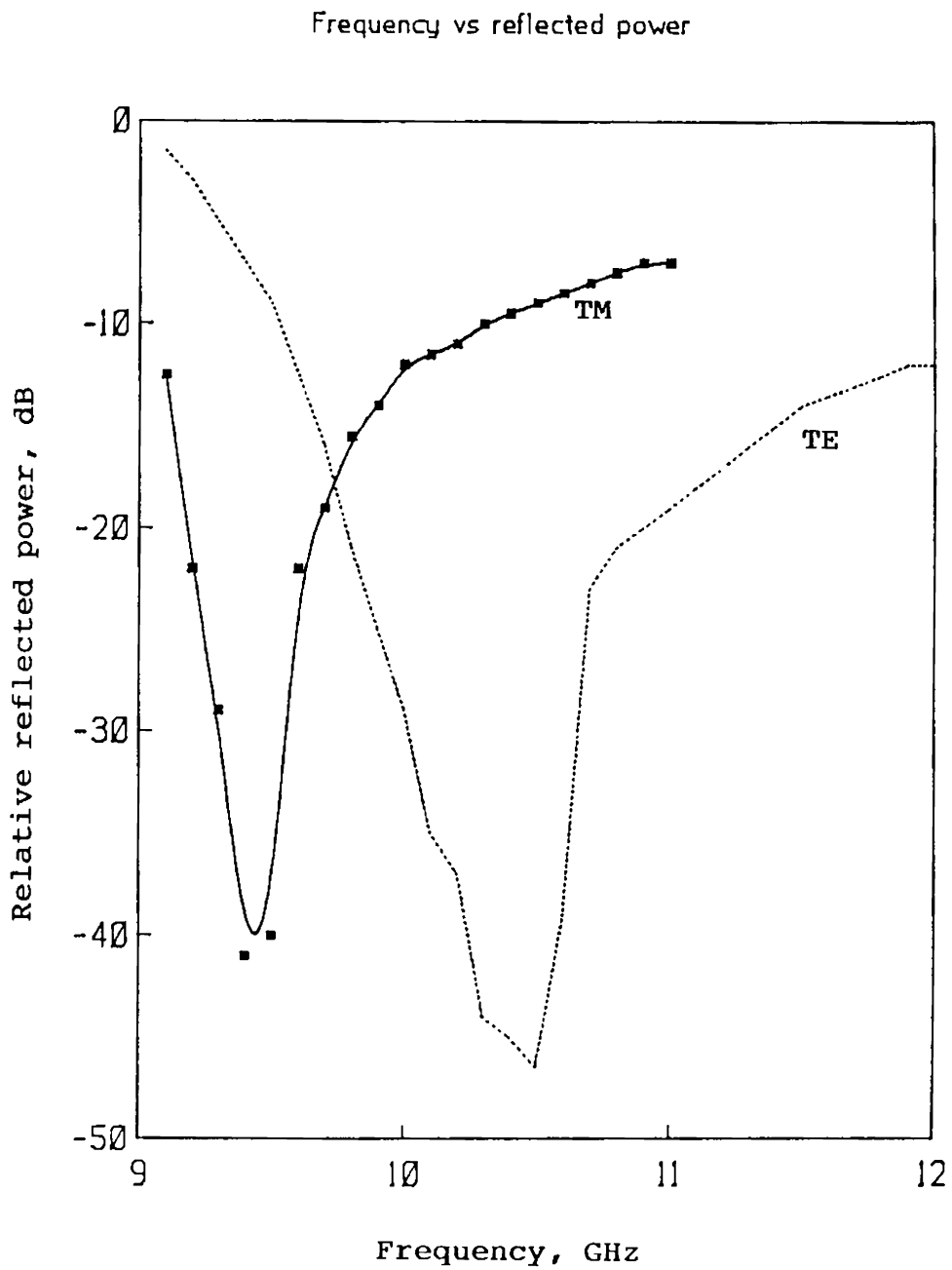
Frequency, GHz

Fig. 4.9 Variation of reflected power against frequency for corrugated metallic plate P_1 ; a=0.851d

excited on the grating surface is entirely x-directed and hence it is not possible to enter the slots. The theoretical variation of the corrugation depth h for TM polarised reflected power for large aspect ratios [84] is shown in Fig.4.10(a) and for small aspect ratios in Fig.4.10(b).

Reflector-backed strip grating, which shows similar behaviour of a corrugated metallic plate, exhibits drastic reduction in necessary condition of corrugation depth. The perfect blazing is possible for a dielectric plate of thickness h = 0.118 λ for TM polarisation as shown in Fig.4.11. Fig.4.11(a) is the observations taken for strip grating S_5 with dimensions a/d = 0.566. Fig.4.11(b) shows the variation of reflected power against the variation of the thickness of dielectric sheet for strip grating S_3, a/d = 0.851. The complete elimination of TE polarised reflected power is obtained for h = 0.178λ at a frequency f = 10.651 GHz.

In the case of strip grating S_5 the perfect blazing for TE polarisation is possible for dielectric thickness of 0.171λ and 0.460 λ .

4.5 ELIMINATION OF NORMAL INCIDENCE AND NEAR-NORMAL INCIDENCE SPECULAR REFLECTION

From equation (4), it is apparent that for a corrugated metallic surface, n = -1, -2 and all higher spectral
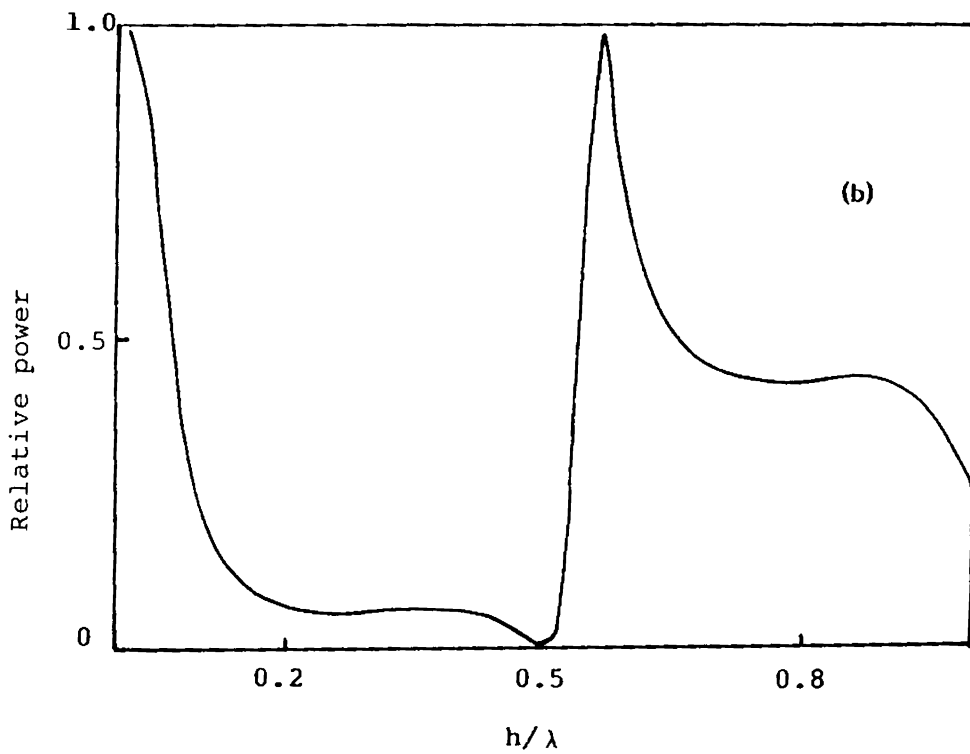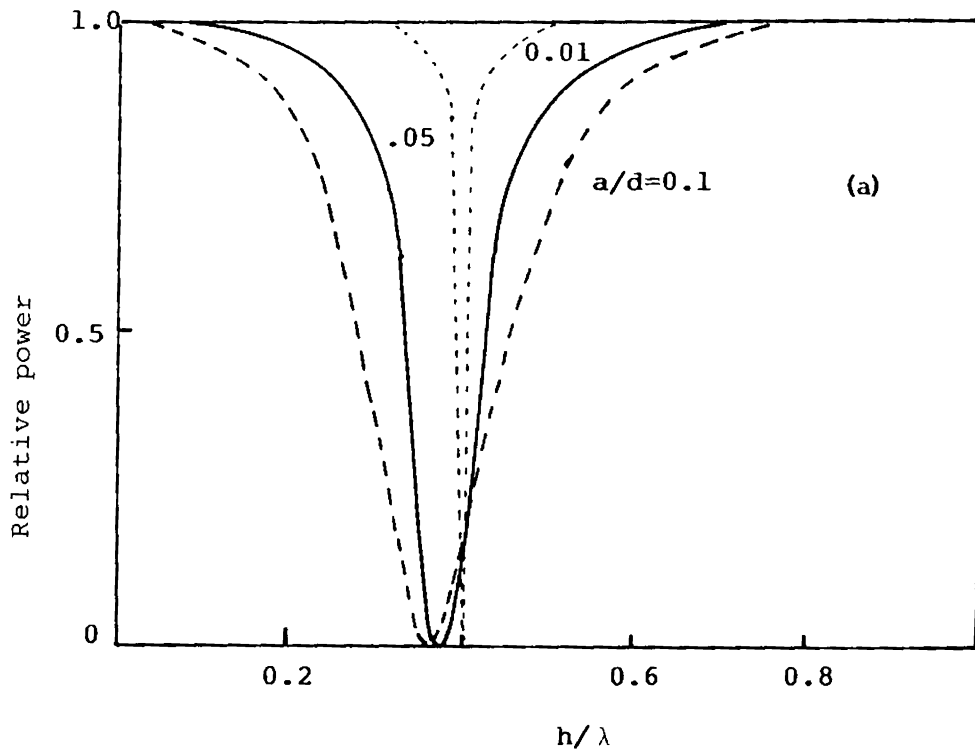
Fig. 4.10 Variation of reflected power against
corrugation depth [ref.84]

(a) for small aspect ratios
(b) for large aspect ratios
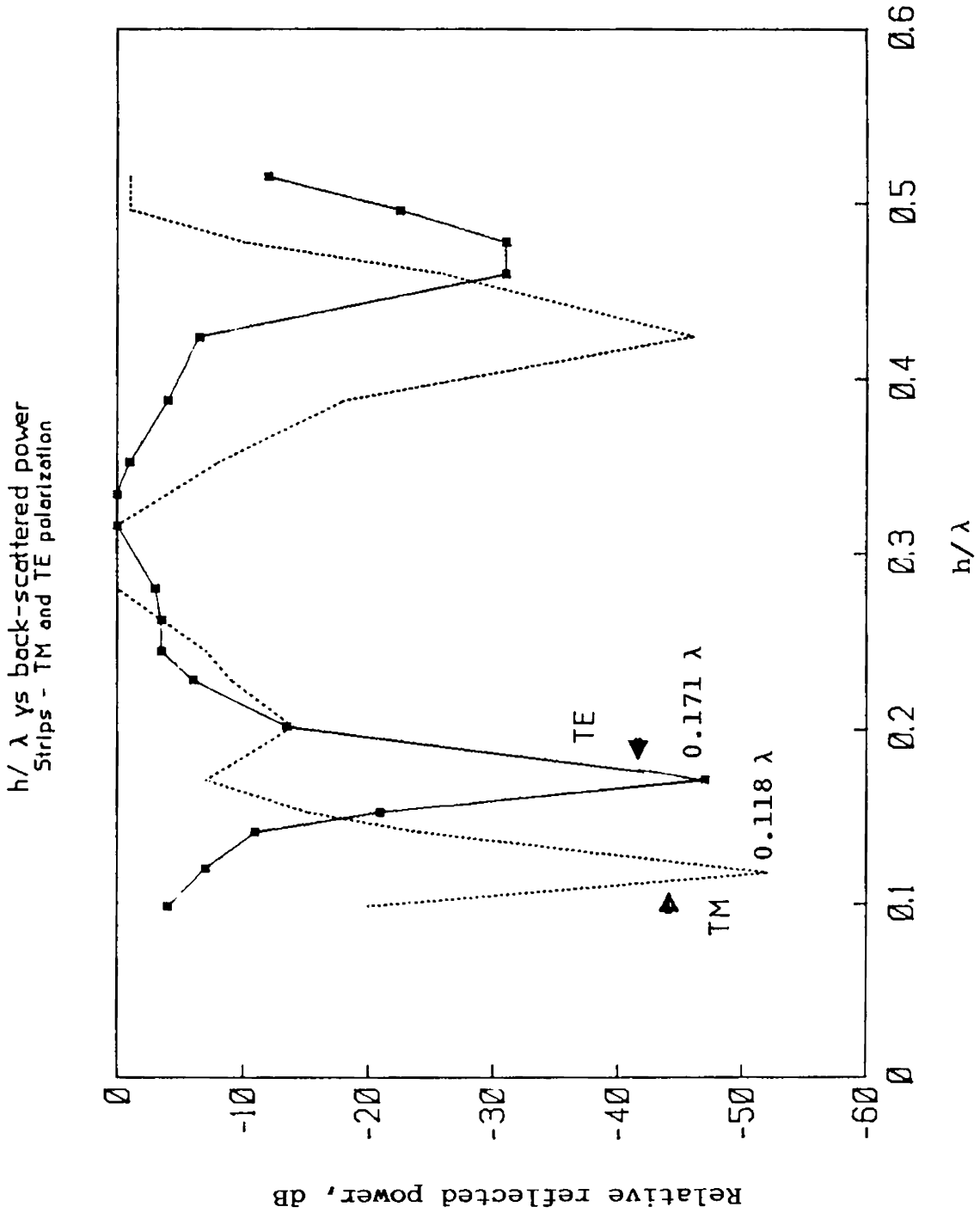
Fig. 4.11 (a) Measured TE and TM polarized reflected power against the variation of the thickness of dielectric sheet for strip grating S_5 ; f=10.90 GHz.

h/λ vs back-scattered power strips-TE polarization

0.178 λ

Relative reflected power, dB

h/λ
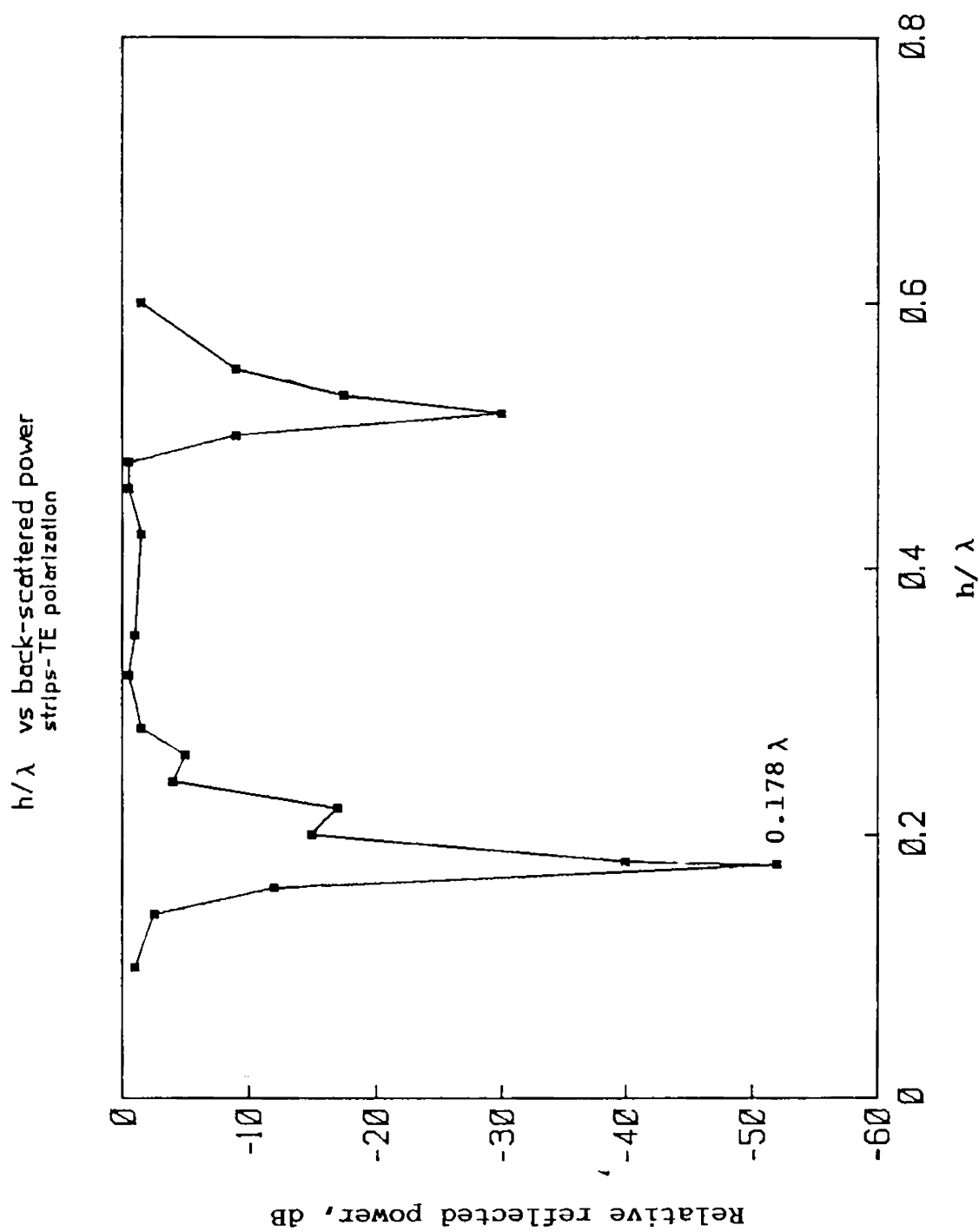
Fig. 4.11 (b) Measured TE polarized reflected power against variation of the thickness of dielectric sheet for strip grating S_3 ; f=10.651 GHz

orders will not appear for real angles θ_n if $d > \lambda/2$ and $\theta_i > \sin^{-1}(1/3) = 19.47°$. Consequently, for minimum specular reflection and maximum back-scattering, the period $d = \lambda/(2 \sin \theta_i)$ is in the angular range of $19.47° < \theta_i < 90°$. It is not possible to get minimum specular reflection for an angle less than $19.47°$ in metallic corrugations.

The normal and near normal incidence specular reflection can be completely eliminated by self-complementary strip grating with $a/d = 0.50$. Fig.4.12 shows the variation of the back-scattered power against the period for normal incidence. The reflected power is minimum when grating period $d = \lambda$ and this shows excellent agreement with the reflection coefficients obtained by Richmond [127]. He has developed theory of scattering for a single strip and then for a strip grating with the basic functions including edge mode, which improves the convergence of the moment-method solution with entire time domain expansion functions. Fig.4.13 illustrates the reflection coefficient versus spacing for a strip grating with normal incidence using Richmond's theory.

Another peculiarity of the reflector-backed strip grating system is the elimination of near-normal incidence specular reflection, which is not possible in corrugated metallic plate. Fig.4.14 shows the observations of strip
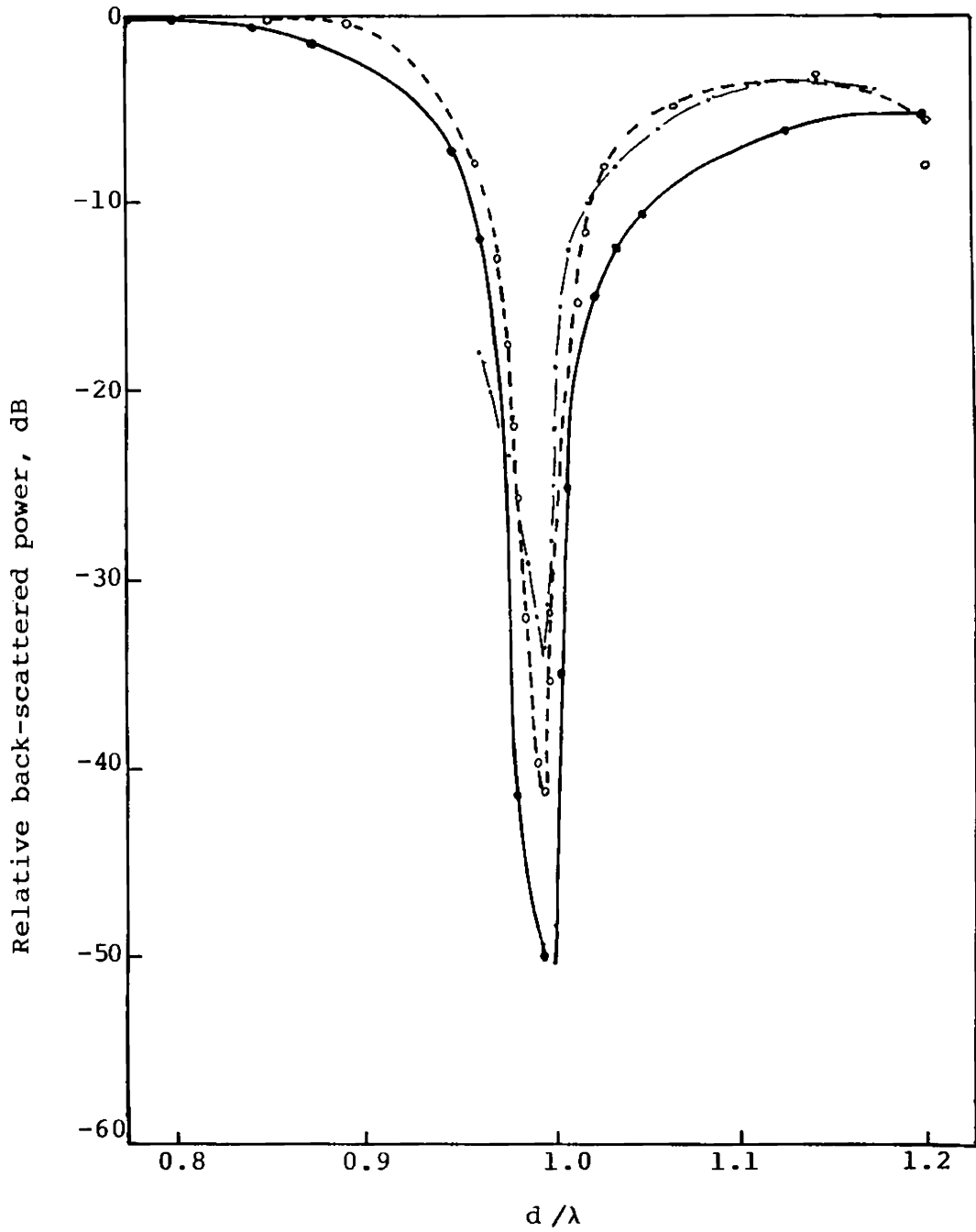
Fig. 4.12. Measured back-scattered power against normalized
grating period, TM polarization, normal incidence

```
————————————  Strip grating S_9  , d = 3.0cm
—·——————··—  Strip grating S_10, d = 2.8cm
·— · —··—  Strip grating S_14, d = 3.6 cm
```
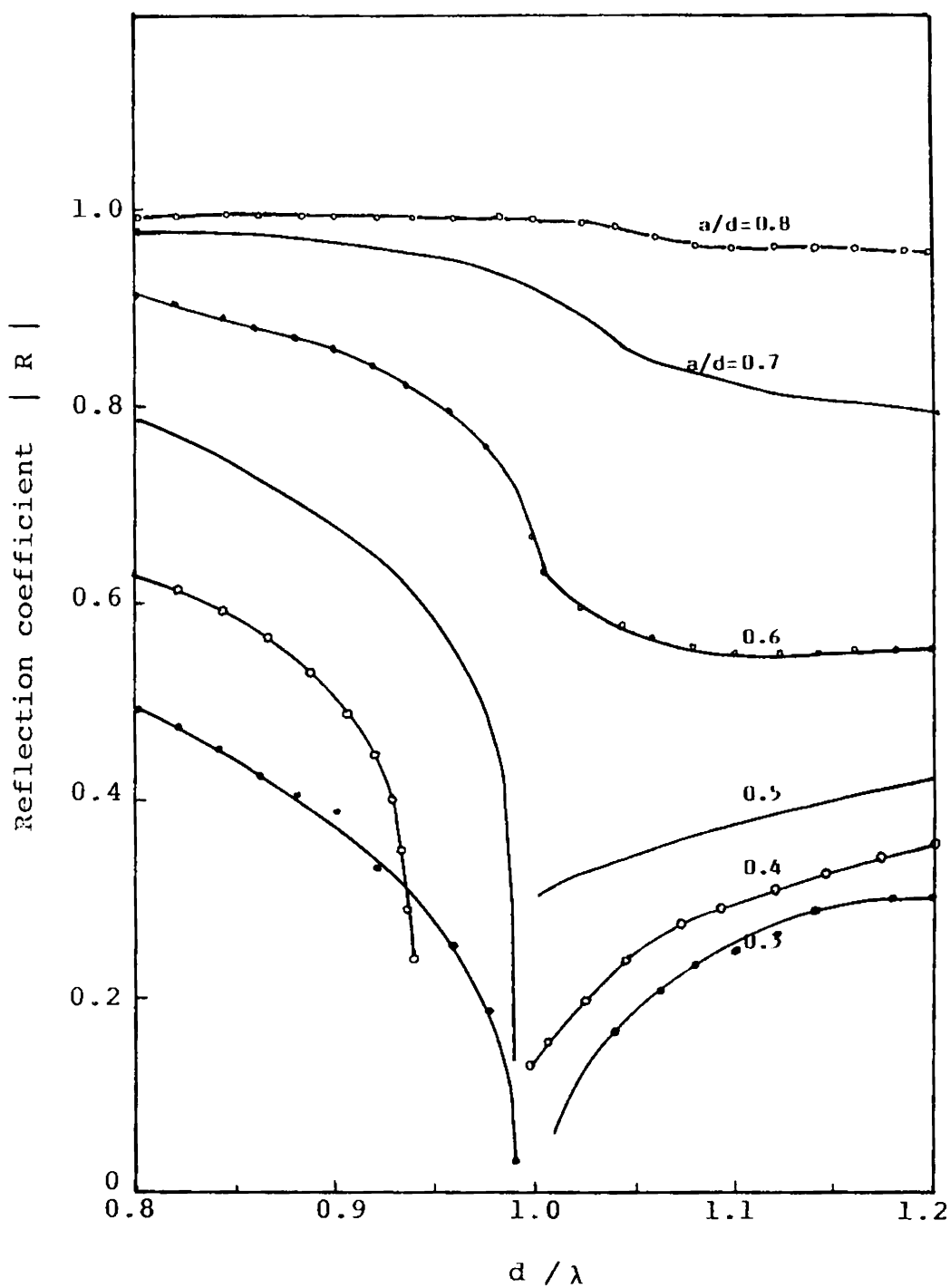
Fig. 4.13 Variation of reflection coefficient against period for strip grating alone.[Richmond's theory] Normal incidence.

Reflected power vs angle of Incidence
Self-complementary strip grating
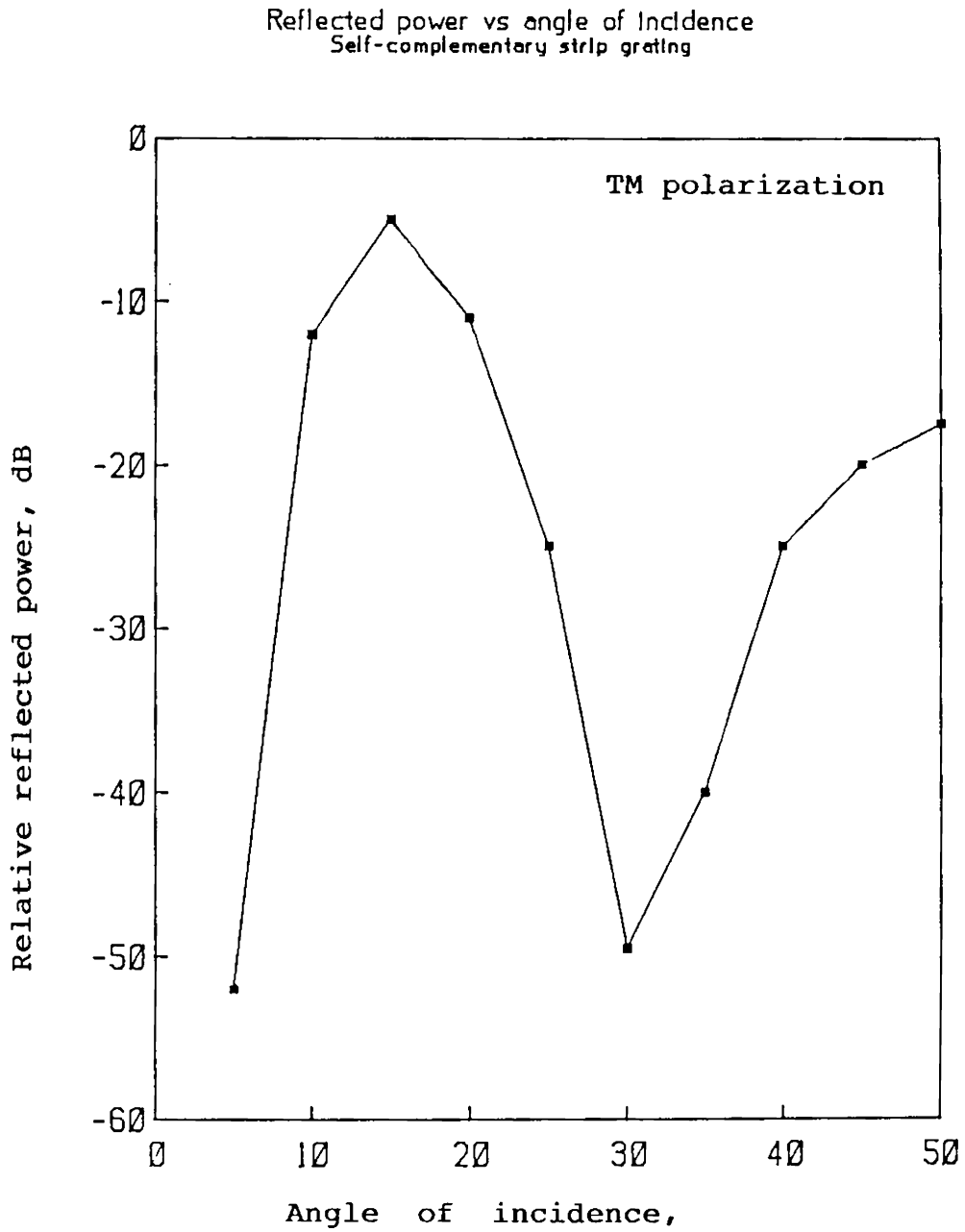
Fig. 4.14. Measured reflected power against incident angle self complementary strip grating S_9
$a = 0.5d$; $h = 0.109\lambda$; $f = 8.2$ GHz

grating S_9 with a/d = 0.50 and dielectric thickness h = 0.109 λ. The reflected power is completely eliminated at angles of incidence of 5°, the near-normal incidence and 30.46°, the perfect blazing angle θ_i of the grating system.

The recorded back-scattered power for self-complementary strip grating, using magic tee analog cancellation technique is shown in Figs.4.15(i),(ii) and (iii). The grating with a conducting plate behind it is placed on a turn-table, and the back-scattered power is recorded by rotating the strip grating system. Compared to the normal incidence back-scattered power for a plane metallic plate, the normal incidence back-scattering from the strip grating is minimum and maximum back-scattering occurs at the blazing angle.

The low back-scattering for normal incidence can be explained as a consequence of the equation,

$$\sin \theta_n = \sin \theta_i + n\lambda/d$$

when θ_i = 0, the diffraction angle will be 90° for d = λ. Also, when θ_i = 90° then θ_n will be zero. This is experimentally proved in Fig.4.16. The back-scattered power is plotted by rotating the receiver along the circumference of a circle with geometric centre of the plate as the centre,

in a horizontal plane. The maximum diffracted power is obtained when the receiving angle becomes 90° as shown in Fig.4.16(i). The same results are repeated when θ_i = 90°, i.e., when the incident ray is parallel to the plane of the grating (Fig.4.16(ii)).

4.6 THE EFFECT OF VARIATION OF THE THICKNESS OF THE DIELECTRIC MEDIUM 'h'

The thickness of the dielectric medium, in between the strip gratings and the ground plane is an important parameter in the elimination of normal incidence specular reflection of a self-complementary strip grating. Fig.4.17 presents the variation of back-scattered power due to the variation of thickness of dielectric sheet h for normal incidence for different gratings. This observation is taken by magic tee analog cancellation technique.

The recorded back-scattered power (Fig.4.15) also changes due to the change in dielectric medium. Various plots are obtained for strip grating S_9, with dielectric plates of different thickness. These are shown in Fig.4.18. The main change in the recorded power level is the change in the back-scattered power only for normal incidence.

The variation of the diffracted power, for an incident angle θ_i = 0 and receiving angle θ_n = 90°, due to the
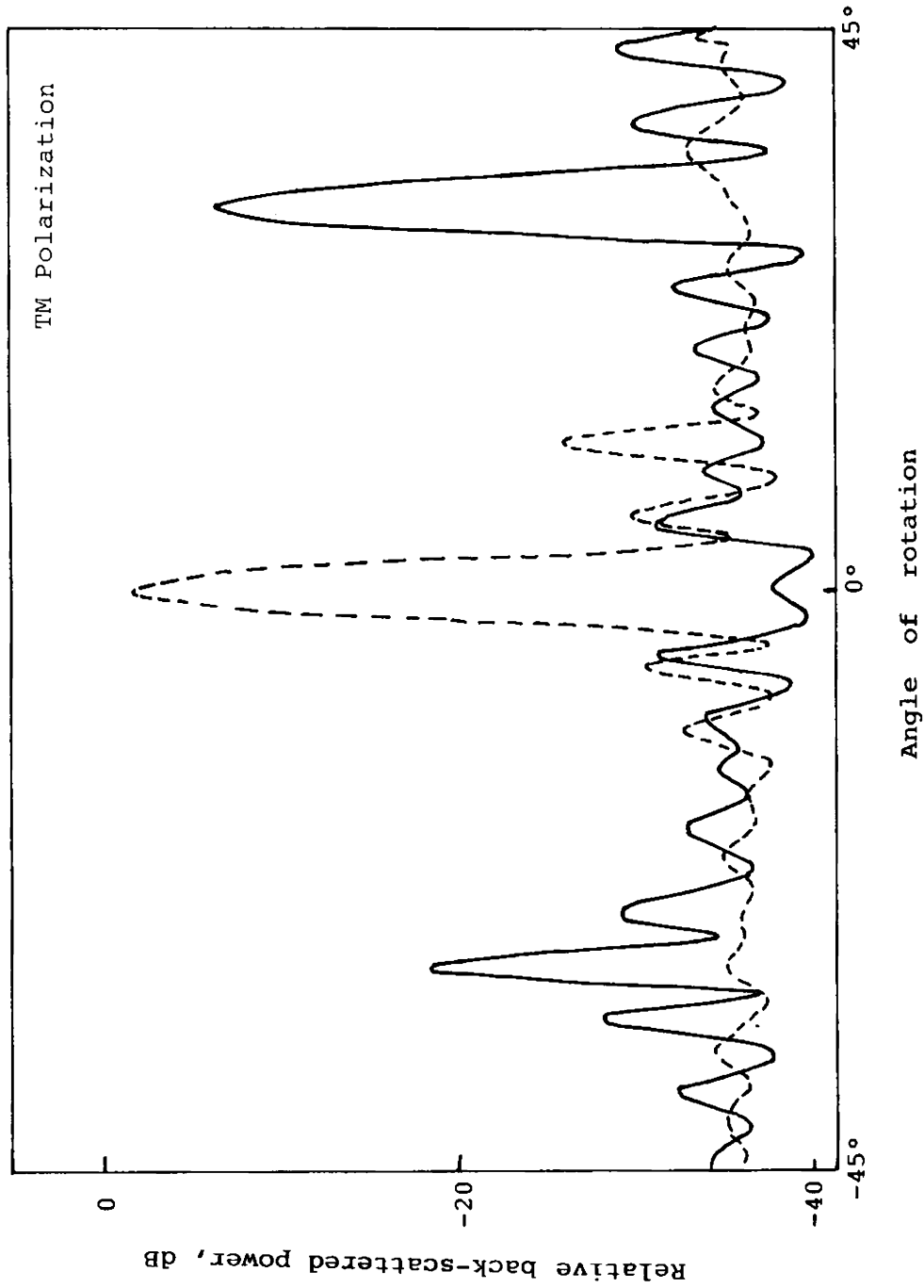
Fig. 4.15 (i). Recorded back-scattered power for self complementary strip grating, S_{11}; monostatic method. f = 12.25 GHz

———— strip grating, ------- plane metallic plate.
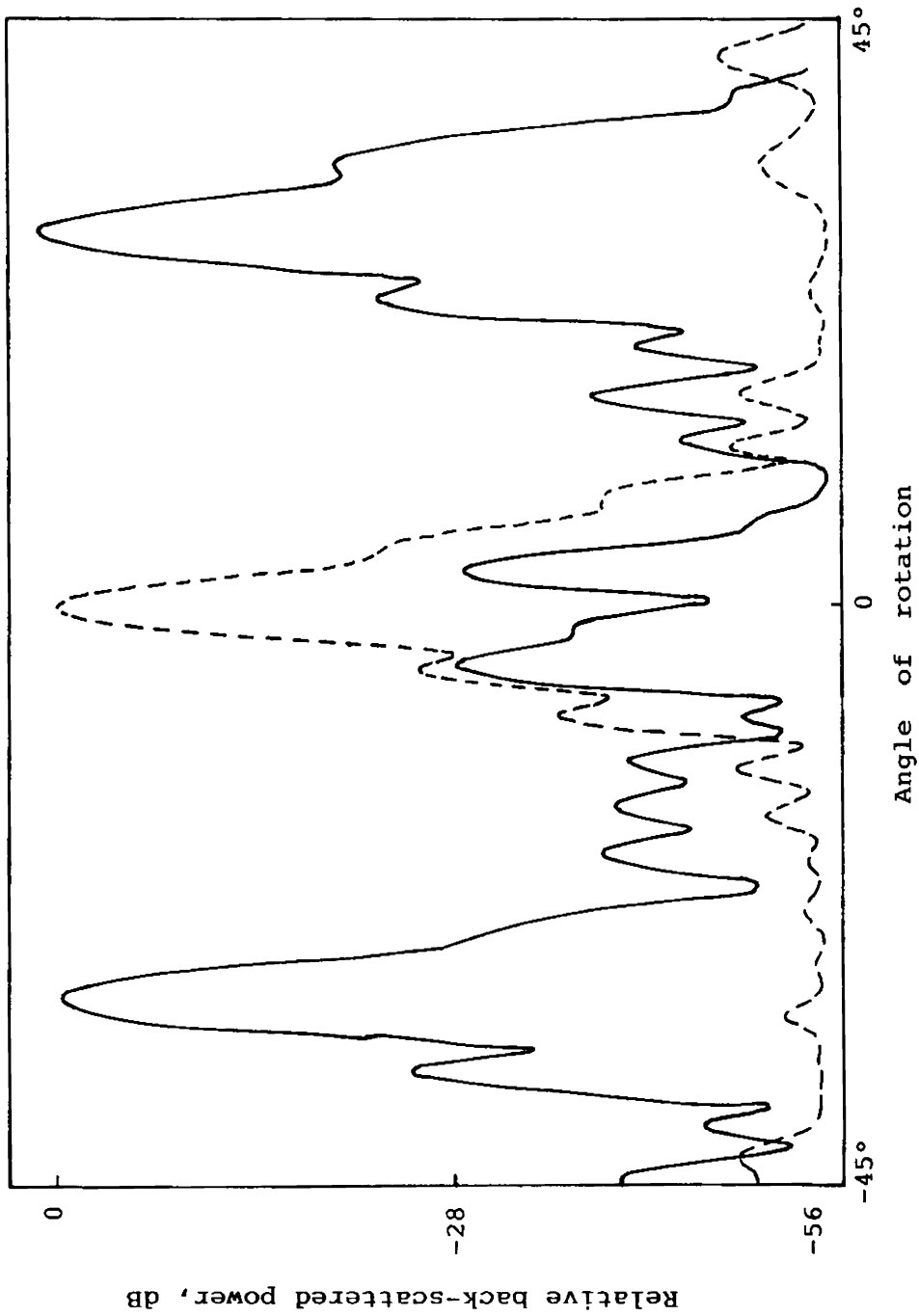
Fig. 4.15 (ii). Recorded back-scattered power for self complementary strip grating, S_{14}; monostatic method. $f = 8.30$ GHz.

———— strip grating, ──────── plane metallic plate.
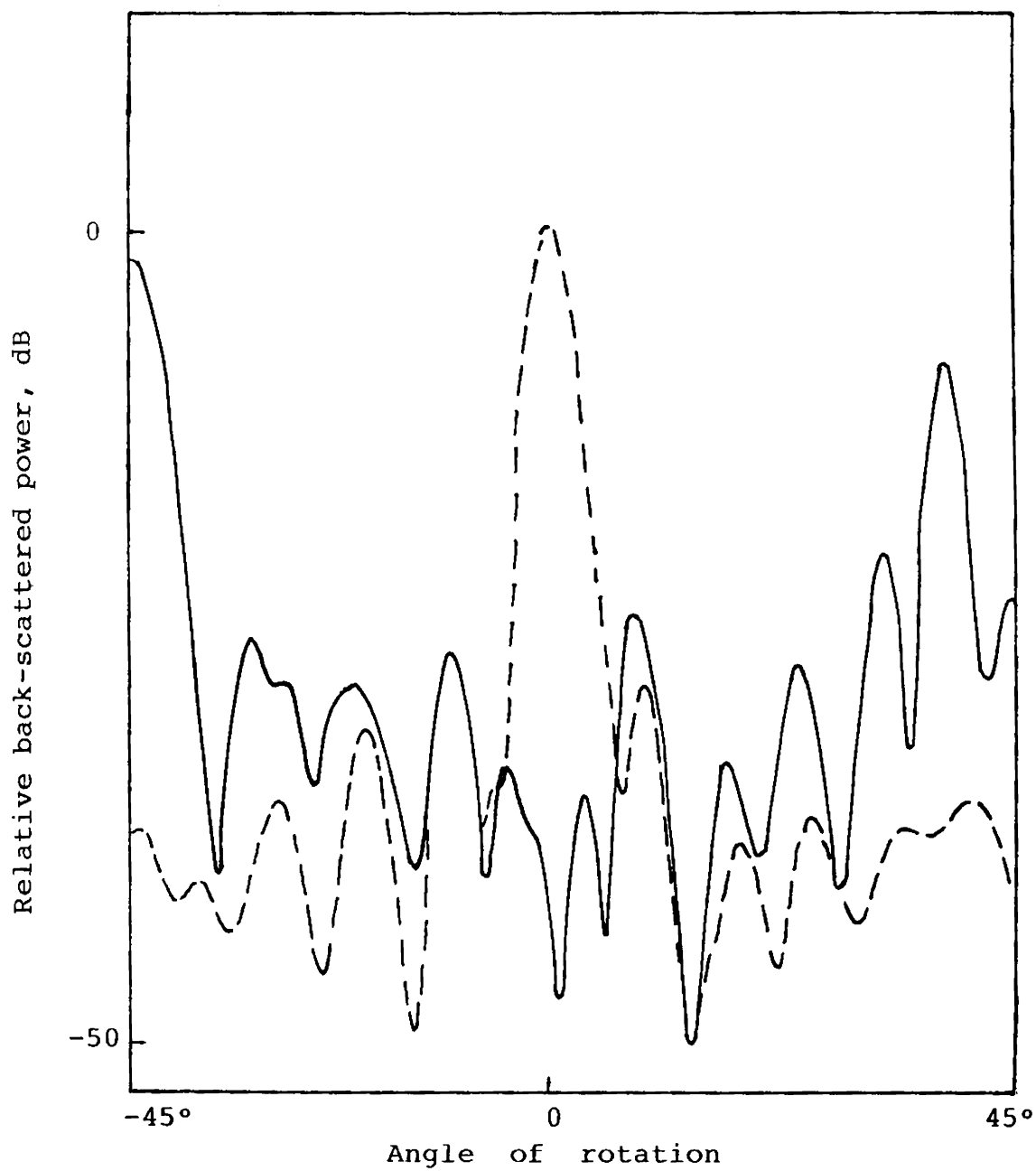
Fig. 4.15 (iii). Recorded back-scattered power for self-complementary strip grating S_9; f=9.85 GHz TM polarization.

——————— strip grating
- - - - - - - plane metallic plate.
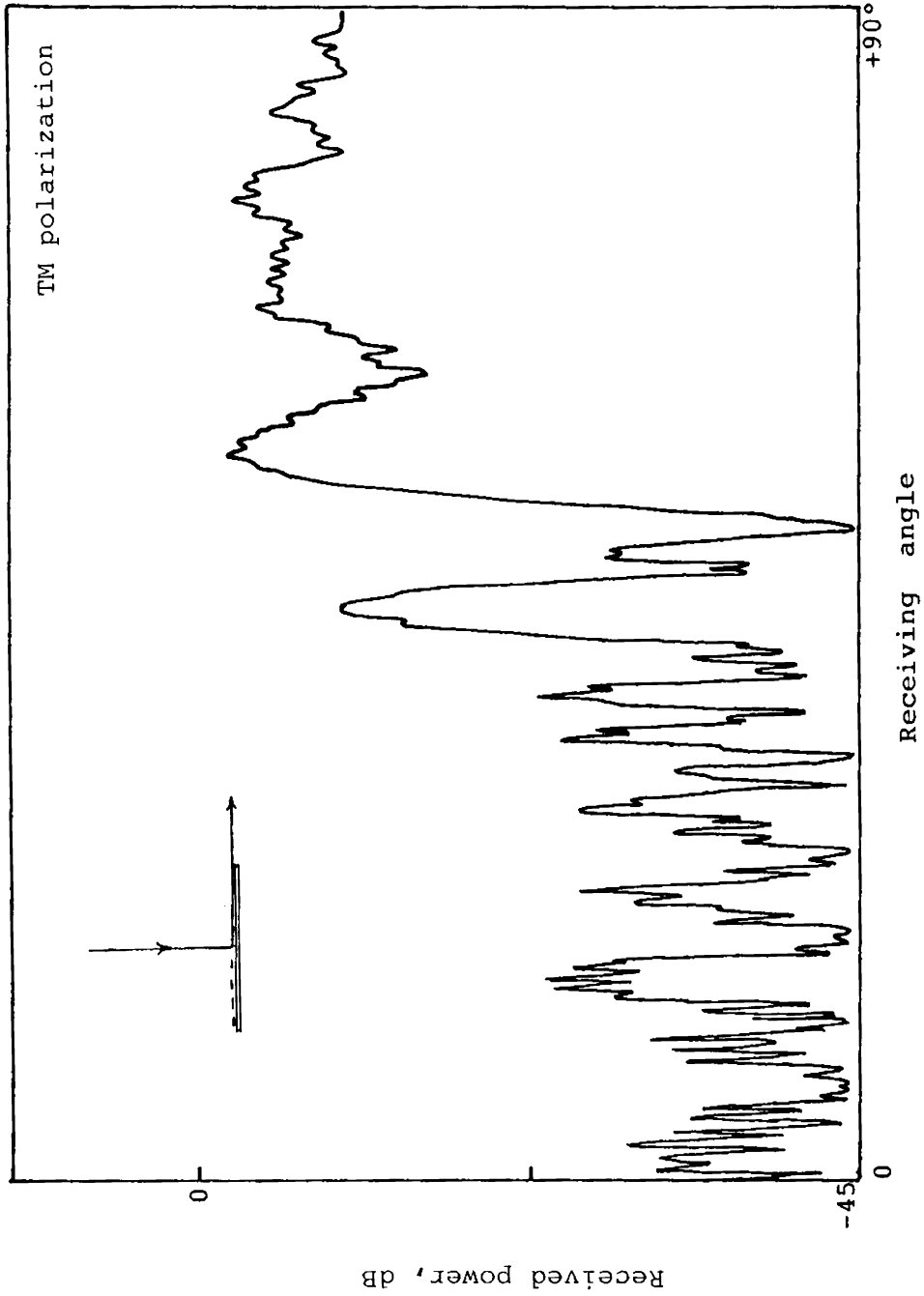
Fig. 4.16 (ia). Measured scattered power for normal incidence and
different receiving angles (0 → +90°)
grating S_{10}, f = 9.751 GHz
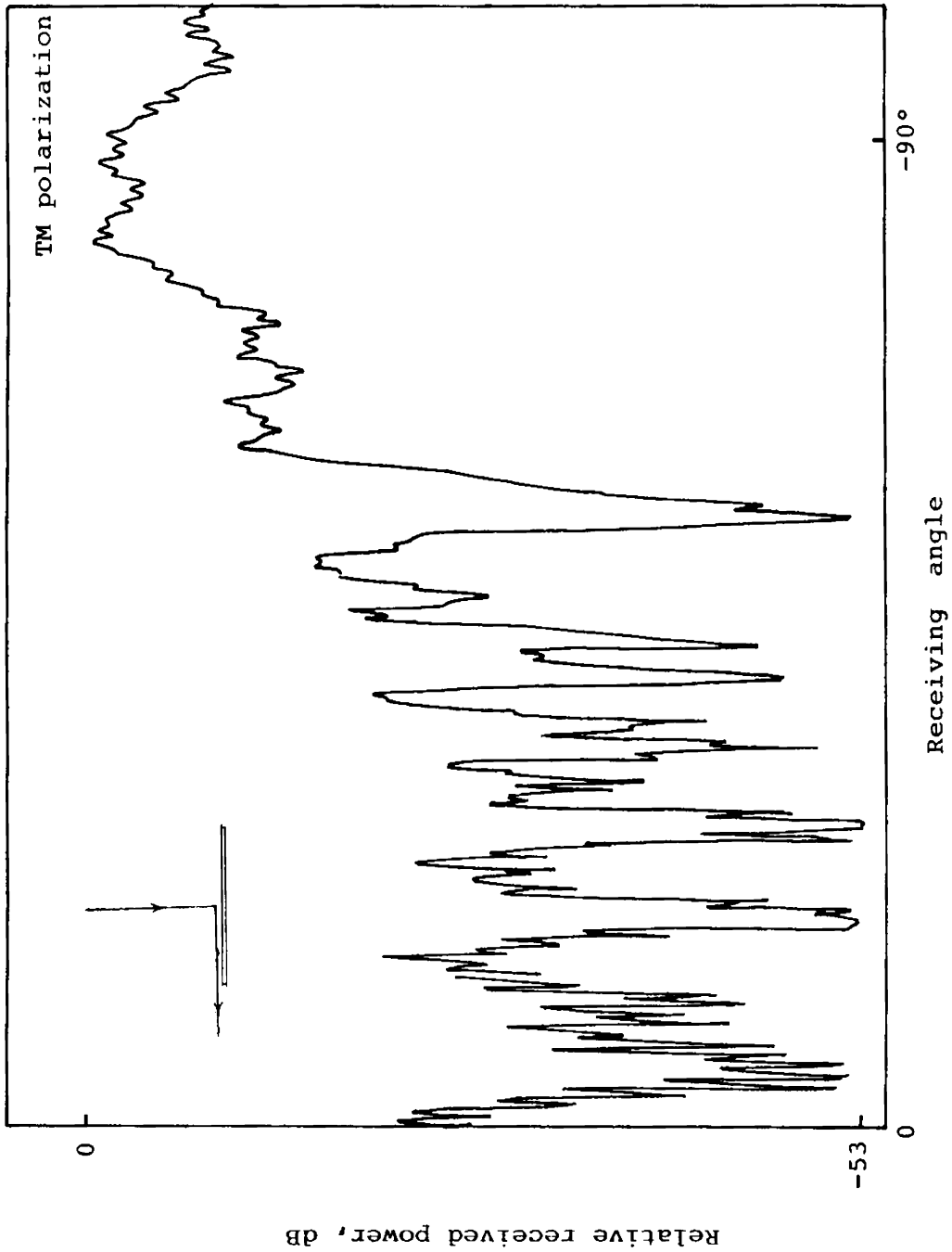
Fig. 4.16 (ib). Measured scattered power for normal incidence and different receiving angles (0 → -90°) grating S_9 , f = 9.850GHz.
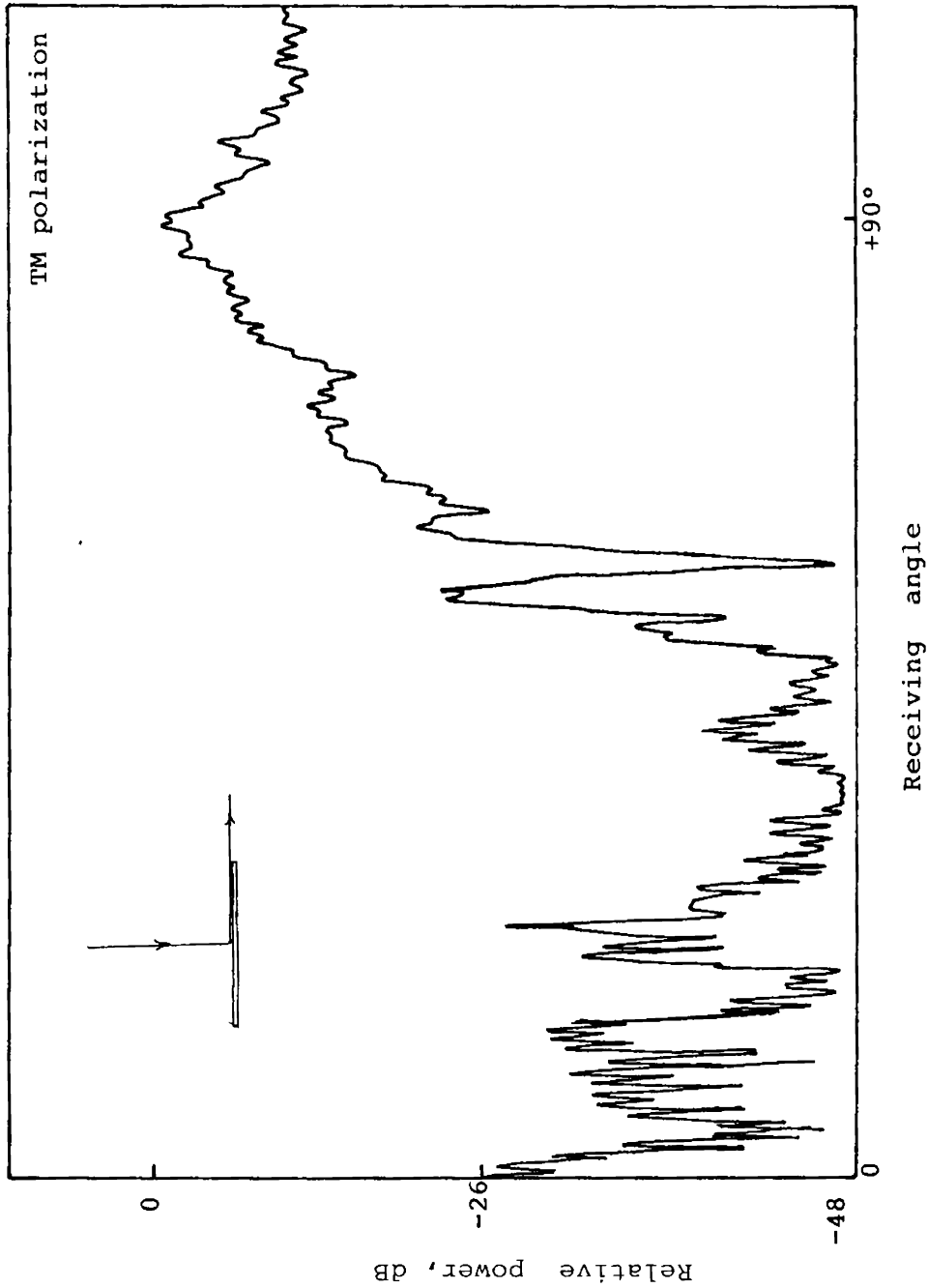
Fig. 4.16 (ic). Measured scattered power for normal incidence and different observation angles ($0 \rightarrow +90°$) grating S_9 , f = 9.850 GHz.
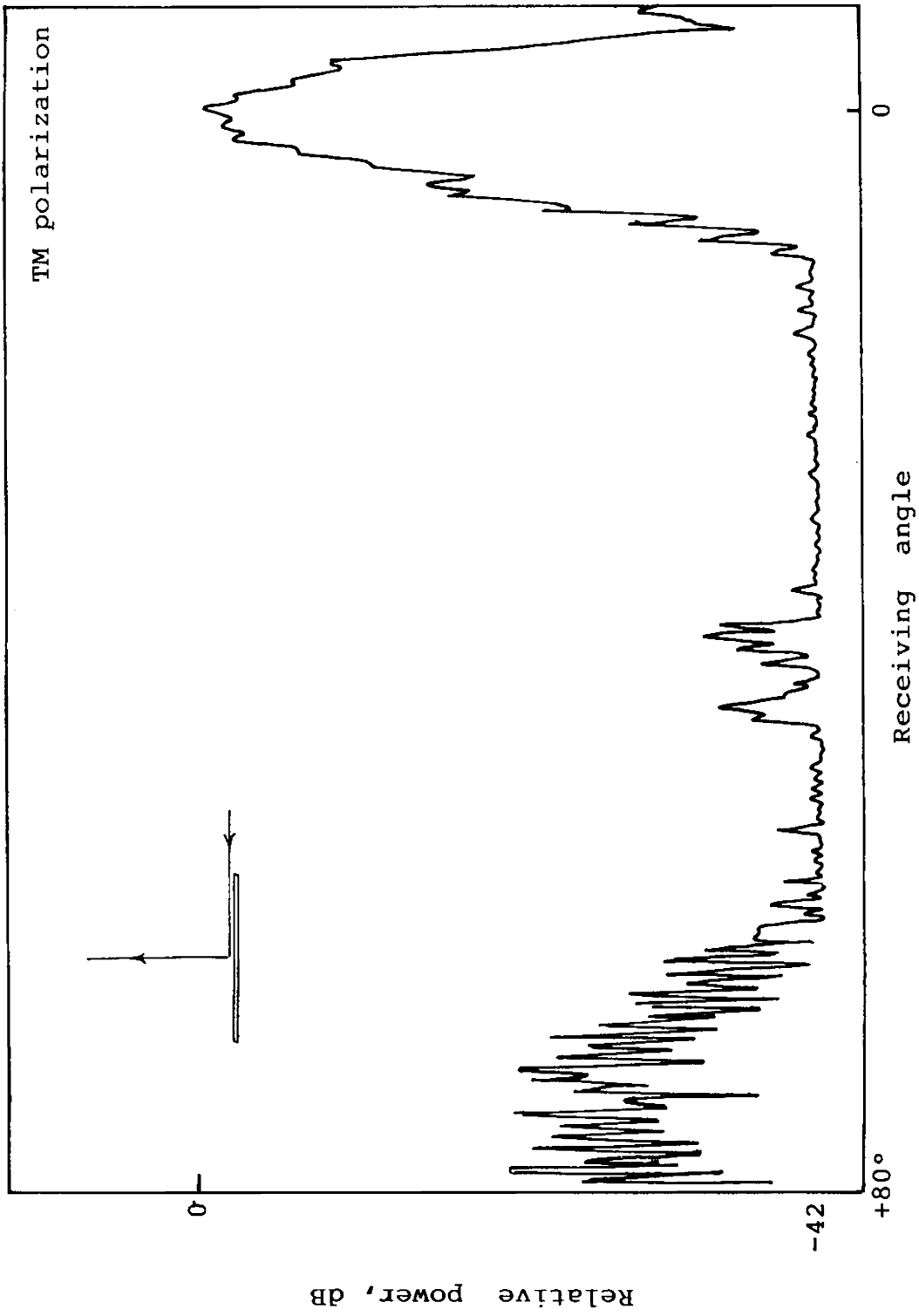
Fig. 4.16 (iia). Measured scattered power for 90° incidence and observing angles +80° to 0. grating S_9, f = 9.840 GHz.
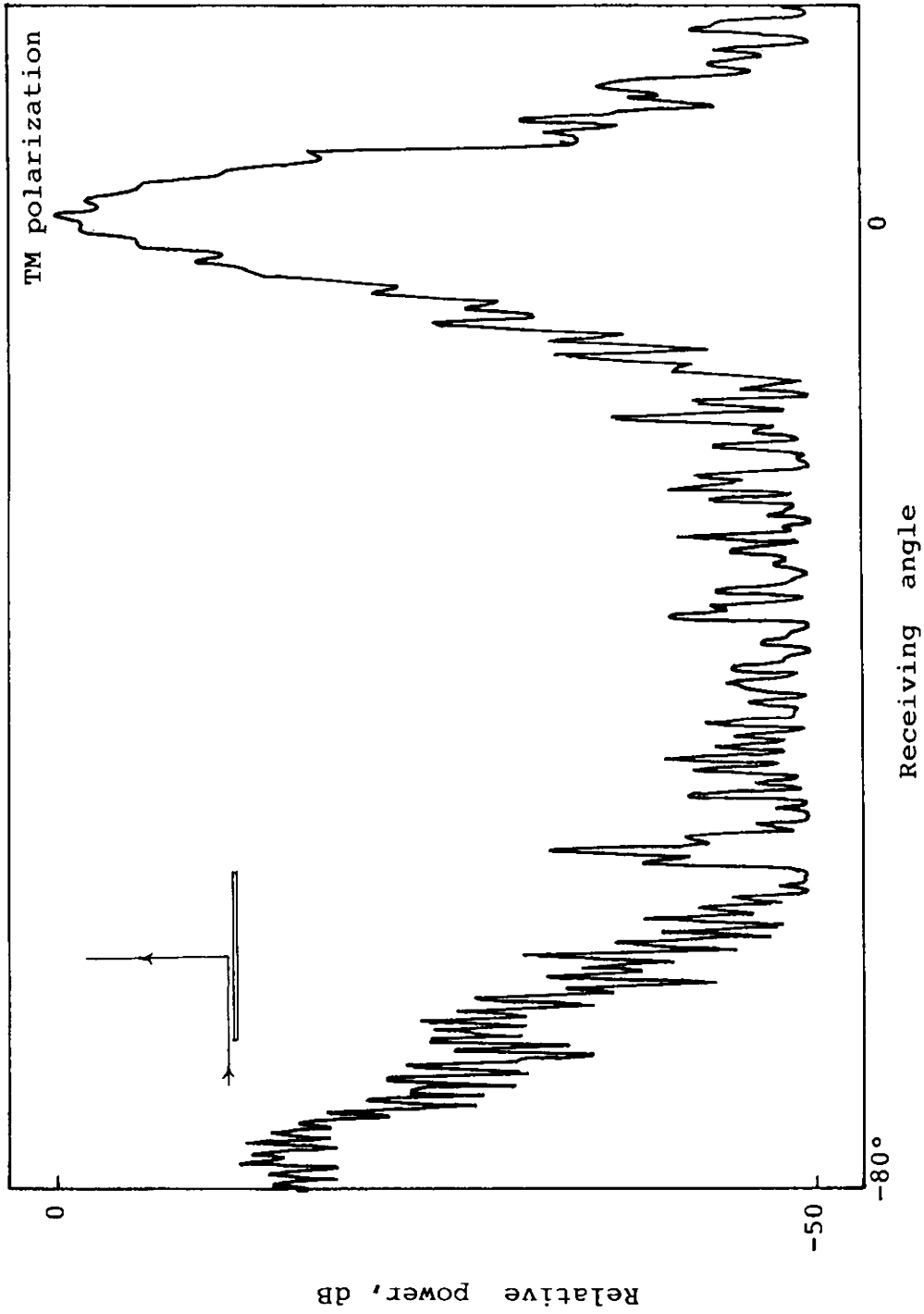
Fig. 4.16 (ii b). Measured scattered power for 90° incidence and observing angles -80° to 0° grating S9 , f = 9.840 GHz.
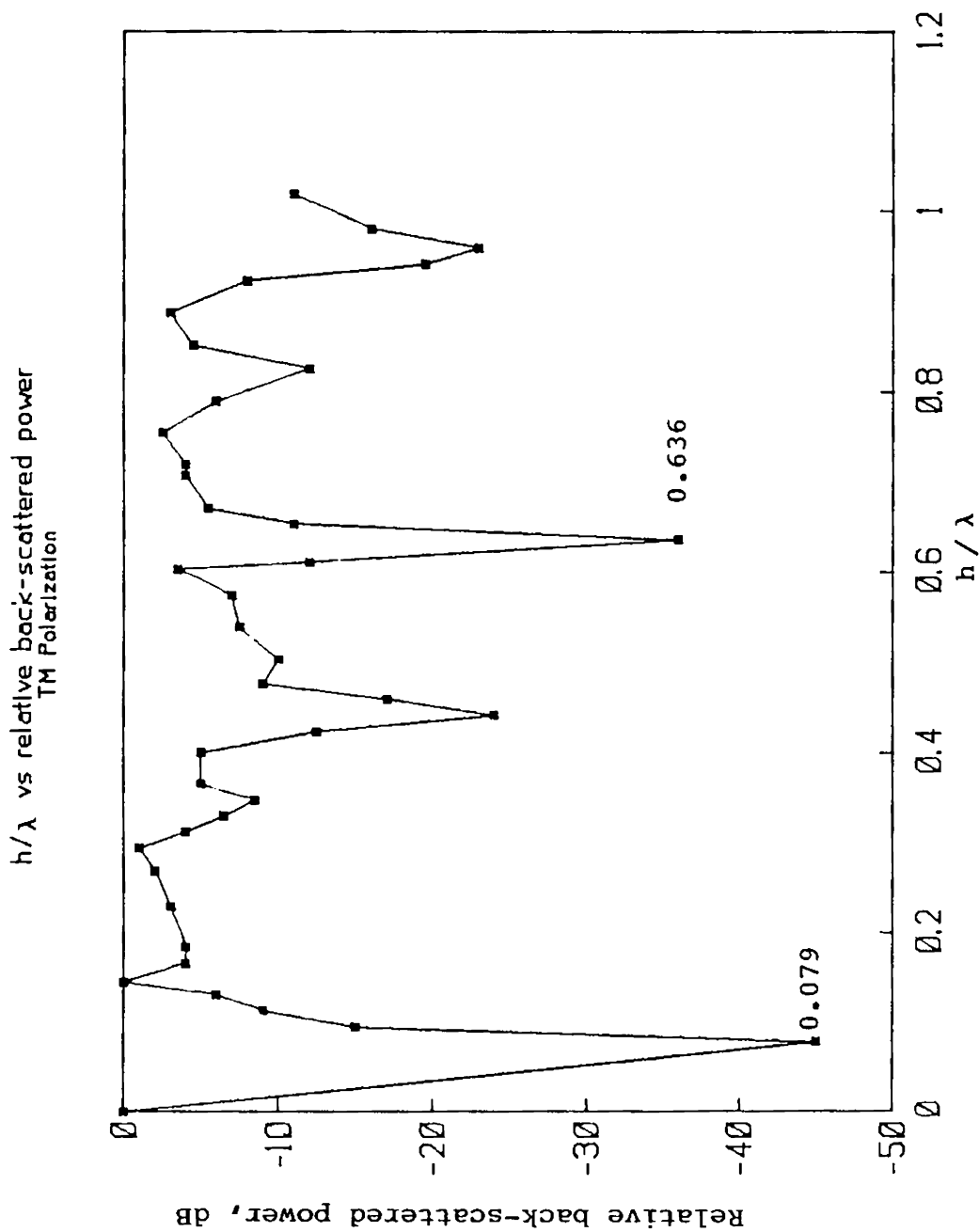
Fig. 4.17 (i). Variation of backscattered power due to the change in the thickness of dielectric sheet; monostatic method, normal incidence, grating S_{10}; $f = 10.635$ GHz
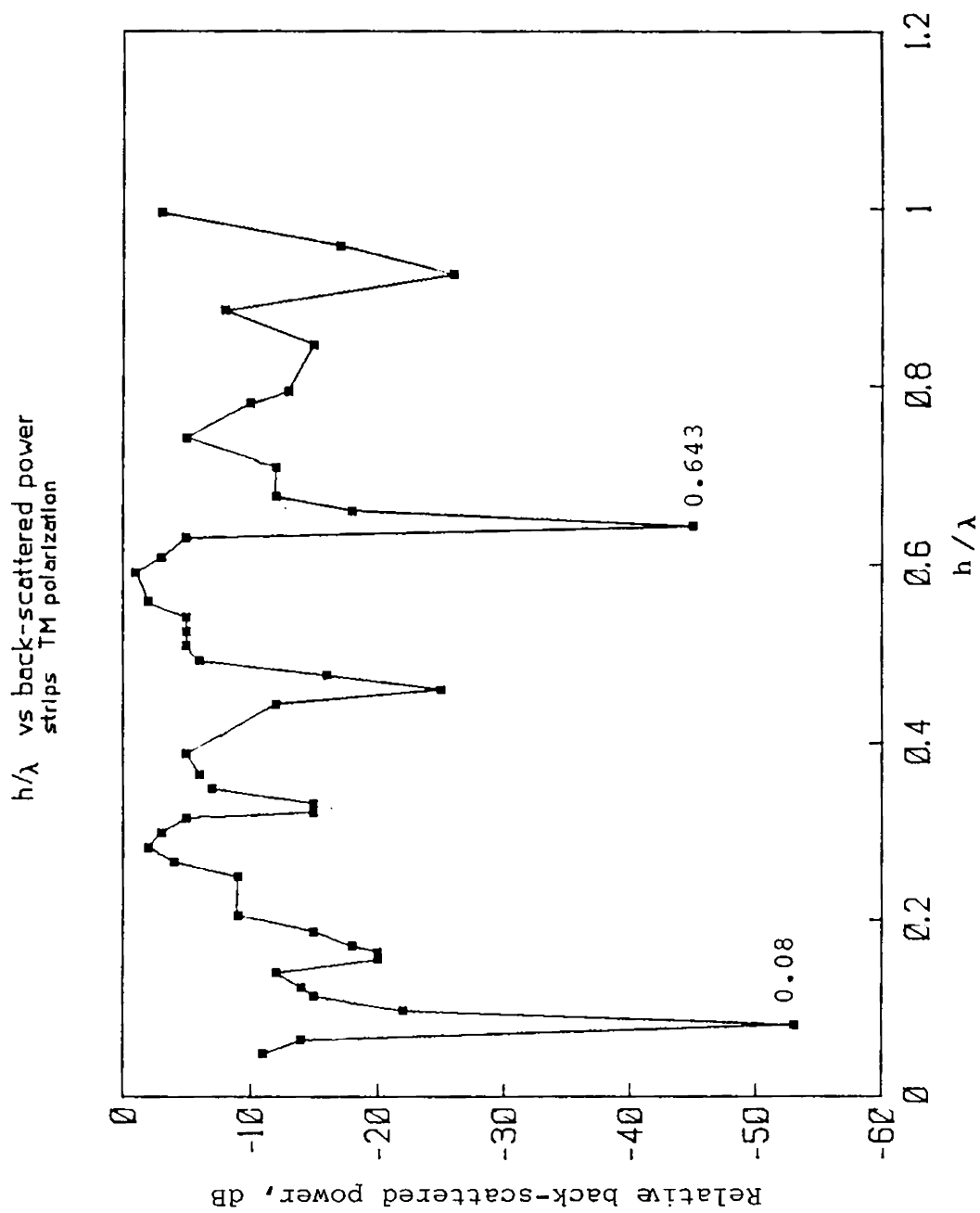
Fig. 4.17 (ii). Variation of back-scattered power against the change in thickness of dielectric sheet; monostatic method, normal incidence, grating S_9; $f = 9.850$ GHz.
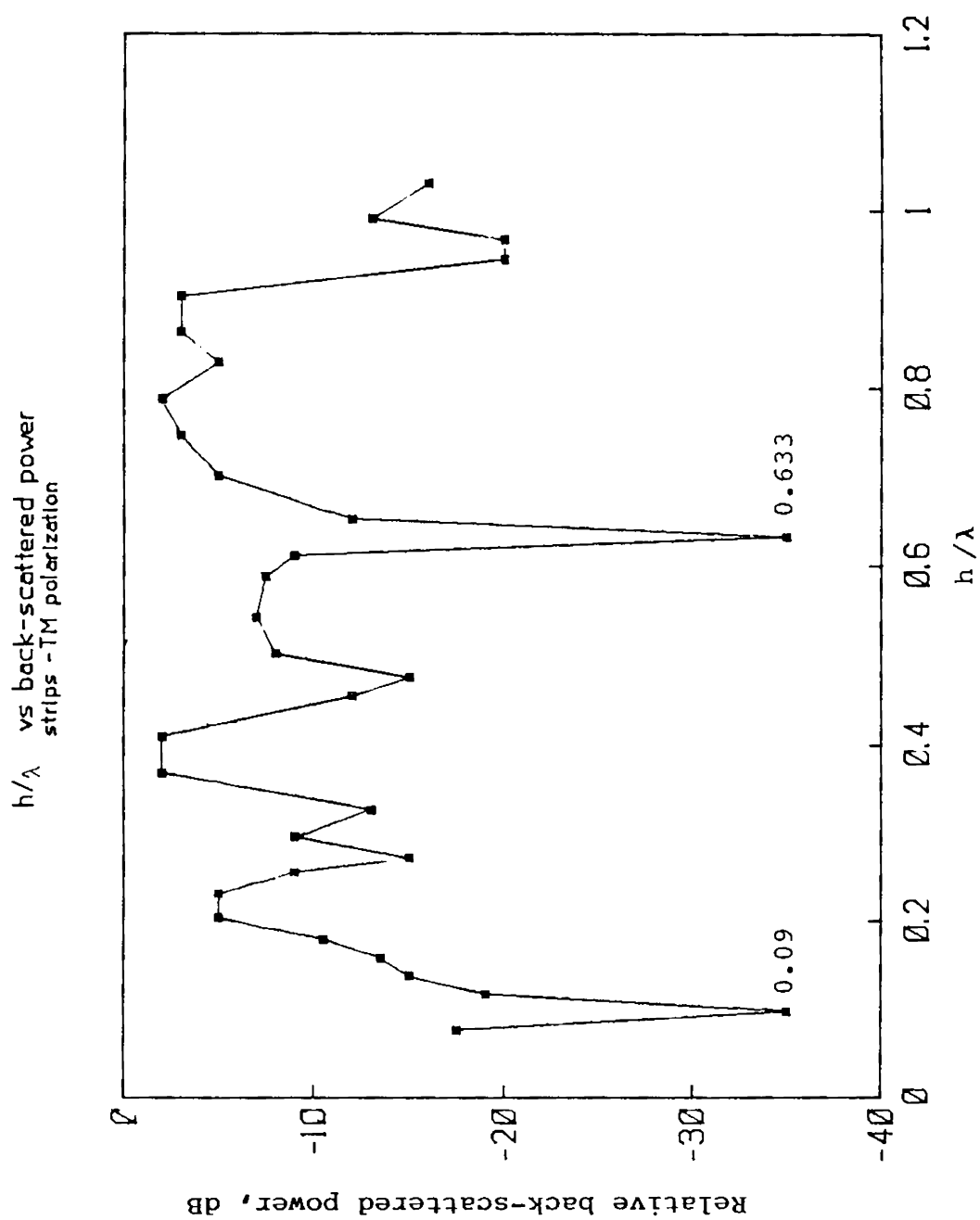
Fig. 4.17 (iii). Variation of back-scattered power against the change in thickness of dielectric sheet; monostatic method, normal incidence, grating S_{11}; f = 12.25 GHz.
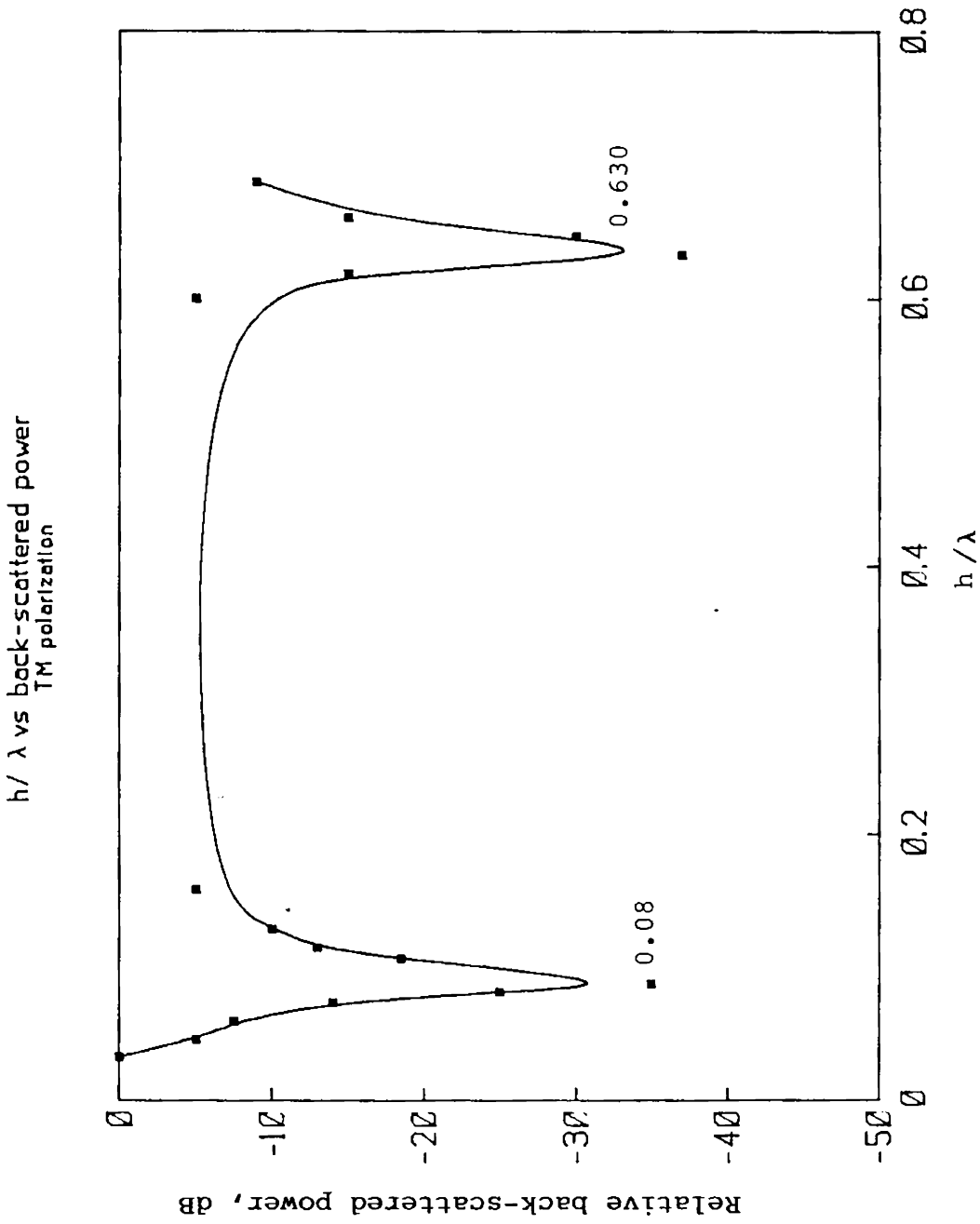
Fig. 4.17 (iv). Variation of back-scattered power against the change in thickness of dielectric sheet; monostatic method, normal incidence, grating S_{14}; f = 8.250 GHz.
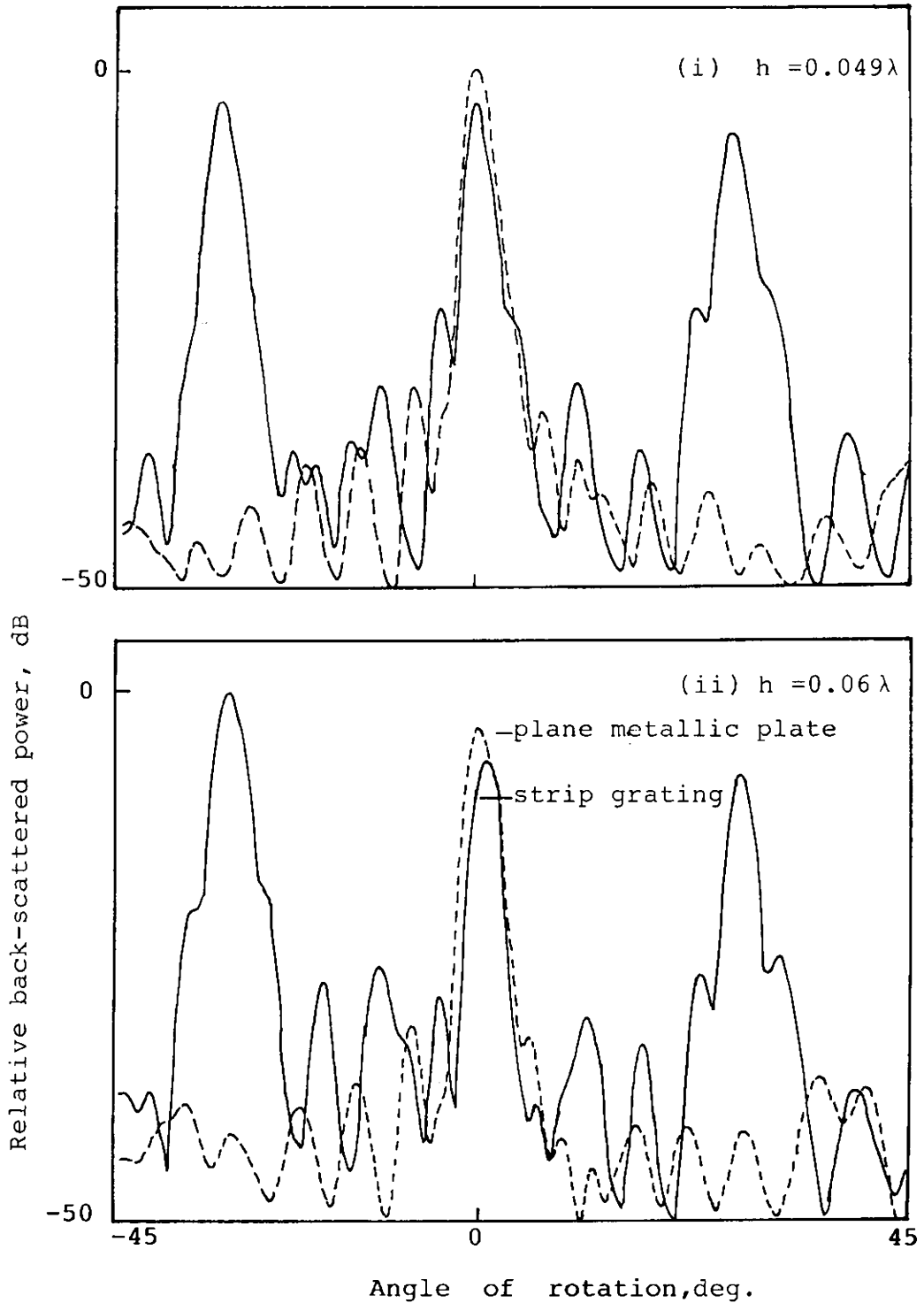
Fig. 4.18. Recorded back-scattered power for dielectric medium of different thickness, h; monostatic method, f = 9.850 GHz.

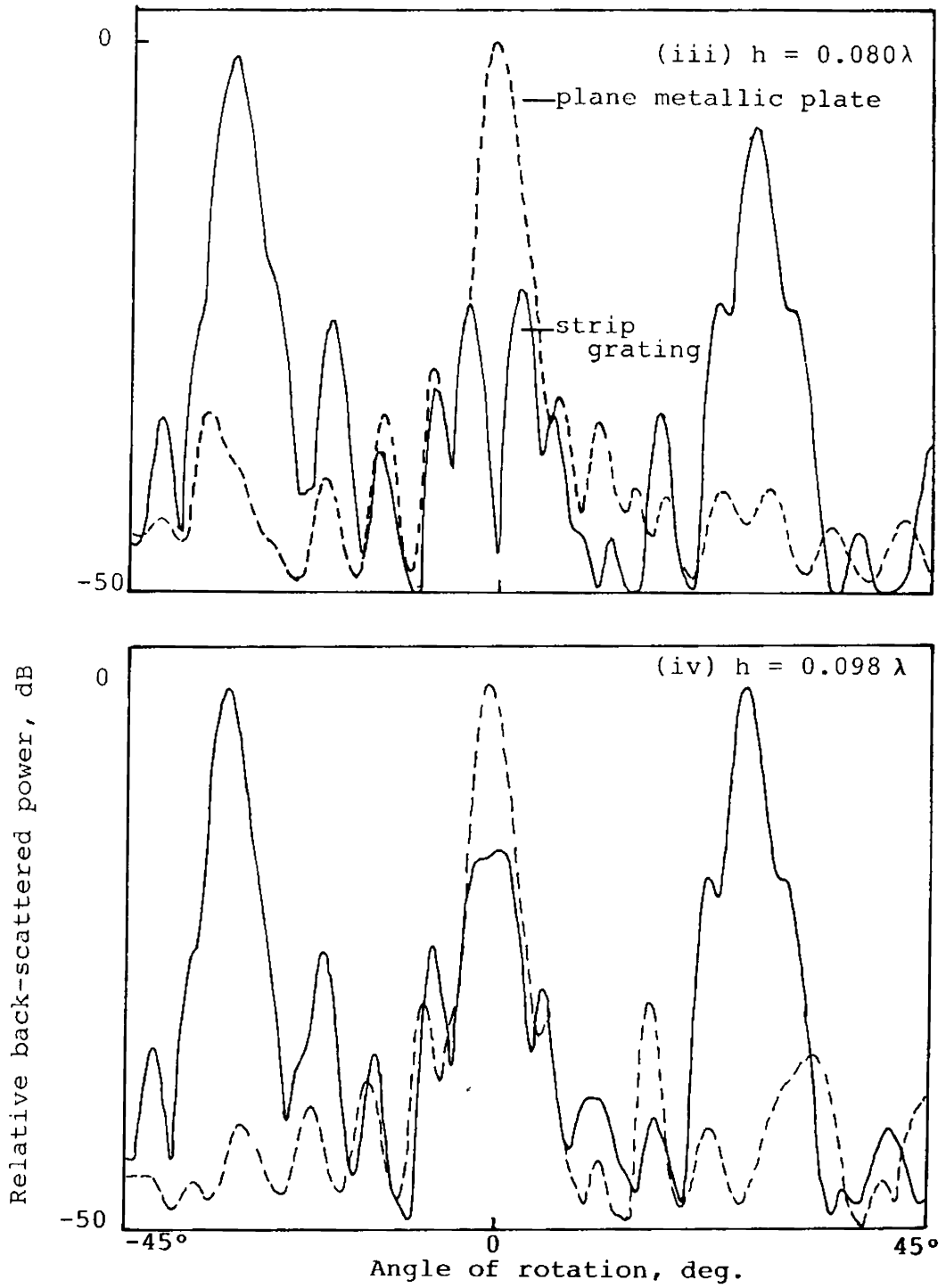
Fig. 4.18. Recorded back-scattered power for dielectric medium of different thickness, h. monostatic method, f = 9.850 GHz.
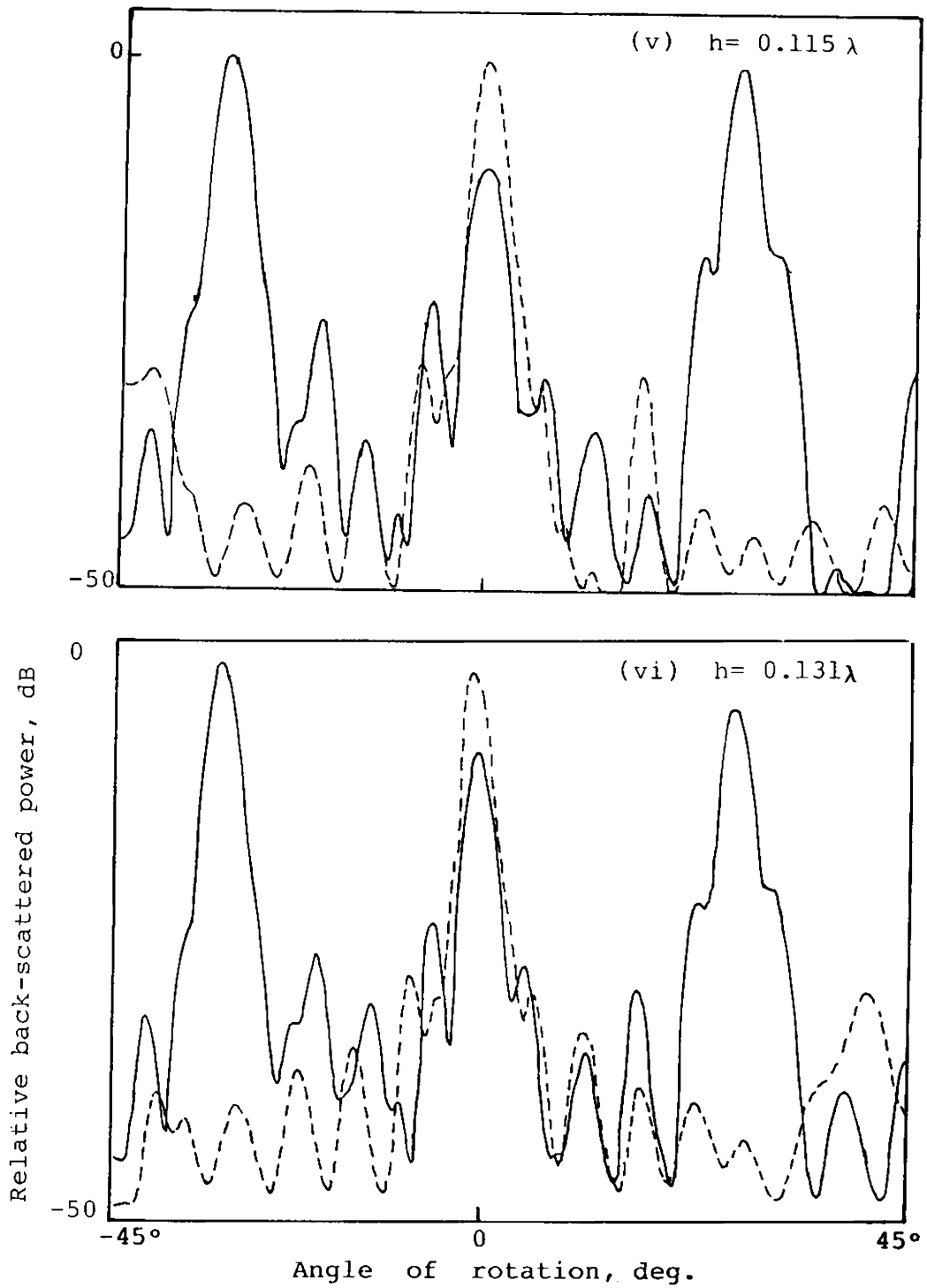
Fig. 4.18. Recorded back-scattered power for dielectric medium of different thickness, h. monostatic method, f = 9.850 GHz
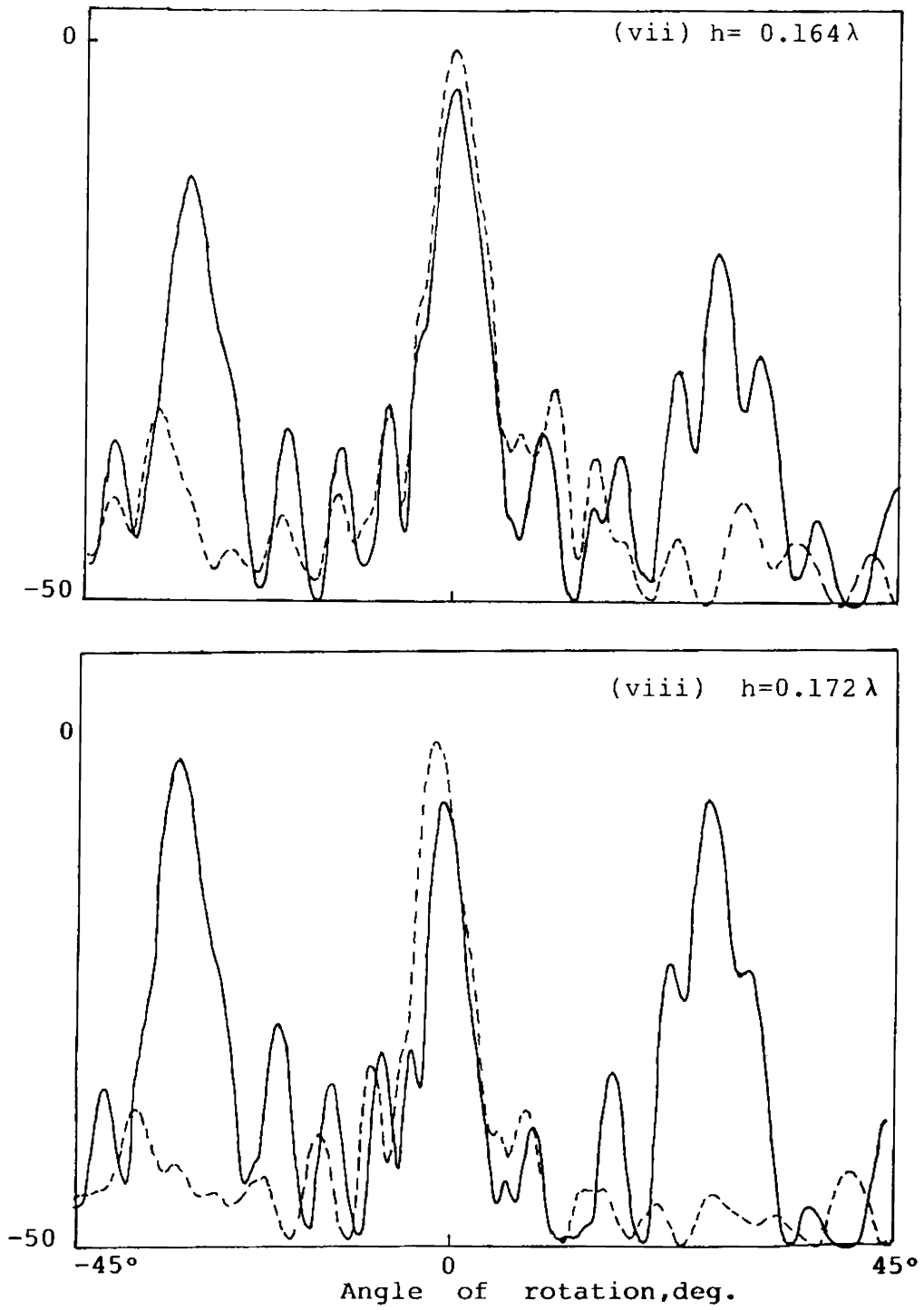
Fig. 4.18. Recorded back-scattered power for dielectric medium of different thickness, h. monostatic method, f = 9.850 GHz.

variation of the thickness of the dielectric sheet is shown in Fig.4.19(i). The same result is presented in Fig.4.19(ii) when the angle of incidence $\theta_i = 90°$ and $\theta_n = 0°$ for the same grating.

The changes in back-scattered power for near-normal-incidence due to the variation of the thickness of dielectric sheet h is shown in Fig.4.20.

4.7 THE EFFECTS OF MULTI-ELEMENTS ON SPECULAR REFLECTION

When the grating period d satisfies Bragg condition for perfect blazing, the specular reflection (n = 0 mode) is completely cancelled and the grating behaves as a back-scatterer (n = -1 mode). When conducting strips are split to thinner elements keeping the grating period d constant, it is possible to reduce the requirement of minimum thickness of dielectric sheet. This multi-element reflector-backed grating system shows similar behaviour of a single periodic grating system. It could be possible to achieve better results from the dual-periodic or multi-element grating without any change in the blazing properties of it. Strip grating S_9, with d = 30 mm is taken for the observations. It shows perfect blazing for angle of incidence $\theta_i = 29°$ and $h/\lambda = 0.113$, a/d = 0.50. The strips of width b = 0.5d is divided such
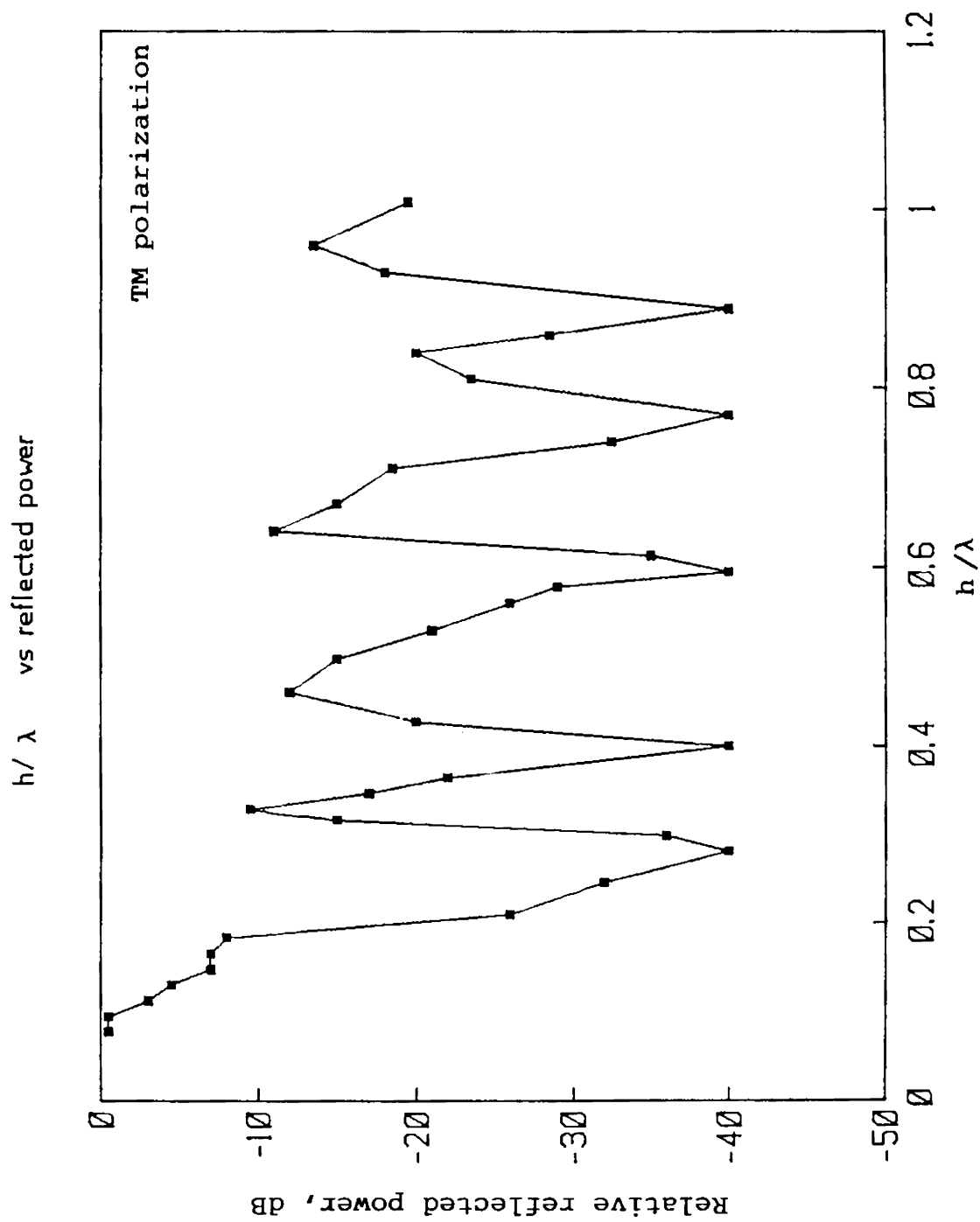
Fig. 4.19 (i a). Variation of scattered power due to the change in thickness of dielectric, for $\theta_i = 0$ and receiving angle $\theta_n = 90°$ grating S_{10} ; $f = 10.635$ GHz.

h/λ vs reflected power
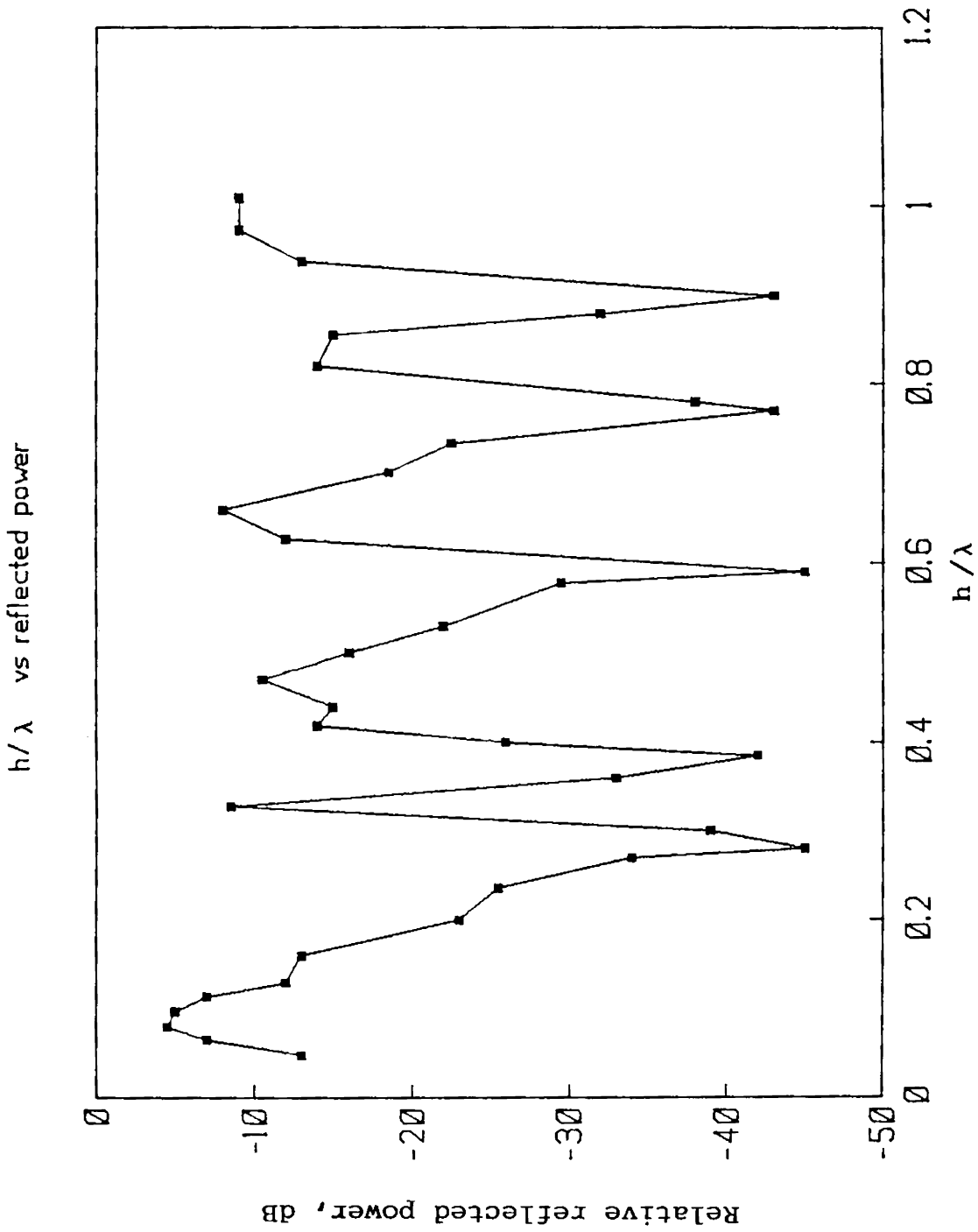
Fig. 4.19 (i b). Variation of scattered power due to the change in thickness of dielectric, for $\theta_i = 0$ and receiving angle $\theta_n = 90°$ grating S_g ; f = 9.750 GHz
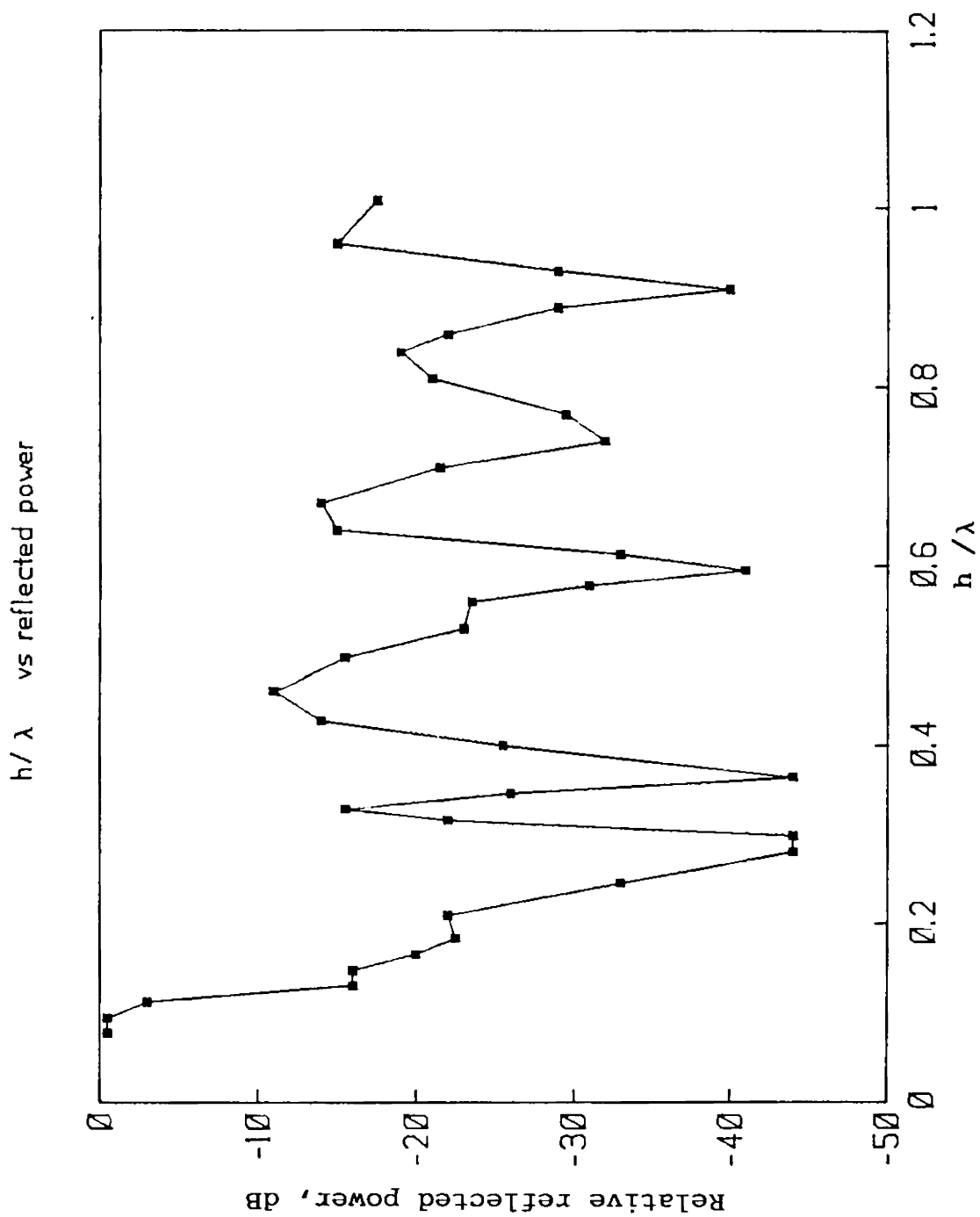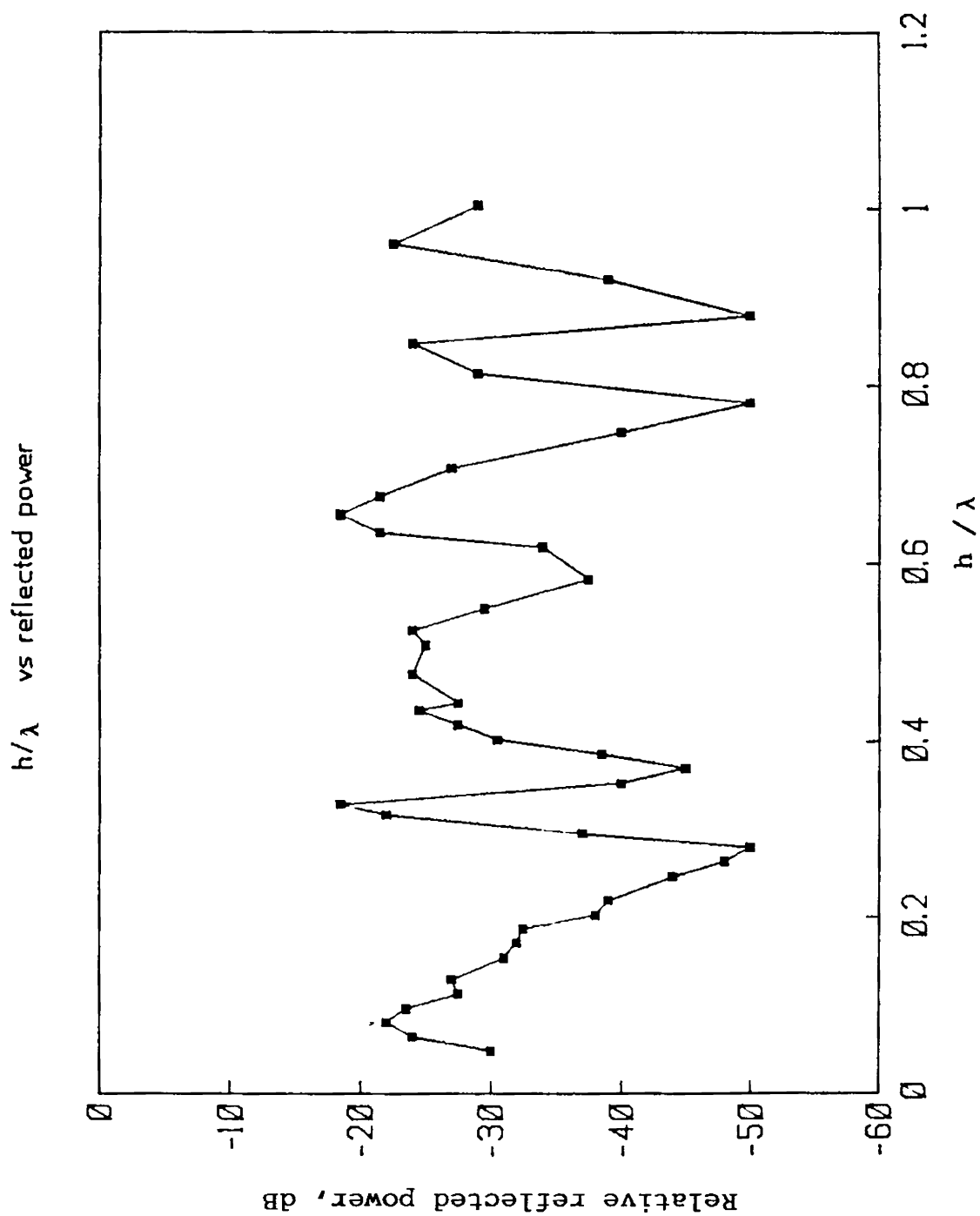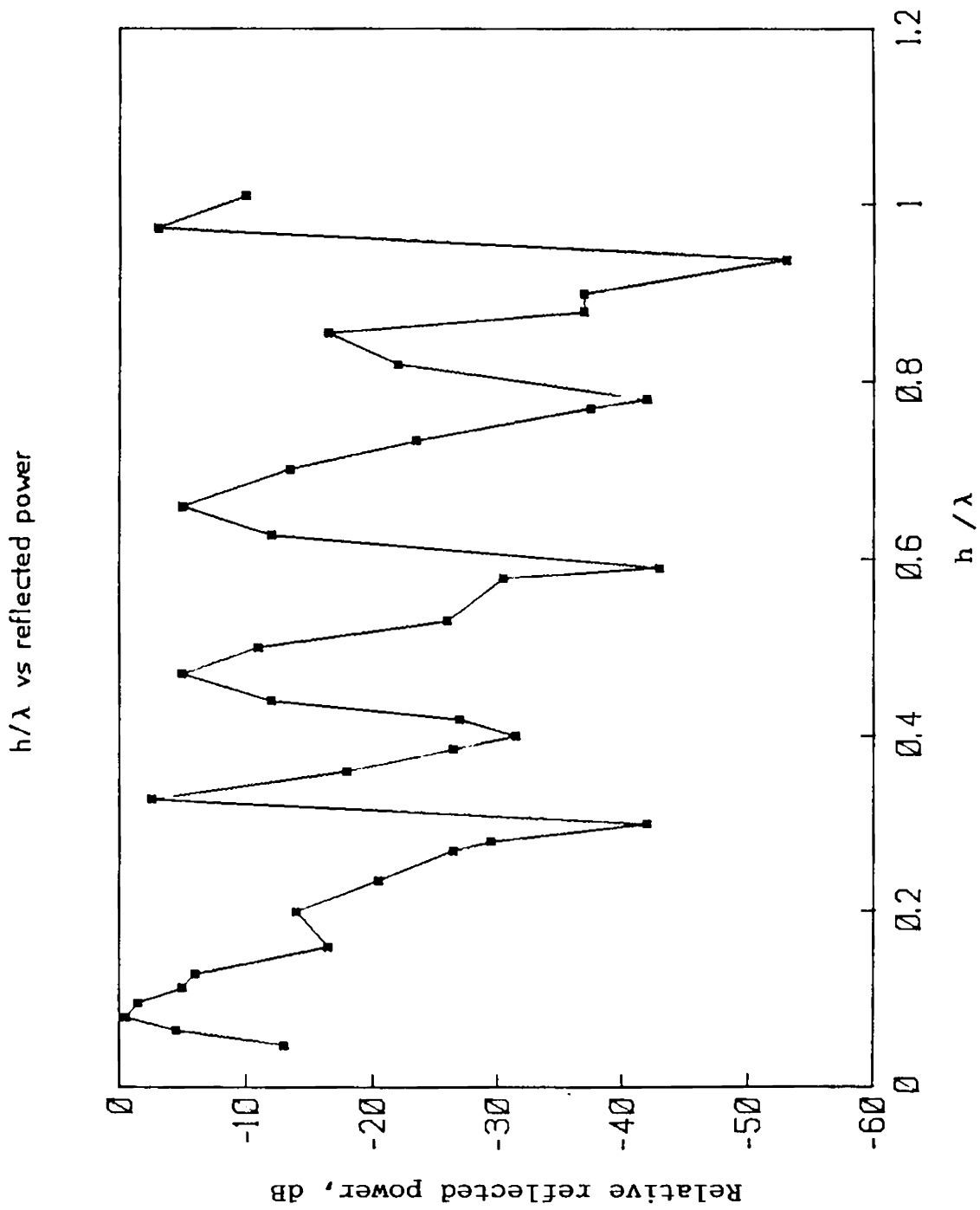
h/λ   vs reflected power
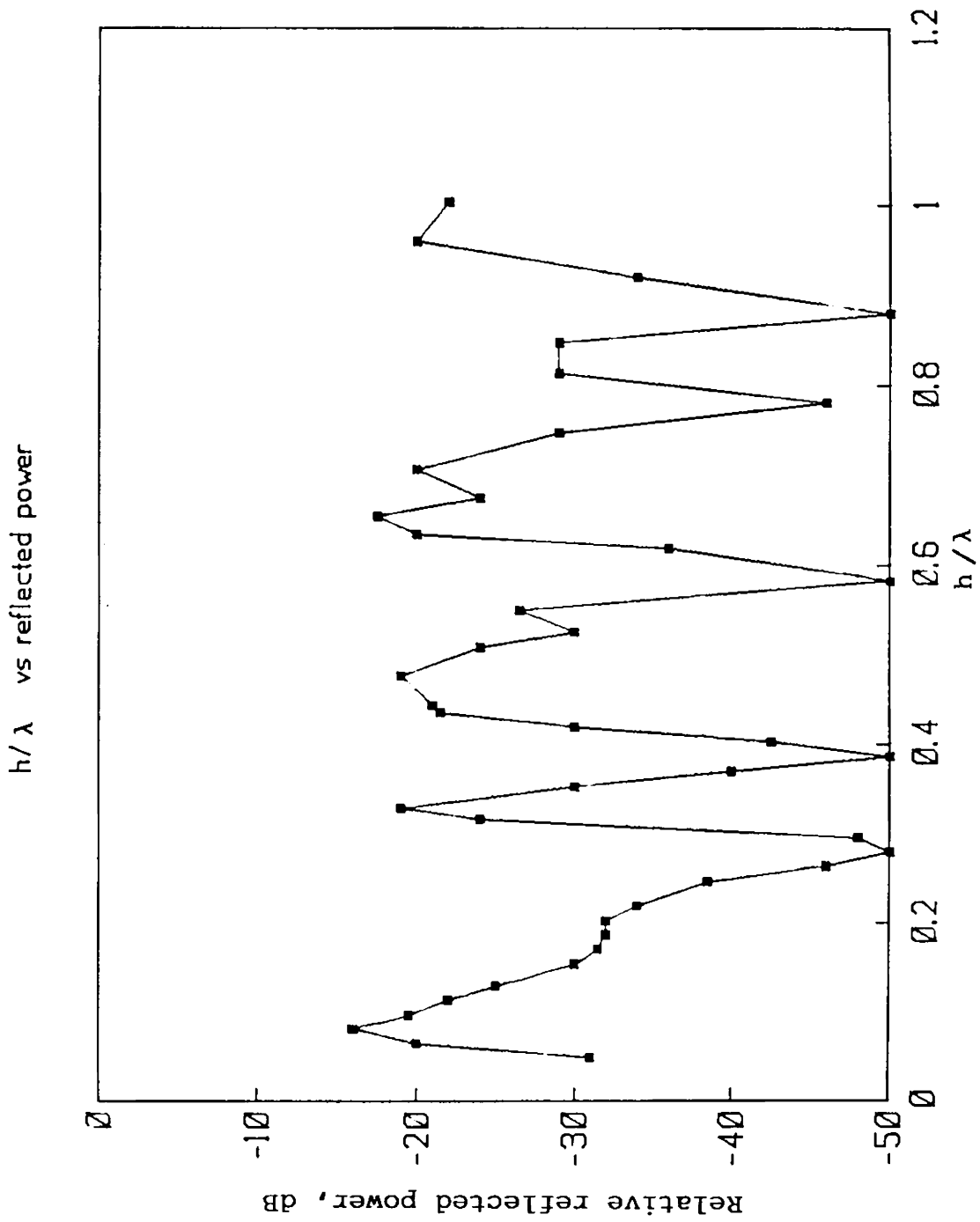
Fig. 4.19 (i c).   Variation of scattered power due to change in thickness of dielectric, for $\theta_i = 0$ and receiving angle $\theta_n = 90°$ grating S_9 ; $f = 8.850$ GHz.

h/λ   vs reflected power

Fig. 4.19 (ii a).   Measured scattered power due to the change in thickness
of dielectric, for $\theta_i = 90°$ and receiving angle $\theta_n = 0°$
grating S_{10}; $f = 9.850$ GHz

h/λ   vs reflected power

Fig. 4.19 (ii b). Measured scattered power due to the change in thickness of dielectric, for $\theta_i = 90°$ and receiving angle $\theta_n = 0°$ grating S_g; $f = 9.850$GHz.

h/λ vs reflected power

Fig. 4.19 (ii c). Measured scattered power due to the change in thickness of dielectric, for $\theta_i = 90°$ and receiving angle $\theta_n = 0°$ grating S_9 ; f = 8.850 GHz.
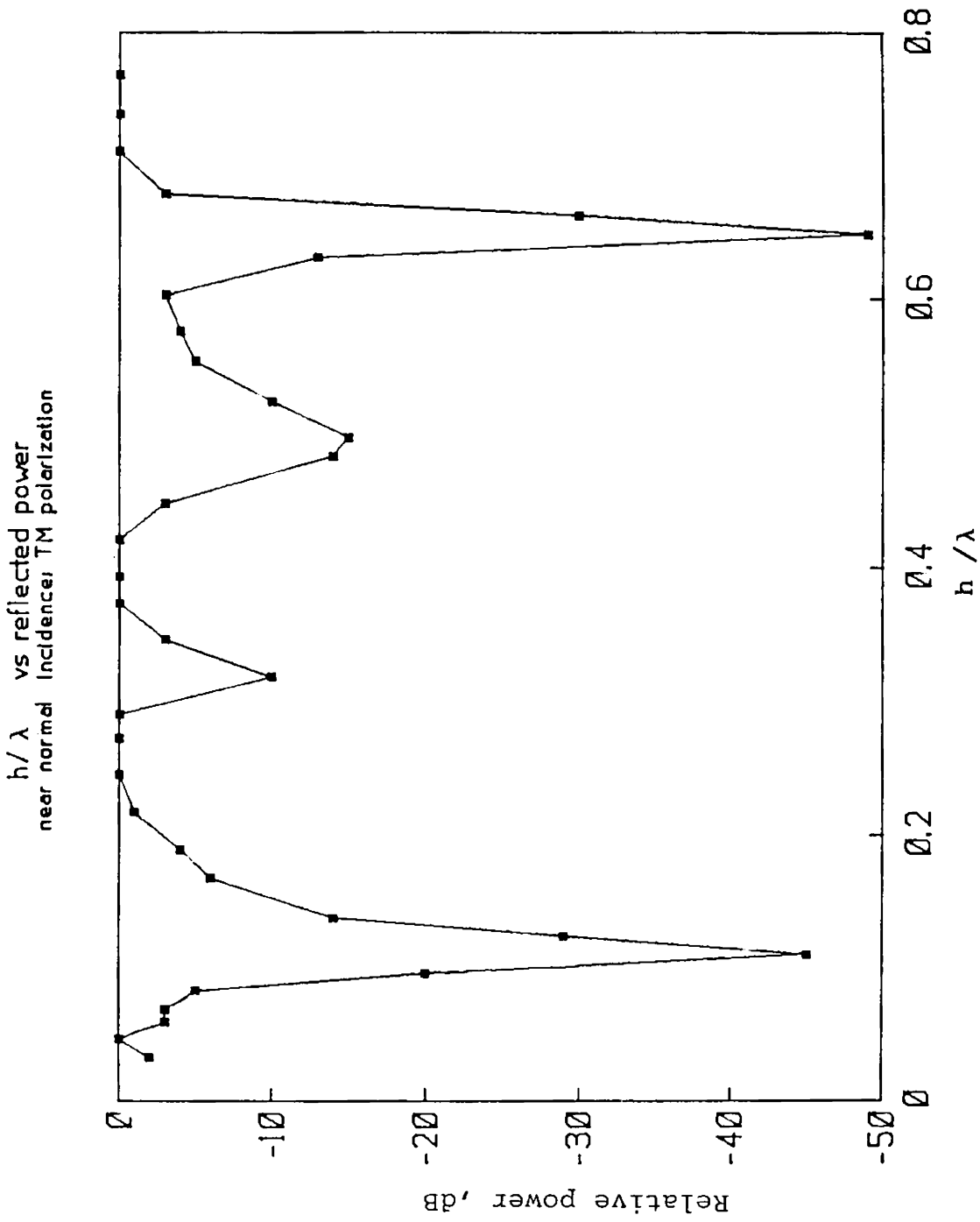
Fig. 4.20. measured back-scattered power for near normal incidence, for different h, the thickness grating S_{14} ; f = 8.30 GHz.

that $b_1 + b_2 + b_1 = 0.5d$ (Fig.3.8) and the observations were repeated. The experimental results are shown in Fig.4.21(i) and (ii). Fig.4.21(i) shows the variation of reflected and back-scattered power for different angles of incidence θ_i, for single periodic strip grating. For perfect blazing, the thickness h of the dielectric sheet is 0.113λ. Fig.4.21(ii) shows the results of dual-periodic strip grating. It exhibit same properties of single periodic grating when the thickness h of dielectric sheet becomes 0.058λ.

In Fig.4.22, a graph is presented in which, the reflected power is plotted against the thickness of dielectric sheet for dual-periodic and single periodic strip gratings.

The frequency behaviour of the multi-element strip grating is shown in Fig.4.23. The slight difference in frequency for single-periodic and dual-periodic gratings is due to the design discripancies. The bandwidth of effective elimination of specular reflection is very much increased by splitting the conducting strips.

4.8 ELIMINATION OF NORMAL INCIDENCE SPECULAR REFLECTION-- MULTI-ELEMENT GRATINGS

The elimination of specular reflection for normal incidence (i.e., low-back-scattering), the characteristic

Reflected power vs angle of Incidence
Strip grating- single period
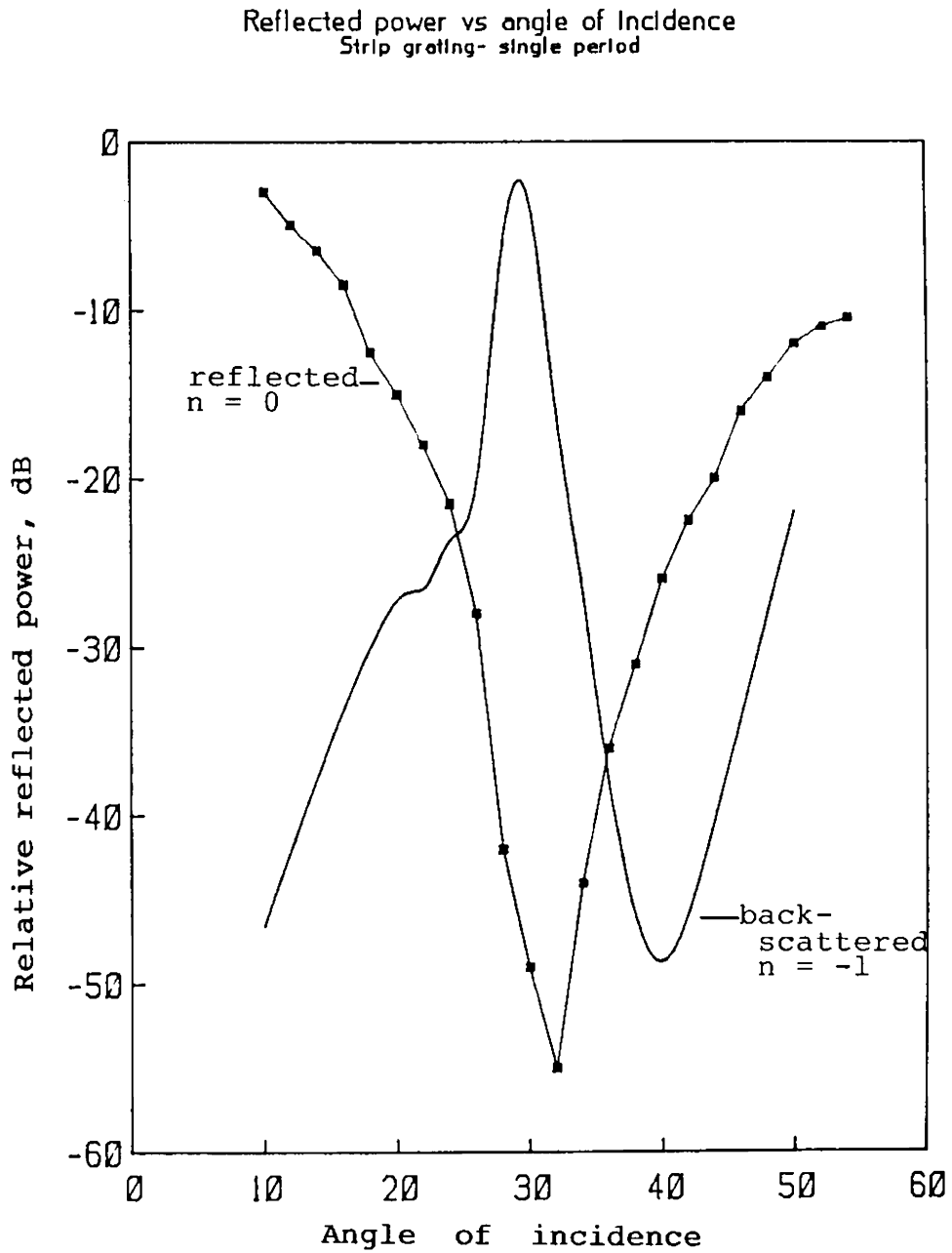
Fig. 4.21 (i). Measured TM polarized reflected and back-scattered power for single-periodic grating system S_9 ; f = 9.650 GHz, h = 0.113λ

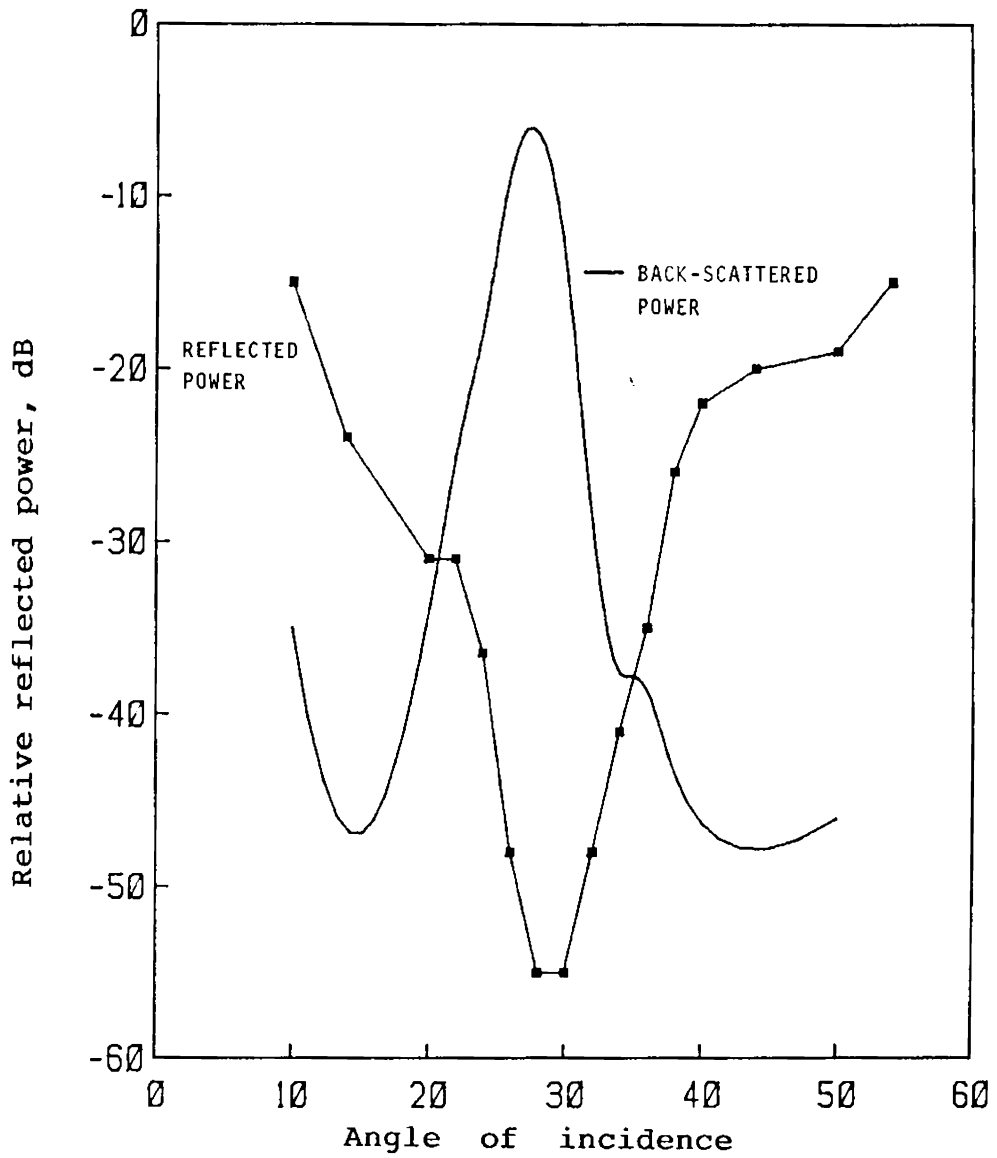Reflected power vs angle of incidence
Strip grating- dual period

Fig. 4.21 (ii). Measured TM polarized reflected and back-scattered power for dual-periodic grating system ; f = 9.850 GHz, h = 0.058λ
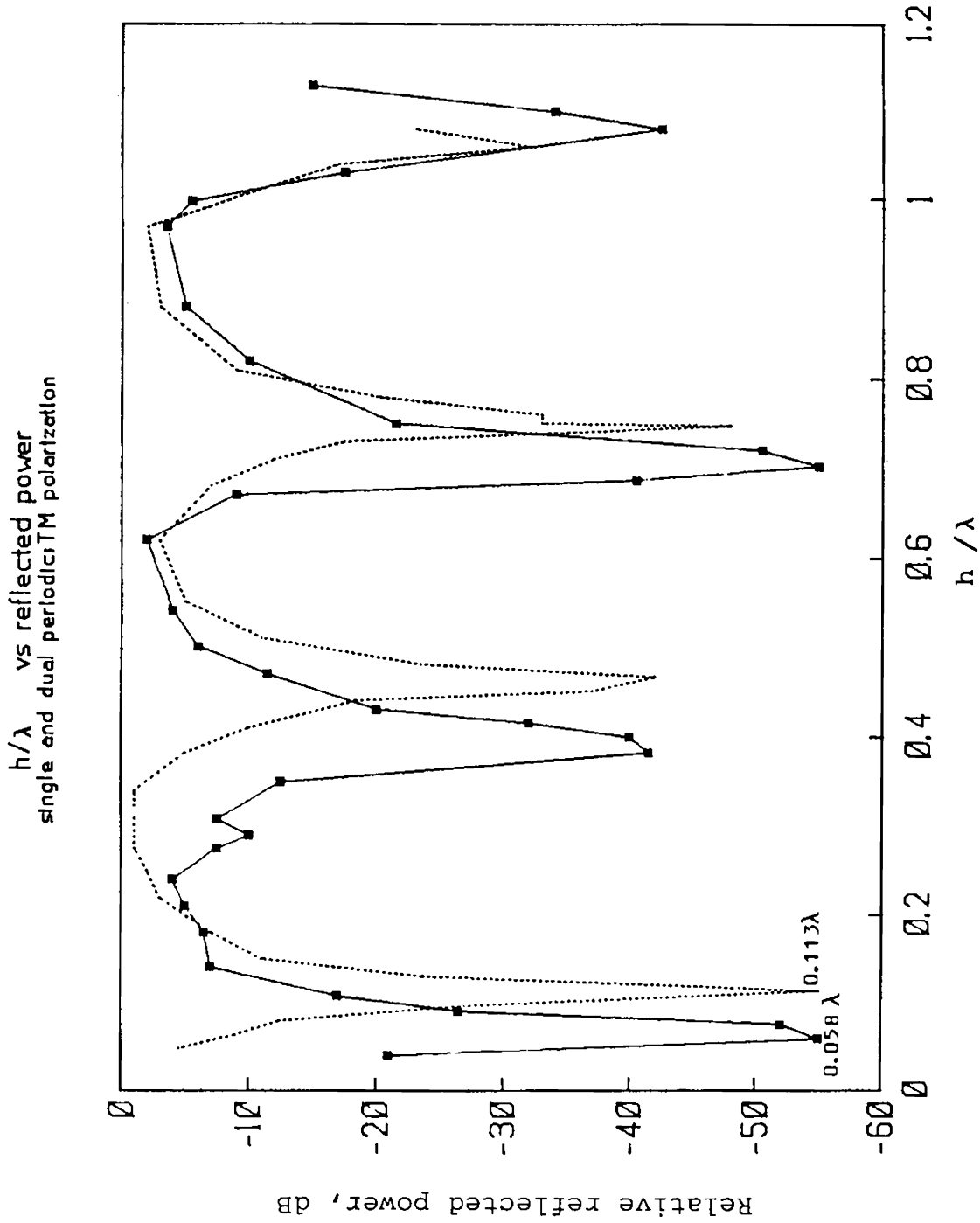
Fig. 4.22. Variation of reflected power due to the change in thickness of dielectric sheet.

Frequency vs reflected power
single and dual periodic
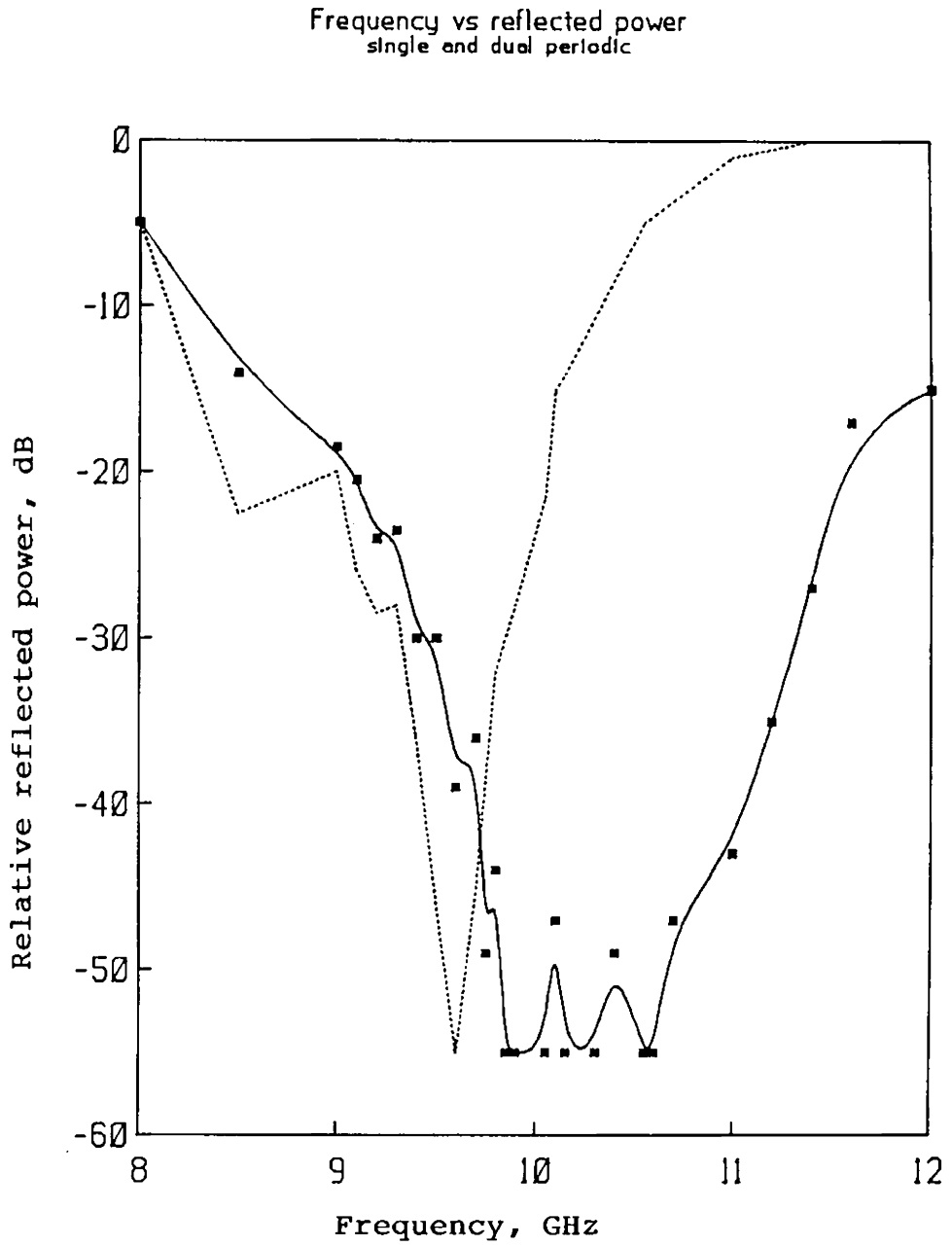
Fig. 4.23. Measured reflected power against frequency
Incident angle, $\theta_i = 30°$

————————— dual periodic
.... single periodic

of a grating system, is also possible for multi-element grating. The strip grating is placed on a turn-table and the back-scattered power is recorded using a magic-tee. The received signal is recorded after proper amplification. Fig.4.24 presents the variation of back-scattered power recorded for different gratings.

There is also considerable reduction in dielectric thickness by employing multi-element gratings. The normal incidence back-scattered power is minimum when the thickness h of the dielectric sheet is 0.042λ for multi-element system and the same result is obtained for single periodic system for h = 0.082λ.

Fig.4.25 shows the performance comparison between the single and dual-periodic gratings. The reflected power is recorded for θ_i = 5°, (near-normal incidence) at different frequencies. From the figure, it is clear that dual-periodic grating system shows better performance, compared to single periodic gratings. The back-scattering level is much smaller.

4.9 LIMITATIONS

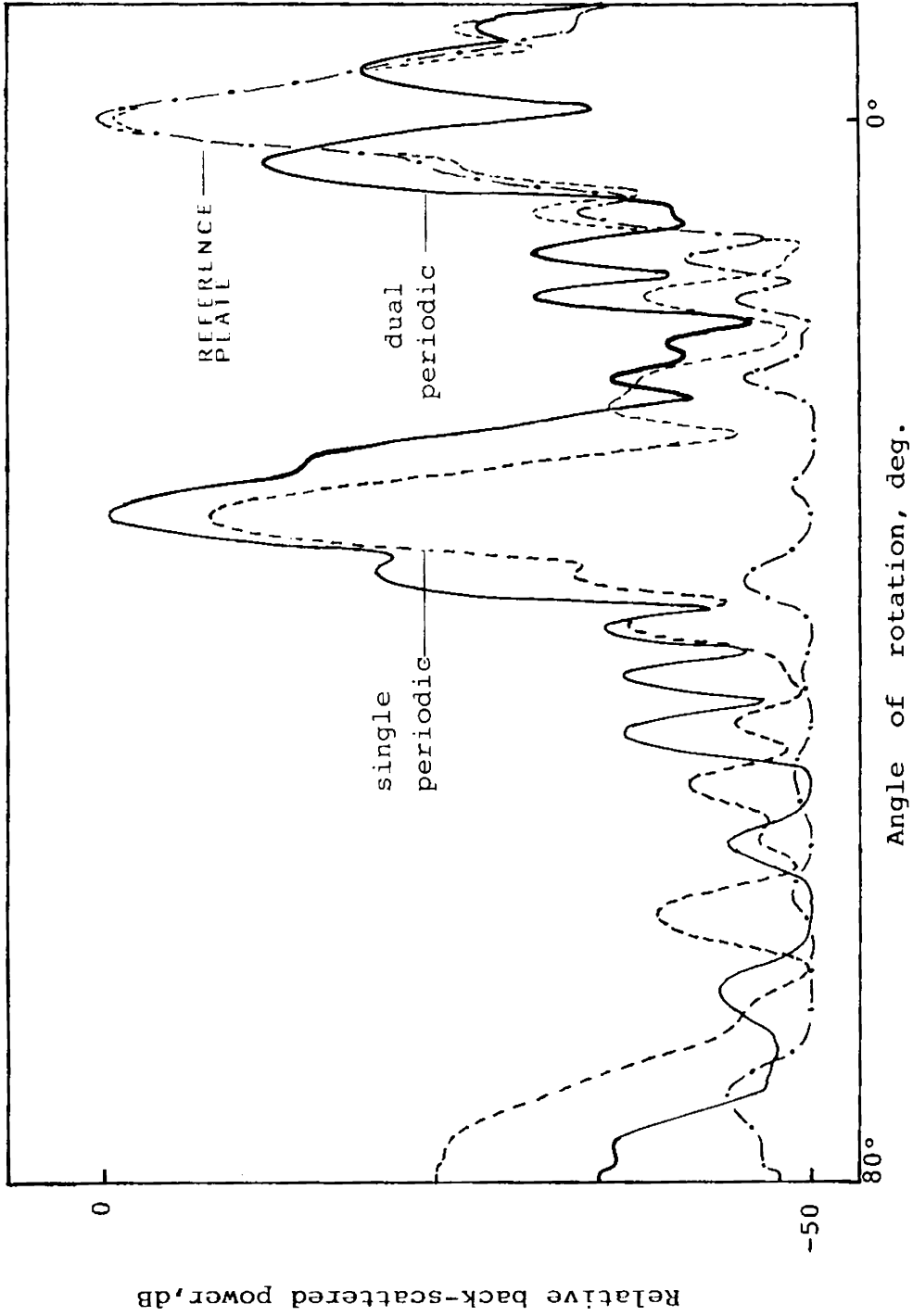It is not possible to increase the coupling gap b_2 in dual-strip grating beyond certain limit. Normal blazing

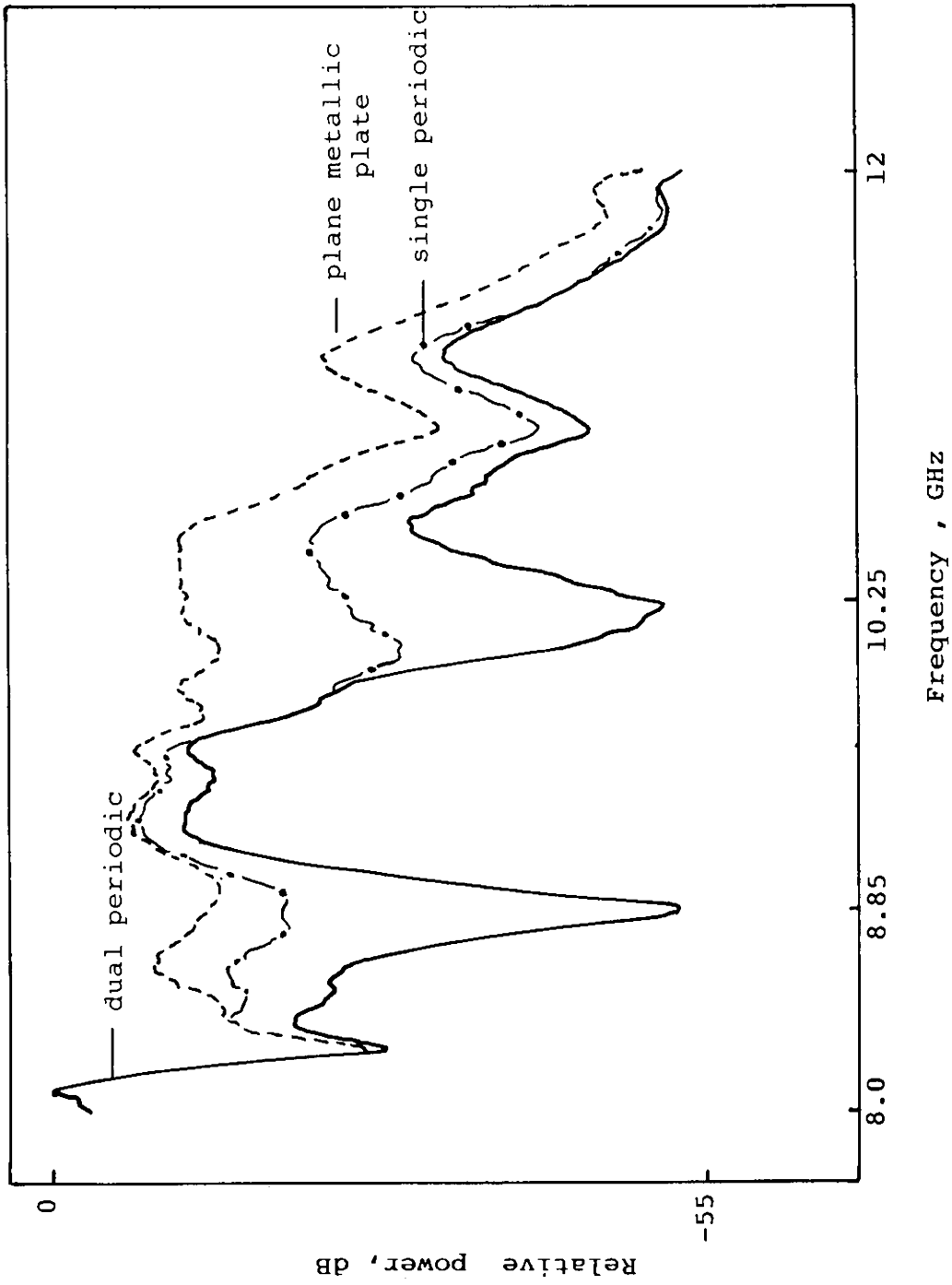Fig. 4.24. Recorded variation of back-scattered power for different gratings monostatic method, f = 9.850 GHz.

Fig. 4.25. Performances of single and dual periodic gratings against change in frequency, bistatic method; $\theta_i = 5°$
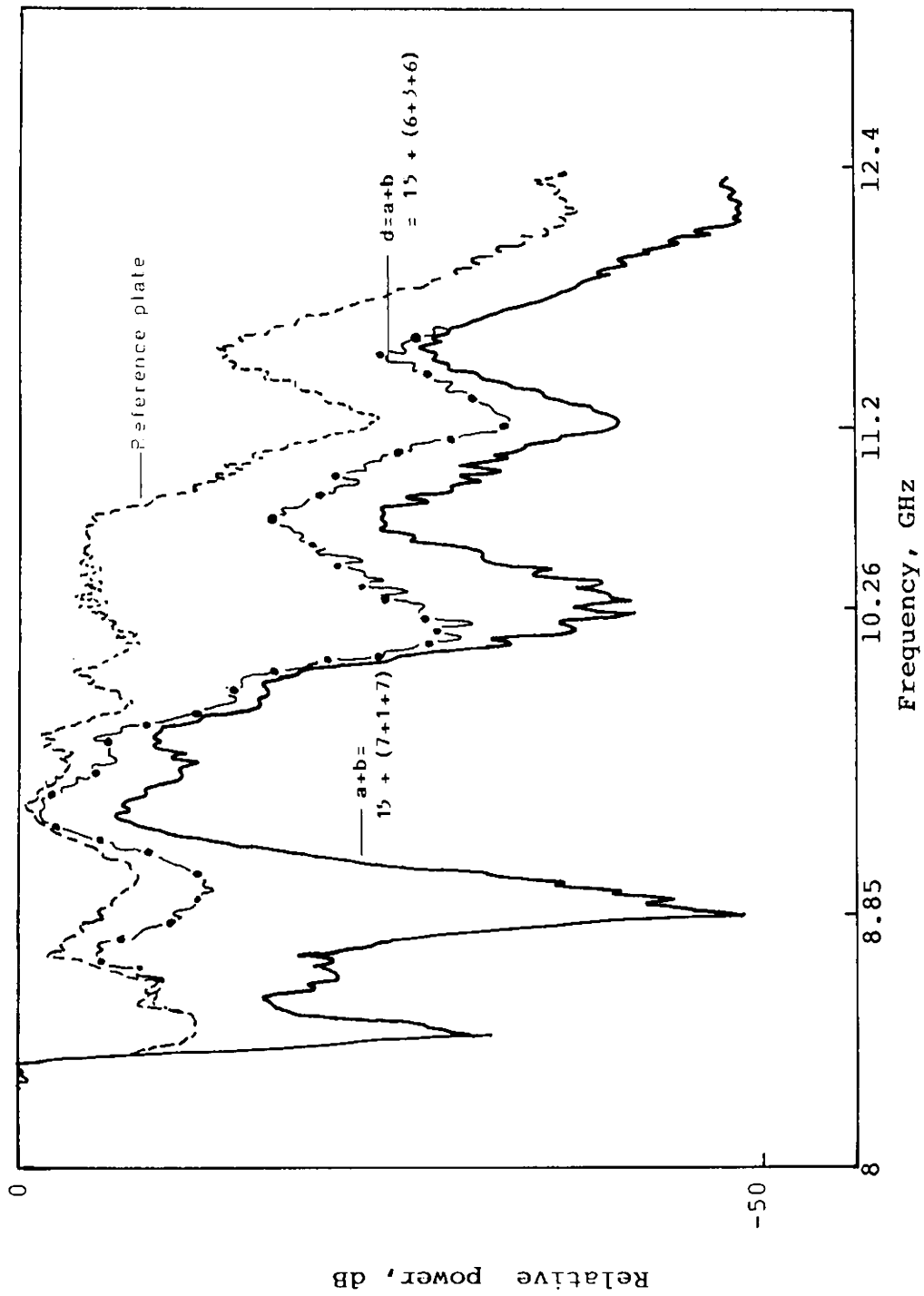
Fig. 4.26. Measured reflected power for dual periodic gratings of different spacing; bistatic, $\theta_i = 5°$.

properties are obtained for a gap-width less than 0.066λ . If the spacing b_2 is further increased, the property of elimination of specular reflection will gradually vanish and the grating will act as a single periodic system. Fig.4.26 shows the performance comparison of gratings with different coupling gap. The limiting factor in this case is depending on the incident wavelength and the dielectric medium between the reflector and the grating elements.

The non-availability of dielectric sheets of appropriate electrical properties and required thickness restricted the present study to concentrate only on a single medium of $\varepsilon_r = 2.57$. For proper analysis, the most essential condition is the perfection of the plane dielectric sheets with respect to the thickness and uniformity.

Chapter   5

NUMERICAL   RESULTS

147

Chapter 5

NUMERICAL RESULTS

5.1 INTRODUCTION

The objective of this chapter is to present a theoretical explanation for the observed phenomena of scattering from periodic strips over a dielectric sheet with a conducting ground plane. Numerical solutions for scattering from periodic strips are available in literature [99,116-118, 155]. Richmond [127] developed a convergence solution for a strip and for strip grating, in which the basis function include the edge mode. This shows great improvement in convergence of the moment method solution with entire-domain expansion function. In this chapter, the same technique is extended to find the solutions for a strip grating with metallic ground plane. The scattering from a single period is determined first and is expanded to N such elements.

Here, the strips are considered to be perfect conductors with infinite length and negligible thickness. The current density on the strip is expanded as Fourier series, and simultaneous linear equations are developed.
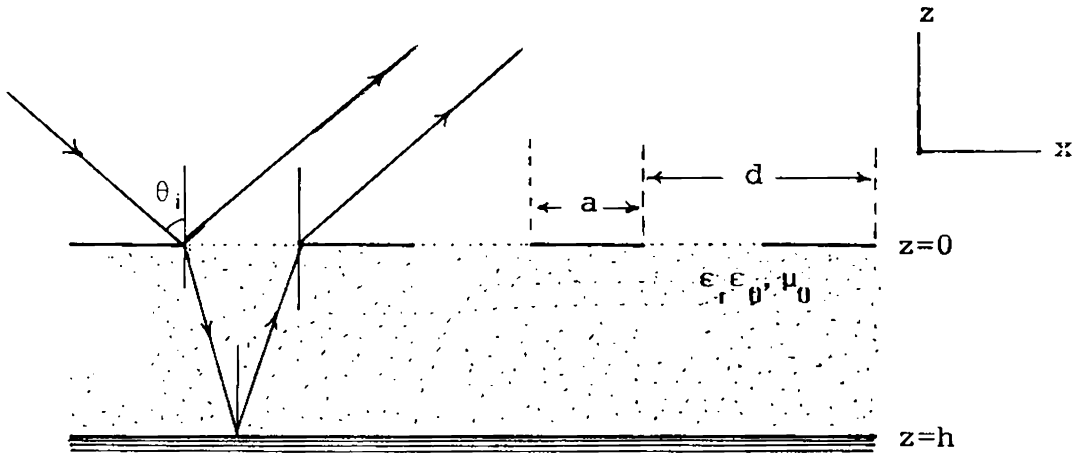
148

5.2 FORMULATION OF THE PROBLEM

Fig. 5.1 Structure of the reflector-backed strip grating.

The dielectric sheet of thickness h loaded with a periodic array of perfectly conducting thin strips over a ground plane is shown in Fig.5.1. The dielectric is assumed to be lossless with parameters $\varepsilon_r \varepsilon_0$ and μ_0 where ε_r is the dielectric constant and ε_0, μ_0 the permittivity and permeability of free space. The conducting strips of width 'a' are fixed at a separation 'b' having period d. Consider a time-harmonic plane electromagnetic wave in free space, having an incident angle θ_i on this periodic array. The incident magnetic field intensity is

$$H_i = \hat{a}_y \, H_o \, \exp[-j(\beta x + \gamma z)] \tag{1}$$

The time harmonic factor $e^{j\omega t}$ is suppressed here for avoiding repetitive reproduction.

The scattered field, which is the sum of the fields reflected from the periodic strips and that from the dielectric and ground plane, is given by

$$H_s = \hat{a}_y H_o R_1 \exp[-j(\beta x + \gamma z)] +$$

$$\hat{a}_y H_o R_2 \exp[-j(\beta x + \gamma z)] \tag{2}$$

where

$$\beta = k_o \sin \theta_i \tag{3}$$

$$\gamma = k_o \cos \theta_i \tag{4}$$

and R_1 is the reflection coefficient of the strip grating alone and $R_2 = (1 + R_1)R$, R being the reflection coefficient for the gap. The total reflection coefficient of the system is calculated by the vector addition of R_1 and R_2.

5.2.1 Evaluation of R_1

The scattered fields from the strip alone are given by

$$E_s = \hat{z} E_o \exp(jkx \sin \theta_i) \sum_{-\infty}^{\infty} a_n \exp(-\gamma_n |z|)$$
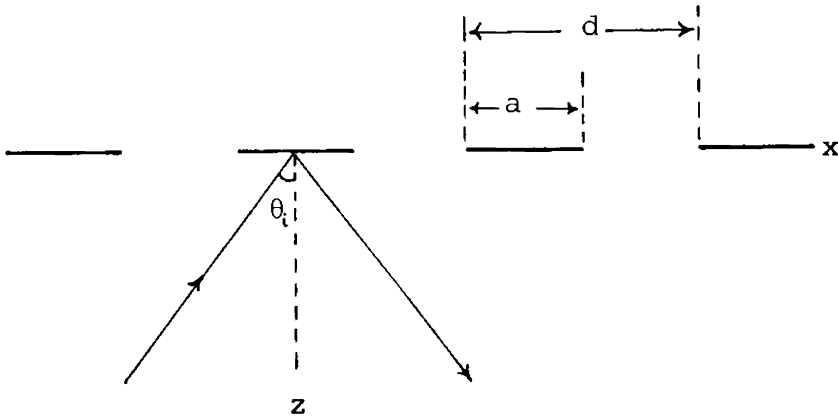
$$\exp(j2n\pi x/d) \tag{5}$$

Fig. 5.2 Geometry of the planar array of strips
d = a+b,   a = 2s.

and $H_x^s = \hat{a}_y \dfrac{E_o}{j\omega\mu}$ exp(jkx sin θ_i)

$$\sum_{-\infty}^{\infty} a_n \gamma_n \exp(-\gamma_n |z|) \exp(j2n\pi x/d) \tag{6}$$

where

$$\gamma_n = (k \sin\theta_i + 2n\pi/d)^2 - k^2 \tag{7}$$

and θ_i is the angle of incidence.

The surface current density $\vec{J}$ can be expanded as a Fourier series.

$$\vec{J} = \hat{y} \exp(jkx \sin\theta_i) \sum b_\ell \exp(\ell\pi x/s) \tag{8}$$

Applying boundary condition on tangential H,

$$E_o \sum a_n \gamma_n \exp(j2n\pi x/d) = \begin{cases} \dfrac{-i\,k\eta}{2} \sum b_\ell \exp(j\ell\pi x/s), & -s < x < s \\ 0. & \text{in the apertures} \end{cases} \tag{9}$$

where $\eta = \sqrt{\mu/\epsilon}$.   Multiplying both sides of equation (9) by $\exp(j2n\pi x/d)$ and integrating between $-d/2$ and $d/2$, we get

$$a_o = \frac{-\eta a b_0}{2dE_o \cos\theta_i} \tag{10}$$

$$a_n = \frac{-jk\eta}{2d\gamma_n E_o} \Sigma\ b_\ell\ F_{\ell n} \tag{11}$$

$$F_{\ell n} = \int_{-s}^{s} \exp[j2\pi(\ell/a - n/d)]x\ dx \tag{12}$$

$$= \frac{a\ \sin\pi\ (\ell - na/d)}{\pi(\ell - na/d)} \tag{13}$$

$$Z_{i\ell} = \frac{jk\eta}{2da} \sum_n \frac{F_{\ell n}^* F_{in}}{\gamma_n} \tag{14}$$

The numerical data is found by substituting (13) in (14) and solving equation (14)

$$Z_{i\ell} = \frac{jk\eta}{2ad} \sum_{-\infty}^{\infty} \left[\frac{a\ \sin\pi(\ell-na/d)}{\pi(\ell-na/d)}\right]^* \left[\frac{a\ \sin\pi(\ell-na/d)}{\pi(\ell-na/d)}\right] \Big/ \gamma_n \tag{15}$$

Applying boundary conditions for E tangent on the conducting strips, we have,

$$\sum_n a_n \exp(j2n\pi x/d) = -1; \quad -a/2 < x < a/2 \tag{16}$$

Multiplying both sides of the above equation with $\exp(-ji\pi x/s)$ and integrating over the region $-s < x < s$, we get,

$$\sum_n a_n F_{in}^{*} = \begin{cases} -a & \text{if } i = 0 \\ 0 & \text{if } i \neq 0 \end{cases} \tag{17}$$

Substituting the values of a_o and a_n from equations (10) and (11), equation (17) yields the following set of simultaneous linear equations.

$$\sum_\ell b_\ell Z_{i\ell} = V_i \qquad i = 0, \pm 1, \pm 2, \ldots$$

i.e., $[b][Z_{i\ell}] = [V_i]$ \hfill (18)

$$[b] = [V_i][Z_{i\ell}]^{-1} \tag{19}$$

where $V_o = E_o$ and $V_i = 0$ if $i \neq 0$.

Substituting the value of $[b_o]$ from equation (19) in equation (10), the $n = 0$ mode reflection coefficient of the strip

grating alone is given by,

$$R_1 = a_o = (x_o + iy_o) \tag{20}$$

$$= -\eta ab_o/2dE_o \cos\theta_i$$

where x_o is the real part of a_o and y_o is the imaginary part of a_o. In general R_1 is complex in nature, so the resultant amplitude of the reflection coefficient is the absolute value of a_o. The phase of the reflection coefficient is given by

$$\phi = \tan^{-1}[y_o/x_o] \tag{21}$$

and the transmission coefficient as

$$T = 1 + R_1 \tag{22}$$

Equation (20) is solved using the available LSACG routine in IMSL for solving complex linear equations.

5.2.2 Determination of R_2

The incident and reflected fields in dielectric metallic ground plane boundary are
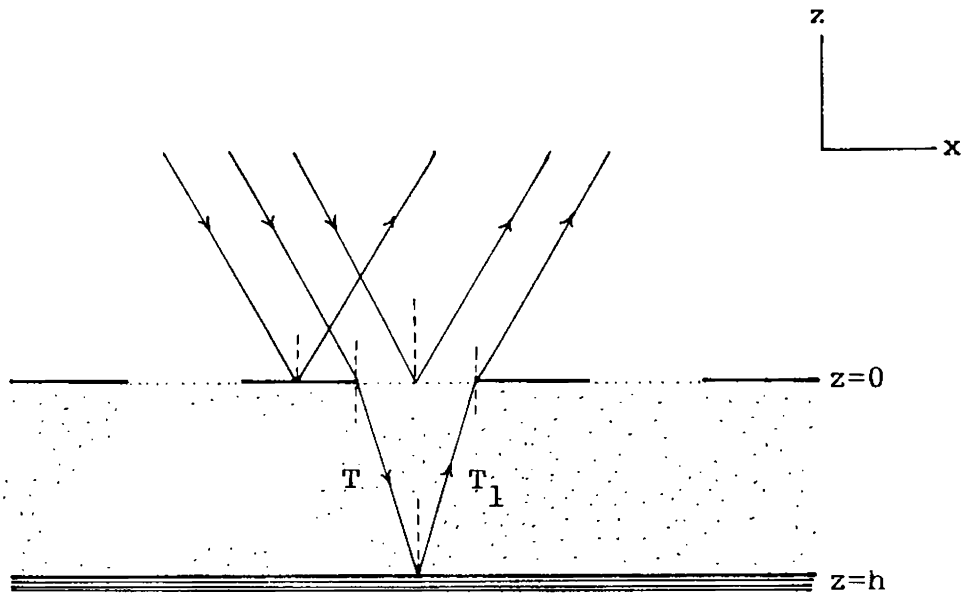
Fig. 5.3 Arrangement of reflector-backed strip grating under consideration with co-ordinates

$$H_{d_1} = \hat{a}_y \, H_o T \, \exp[-j(\, \beta x + \gamma_d z \,)] \tag{23}$$

$$H_{d_2} = \hat{a}_y \, H_o T_1 \exp[-j(\, \beta x - \gamma_d z \,)] \tag{24}$$

where

$$\beta = k_o \sin \theta_i$$

$$\gamma = k_o \cos \theta_i$$

$$\gamma_d = \sqrt{k^2 - \beta^2}$$

$$k_o = 2\pi / \lambda$$

$$k = k_o \sqrt{\varepsilon_r}$$

The corresponding electric fields are,

$$E_{d_1} = \hat{a}_x \frac{H_0}{\omega\epsilon} T \gamma_d \exp[-j(\beta x + \gamma_d z)]$$

$$-\hat{a}_z \frac{H_0}{\omega\epsilon} \beta T \exp[-j(\beta x + \gamma_d z)] \qquad (25)$$

$$E_{d_2} = -\hat{a}_x \frac{H_0}{\omega\epsilon} T_1 \gamma_d \exp[-j(\beta x - \gamma_d z)]$$

$$-\hat{a}_z \frac{H_0}{\omega\epsilon} \beta T_1 \exp[-j(\beta x - \gamma_d z)] \qquad (26)$$

Since the above equation must be valid for all values of x and the exponential functions are linearly independent as the values of x, and the equation must hold termwise. Applying boundary conditions for tangential component of E at Z = h,

$$E_{d_1} = -E_{d_2}$$

$$\therefore T_1 = T \exp(-2j \gamma_d z) \qquad (27)$$

Substituting the value of T_1 in equation (25) and (26)

$$E_{d_1} = \hat{a}_x \frac{H_0}{\omega \epsilon} \, T \, \gamma_d \exp[-j(\beta x + \gamma_d z)]$$

$$-\hat{a}_z \frac{H_0}{\omega \epsilon} \, \beta \, T \, \exp[-j(\beta x + \gamma_d z)] \qquad (28)$$

$$E_{d_2} = \hat{a}_x \frac{H_0}{\omega \epsilon} \, \gamma_d \, T \, \exp(-2j \, \gamma_d h) \exp[-j(\beta x - \gamma_d z)]$$

$$-\hat{a}_z \frac{H_o}{\omega \epsilon} \, \beta \, T \, \exp(-2j \, \gamma_d h) \exp[-j(\beta x - \gamma_d z)] \qquad (29)$$

The total electric field inside the dielectric is,

$$E_{d_i} = (1-R_1) \frac{H_0}{\omega \epsilon} T \, \exp(-j\beta x)$$

$$[\hat{a}_x \, \gamma_d \{ \exp(-j\gamma_d z) - \exp[j\gamma_d z (z-2s)] \}$$

$$-\hat{a}_z \{ \beta \, \exp(-j\gamma_d z) + \exp[-j\gamma_d z(z-2s)] \}] \qquad (30)$$

The total magnetic field inside the dielectric is,

$$H_{d_i} = (1-R_1)H_o T \, \exp(-j\beta x) \hat{a}y \, [\exp(-j\gamma_d z) +$$

$$\exp(j\gamma_d z)] \qquad (31)$$

The corresponding magnetic and electric fields in air are

$$H_{air} = (1-R_1)H_o \, \exp(j\beta x) \{ \exp(-j\gamma z)$$

$$+ R \, \exp(j\gamma z) \} \, \hat{a}_y \qquad (32)$$

$$E_{air} = (1-R_1)\frac{1}{\omega\varepsilon_0} \exp(j\beta x)$$

$$[\hat{a}_x\{\gamma \exp(-j\gamma z) - \gamma R \exp(j\gamma z)\}$$

$$-\hat{a}_z\{\beta \exp(-j\gamma z) + \beta R \exp(j\gamma z)\}] \qquad (33)$$

Applying boundary conditions for tangential E and H fields at z = 0, we get

$$\frac{\varepsilon_r \gamma(R-1)}{\gamma_d[\exp(-2j\gamma_d s) - 1]} = \frac{1+R}{1+\exp(-2j\gamma_d s)} \qquad (34)$$

where

$$\varepsilon_r = \varepsilon/\varepsilon_0$$

$$R = \frac{P+Q \exp(-2j\gamma_d s)}{Q+P \exp(-2j\gamma_d s)} \qquad (35)$$

where R is normalized reflection coefficient for the gap

$$P = \varepsilon_r \gamma - \gamma_d$$

$$Q = \varepsilon_r \gamma + \gamma_d$$

and

$$\Phi = \tan^{-1}\left[\frac{(P_1 S_1 + Q_1 T_1)}{(P_1 T_1 - Q_1 S_1)}\right] \qquad (36)$$

where

$$P_1 = P + Q \cos 2\gamma_d h$$

$$Q_1 = Q \sin 2\gamma_d h$$

$$S_1 = Q + P \cos 2\gamma_d h$$

$$T_1 = P \sin 2 \gamma_d h$$

$$R_2 = (1+R_1) R$$

The total reflection coefficient of an element is ,

$$R_1 \exp(j \phi_1) + (1+R_1 \exp(j\phi_1) R \exp [-j(\phi +\alpha)] \qquad (37)$$

where,

$$\alpha = k_o \frac{d}{2} \sin \theta_i$$

Using array principle, it is possible to evaluate the reflection coefficient of N such elements.

5.3 CONCLUSION FROM THEORETICAL CALCULATIONS

Substituting the value of b_o from equation (19) in equation (10) and solving for a_o, we get the reflection coefficient of the strip grating alone, as shown in Fig.5.4. This graph shows the variation of reflection coefficient with normalized grating period d. It is predicted theoretically that minimum reflection occurs when $d/\lambda = 1$ for normal incidence , corresponding to $a/d = 0.5$.

The total reflection coefficient of the system and hence the reflected power is given by solving equation (35) for R and then by vector addition of R_1 and R, using equation (37). The theoretical and experimental results of the back-scattered power are shown in Fig.5.5. The variation of back-scattered power due to the variation of the grating period d is determined numerically and the experimental results are found to be in agreement with it. For a reflector-backed strip grating the minimum back-scattering occurs when $d = \lambda$ for $a/d = 0.5$. Theoretical results also confirm this result.

The normal incidence low back-scattering is measured experimentally for a self-complementary strip grating, for the thickness of dielectric medium $h = 0.078\lambda$ (Fig. 4.17). The variation of scattered power for normal incidence
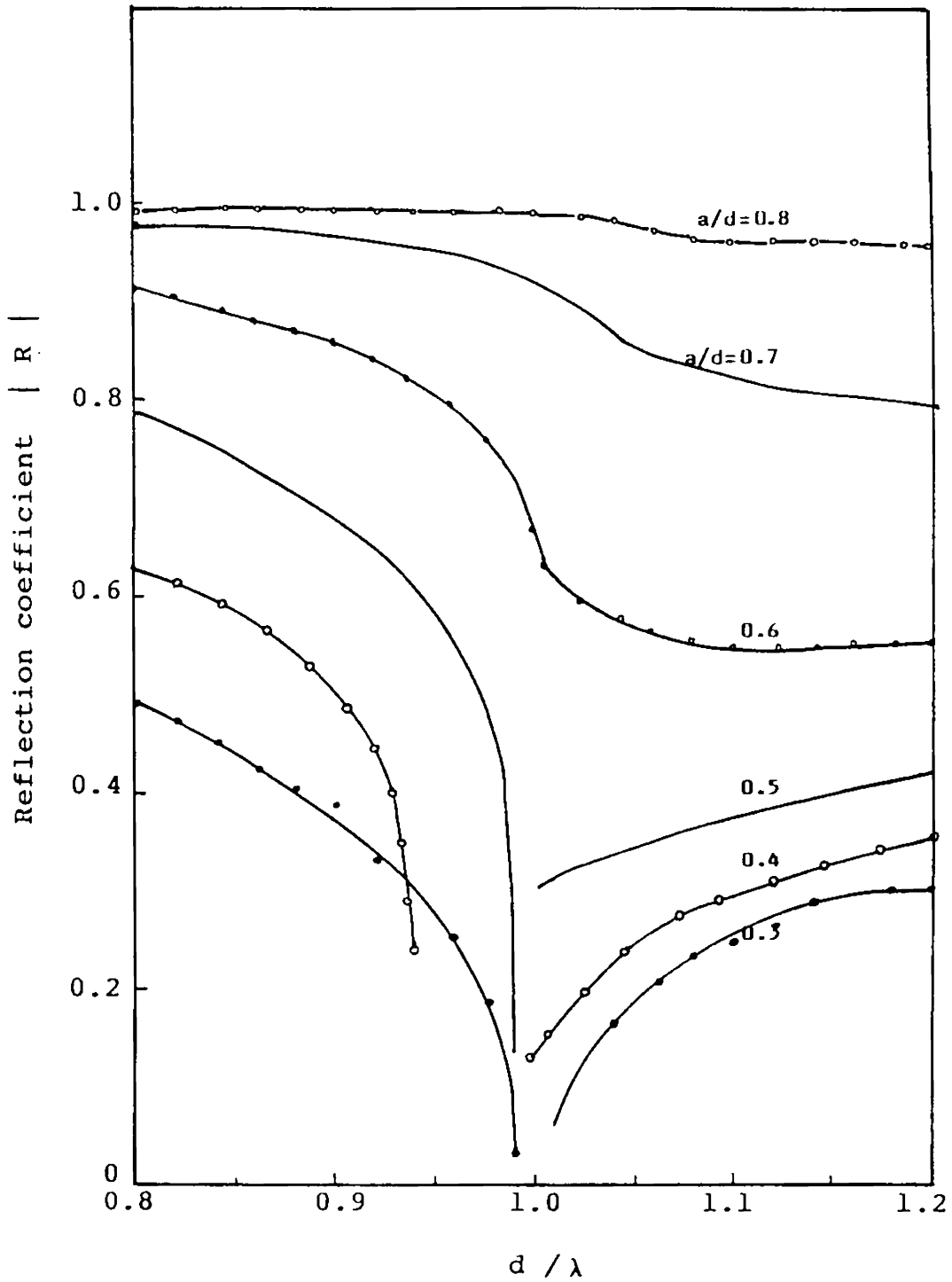
Fig. 5.4 Variation of reflection coefficient against period for strip grating alone.[Richmond's theory]
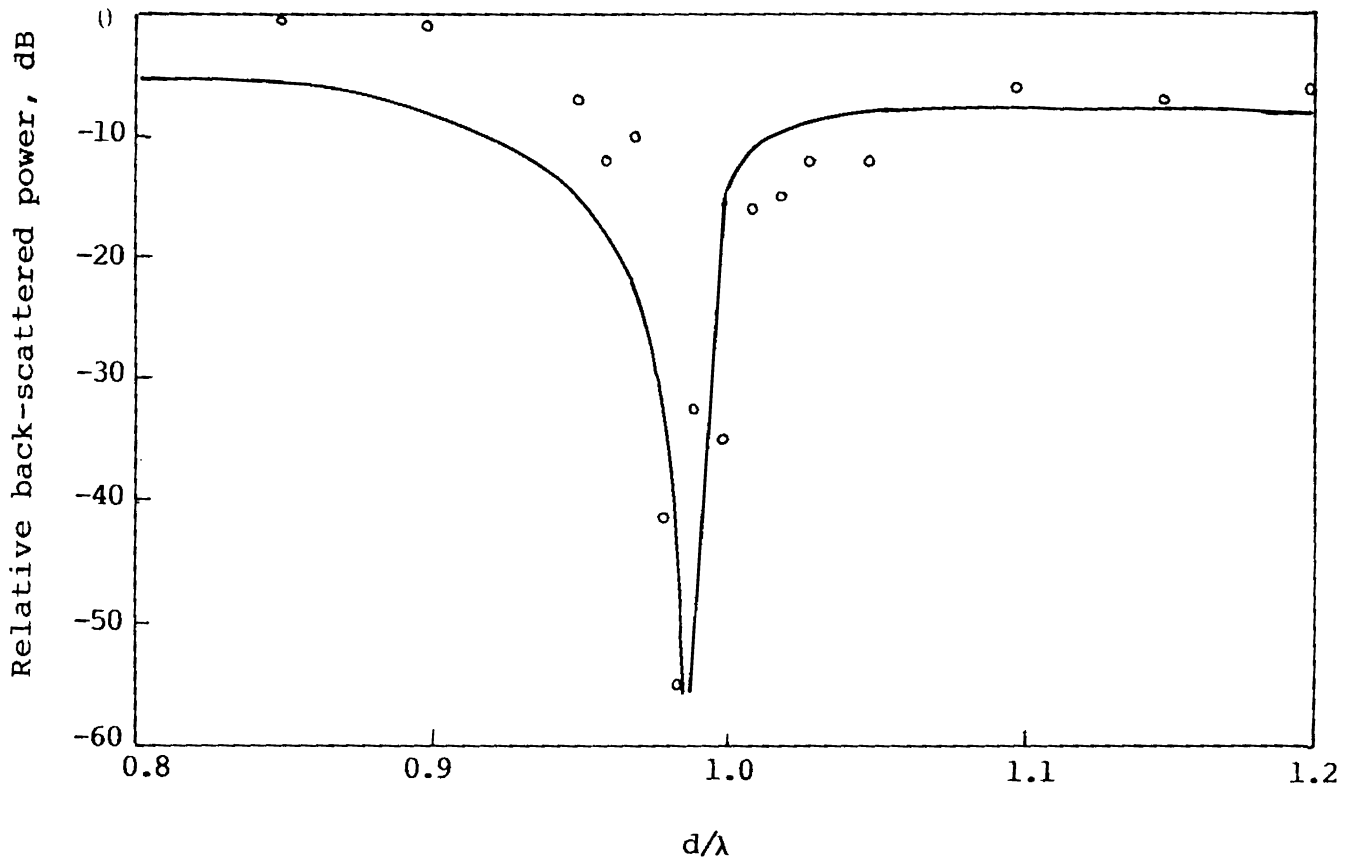
Fig. 5.5 Variation of back-scattered power against grating
period d for normal incidence.
h = 0.078 λ ; a/d = 0.5.

———————— Theory   o o o o o o o o Experimental
                                          values

for different angles of observation is shown in Fig.5.6. The normal incidence back-scattered power is minimum in both experiment and theory, and maximum scattering is observed when the receiving angle is 90°.

According to the above theory, when back-scattered power is minimum, most of the power is scattered to an angle 90°. This could be explained with the help of Bragg's law, which gives the condition for 90° scattering. However, the analysis using the present theory also incorporates the power scattered in other directions, since the theory is consistent with Bragg's law and the direction in which the maximum power is scattered.

Fig.5.7 shows the variation of back-scattered power due to the change in the thickness of the dielectric sheet h. Theoretical results show that minimum back-scattering occurs when the thickness of the dielectric sheet h = 0.079 λ . The experimental results are exactly following the theoretical values.

The variation of specularly reflected power for near-normal incidence is calculated and is shown in Fig.5.8.
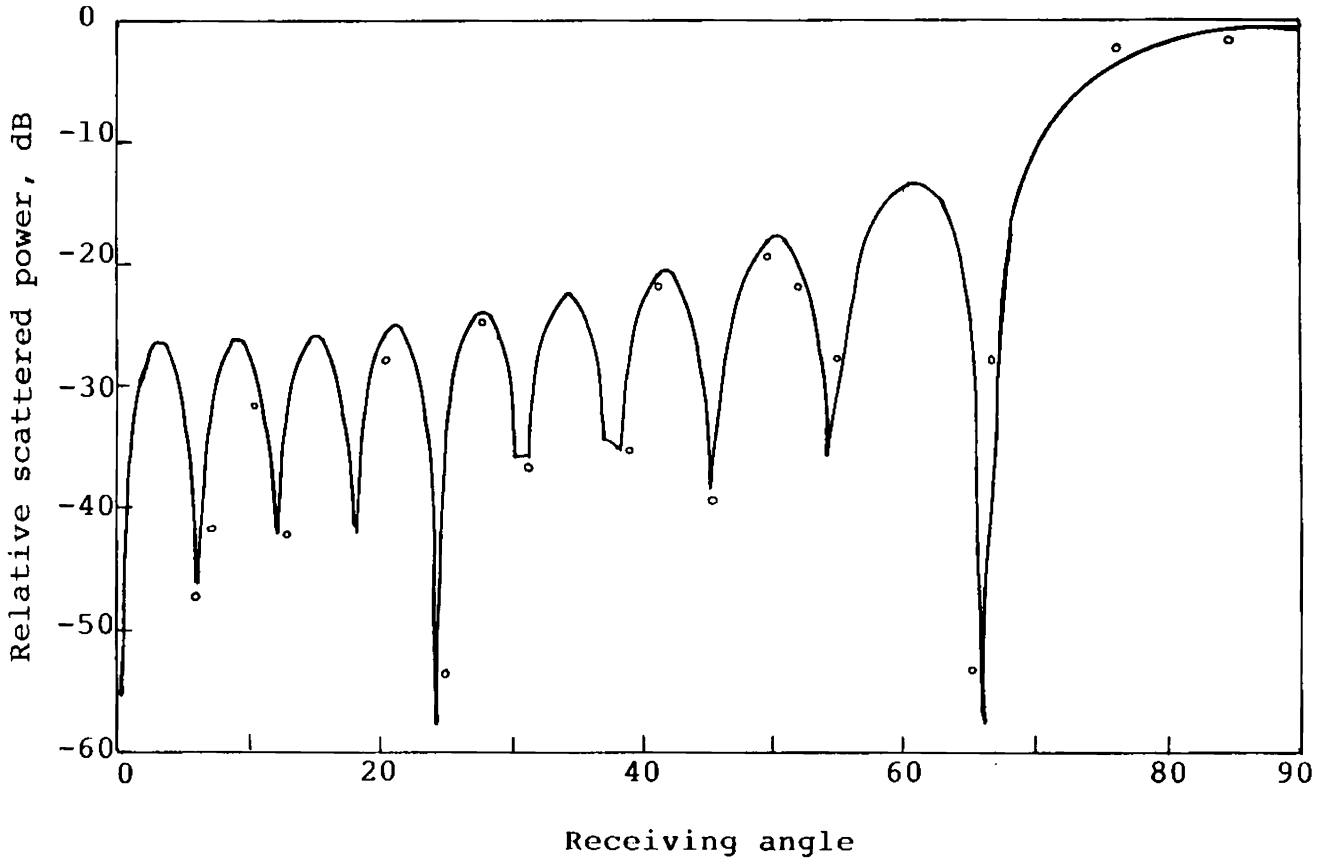
Fig. 5.6 Variation of scattered power for normal incidence
for different angle of observation.
h = o.078 λ ; a/d = 0.5 ; f = 9.751 G Hz

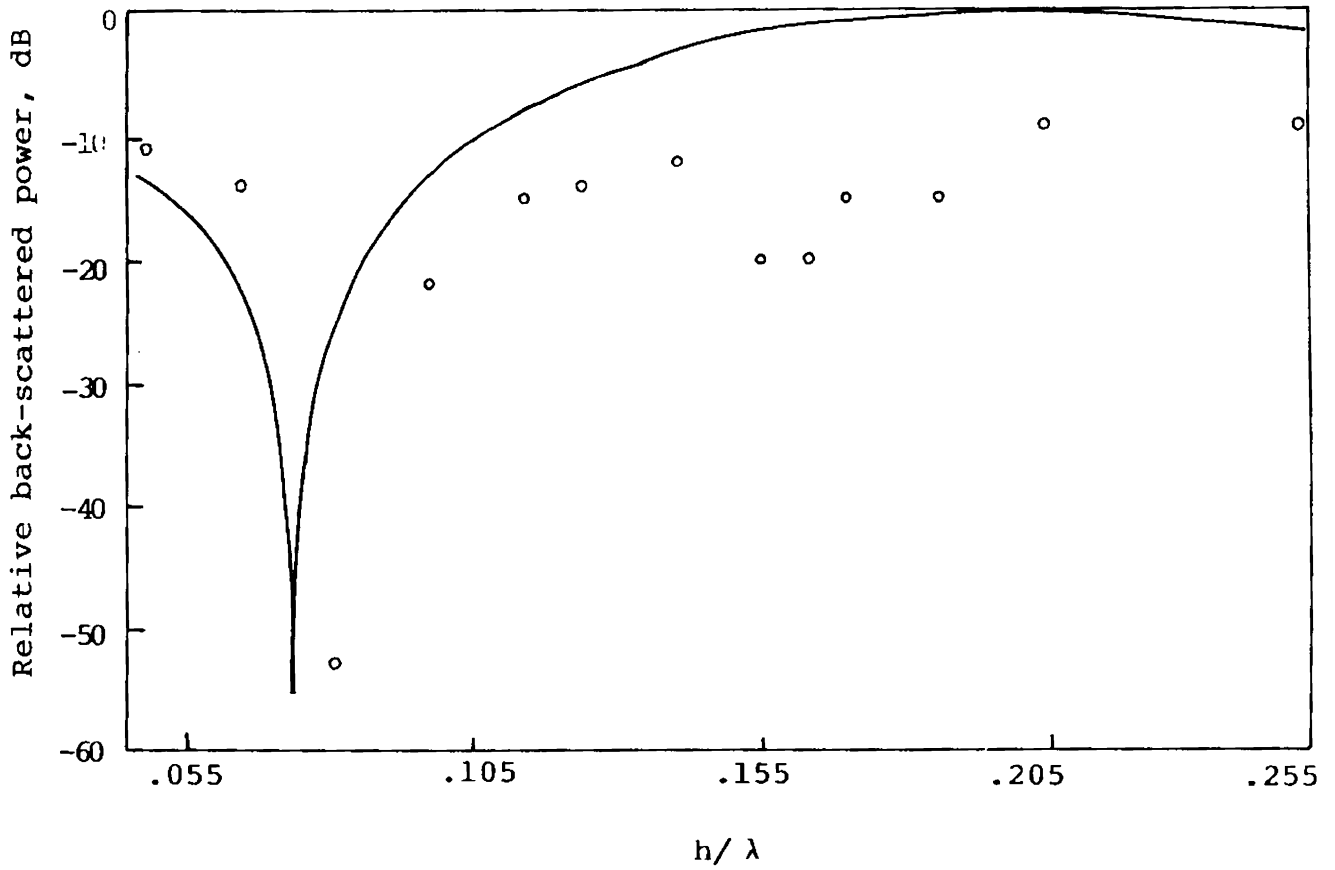————— Theory   o o o o o o o o Experimental
values

Fig. 5.7 Variation of the back-scattered power against the change in the thickness of the dielectric sheet, h

——————— Theory   o o o o o o o o o o Experimental values

a = 0.5 d   f = 10.635 GHz.
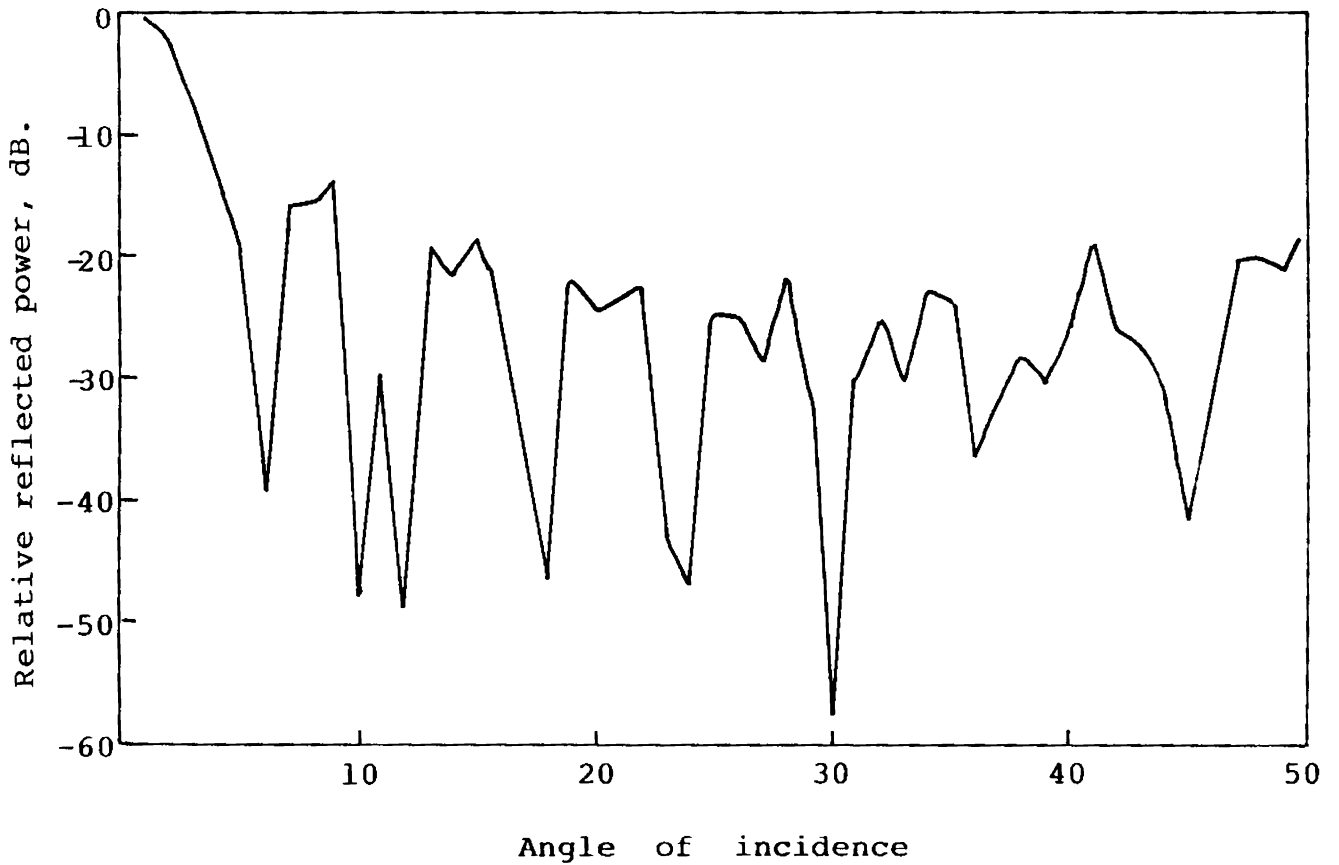
Fig. 5.8 Variation of specularly reflected power for different
incident angles.

h = 0.078 λ   ;   a/d = 0.5 . f = 9.751 GHz

The above theory is adequate to explain most of the experimental observations, especially for normal incidence. However, the theory developed is not fully satisfying the scattering behaviour of other incident angles. This may be due to the following assumptions and approximations in the theory.

It is assumed that the strip is not blocking any reflected energy. This is true in normal incidence. But when the angle of incidence is changed from normal to other angles, the reflected energy would be blocked in between the strip and the ground plane. This is ignored in the theory. However, in normal incidence, the blockage is almost zero and predicts·the experimental results accurately.

To predict the specular reflection behaviour for other angles, the theory requires further modifications and this is left for future work.

Chapter 6

CONCLUSIONS

Chapter 6

CONCLUSIONS

1. INTRODUCTION

This chapter presents the main conclusions drawn from the experimental investigations and theoretical analysis of the strip grating system, which possesses the properties of reduction of RCS of metallic targets. Eventhough, the main aim is development of a technique to reduce RCS of planar surfaces, the present study is concentrated in determining the reflected and back-scattered power-level from the metallic targets and thus to estimate their reflectivity. The electromagnetic power reflected from plane metallic targets are compared with that from strip grating system. From these, it would be possible to evaluate the level of RCS of the target. This would be beneficial in many ways, since the absolute value of RCS is not always necessary when the reflectivity of the target is known, provided the other parameters like range, transmitting power, isolation between transmitter and receiver were kept unchanged. The main motivation of the present work is to develop an alternative system for metallic corrugations. Jull et al. [92] presented elaborate investigation

169

of different aspects of metallic corrugations in numerical and experimental methods and they have already established that RCS of a metallic target could be reduced by corrugation techniques. In a way, the present work is an extension of this reported result. The exact estimation of RCS of strip gratings, and implementation of the techniques in real-time targets are leaving enough scope for further work in the field.

6.2 COMPARISON BETWEEN STRIP GRATINGS AND METALLIC CORRUGATED SURFACES

Metallic strips with proper period, on a dielectric sheet, with a conducting ground plane behind it behaves similar to rectangular metallic corrugations, which are widely used at present, for the elimination of specular reflections. The effect of strip gratings is studied in detail and it is found that the strip gratings are superior to metallic corrugations, in many ways.

In metallic corrugations, perfect blazing or elimination of specular reflection is possible only when the depth h of corrugations is nearly 0.25λ . But in strip grating, perfect blazing has been achieved for much lesser thickness of dielectric sheet for both TE and TM polarisations.

Elimination of normal and near-normal incidence specular reflection (low back-scattering) is a problem in metallic corrugated plates. The specularly reflected power is eliminated only for the angle of incidence θ_i between 19.4° and 90° [6] in metallic corrugations. But the back-scattered and reflected power corresponding to normal and near-normal incidence has been eliminated in strip gratings and they behave like non-reflecting conducting surfaces. Thus, the specularly reflected power is almost zero in strip grating system.

The recorded back-scattered power for self-complementary strip grating is shown in Fig.4.15. It is found that for normal incidence, back-scattering is minimum and it is maximum at the blazing angle. The low back-scattering for normal incidence is demonstrated experimentally in Fig.4.16. In this case, the maximum diffracted power is obtained when the receiving angle becomes 90°.

It is observed that the thickness of the dielectric sheet is an important parameter in elimination of back-scattered power. Variation of back-scattered power due to the change in the thickness of the dielectric sheet is shown in Fig.4.17. This minimum thickness for the reduction of back-scattered power is found to be further reduced

in multi-element strip grating (Fig.4.22). The multi-element or dual-periodic strip grating exhibits same effects as single periodic strip grating system. Meanwhile, it would be possible to attain better performances from dual-periodic gratings, compared to single periodic systems.

6.3 THEORETICAL RESULTS

The technique of convergence of moment method solution by Richmond [127] has been extended to explain the scattering from periodic strips over a dielectric sheet with a metallic ground plane. Fig.5.4 shows the theoretical and experimental results obtained using a self-complementary strip grating. Tne back-scattered power is minimum when $d = \lambda$ and this shows excellent agreement with the reflection coefficients plotted by Richmond.

The theory developed in this work is capable of explaining most of the experimental observations corresponding to normal incidence. However, in explaining the scattering for other angles of incidence, the theory seems to be inadequate. In such cases, the experimental results are not in perfect agreement with theoretical computations. The theory needs further modifications and this leaves scope for further work in this field.

6.4 ADVANTAGES AND DISADVANTAGES OF STRIP GRATING SYSTEM

Reflector-backed strip grating show many advantages over metallic corrugations. The most important one is, the case of implementations of strip gratings for reduction of RCS of metallic targets. It is possible to use strip gratings to reduce the reflectivity and hence the RCS, of targets having complex shapes. For targets of such strategic importance, implementation of conventional corrugated surfaces are not possible mainly due to aerodynamical considerations.

The bandwidth of effective elimination of specular reflection is found to be increased very much in the case of strip gratings, compared to metallic corrugations. The reduction of minimum thickness of the dielectric sheet for perfect blazing is another remarkable advantage of the strip gratings.

The main disadvantage in the case of strip grating system is the enhancement of RCS in some direction like blazing angle, though there is enormous reduction in other directions. Using the strip grating technique, it is possible to reduce the monostatic RCS to a considerable extent. But in the case of bistatic, or when the incident angle

is same as the blazing angle, the reduction is not very significant. This again is a problem for further investigation in the field.

6.5 SCOPE FOR FURTHER WORK IN THIS FIELD

Implementation of the strip grating technique in real-time targets like models of aircrafts, ships and reduction of their RCS is an important work to be taken up in this area. These complex shapes need much attention and careful analysis for implementing strip grating technique. This is because, each portion of such targets must have different types of strip configuration. For example, for an aircraft, 'nose-on-incidence RCS' can be reduced very much by strip gratings of regular period. But the same configuration may not be successful for wings and planar portions. More detailed investigation could be carried out in these directions.

RCS reduction of planar metallic targets for normal incidence could be achieved by the present work. It may be interesting to investigate whether this technique is extendable to targets of other regular shapes, namely cylinders, spheres etc.

Splitting the strips into two parts to form a multi-element or dual-periodic strip grating, has been suggested in the thesis. The advantages of this system have not been fully studied. The splitting of strips may enhance the elimination of specular reflection corresponding to normal and near-normal incidence in many ways. It is possible to take different parameters like, spacing, changes in period etc. for detailed study of the broken strips in different dimensions. This also is a problem of interest for further studies.

The dielectric constant of the medium in between the strips and the ground plane, is another parameter which may be added to the theory. The effect of different dielectric materials for RCS reduction may be taken up for detailed theoretical and experimental investigations.

The main disadvantage encountered in the present study is the enhancement of RCS in certain angles like blazing angles. This requires a further detailed investigation. The elimination of specular reflections for wider angles of incidence may be possible by the critical selection of different grating periods and the spacing between the elements.

Other areas for future work in this field would include the study of broken strips. The particular structure with regular and irregular broken strips can change reflectivity level of targets. The final goal in the above study should be to achieve complete reduction of RCS of targets for all aspect angles.

A P P E N D I C E S

A MICROWAVE METHOD FOR MONITORING THE CURING CONDITIONS
OF A SOLID ROCKET PROPELLANT

APPENDIX-I

A MICROWAVE METHOD FOR MONITORING THE CURING CONDITIONS OF A SOLID ROCKET PROPELLANT

I.1 INTRODUCTION

A new microwave Non-Destructive Test (NDT) method developed to monitor the curing conditions of a solid rocket propellant is presented in this section. Rocket propellants generally contain different ingredients mixed in definite proportions to form a propellant slurry which, on curing gives a solid propellant. After mixing for hours, this paste is casted in the form of cylinders of appropriate size and is treated for curing in hot air ovens. The time taken for accurate curing depends on the size of the propellant and temperature of the oven. Normally, it will take days for proper curing.

At present, no method is available to monitor the curing process. There could be over or under curing of the propellant as hours passed through. The accepted practice now is to monitor the variation of tensile strength of the propellant samples after it is cured and this is a destructive test procedure. The variation of tensile strength is studied continuously for days and it will finally attain a constant value after the required curing.

In this curing process, the mechanical as well as electrical properties of the propellant sample are subjected to changes and they reach stable values after curing. It will be easy to monitor the curing process by monitoring the change in electrical property.

I.2 MICROWAVE METHOD

The dielectric properties of a non-conducting material can be obtained from the characteristics of an electromagnetic wave propagating through the medium. There are different ways to measure the propagation constant or equivalent parameters for a uniform sample of the material [162].

In general, the electrical and magnetic properties of a dielectric sample are all functions of frequency of electromagnetic waves passing through the samples. The measurement methods fall broadly in two groups.

1. Guided wave method

2. Free space method.

The guided wave method may be further subdivided into those which employ resonant cavities and those which use observations on travelling waves in waveguides. The performance of a cavity resonator depends on the dielectric

material inside it. Moreover, any variation in the property of dielectric material within the cavity will result in a corresponding change in resonance frequency.

Standard transmission line techniques are used to measure the impedance at the face of a sample of dielectric medium enclosed in a hollow waveguide. It is also possible to measure the dielectric constant either by measuring the wavelength directly in a dielectric media surrounding a resonant section of a pair of lecher wire, or by measuring the capacitance of a small capacitor containing the dielectric, which is closely attached to the lecher wire.

In waveguide method, the dielectric sample is placed against a perfectly reflecting surface. A general solution of the transmission line for a dielectric-filled line has been given by Roberts and von Hippel [163]. This method has been discussed in detail by Dakin and Works [164] and they developed a modification.

I.3 MEASUREMENT OF DIELECTRIC CONSTANT

The block diagram of the experimental set up for measurement of dielectric constant is shown in Fig.I.1. A rectangular waveguide is excited in TE_{10} mode in x-band.
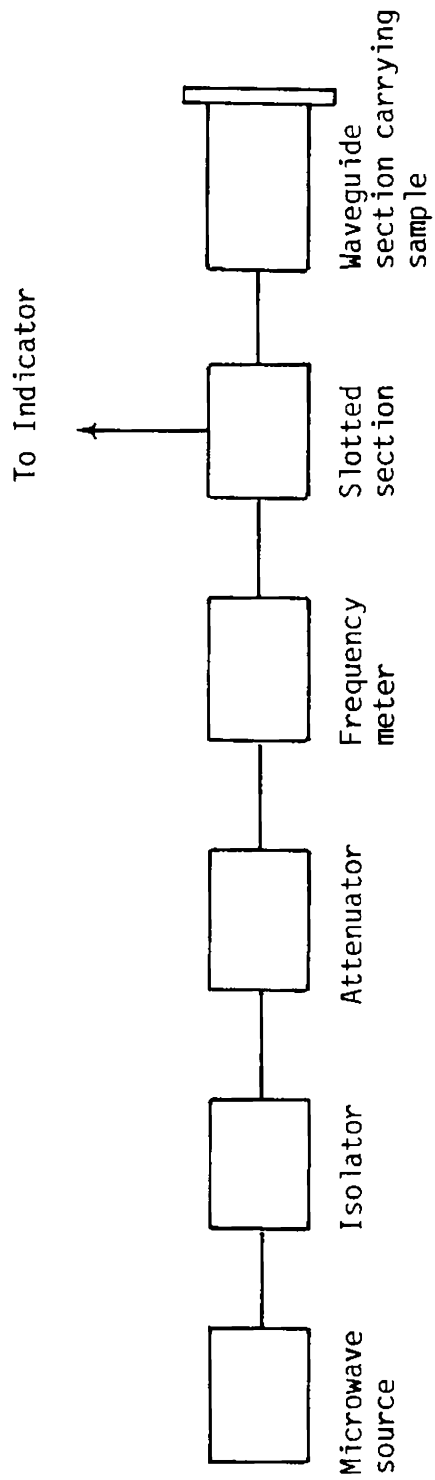
Fig. I.1 Experimental set up for the determination of dielectric properties of the propellant sample.

182

A section of the waveguide with a short circuiting plate at one end is connected to the termination of the waveguide slotted section with probe carriage. After noting the position of the minimum, the sample is introduced into the waveguide in paste-form and the shift of the first minimum is observed. The sample is then placed in an oven which maintains a constant curing temperature. After the required time for curing, the sample is taken out and by connecting it to the same waveguide termination, the shift in first minimum is again observed. The experiment is repeated for samples of different length.

I.3.1 Theoretical considerations

As shown in Fig.I.2, standing waves are formed within the sample as a result of the superposition of the incident and reflected waves. The first minimum from the face of the sample is an integral multiple of half-wavelength. The position of the first minimum from the face of the sample, thus depends on the wavelength of the electro-magnetic radiation in the sample and the sample thickness. When the dielectric sample is introduced in the waveguide, the minimum shifts towards one end. This shift provides a measure of the dielectric constant of the sample.
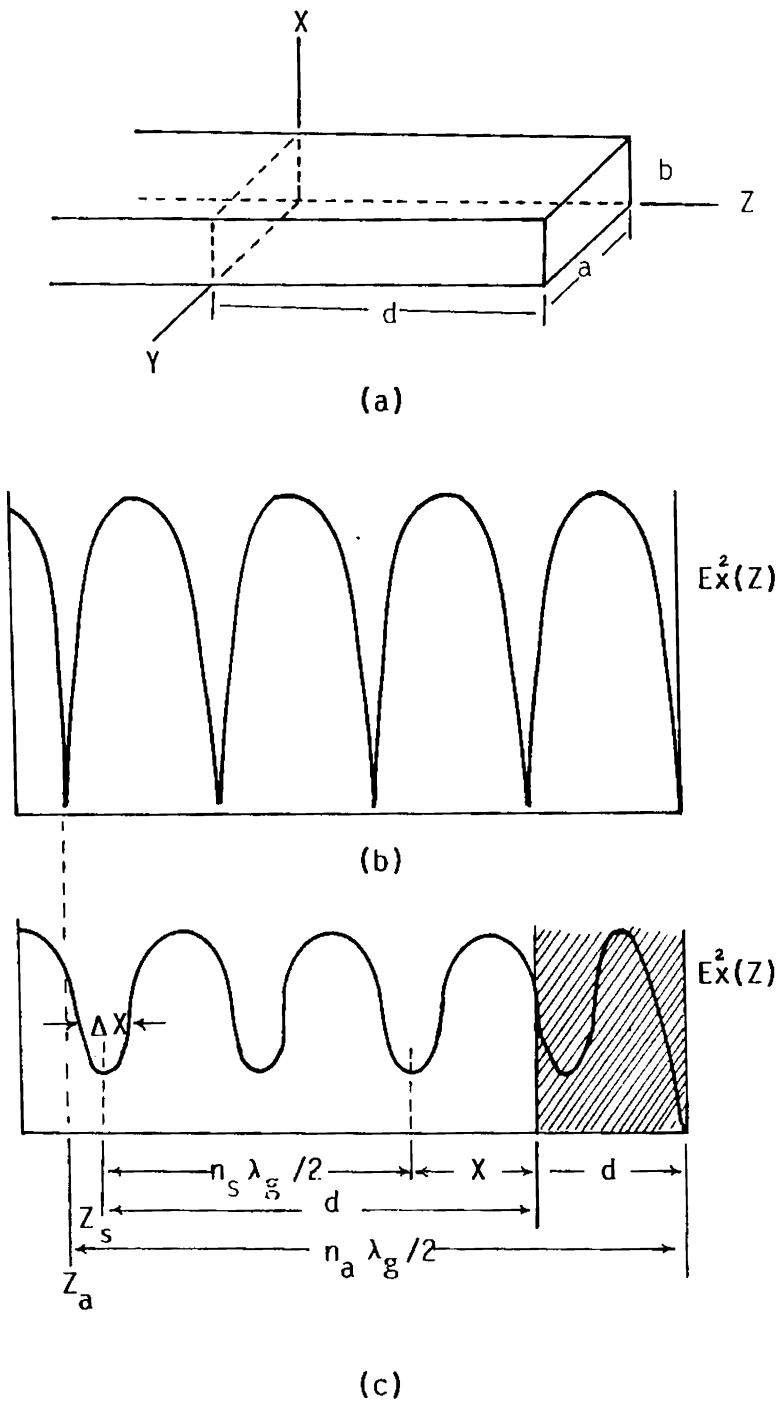
Fig. I.2. (a) Short-circuited rectangular waveguide with dielectric
sample of length d at the shorted end
(b) & (c) Voltage standing-wave patterns in an empty and
dielectric filled waveguide.

The separation of the first minimum of the standing wave from the face of the sample is given by [163]

$$\chi_0 = (n_a - n_s) \lambda_g /2 - [d + Z_a - Z_s] \qquad (1)$$

The dielectric constant of the sample is related to the attenuation constant and the standing wave ratio by the relation [164]

$$\left[\frac{\dfrac{E_{min}}{E_{max}} - i \tan [360 \chi_0 / \lambda_g]}{1 - i \dfrac{E_{min}}{E_{max}} \tan [360 \chi_0 / \lambda_g]} \right] \frac{\lambda_g}{2 \pi d i} = [\tan \gamma_2 d]/ \gamma_2 \qquad (2)$$

where,

   χ_0 = the distance of the first minimum from the face of the sample

   d = thickness of the sample

   γ = propagation constant, and

   λ_g = guide wavelength.

The solution of the above complex transcendental equation can be obtained by separating eqn.(2) into real and imaginary parts and equating them separately.

Thus, we have,

$$\frac{\tan \beta_2 d}{\beta_2 d} = -\lambda_g \tan [360 \chi_0 / \lambda_g] / 2\pi d \qquad (3)$$

Equation (3) can be solved for $\beta_2 d$ and hence the dielectric constant is calculated from the relation,

$$\varepsilon' = \frac{1/\lambda_c^2 + [\beta_2 d / 2\pi d]^2}{1/\lambda_c^2 + 1/\lambda_g^2} \qquad (4)$$

where ε' is the dielectric constant and λ_c is the cut off wavelength of the waveguide.

The solution of eqn.(3) for $\beta_2 d$ is multi-valued and will give different values of ε' . From these values of ε' , it is not possible to select the exact value without knowing the properties of the material. Hence a second measurement using samples of different length d is necessary for correct determination of ε'.

Equating the imaginary parts of eqn.(1), the loss tangent,

$$\tan \delta_2 = \frac{\Delta x}{d} \left[\frac{(1/\lambda_c^2 + 1/\lambda_g^2) - 1/\lambda_c^2 \varepsilon'}{1/\lambda_c^2 + 1/\lambda_g^2} \right] \left[\frac{\beta_2 d [1 + \tan^2 (360 \chi_0/\lambda_g)]}{\beta_2 d (1 + \tan^2 \beta_2 d) - \tan \beta_2 d} \right]$$

$$(5)$$

where Δx is the width of the minimum of the standing wave to the double power points.

I.4 EXPERIMENTAL RESULTS

The variations of dielectric constant are plotted against curing time for two different types of propellants of composition I (live) and of composition II (dummy) and these are shown in Fig.I.3. For propellant composition I, the dielectric constant decreases with time until it finally reaches a stable value.

The experimental observations with propellant composition II, which cured at room temperature show that the dielectric constant increases with curing time and levels off after curing [Fig.I.3(b)]. The change in propellant compositions I and II accounts for the opposite nature of the curves. Fig.I.3(d) and (e) shows the dielectric constant variation of propellants of different size. From the above graphs, it can be seen that the dielectric constant attains a steady value after curing.

I.4.1 Correlation of mechanical and electrical properties

The change in dielectric constant can be co-related with the changes of mechanical properties of the propellant.

Fig.I.4 shows that tensile strength increases with curing and then becomes constant.

The graph connecting electrical property and curing time reaches a steady state much earlier, compared to the curves of tensile strength versus curing time. This is explained as follows: In the normal curing procedure, the sample is cured in bulk in a plastic container. In this situation, the curing process is slow because of the poor conductivity of the plastic container. This type of sample was used to study the variation of tensile strength. But to study the electrical properties, the sample was subjected to 'accelerated curing'. A small amount of propellant sample was placed in a highly conducting copper waveguide cell so that it attains the curing temperature rapidly. The curing was faster and hence the curve levelled off much earlier than in the normal curing case.

I.4.2 Variation of loss tangent, tan δ

The loss factor of the dielectric sample is also changing due to curing of the rocket propellant. Fig.I.5 shows the variation of loss factor with respect to curing time, for propellant composition II of different length d. ε'' is found to be decreasing while curing progresses and reaches steady value with proper curing.
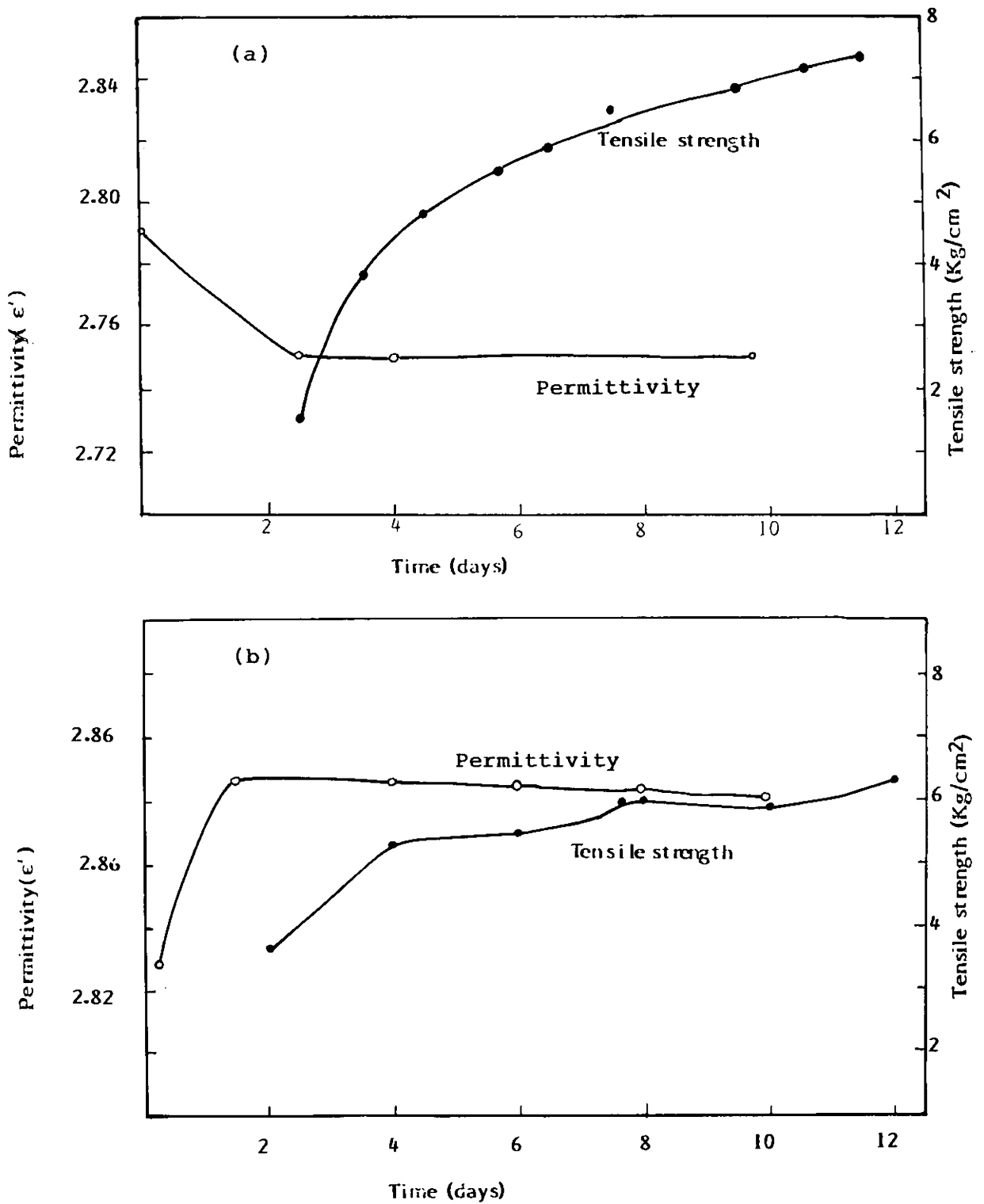
Fig. I.3 Curves co-relating the electrical and mechanical properties of the propellant samples
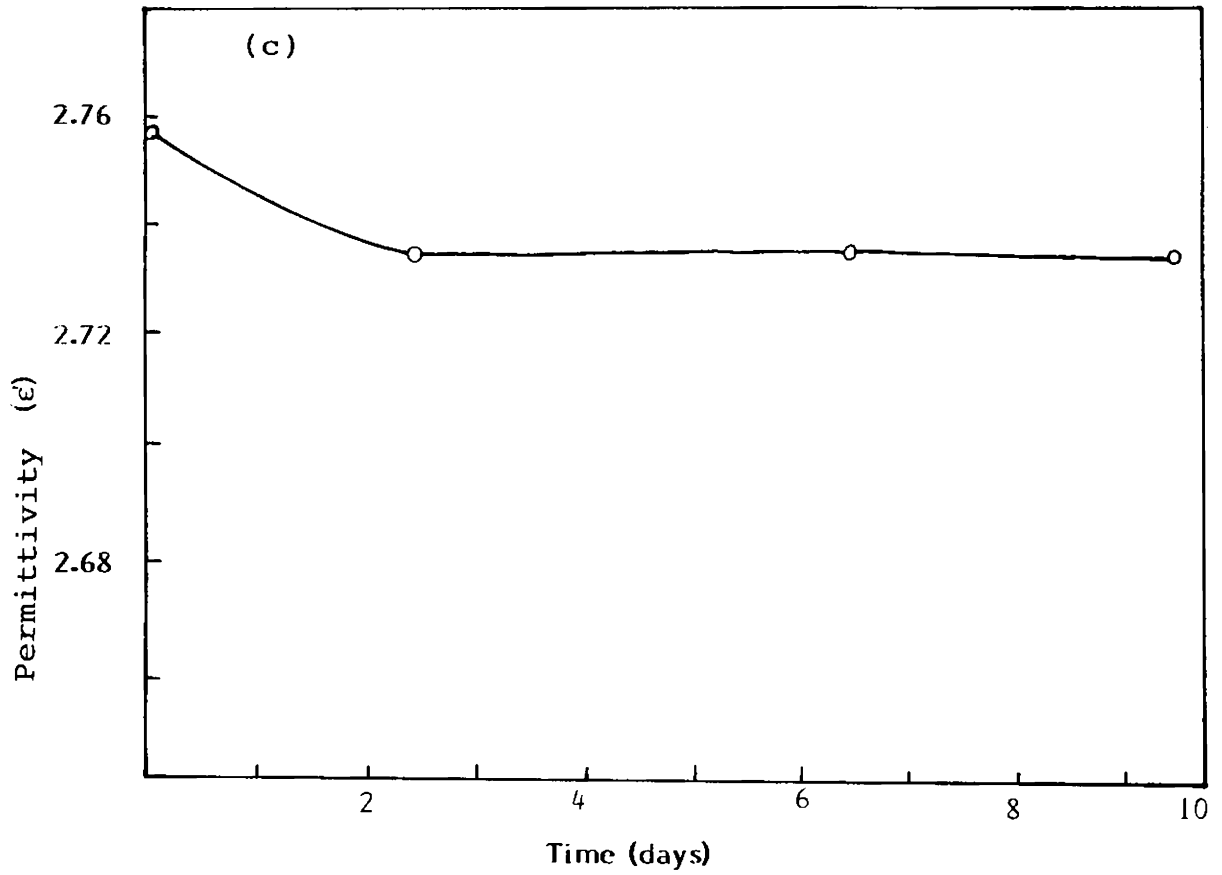
(A) Live sample: (B) Dummy.

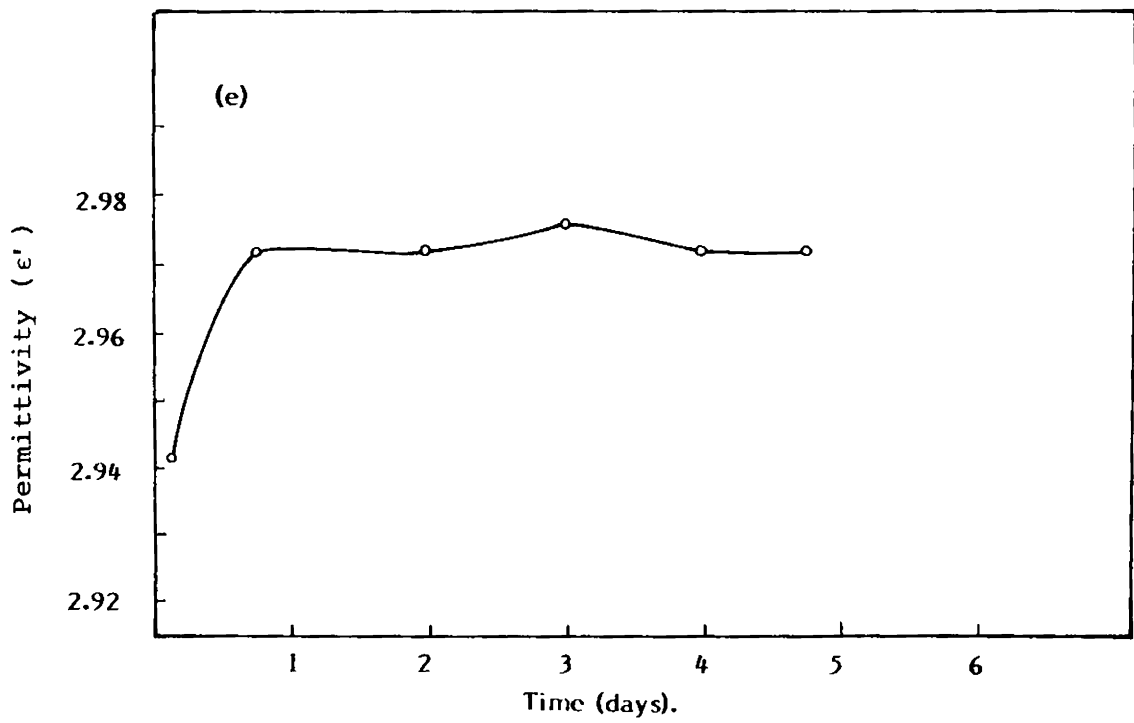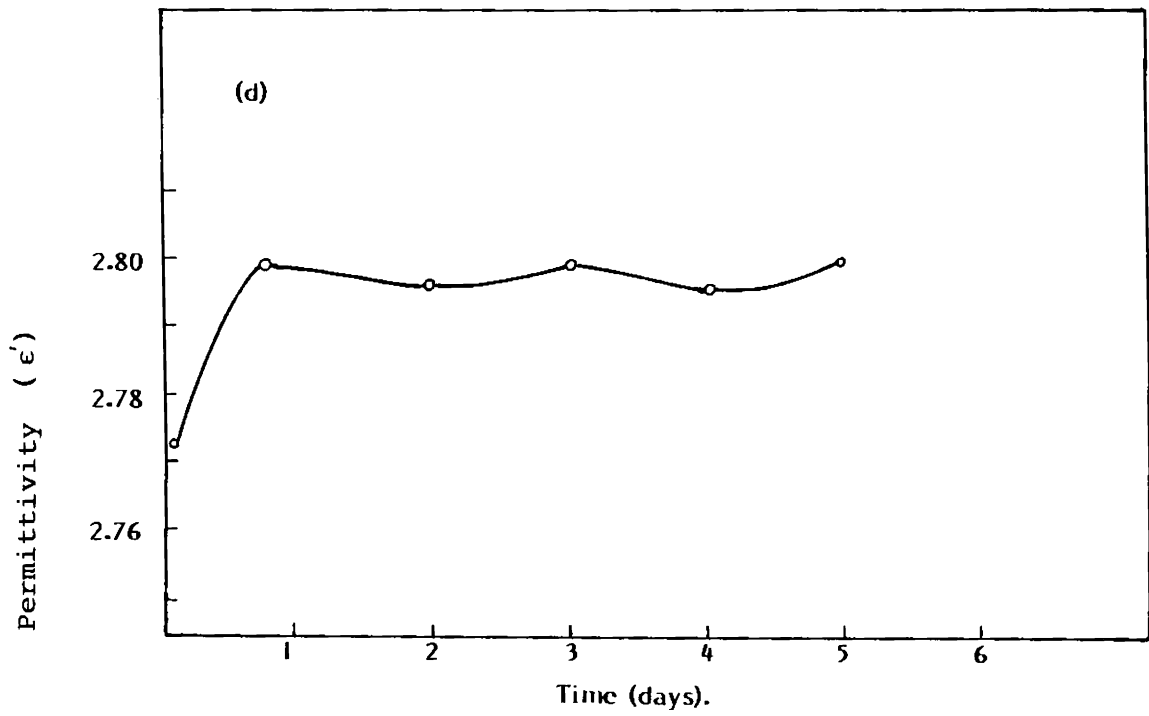**Fig.J.3.(c).** Variation of electrical property against curing time-Live propellant.

Fig.I.3.(d) & (e). Variation of permittivity versus curing time: IPP-40 dummy
propellant of different length d
(d) d= 1.2 cm: (e) d= 5.13 cm.

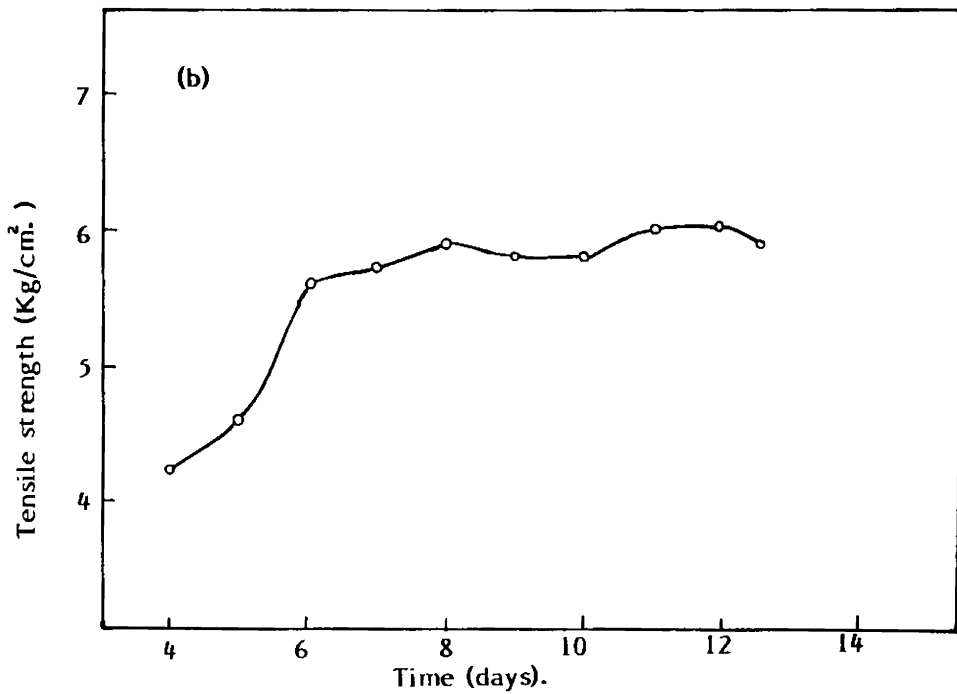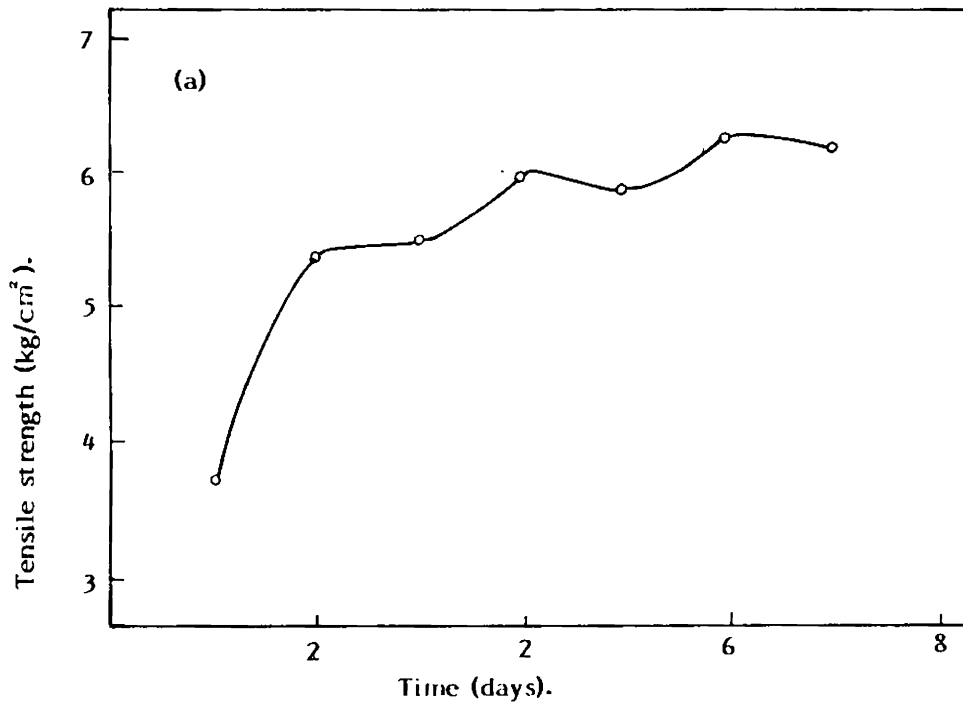Fig.1.4.(a) & (b) Variation of mechanical property against curing time
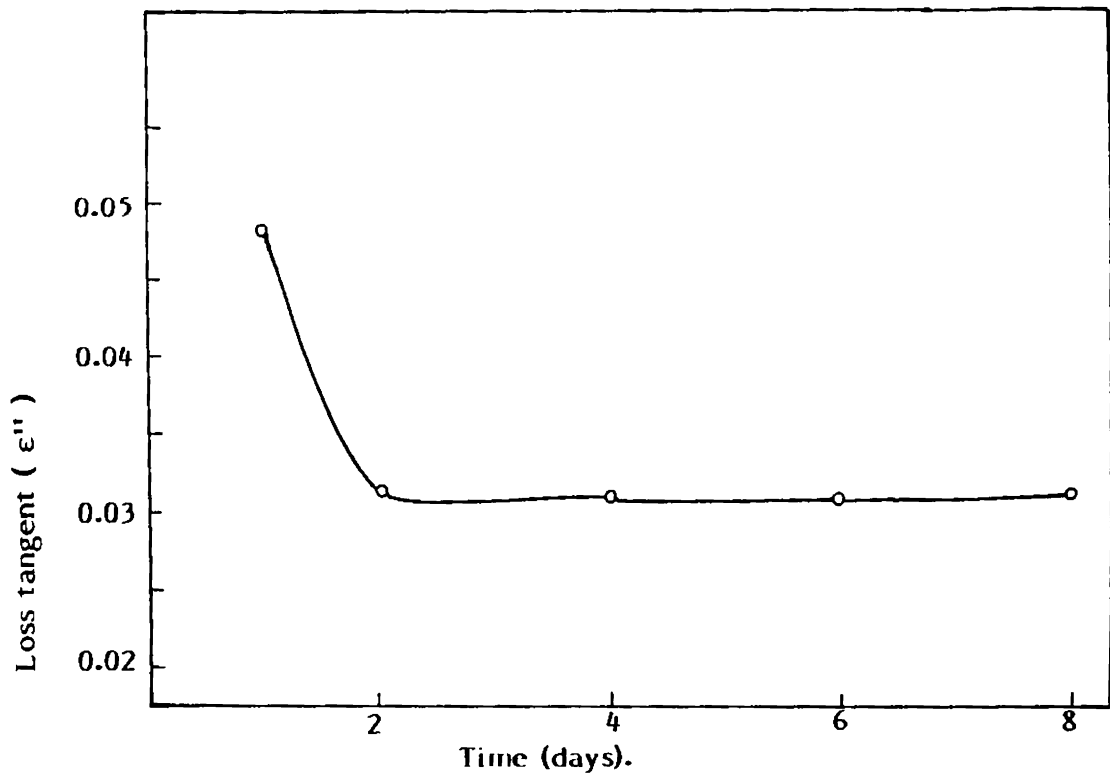IPP-40 dummy propellant of different size.

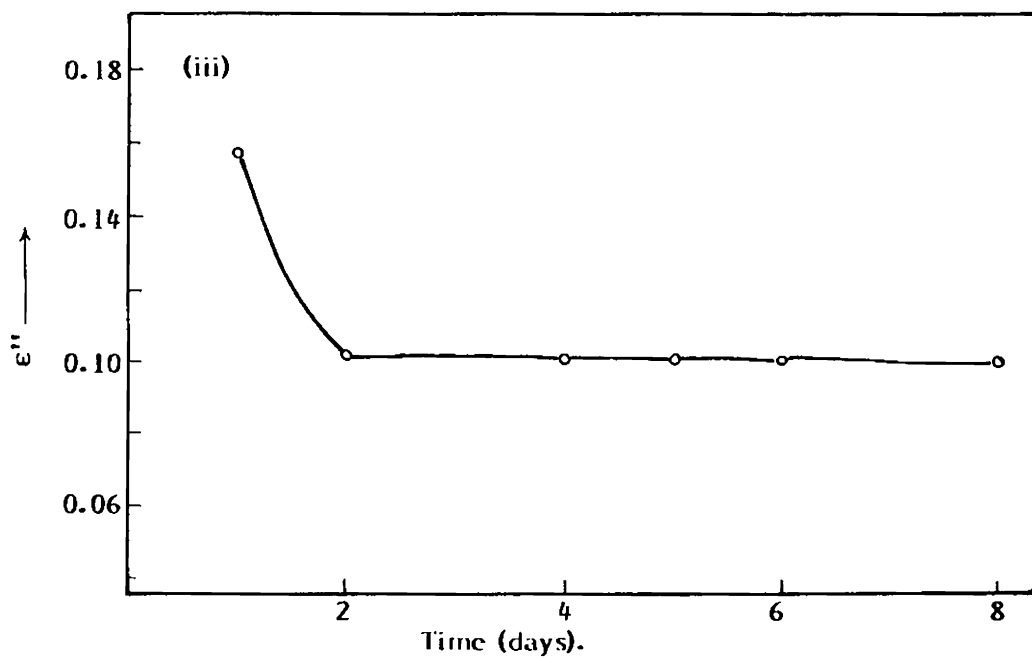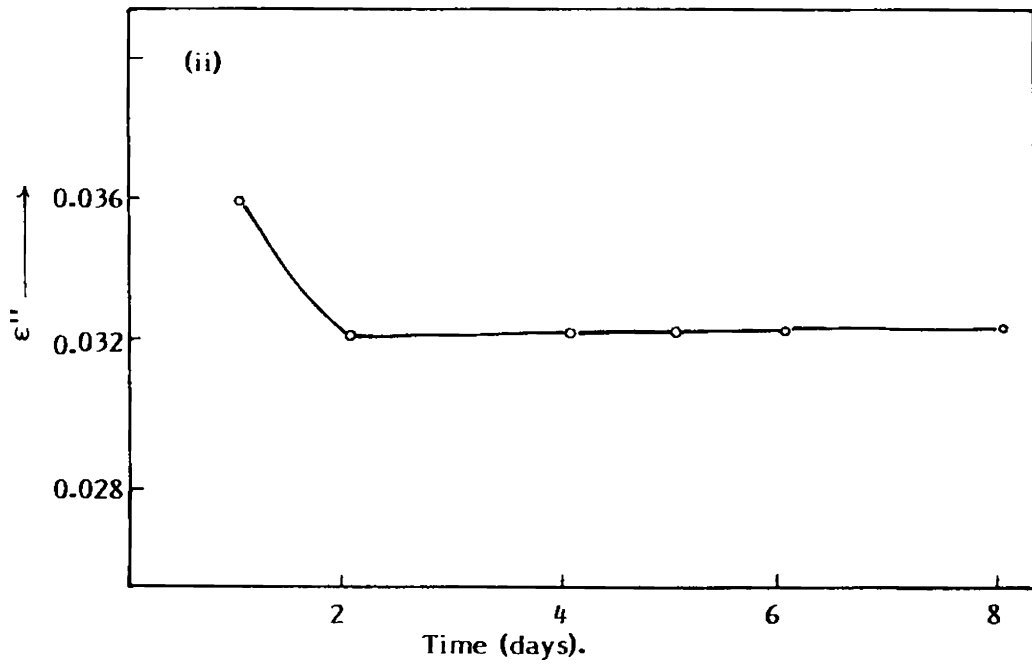Fig.I.5.(i) Loss factor versus curing time for IPP-40 dummy propellant of length: 5.05 cm.

Fig. 1.5. (ii) & (iii) Loss factor versus curing time: IPP-40 dummy
propellant.

(ii) for d= 3.2 cm
(iii) for d= 2.5 cm.

I.4.3 VSWR variation

Fig.I.6 shows the variation of VSWR for propellant composition II. Variation of VSWR shows that the reflections from the interface of the propellant sample is increased with curing and this increase in reflection causes a corresponding decrease in output power [Fig.I.8(b)].

I.5 ATTENUATION MEASUREMENTS

When the propellant starts curing from paste to solid form, the corresponding changes in electrical property affect the propagation of microwaves through it. The curing state can be predicted by monitoring the change in the amplitude of the transmitted signal through the sample. The experimental set up for monitoring the curing state is shown in Fig.I.7. The sample in paste-form is filled in a waveguide cell surrounded by an outer-jacket through which non-volatile oil at curing temperature is circulated. Microwave energy is fed into the waveguide cell and the transmitted microwave power is measured with high accuracy keeping the input constant. The results are shown in Fig.I.8. For propellant composition I, the output power is found to be increased as curing progresses and attained a steady level after the completion of curing.
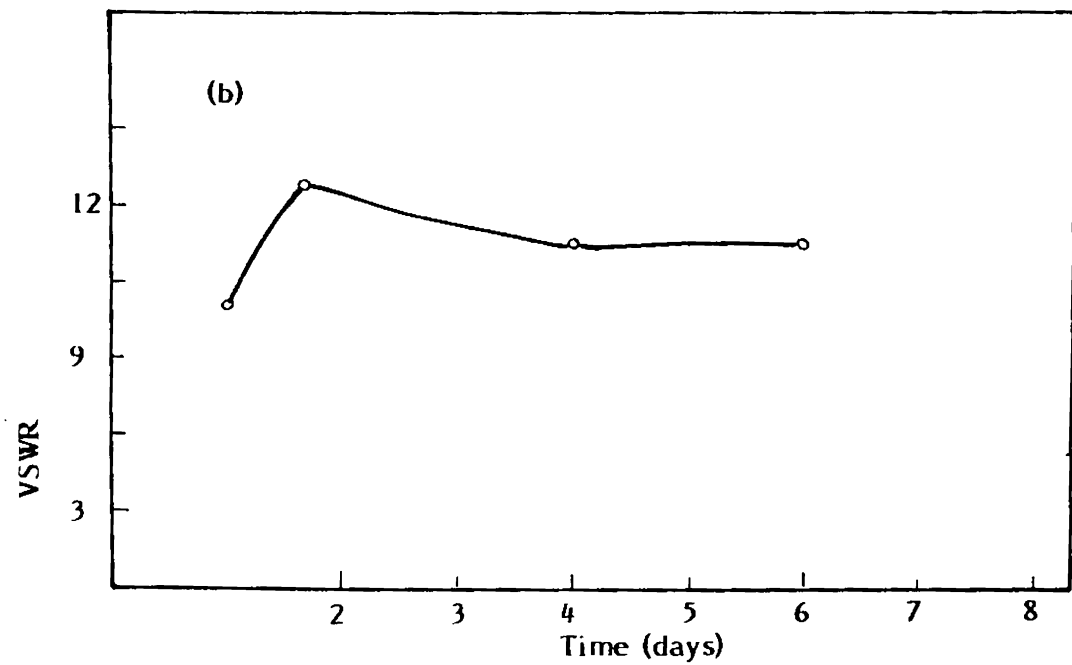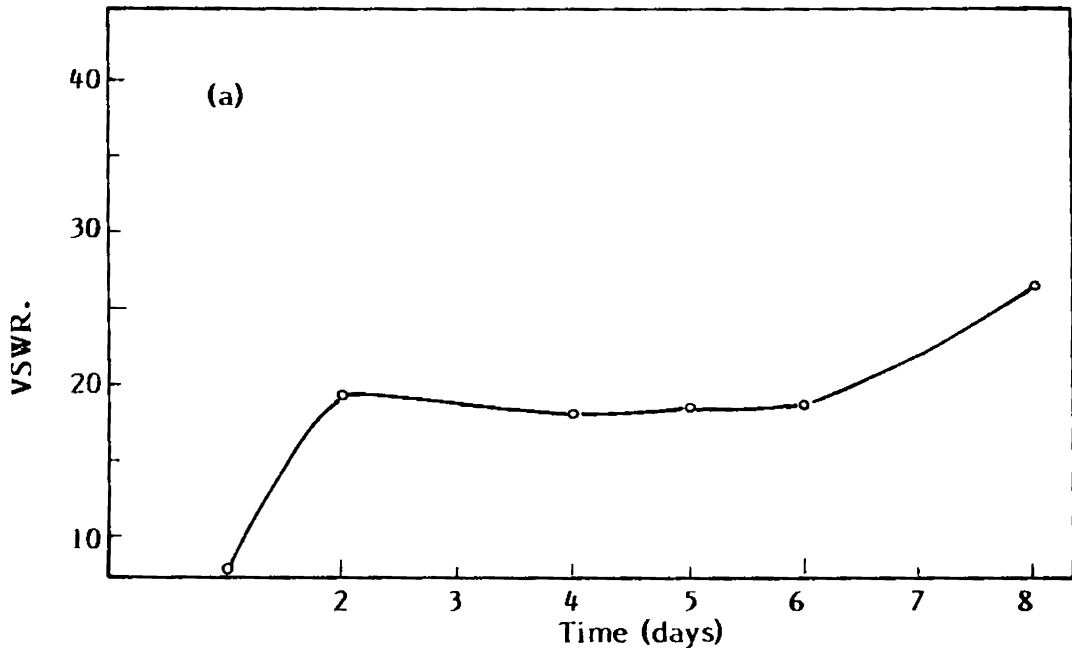
Fig.l. 6.(a) & (b)   Variation of VSWR against curing time: IPP-40
dummy propellant
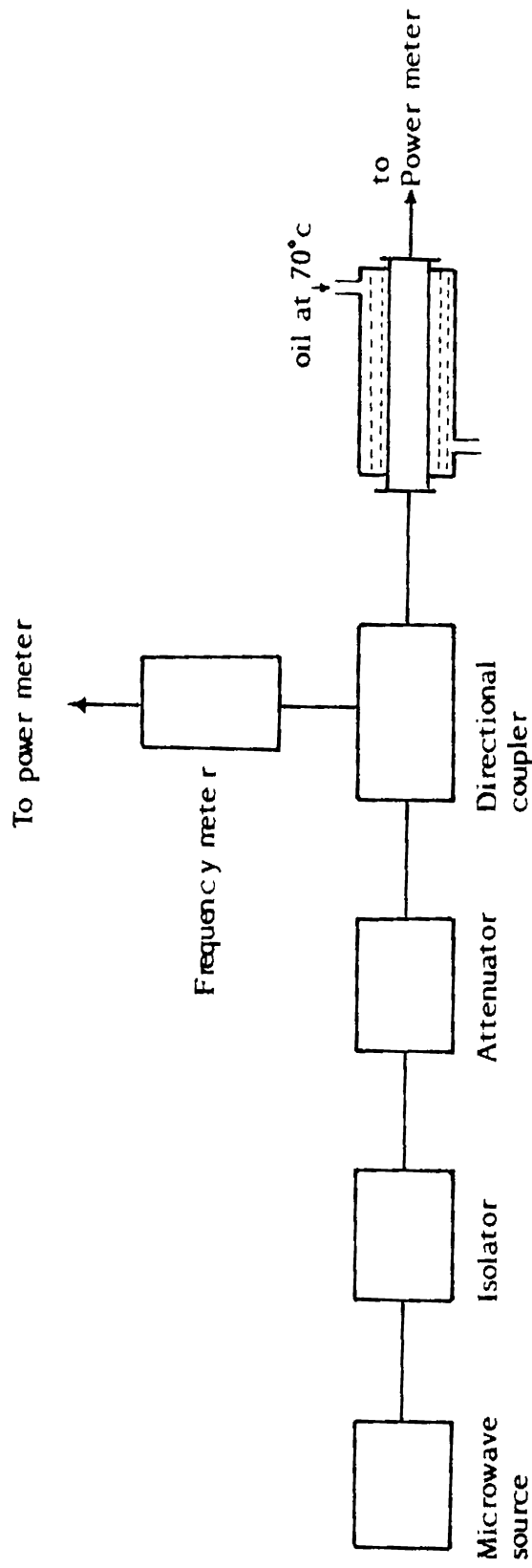(a) for d= 1.2 cm
(b) for d= 5.13 cm.

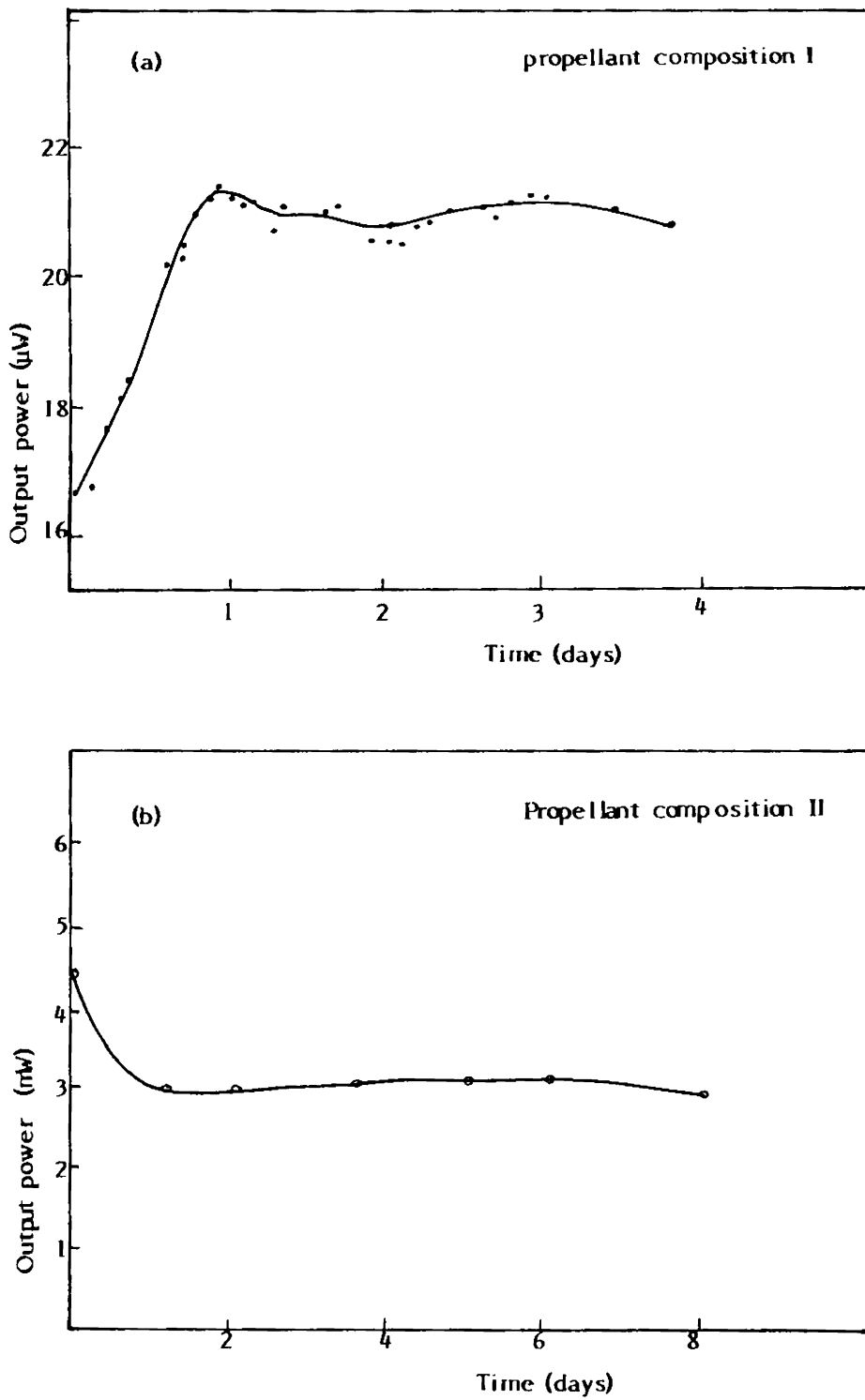Fig. I. 7. Experimental set up for attenuation measurements

Fig. I.8. Output power against curing time
(a) for propellant composition I
(b) for propellant composition II

Fig.I.8(b) shows the variation of output power for propellant composition II. In this case it is found that the VSWR of the system is increasing due to curing (Fig.I.6) and this result is very much supporting Fig.I.8.

I.6 CONCLUSIONS

The curing state of a rocket propellant can be monitored by studying the variation of electrical property of the sample in real time. This enables to avoid many problems like improper curing, variation of temperature, over or under curing during process etc. A better conclusion, regarding the curing state of the propellant sample is obtained by comparing the mechanical properties of the sample with its electrical property.

Appendix II

MICROWAVE METHOD FOR LOCATING INHOMOGENEITIES

IN NON-METALLIC MEDIA

199

APPENDIX-II

MICROWAVE METHOD FOR LOCATING INHOMOGENEITIES IN NON-METALLIC MEDIA

II.1 SOLID ROCKET PROPELLANT

II.1.1 Introduction

The main aim of this work is to develop a method to locate the exact position of the inhomogeneities inside a non-metallic media like solid rocket propellant. Determination of exact position of inhomogeneities in cured propellant is vital, because the ultimate selection of a rocket motor for a launch vehicle depends on the position, size and nature of the crack or flaw inside it.

Microwaves interact with non-metallic materials in different ways which depend on the internal properties of the materials. The analysis of the transmitted signal, however, can give information about the internal state of the material. This leads to the possibility of using microwaves to detect inhomogeneities like under or over cured portions, flaws, cracks or metallic inclusions inside a curved rocket propellant sample [166].

II.1.2   Experimental set up

Microwaves are allowed to pass through the propel-
lant sample and the phase as well as the amplitude of the
received signals are analysed.   The experimental set up is
shown in Fig.II.1.   The sample is mounted on a turn-table
exactly symmetric with respect to transmitter and receiver.
The propellant sample is capable of rotating about a vertical
axis.   High gain pyramidal horn antennas are used for signal
transmission and reception.   To analyse the receiver signal
an HP-8410 Network Analyser is used.

For a fully cured sample with no flaws, a flat
response curve is obtained in both phase and amplitude
patterns as the sample is rotated 180° (Fig.II.2).   When
artificial flaws are introduced inside the sample, the recorded
curves show change in phase and amplitude. The two peaks
in recorded patterns correspond to the flaw position when,
the flaw is closest to the transmitter and then closest to
the receiver respectively, as it rotates, as in Fig.II.3.
Since the propellant test sample is mounted symmetrically
with respect to the transmitter and receiver, two peaks,
obtained in the resulting signal, are separated by 180°
(Fig.II.3a).   Fig.II.3(b) shows the transmitter and receiver
in same positions, but the sample is given a lateral displace-
ment of d cm.
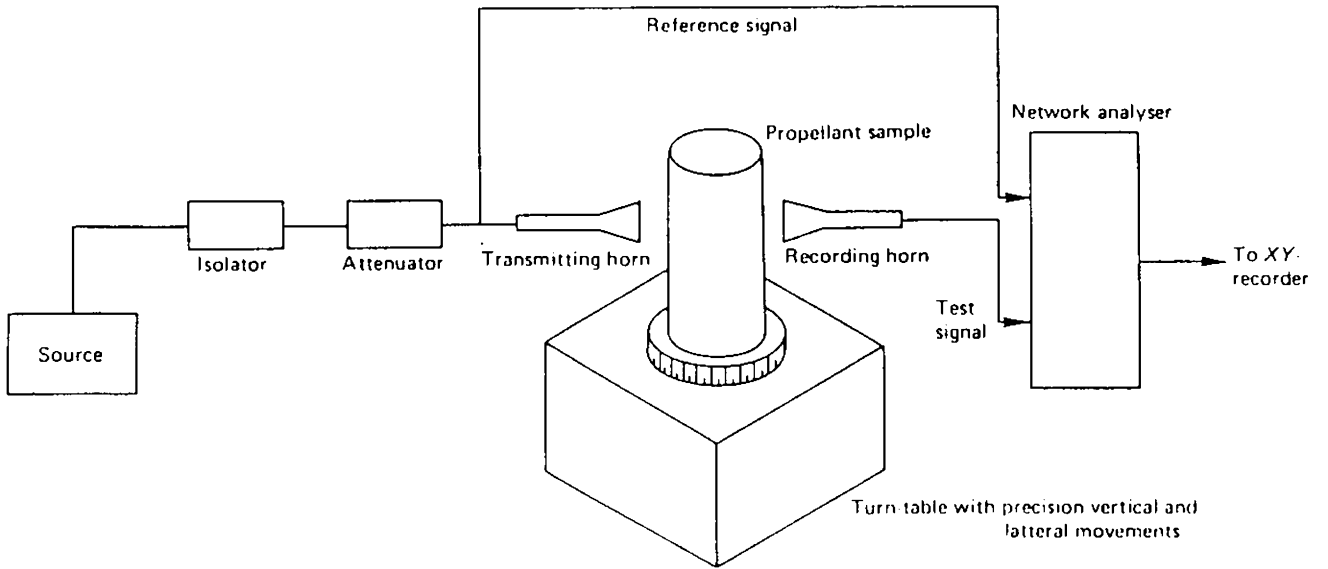
Fig. II.1 Microwave transmission set up to locate defects or flaws.
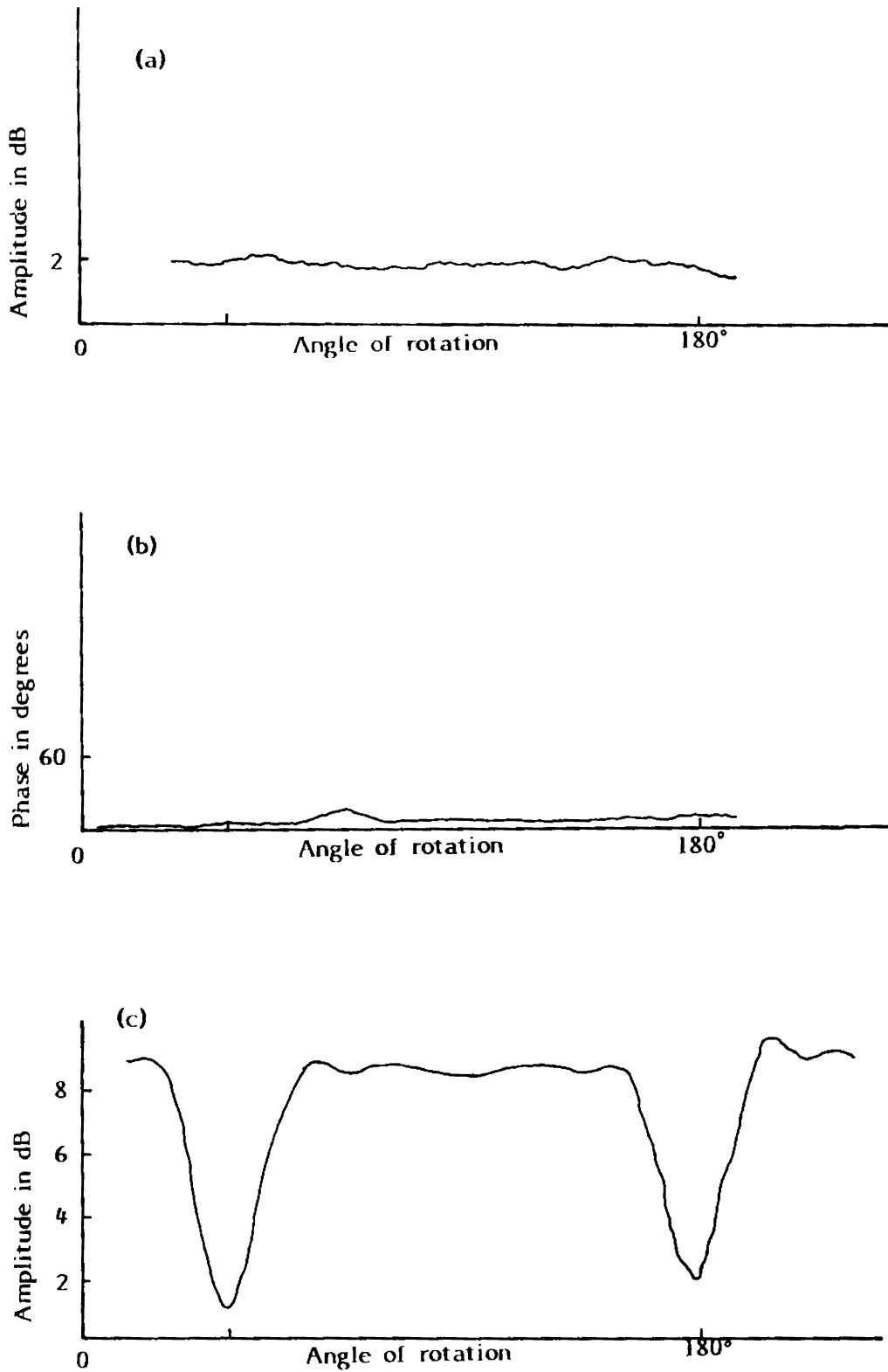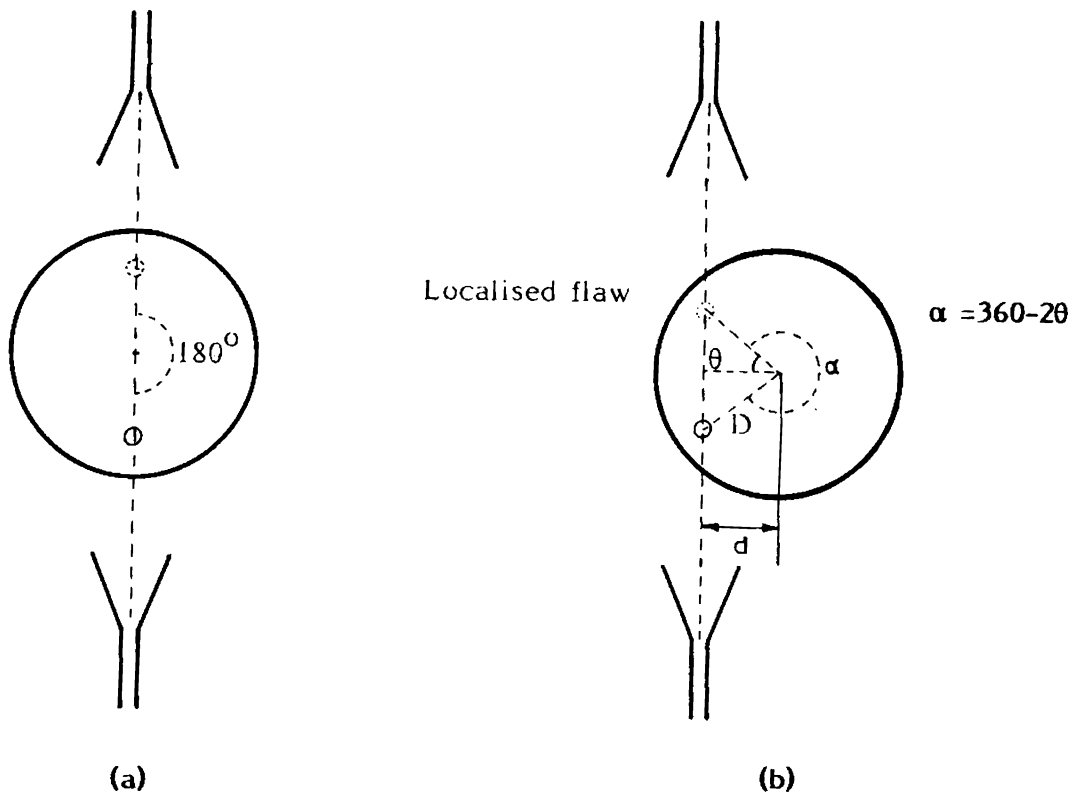
203

Fig. II.2 (a). Amplitude patterns of flawless homogeneous sample
(b). Phase pattern of a flawless homogeneous sample
(c). Amplitude pattern of propellant sample with a cylindrical flaw.

Fig. II.3 (a) Propellant sample mounted symmetrically with respect to transmitter and receiver
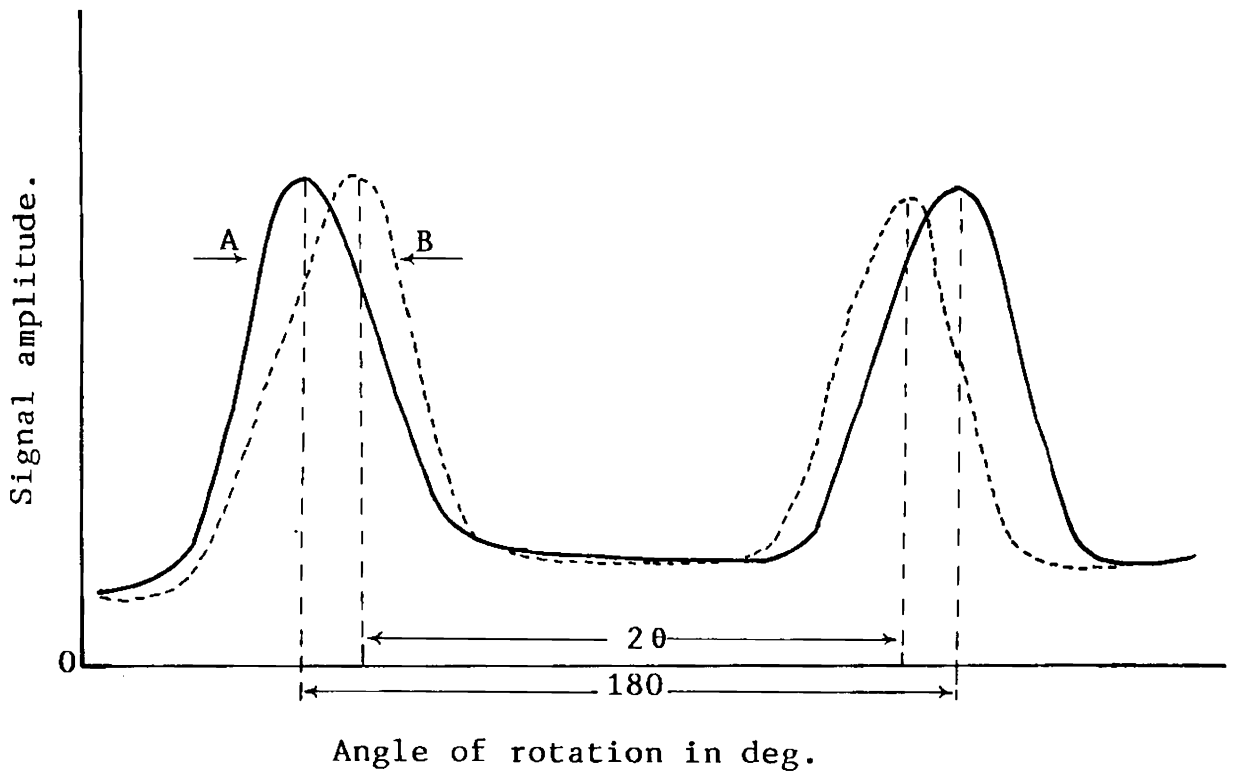
(b) Sample is given a lateral displacement

Fig. II.4. Amplitude patterns of transmitted signal as the
sample is rotated about the vertical axis.
(A) When sample is mounted symmetrically
(B) When sample is given a lateral displacement.

When the sample is rotated, it has been found that the separation of the two peaks is not 180°. As shown in Fig.II.4, the separation is smaller or greater depending on the direction of rotation of the turn-table. This rotation can be adjusted in both directions to determine the angular separation of the two positions exactly. If, in one direction, 2θ is the angle subtended by the two positions at the centre of the rocket motor, in the other direction the angle will be $(360 - 2\theta)$. In both cases, it is possible to determine the exact value of θ. If 2θ is the angular separation between two peaks, from Fig.II.3 we have

$$d/D = \cos\theta$$

where D is the distance between the localized flaw and the axis of the motor, and d is the lateral displacement.

Artificial cylindrical flaws of diameters 1.25 cm, 1.10 cm, 0.90 cm were created in different samples, 9.25 cm, 9.0 cm and 6.90 cm respectively from the centre of the sample. The sample is then mounted vertically on a turn-table and kept symmetrical with respect to the transmitter and receiver. The turn-table is rotated about a vertical axis and the received power is plotted. The sample is next given a small

lateral displacement of 0.50 cm, 1.0 cm and 1.50 cm and 2 cm
and curves are plotted in each case. The curves obtained
are shown in Fig.II.5.

Table I.1 shows a few estimated values of D from
the experiment and the actual distance D. The accuracy of
the method is well within 7.6% which is well within tolerable
limit of 10%.

II.1.3 Limitations

Eventhough the above method is simple, it has
following limitations:

1. The method is applicable only if the flaw or defect is
   localized. If the defect is spread out, it may be possible
   to detect the defect indicated by the recorded trace,
   but impossible to predict the location. However, only local-
   ized defects could give sharp curve with distinct separa-
   tion.

2. Theoretically, the variation $D = d/\cos \theta$ holds good for
   any displacement. However, the accuracy of the method
   will depend on the accuracy with which θ is extrapolated
   from the amplitude patterns of the received signal. For
   a small displacement d, θ will normally be large and in
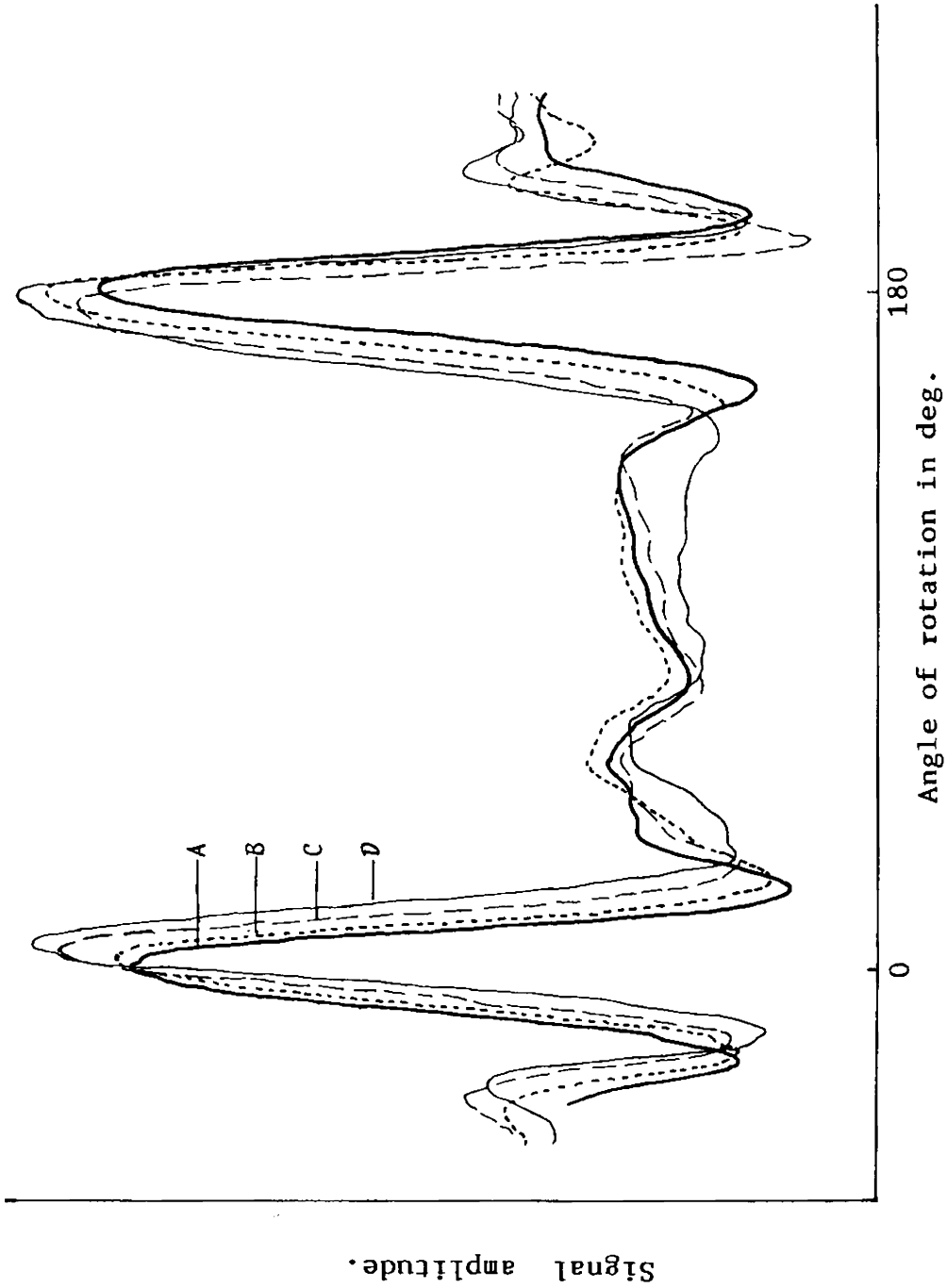
Fig. II.5. Experimentally recorded amplitude patterns of a rocket propellant sample.
(A). Sample is mounted symmetrically., (B). with a lateral shift of 0.3 cm., (C) & (D). with a lateral shift of 0.6 and 0.9 cm respectively.

Table I.1 Details of flaws and detection results

Sl.No.	Flaw size (Diameter) cm.	Actual distance from the centre cm.	Displacement of motor axis cm.	2θ	Estimated value of D $D=\dfrac{d}{\cos\theta}$ cm	Percentage of variation
1.	1.5	9.25	0.3	176.14	8.91	3.67
			0.6	172.28	8.92	3.56
			0.9	168.42	8.93	3.45
2.	1.1	9.0	0.5	173.33	8.60	4.4
			1.0	171.33	13.23	4.7
			1.5	158.0	7.86	12.6
			2.0	153.33	8.67	3.6
			2.5	144.0	8.09	10.1
3.	0.9	6.9	1.2	159.01	6.59	4.4
			1.4	155.24	6.53	5.3
			1.6	155.13	7.43	7.6

this case, the variation of $\cos \theta$ with θ will be abrupt. As the displacement d increases, θ will decrease and a small error in measuring θ will cause significant uncertainty in the calculation of D.

II.2 NDT OF SYMMETRICAL SOLID BODIES LIKE VEHICULAR TYRES

The detection and monitoring of inhomogeneities or defects in an automobile tyre is of great concern, especially when it is used in heavy torque conditions. At the landing and take-off time, the aircraft tyres are under high pressure condition and even minute defects may cause serious problems. Using microwaves, a simple and effective method has been developed to detect flaws or defects inside the automobile tyre. The received signal, which gives an indication of the characteristics of the inside portions of the tyre, is analysed by a signal processing unit incorporating in 8085 microprocessor.

II.2.1 Experimental set up

The schematic diagram of the experimental set up is shown in Fig.II.6. The tyre is mounted on a turn-table controlled by a microprocessor system, symmetric between transmitter and receiver. The tyre is rotated about its own axis. A dipole antenna is kept inside the tyre as shown in Fig.II.7 to transmit microwave signals. The receivers
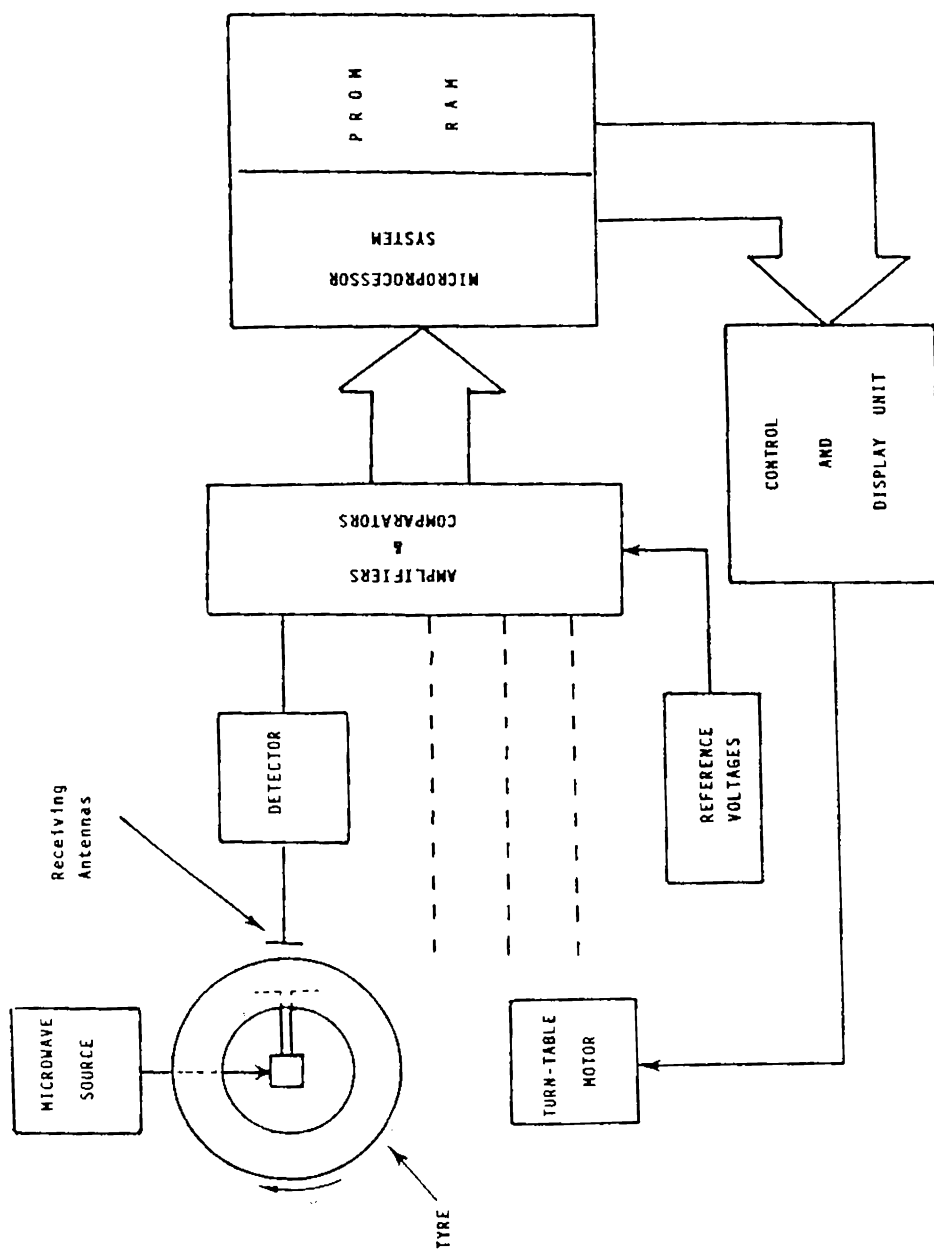
Fig. II. 6 Experimental set-up showing Microwave transmitting and microprocessor controlled system.
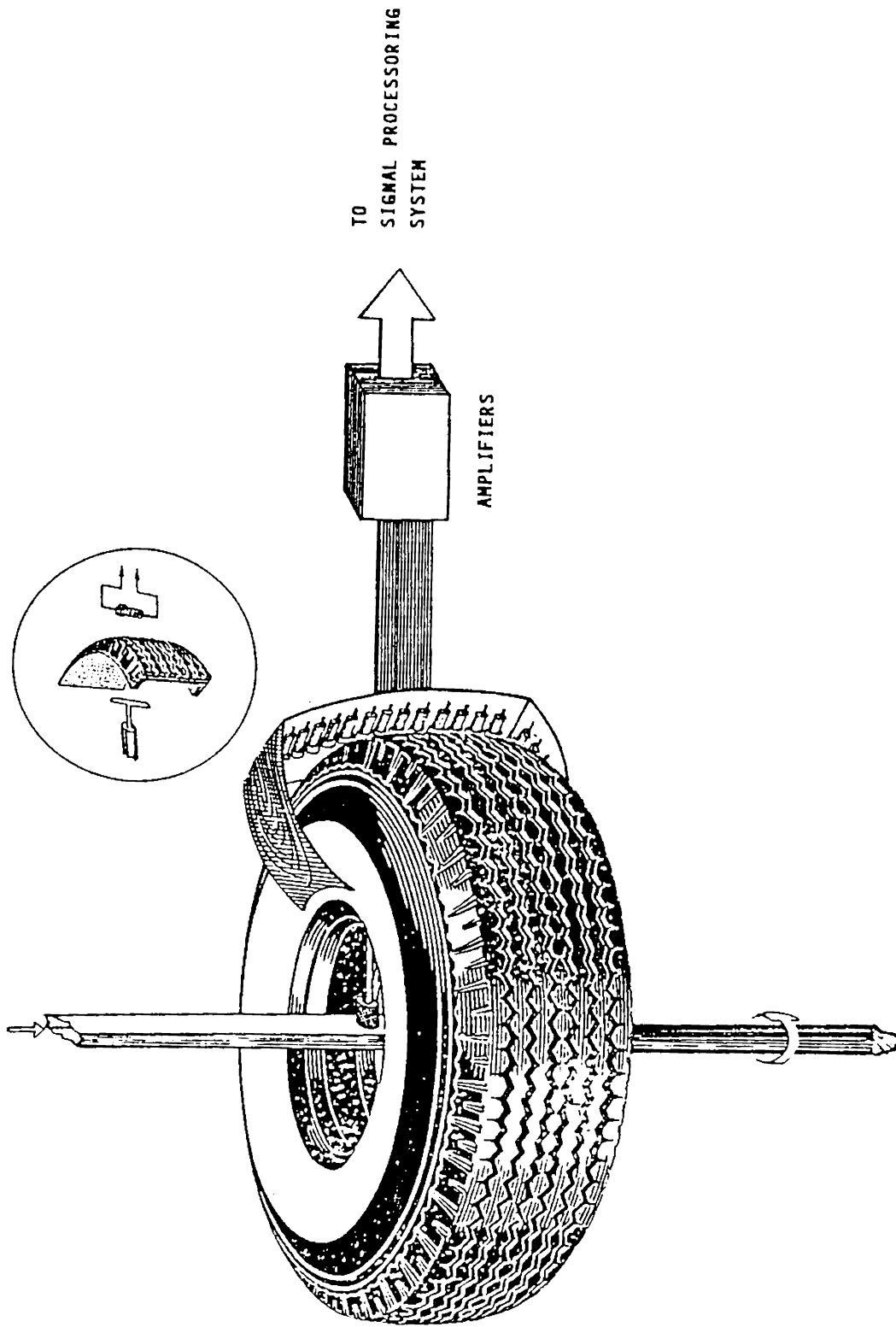
Fig. II.7. Arrangement of Microwave transmitter and detecting diodes.
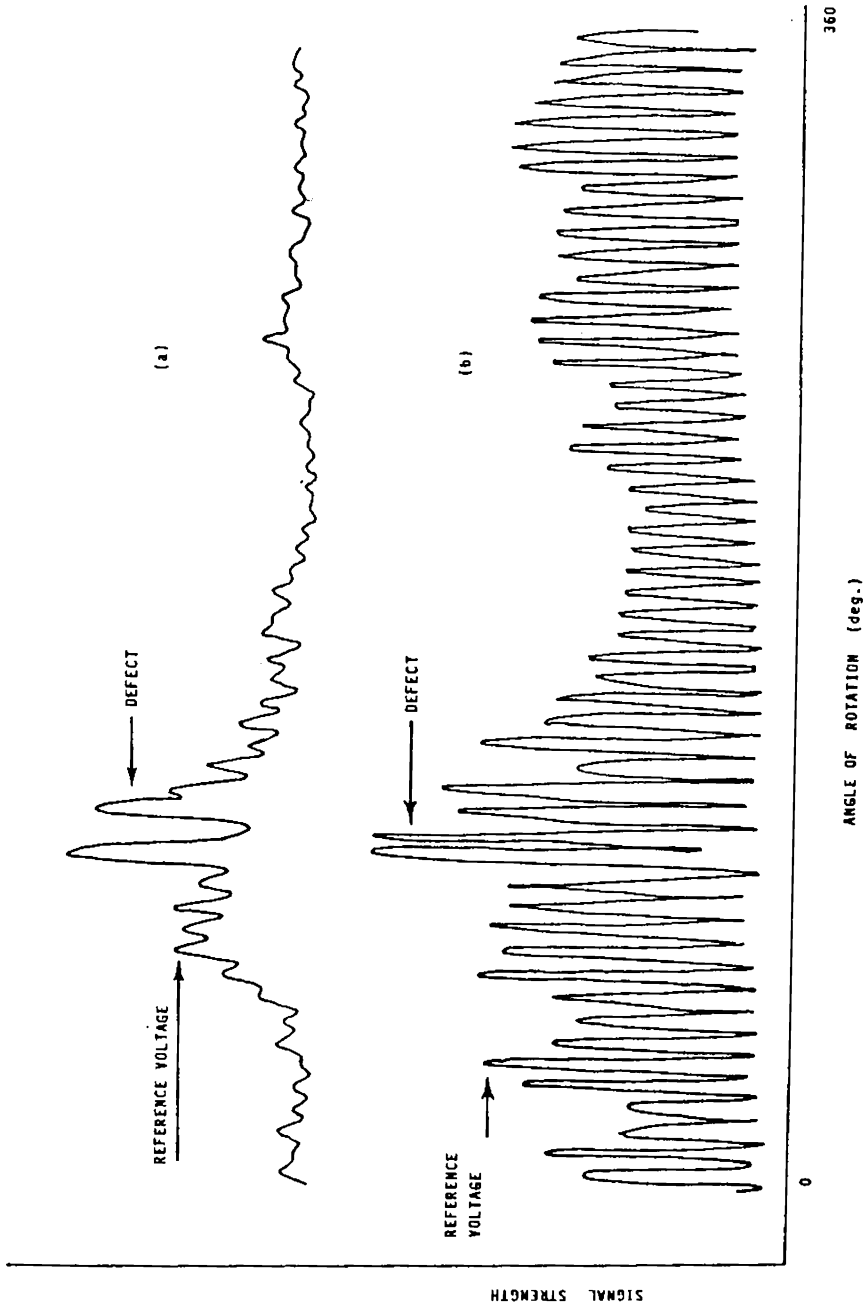
Fig. II.8. Variation of output power recorded using two detecting diodes at different positions
(a) variations corresponding to the side of the tyre.
(b) variations from the thread area.

are microwave detecting diodes, arranged along the outer radial azimuth of the tyre so that the tyre can be scanned for its entire area. Any inhomogeneity in between the transmitter and the receiver, gives abrupt changes in the amplitude of the transmitted signal. The output signal from all receivers are amplified and is given to a voltage comparator.

The reference voltage of the voltage comparator is set such that the output voltage of a particular receiver, which is receiving microwave signal from a portion of the tyre having no inhomogeneity. Then the output voltage gives an indication of the nature of the region of the tyre in between the transmitter and the particular detector. The outputs from all comparators form an "input word" for the microprocessor system. The control and display units are interfaced to a 8085 processor, which derives control signal for the turn-table and monitor the defect and displays it.

When the tyre is rotated, the processor will read the data from the input port and checks for the defect. Once, the defect is detected, it sends a STOP signal to the turn-table and identifies the detector to locate the defect. Necessary delay is included for proper marking of the defective portion. After the delay time, the processor sends START
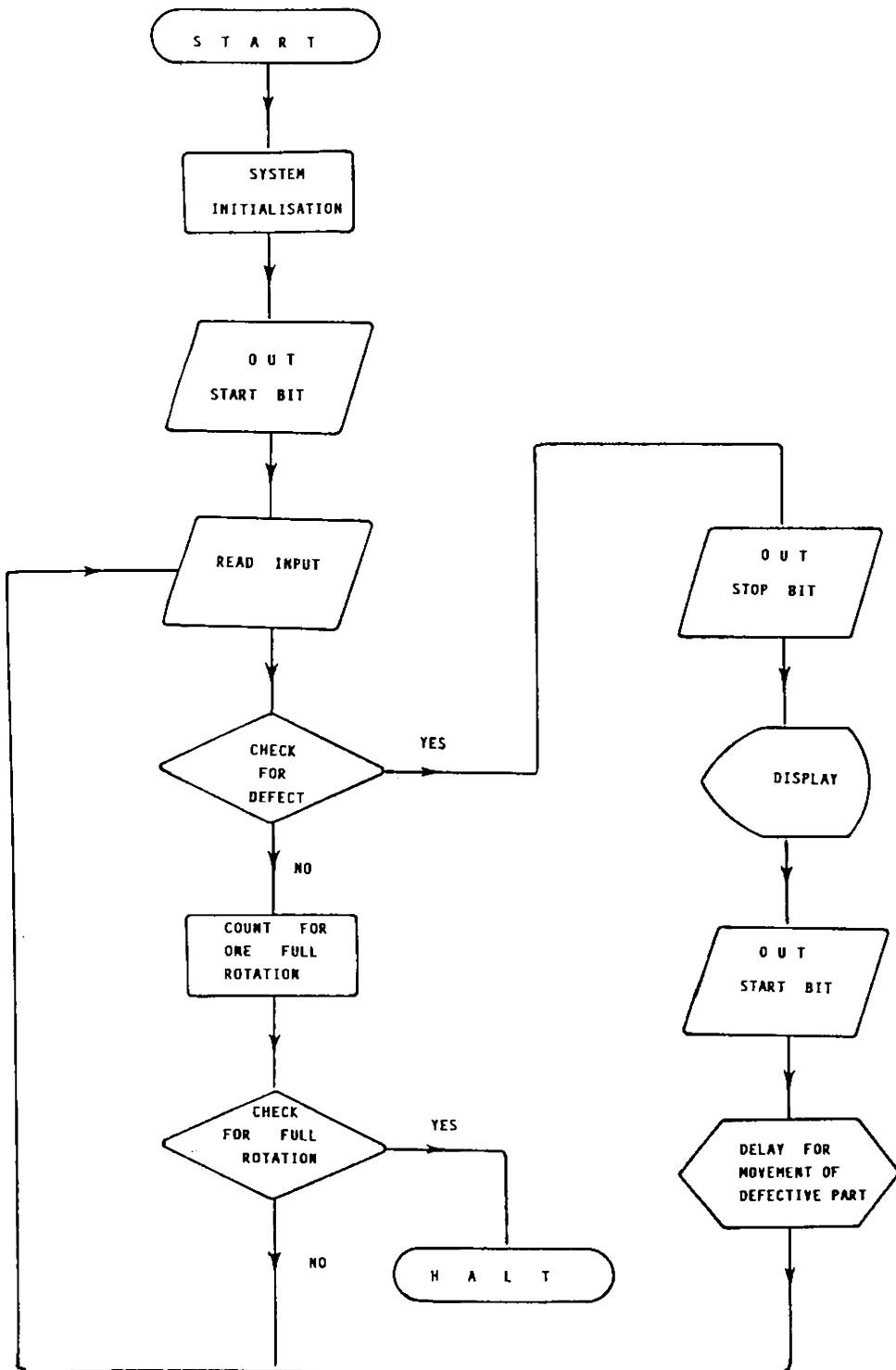
Fig. II.9.Flow chart.

signal to the turn-table and the process of detection is repeated, till the identified defect moves off from the line of sight.

The output of the detectors are plotted using an XY/t recorder and is shown in Fig.II.8. The graph (a) represents the variation corresponding to the side of the tyre and (b) that of the tread. The periodic variations in (b) correspond to the tread and high level peaks indicate the flaws or defects.

Detailed flow chart of the process is shown in Fig.II.9.

II.2.2 Conclusion

The new microwave NDT technique provides a simple and effective method to monitor the defects and inhomogeneities in non-metallic media. The microprocessor based system provides an error-free detection of defects and an accurate production control. The acceptable defect level can be adjusted for different types of tyres by adjusting the comparator reference voltage. For example, the level setting can be critical for aviation tyres, but can be compromised to a great extent for automobile tyres.

DESIGN AND EVALUATION OF A CONVERTIBLE MICROWAVE

ANECHOIC CHAMBER

217

DESIGN AND EVALUATION OF A CONVERTIBLE MICROWAVE

ANECHOIC CHAMBER

III.1 INTRODUCTION

The progress of electromagnetic scattering studies leads to the necessity of the knowledge of the accurate performances of microwave antennas. This precision measurement must be executed either in free space, which is devoid of any kind of perturbations or in a simulated free space condition like modern anechoic chambers. Though the anechoic chambers are not exactly satisfying all conditions of free space, it is very much helpful for accurate performance evaluation of antennas. Besides, the increasing interests in Radar Cross Section measurements, necessitates improvements in state-of-art of the chamber and the reflecting materials.

The earlier general purpose chambers [167-169] like tapered or rectangular were designed for antenna measurements or scattering studies. Each design is devoted to a particular measurement, and it could not be used effectively for other measurements.

For example, a tapered microwave anechoic chamber is mainly intented to use for antenna studies and it cannot be used effectively for scattering studies which need a rectangular chamber, for many reasons. In this Appendix, the development of a microwave anechoic chamber with convertible features is presented. This chamber can be converted from rectangular to tapered configuration or vice-versa, with little time and effort.

III.2 DESIGN OF THE CONVERTIBLE MICROWAVE ANECHOIC CHAMBER

The performance of anechoic chambers are determined by the proper selection of absorbing materials, with regard to its availability to provide free-space environment. It also depends on the path of the incident RF signal. In the present chamber, the absorber used is pyramidal and wedge shaped polyurethene-form-based material, with some microwave absorbing material dispersed inside. The following type of materials were employed:

1. Small pyramids of base 7.60 cm and height 15.20 cm were used on the ceiling, side walls, a major portion of the floor.

2. Wedges of base width 10.20 cm and height 5.10 cm were used to cover the less important portions of the chamber like surfaces of tapered sections.

3. Large pyramids of base 15.20 cm and height 45.70 cm were used as the central portion of the back wall from where reflections are most likely to occur.

4. A layered flat sheet absorber having five layers and a total thickness of 15.20 cm was used on the walk ways.

5. A densely packed flat absorber of thickness 5.10 cm had been put beneath all of the above mentioned types to increase the total absorption.

These absorbers are finally pasted to the wooden walls using quick drying organic based adhesives.

Electromagnetic Interference (EMI) shielding using thin aluminium sheets is given to avoid the interference from any external sources. The shield is well earthed to prevent the formation of the fringing waves inside the chamber.

For a tapered anechoic chamber using geometrical optics, one can show that, there is a little difference in phase between the direct ray and reflected ray at any point in test region, for a perfectly located transmitting system. That is, a vectorial addition of direct ray and reflected

ray causes a slowly varying interference pattern and a slowly varying signal amplitude in test region. Thus the oscillating behaviour of field prevents the gain measurements based directly upon Friss transmission formula, such as two antenna or three antenna method [170]. So a tapered chamber meant for radiation pattern measurements, has to be converted into rectangular chamber for absolute gain measurements.

The geometry of the convertible anechoic chamber is shown in Fig.III.1. The length of the chamber was chosen in such a way that the test antenna should be illuminated by a plane wave front. The condition of minimum separation between the transmitting and receiving antenna for a plane wavefront, $R = 2D^2/\lambda$ where D is the aperture diameter, R is the separation between the antennas, is to be satisfied. The length of the chamber should be more than this, since the test antenna has to be put in the "quiet-zone", which occurs at some distance from the chamber walls. The height and overall width of the chamber is chosen to $W \geq R/2.75$, where R is the distance between source and test antenna, W is width or height of the chamber.

A rectangular room of size 9.00 x 5.00 m is used for the anechoic chamber. The tapered portion begins with a slope of 25° from the mid-portion of the chamber. The

CONVERTIBLE MICROWAVE ANECHOIC CHAMBER
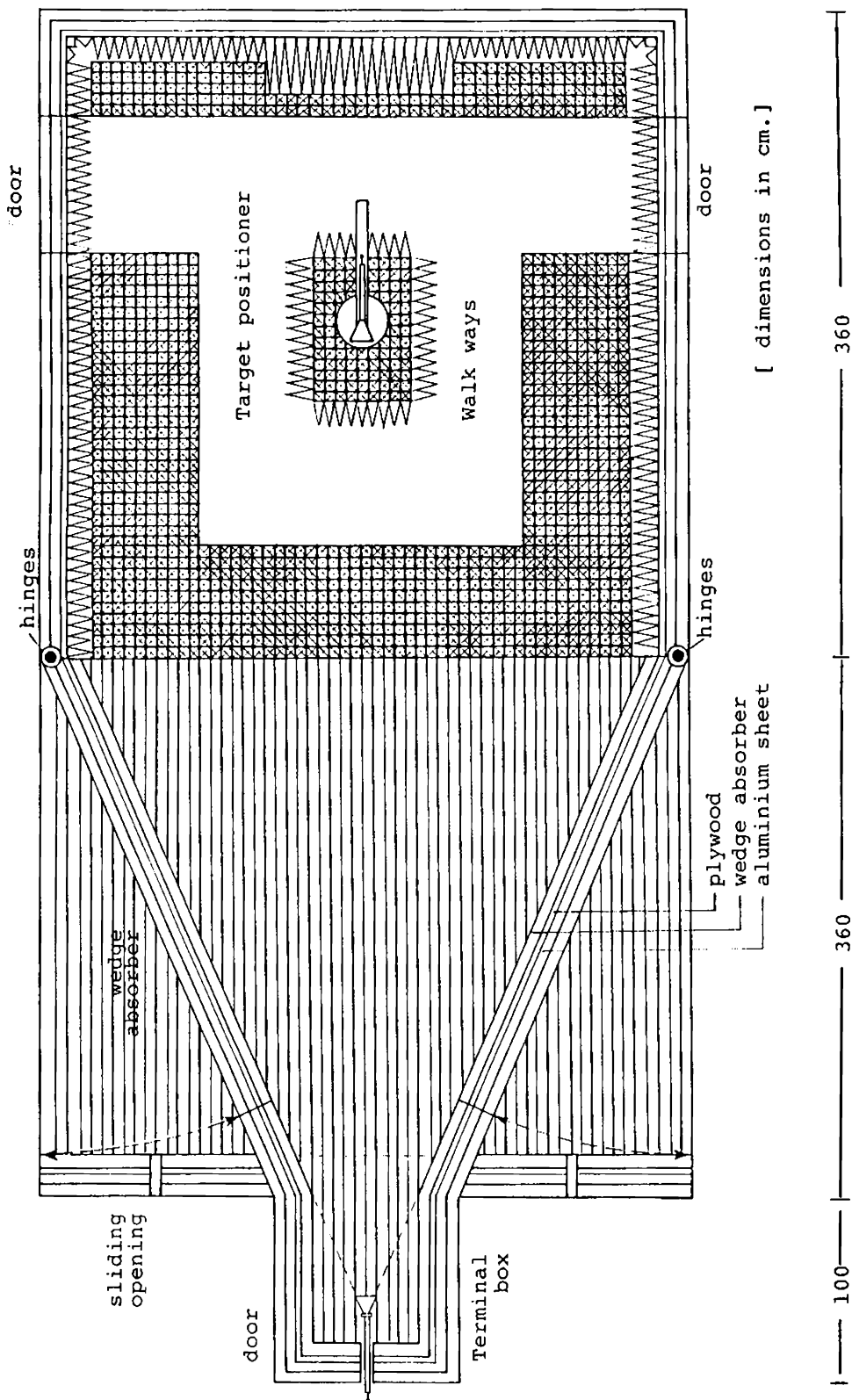
[view from the top]

Fig. III. 1 Geometry of convertible microwave anechoic chamber.

[dimensions in cm.]

convertible chamber is a modification over the earlier tapered chamber. Keeping the quiet zone same, the tapering pads are moved out to change to a rectangular form. For this purpose, the tapered section offers an additional degree of freedom in the sense that it can choose appropriate tapering angle so as to retain the same chamber behaviour in rectangular shape. The remaining portions, when the tapered is converted to rectangular, is also covered with same kind of absorbers.

The transmitting portion of the rectangular chamber is given an adjustable sliding opening, which provides additional facility like the proper insertion of transmitting and receiving antenna to the chamber and the remaining parts can be covered. The side walls of the tapered portions are fitted with caster wheels. The lower (floor) portion is pushed down while the upper pad is pulled up using a pully and rope mechanism. The conversions from rectangular to tapered shape and vice-versa are simpler and it requires very little effort and time.

The antenna turn table (positioner) and associated gadgets are placed below the ground level in a 'cellar', beneath the quiet zone. The positioner's axial rod only will be protruding out. This avoid multiple reflections

and the complexity to avoid the reflection from the positioner, since the 'quietness' of the zone depends upon the magnitudes of the reflections from the walls, floor and ceiling of the chamber.

III.3 PERFORMANCE EVALUATION

III.3.1 Antenna pattern comparison technique

The chamber reflectivity which is a measure of the average reflectivity level in quiet zone, is measured using pattern comparison technique [171]. The level of the reflected signal was determined by recording radiation patterns of an antenna at different locations within the test region of the chamber and superimposing these recordings. Even though the chamber performance depends on the directivity of the measuring antennas, the deviation of different recorded patterns attributed to the phase relationships between the actual pattern and the specularly reflected signals. The deviation of each pattern level from the reference pattern at -10, -15, -20, -25 dB levels on each side of the reference pattern is determined.

Fig.III.2(a) and (b) shows the superimposed radiation pattern for a metallic corrugated horn, recorded, in tapered and rectangular anechoic chamber. Fig.III.2(c) shows the radiation patterns of ordinary horn.
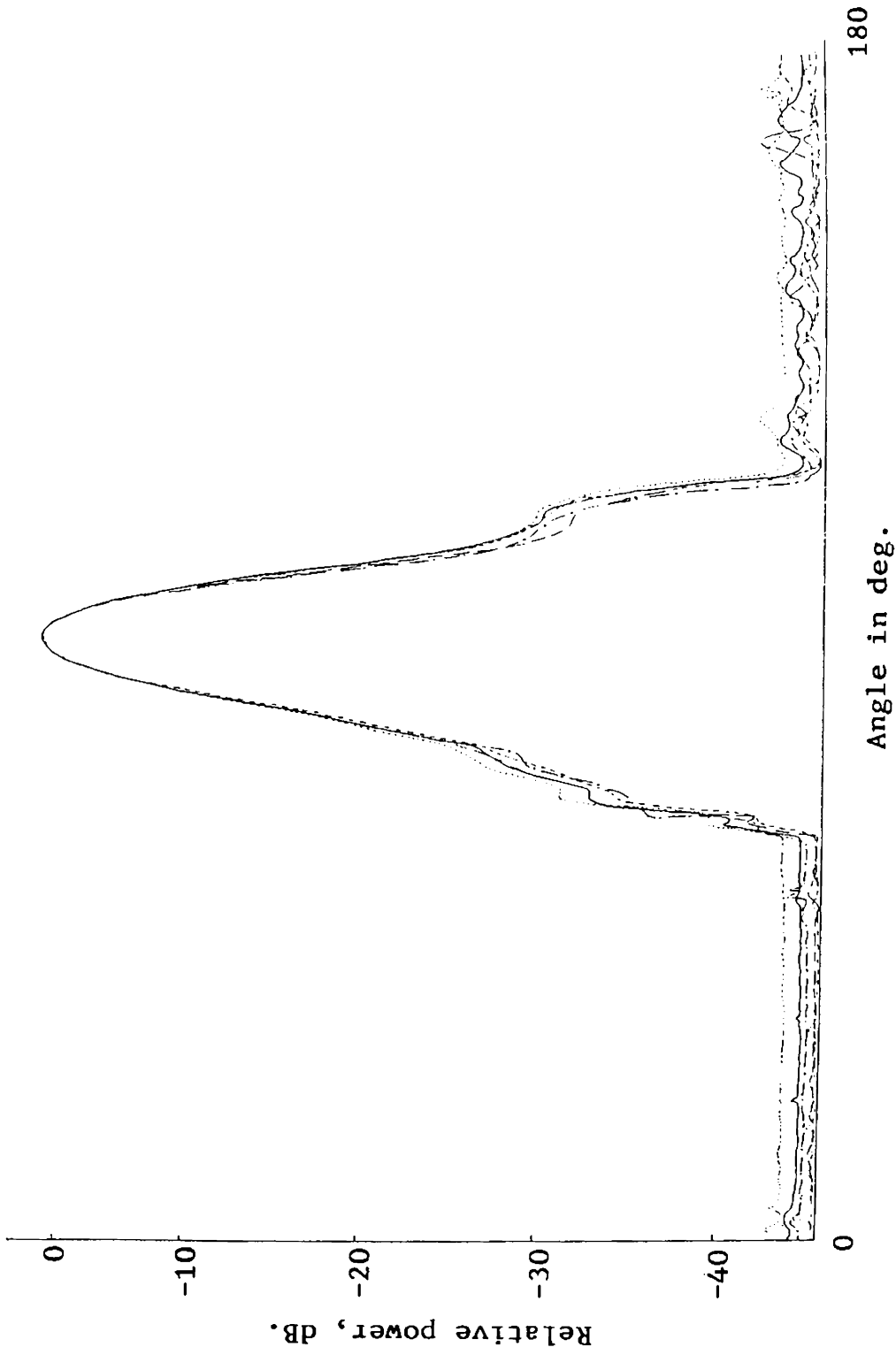
Fig. III.2.a. Comparison of antenna patterns recorded in tapered anechoic chamber at 15,30,45, & 60 cm off axis. Corrugated horn; f=9.15 GHz.
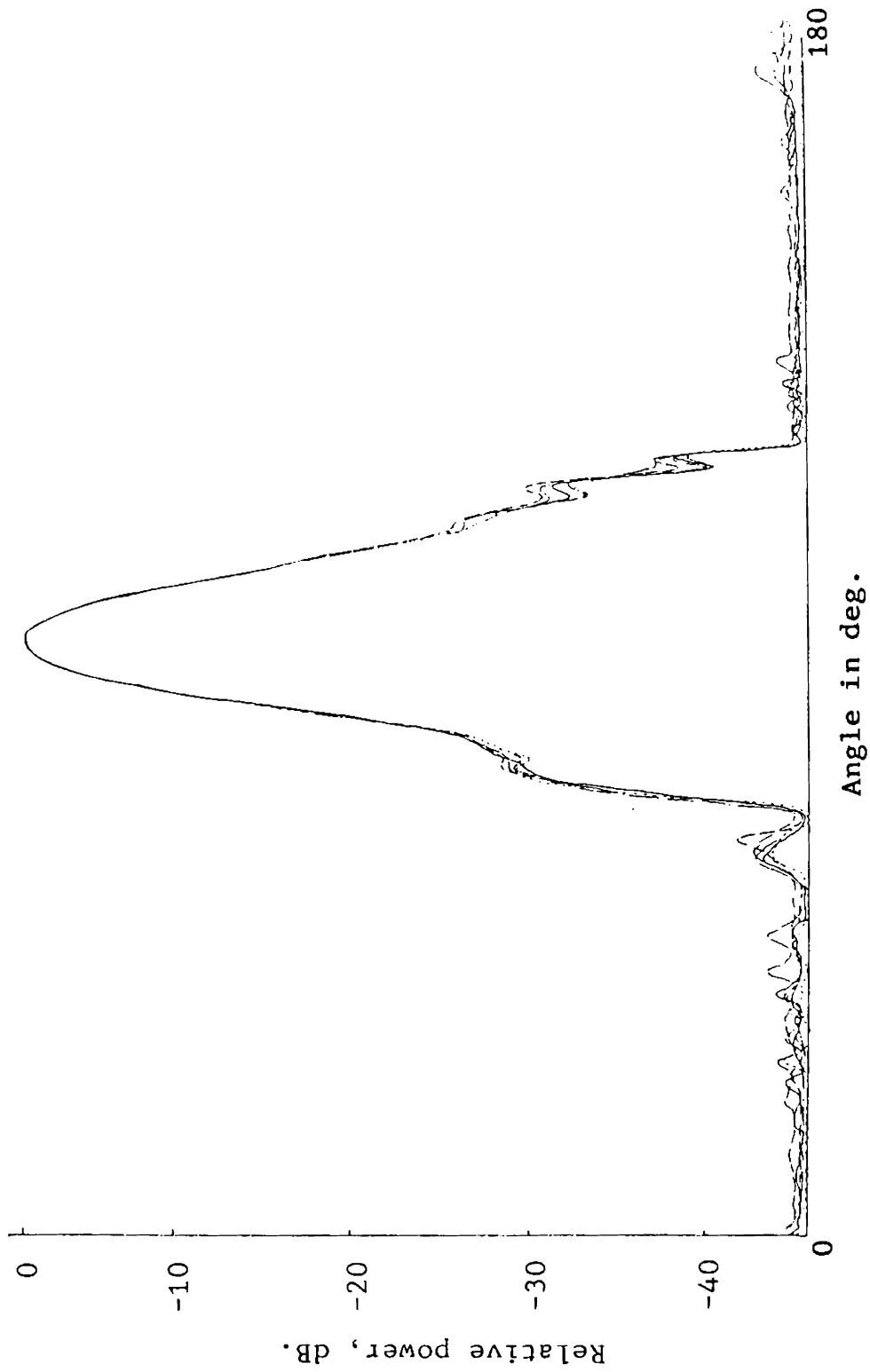
Fig. III.2.b. Comparison of antenna patterns recorded in rectangular anechoic chamber at 15,30,45 & 60 cm off axis. Corrugated metallic horn; f=9.15 GHz.
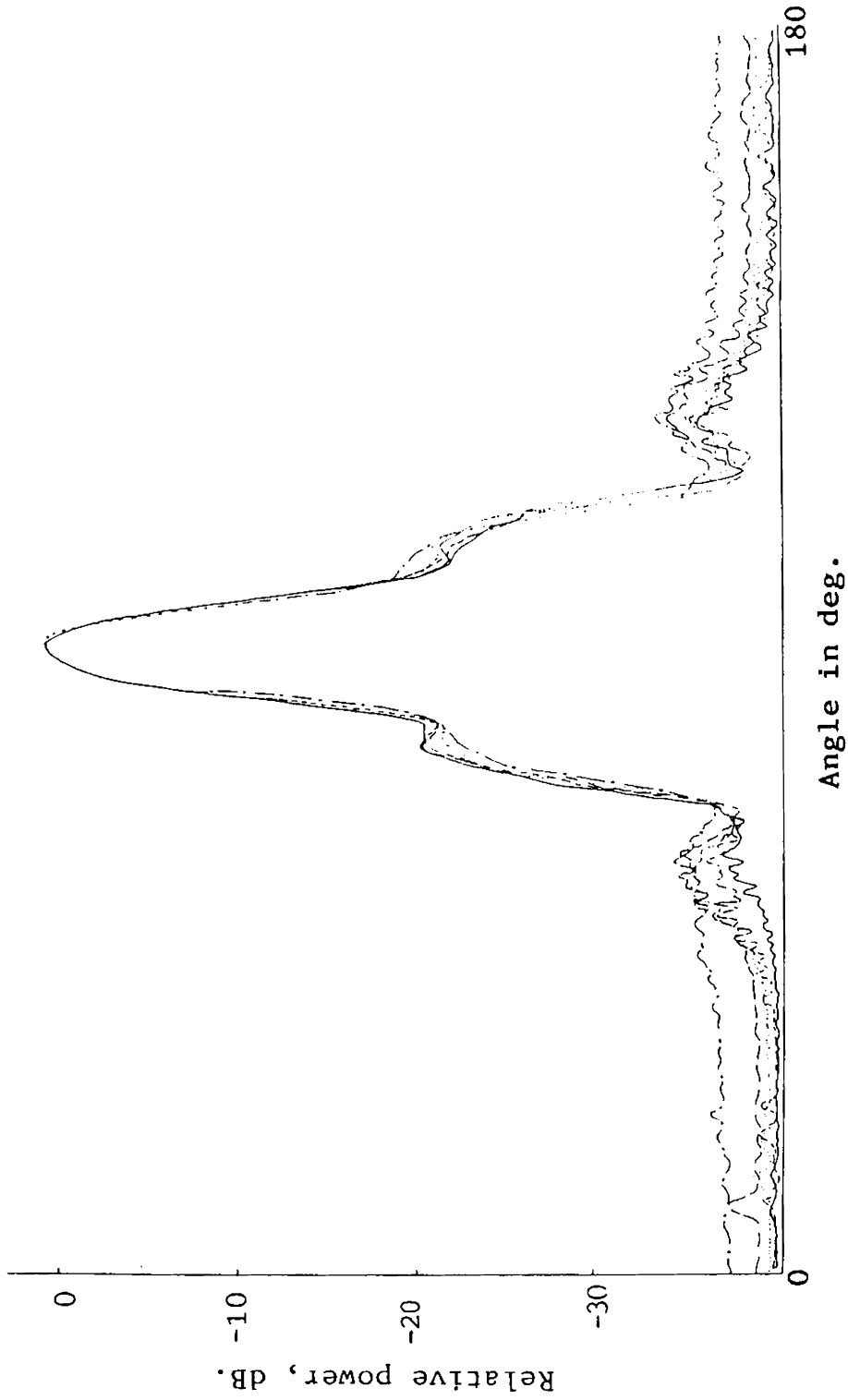
Fig. III.2.c. Comparison of antenna patterns recorded in rectangular anechoic chamber at 5,15,30 & 50 cm off axis: Ordinary horn antenna; f=10.0 GHz.

The considerable difference for the two sets of patterns shows the superiority of the tapered chamber for radiation pattern measurements. The deviation of each pattern from the reference pattern level, is plotted versus radial distance between the chamber axis and test point. Fig.III.3 shows the deviation curve. The chamber reflectivity can be determined from the standard curves of Backley [172]. The average reflectivity of the chamber is found to be -35 dB.

III.3.2 Free space VSWR measurements

One of the important chamber characteristics is the termination VSWR. All conventional VSWR measurements will give only the information about the terminating load. So the VSWR measurement using a 'moving probe technique' cannot be adopted for the evaluation of chamber. This problem is solved by the 'moving termination' technique [170]. The measurement usually consists of setting the frequency to a fixed value and moving the slotted section along with the probe, towards the side walls. The measured values of the VSWR of the rectangular and tapered chamber is less than 1.01 which is quite satisfactory.

The anechoic chamber is equipped with automatic facilities like remote controlled antenna positioner, and automatic pattern recorder.
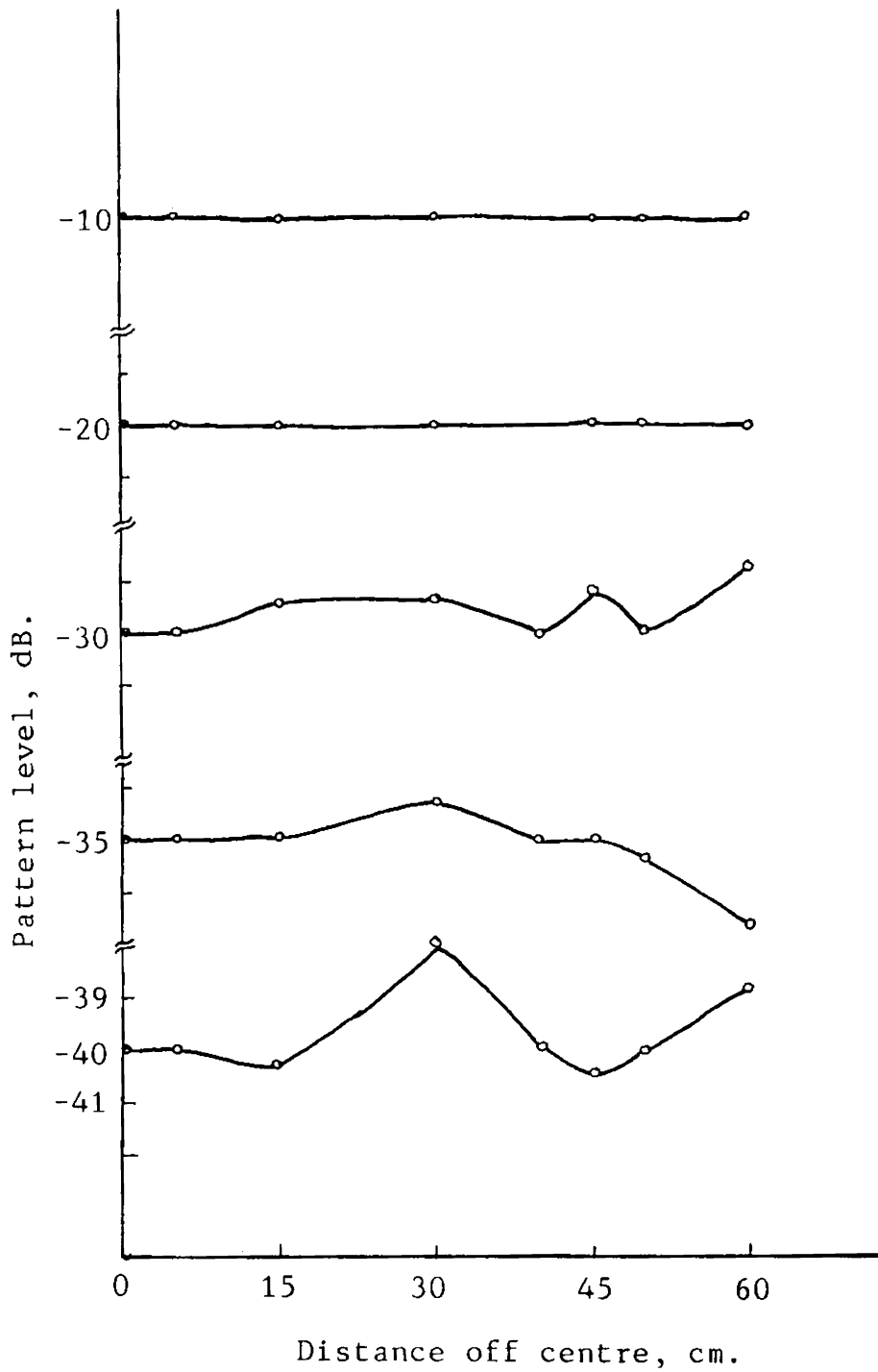
Fig. III.3. Deviation of radiation patterns from
reference pattern with radial distance.

III.4 CONCLUSION

A convertible microwave anechoic chamber with modern instrumentation is constructed and its performance is evaluated. The important chamber performance characteristics like reflectivity and termination VSWR show that the performances of the chamber are well within the specified range. The convertible nature of the chamber enables us to change it from tapered to rectangular chamber configuration. This makes anechoic chamber facility unique in the sense that it is now possible to use it for multiple purposes like studies of antenna characteristics, scattering of electromagnetic waves, RCS reduction studies, EMI and EMC etc.

REFERENCES

1. Nicholas C.Currie (Ed.), "Techniques of radar reflectivity measurements", Artech House Inc., Dedham, M.A. 1984.

2. George T.Ruck (Ed.), "Radar cross section handbook", Vols.I and II, Plenum Press, New York, 1970.

3. Eugene F.Knott, John F.Shaeffer and Michael T.Tuley, "Radar cross section", Artech House, Inc., Dedham, M.A. 1985.

4. M.I.Skolnik, "Introduction to radar systems", McGraw-Hill, 1962, Ch.2-4.

5. J.W.Crispin and K.M.Siegel (Ed.), "Methods of radar cross section analysis", Academic Press Inc., New York, 1968.

6. E.V.Jull and J.W.Heath, "Conducting surface corrugations for multipath interference suppression", Proc.IEE, Vol.125, No.12, pp.1321-26, Dec. 1978.

7. E.V.Jull and G.R.Ebbeson, "The reduction of interference from large reflecting surfaces", IEEE Trans.Antennas Propagat. Vol.AP-25, No.4, pp.565-570, July 1977.

8. A.Hessel, J.Schmoys and D.Y.Tseng, "Bragg-angle blazing of diffraction gratings", Jour.of Opt.Soc.Am. Vol.65, No.4, pp.380-384, April 1975.

9. C.W.Harrison and R.O.Heinz, "On the radar cross section of rods, tubes, and strips of finite conductivity", IEEE Trans.Antennas Propagat. Vol.AP-11, No.4, pp.459-468, July 1963.

10. Charles M.Knop, "On the radar cross section of a coated plate", IEEE Trans.Antennas Propagat. Vol.AP-11, No.6, pp.719-721, Nov.1963.

11. W.E.Blore, "The radar cross section of ogives, double-backed cones, double-rounded cones, and cone spheres", IEEE Trans.Antennas Propagat. Vol.AP-12, No.5, pp.582-590, Sept.1964.

12. John Rheinstein, "Scattering of electromagnetic waves from dielectric coated conducting spheres", IEEE Trans. Antennas Propagat. Vol.AP-12, No.3, pp.334-340, May 1964.

13. Y.Y.Hu, "Back-scattering cross section of a center-loaded cylindrical antenna", IRE Trans.Antennas Propagat. Vol. AP-6, No.1, pp.140-148, Jan.1958.

14. W.E.Blore, P.E.Robillard and R.I.Primich, "35 and 70 Gc. phase-locked CW balanced - bridge model measurement radars", The Microwave Journal, pp.61-65, Sept.1964.

15. P.Blacksmith, R.E.Hiatt and R.B.Mack, "Introduction to radar cross section measurements", Proc.of IEEE, Vol.53, pp.901-920, Aug.1965.

16. T.B.A.Senior, "A survey of analytical techniques for cross section estimation", Proc.of IEEE, Vol.53, pp.822-832, Aug.1965.

17. J.W.Crispin and A.L.Maffett, "Radar cross-section esti-
    mation of simple shapes", Proc. of IEEE, Vol.53,
    pp.83-848, Aug.1965.

18. J.W.Crispin and A.L.Maffett, "Radar cross section esti-
    mation of complex shapes", Proc.of IEEE, Vol.53,
    pp.972-982, Aug.1965.

19. R.G.Kouyoumjian and L.Peters, 'Range requirements in
    the radar cross section measurements", Proc.of IEEE,
    Vol.53, pp.920-928, Aug.1965.

20. C.C.Freeny, "Target support parameters associated with
    radar reflectivity measurements", Proc. of IEEE, Vol.53,
    pp.929-936, Aug.1965.

21. Robert E.Kell, "On the derivation of bistatic RCS from
    monostatic measurements", Proc. of IEEE, Vol.53, pp.983-
    988, Aug.1965.

22. O.Lowenschuss, "Scattering matrix applications", Proc.
    of IEEE, Vol.53, pp.988-992, Aug.1965.

23. R.E.Kell and N.E.Pedersen, "Comparison of experimental
    radar cross section measurements", Proc.IEEE, Vol.53,
    pp.1092-93, Aug.1965.

24. V.V.Liepa and T.B.A.Senior, "Modification of the scatter-
    ing behaviour of a sphere by reactive loading", Proc.
    IEEE, Vol.53, pp.1004-1011, Aug.1965.

25. Petr Beckmann, "Scattering by composite rough surfaces",
    Proc.IEEE, Vol.53, pp.1012-1015, Aug.1965.

26. H.A.Corriher and Berry O.Pyron, "A bibliography of arti-
    cles on radar reflectivity and related subjects 1957-
    1964", Proc. IEEE, Vol.53, pp.1025-1058, Aug.1965.

27. A.V.Alongi, R.E.Kell and D.J.Newton, "A high resolution
    X-band FM/CW radar for RCS measurements", Proc.IEEE,
    Vol.53, pp.1072-1076, Aug.1965.

28. Daniel P.Springston, "High-data-rate radar cross section
    instrumentation system", Proc.IEEE, Vol.53, p.1076,
    Aug.1965.

29. C.R.Millin, R.Sandburg and C.O.Velline, "A numerical
    technique for the determination of scattering cross
    section of infinite cylinders of arbitrary geometrical
    cross section", IEEE Trans.Antennas Propagat. Vol.AP-13,
    No.1, pp.141-149, Jan.1965.

30. R.A.Cross, "Radar cross section of rectangular flat plate
    as a function of aspect angle", IEEE Trans.Antennas
    Propagat. Vol.AP-14, No.3, pp.329-335, May 1966.

31. R.G.Hajovsky, A.P.Deam and A.H.Lagrone, "Radar reflections
    from insects in the lower atmosphere", IEEE Trans.
    Antennas Propagat. Vol.AP-14, No.2, pp.224-227, March
    1966.

32. J.H.Van Vleck, F.Bloch and M.Hamermesh, "Theory of radar
    reflection from wires or thin metallic strips", Jour.
    Appl.Phys. Vol.18, pp.274-294, March 1947.

33. Michel S.Macrakis, "Theoretical and experimental study
    of the back-scattering cross section of an infinite
    ribbon", Jour.Appl.Phys. Vol.31, No.12, pp.2261-2266,
    Dec.1960.

34. E.K.Miller, G.J.Burke, B.J.Maxum, G.M.Pjerrou and A.R.Neureuther, "Radar cross section of a long wire", IEEE Trans.Antennas Propagat. Vol.AP-17, No.3, pp.381-383, May 1969.

35. Nicholas G.Alexopoulos, "Radar cross section of perfectly conducting spheres coated with a certain class of radially inhomogeneous dielectrics", IEEE Trans.Antennas Propagat. Vol.AP-17, No.5, pp.667-669, Sept.1969.

36. R.C.Johnson, H.A.Ecker and R.A.Moore, "Compact range techniques and measurements", IEEE Trans.Antennas Propagat. Vol.AP-17, No.5, pp.568-576, Sept.1969.

37. E.K.Miller and J.B.Morton, "The RCS of a metal plate with resonant slot", IEEE Trans.Antennas Propagat. Vol. AP-18, No.2, pp.290-292, Mar. 1970.

38. Jiunn S.Yu, "Radar cross section of a thin plate near grazing incidence", IEEE Trans.Antennas Propagat. Vol. AP-18, No.15, pp.711-713, Sept.1970.

39. Y.Rahmat-Samii and Raj Mittra, "Integral equation solution and RCS computation of a thin rectangular plate", IEEE Trans.Antennas Propagat. Vol.AP-22, No.4, pp.608-610, July 1974.

40. J.L.Lin, W.L.Curtis and M.C.Vincent, "Radar cross section of a rectangular conducting plate by wire mesh modelling, IEEE Trans.Antennas Propagat. Vol.AP-22, No.5, pp.718-720, Sept.1974.

41. W.B.Weir, L.A.Robinson and Don Parker, "Broadband auto-mated radar cross section measurements", IEEE Trans. Antennas Propagat. Vol.AP-22, No.6, pp.780-784, Nov.1974.

42. Leonard L.Tsai, "Radar cross section of a simple target: A three-dimension conducting rectangular box", IEEE Trans. Antennas Propagat. Vol.AP-25, No.6, pp.882-884, Nov.1977.

43. Jorgan Appel-Hansen, "Accurate determination of gain and radiation patterns by radar cross section measure-ments", IEEE Trans.Antennas Propagat. Vol.AP-27, No.5, pp.640-646, Sept.1979.

44. Keith M.Keen, "New technique for the evaluation of the scattering cross-section of radar corner reflectors", IEE Proc.H., Vol.130, No.5, pp.322-326, Aug.1983.

45. C.C.Huang, "Simple formula for the RCS of a finite hollow circular cylinder", Electron.Lett. Vol.19, No.20, p.854, Sept.1983.

46. David M.Le Vine, "The radar cross section of dielectric disks", IEEE Trans.Antennas Propagat. Vol.AP-32, No.1, pp.6-12, Jan.1984.

47. S.Sanyal and A.K.Bhattacharyya, "Radar cross section of curved plate using uniform asymptotic theory of diffra-ction", IEEE Trans.Antennas Propagat. Vol.AP-32, No.2, pp.187-189, Feb.1984.

48. Bernhard Rembold, "Radar cross section of long wires", IEEE Trans.Antennas Propagat. Vol.AP-32, No.10, pp.1124-1126, Oct.1984.

49. A.K.Bhattacharyya, S.K.Tandon, Subrata Sanyal and D.R.Sarkar, "A CW radar cross section measurements facility in X-band", IETE Technical Review, Vol.1, No.5, pp.59-64, 1984.

50. P.Corona, G.Ferrara and C.Gennarelli, "A simple and practical reference target for RCS measurements", Atla Frequanze, Vol.LIV, No.4, pp.261-267, 1985.

51. A.D.Yaghjian and R.V.McGahan, "Broadside radar cross section of a perfectly conducting cube", IEEE Trans. Antennas Propagat. Vol.AP-33, No.3, pp.321-329, Mar.1985.

52. Robert B.Dybdal, "Radar cross section measurements", Proc.IEEE, Vol.75, No.4, pp.498-516, April 1987.

53. G.V.Delisle, M.Lecours, G.Gonthier, G.Rette and C.Deshenes, "RCS of projectiles--analytical and experimental results", Proc. of the National Radar Conference, California, pp.83-88, 1986.

54. G.Rette, G.Y.Delisle and M.Lecours, "Experimental techniques for the radar cross section measurements of complex structures", Proc. of the 8th Annual Meeting and Symposium on Antenna Measurement Techniques, Canada, pp.163-168, 1986.

55. Byron M.Welsh and Jon N.Link, "Accuracy criteria for RCS measurements of targets consisting of multiple independent scatters", IEEE Trans.Antennas Propagat. Vol.36, No.11, pp.1587-1593, Nov.1988.

56. C.G.Bachman, H.E.King and R.C.Hansen, "Techniques for measurement of reduced radar cross sections - Part I", The Microwave Journal, Vol.6, pp.61-67, Feb.1963.

57. C.G.Bachman, H.E.King and R.C.Hansen, "Techniques for measurement of reduced radar cross sections - Part II", Microwave Journal, Vol.6, pp.95-101, March 1963.

58. C.G.Bachman, H.E.King and R.C.Hansen, "Techniques for measurement of reduced radar cross sections - Part III", Microwave Journal, Vol.6, pp.80-86, April 1963.

59. W.R.Bradford, "Radar cross section of a corrugated metallic pipe", IEEE Trans.Antennas Propagat. Vol.AP-12, No.4, pp.507-508, July 1964.

60. E.F.Knott, "RCS reduction of dihedral corners", IEEE Trans.Antennas Propagat. Vol.AP-25, No.3, pp.406-407, May 1977.

61. W.H.Emerson, "Electromagnetic wave absorbers and anechoic chambers through years", IEEE Trans.Antennas Propagat. Vol.AP-21, pp.484-490, July 1973.

62. E.F.Knott, "Radar cross section reduction using cylindrical segments", IEEE Trans.Antennas Propagat. Vol.AP-24, No.6, pp.882-884, Nov.1976.

63. E.M.Kennaugh, "Polarisation dependence of RCS - A geometrical interpretation", IEEE Trans.Antennas Propagat. Vol.AP-29, No.2, pp.412-413, March 1981.

64. Asoke K.Bhattacharyya and S.K.Tandon, "Radar cross section of a finite planar structure coated with a lossy dielectric", ibid, Vol.AP-32, No.9, pp.1003-1007, Sept. 1984.

65. Peter Swerling, Swerling, Manasse and Smith, "Some methodological considerations in reducing RCS data to target models", Electromagnetics, Vol.4, pp.111-138, 1984.

66. S.Ray and Raj Mittra, "Scattering from resistive strips and from metallic strips with resistive edge loading", Proc.of IEEE AP-S, International Symposium, May 1985.

67. D.Cuba and N.S.Rawat, "Control of RCS by impedance loading-test done by image plane in X-band", J.Inst.Electron. Telecommu.Engg. Vol.32, No.1, pp.36-38, Jan-Feb. 1986.

68. Rayleigh, "Corrugated gratings", Proc.Royal Soc.London, Vol.A-79, pp.399, 1907.

69. R.A.Hurd, "The propagation of an electromagnetic wave along an infinite corrugated surface", Canad.J.of Phys. Vol.32, No.12, pp.727-734, Dec.1954.

70. V.Twersky, "On the scattering of waves by an infinite grating", IRE Trans.Antennas Propagat. Vol.AP-4, pp.330-345, 1956.

71. T.B.A.Senior, "The scattering of electromagnetic waves by a corrugated sheet", Canad.J. of Phys. Vol.37, No.7, pp.787-797, July 1959.

72. R.E.Lowrie and Leon Peters,Jr., "The control of echo area of ogives by cut-off corrugated surfaces", IEEE Trans.Antennas Propagat. Vol.AP-14, No.6, pp.798-799, Nov.1966.

73. A.Wirgin and R.Deleuil, "Theoretical and experimental investigation of a new type of blazed grating", Jour. of Opt.Soc.Am. Vol.59, No.10, pp.1348-1357, Oct. 1969.

74. John A.De Santo, "Scattering from a periodic corrugated structure - Thin comb with soft boundaries", Jour. of Math.Phys. Vol.12, No.9, pp.1913-1923, Sept.1971.

75. John A.De Santo, "Scattering from periodic corrugated structure - Thin comb with hard boundaries", jour.of Math.Phys. Vol.13, No.3, pp.336-341, March 1972.

76. J.L.Roumiguieres , D.Mystre and R.Petit, "On the efficiencies of rectangular-groove gratings", J.Opt.Soc.Am. Vol.66, No.8, pp.772-775, Aug.1976.

77. Hassan A.Kalhor, "Numerical evaluation of Rayleigh hypo thesis for analysing scattering from corrugated gratings TE polarisation", IEEE Trans.Antennas Propagat. Vol. AP-24, No.6, pp.884-889, Nov.1976.

78. D.Marcuse, "Exact theory of TM-wave scattering from blazed dielectric gratings", The Bell System Technical Journal, Vol.55, No.9, pp.1295-1317, Nov.1976.

79. G.R.Ebbeson, "TM polarised electromagnetic scattering from fin-corrugated periodic surfaces", Jour.Opt.Soc.Am. Vol.66, No.12, pp.1363-1367, Dec.1976.

80. E.V.Jull and G.R.Ebbeson, "Gratings that diffract all incident energy", Jour.Opt.Soc.Am. Vol.67, No.4, pp.557-560, April 1977.

81. E.G.Loewen, M.Neviere and D.Maystre, "Grating efficiency theory as it applied to blazed and holographic gratings", Appl.Opt. Vol.16, No.10, pp.2711-2721, Oct.1977.

82. G.Whitman and F.Schwering, "Scattering by periodic metal surfaces with sinusoidal height profiles--A theoretical approach", IEEE Trans.Antennas Propagat. Vol.AP-25, No.6, pp.869-876, Nov. 1977.

83. L.S.Cheo, "On simultaneous blazing of triangular groove diffraction gratings", J.Opt.Soc.Am. Vol.67, No.12, pp.1686-1688, Dec.1977.

84. J.W.Heath and E.V.Jull, "Perfectly blazed reflection gratings with rectangular grooves", J.Opt.Soc.Am. Vol.68, No.9, pp.1211-1217, Sept.1978.

85. J.W.Heath and E.V.Jull, "Total backscatter from conducting rectangular corrugations", IEEE Trans.Antennas Propagat. Vol.AP-27, No.1, pp.95-97, Jan.1979.

86. G.L.James, "Surface reactance of corrugated planes", Electron.Lett. Vol.15, No.3, pp.751-753, Nov.1979.

87. E.V.Jull and J.W.Heath, "Reflection grating polarisers", IEEE Trans.Antennas Propagat. Vol.AP-28, No.4, pp.586-588, July 1980.

88. E.V.Jull, N.C.Beaulieu and D.C.W.Hui, "Perfectly blazed triangular groove reflection gratings", J.Opt.Soc.Am. Vol.74, pp.180-182, 1984.

89. R.A.Hurd and E.V.Jull, "Theory of a reflection grating with narrow grooves", Radio Science, Vol.16, No.3, pp.271-277, May-June 1981.

90. E.V.Jull and D.C.W.Hui, "Scattering by small reflection gratings", Proc. of APS - International Symposium, 1982.

91. Asoke K.Bhattacharyya and S.K.Tandon, "A corrugated surface with low backscatterer", IEEE Trans.Antennas Propagat. Vol.AP-32, No.8, pp.870-872, Aug.1984.

92. E.V.Jull, D.C.W.Hui and P.Faeq, "Scattering by dual-blazed currogated conducting strips and small reflection gratings", J.Opt.Soc.Am. Vol.2, No.7, pp.1049-1056, July 1985.

93. L.Cai, E.V.Jull and R.Deleuil, "Scattering by pyramidal reflection gratings", Proc.IEEE AP-S International Symposium, pp.45-47, 1984.

94. K.Yasuura and M.Murayama, "Numerical analysis of diffraction from a sinusoidal metal grating", Trans.Inst.Elect. Comm.Engg. Japan, Part B, Vol.J 69B, No.2, pp.198-205, Feb.1986.

95. P.S.Kildal, "Definition of artificially soft and hard surfaces for electromagnetic waves", Electron.Lett. Vol.24, No.3, pp.168-170, Feb.1988.

96. E.A.Lewis and Joseph P.Casey,Jr., "Electromagnetic reflection and transmission by grating of resistive wires", Jour.Appl.Phys. Vol.23, No.6, pp.605-608, June 1952.

97. W.E.Groves, "Transmission of electromagnetic waves through pairs of parallel wire grids", Jour.Appl.Phys. Vol.24, No.7, pp.845-854, July 1953.

98. James R.Wait, "Reflection from a wire grid parallel to a conducting plane", Canad.Jour.Phys. Vol.32, pp.571-579, 1954.

99. Robin I.Primich, "Some electromagnetic transmission and reflection properties of a strip grating", IRE Trans. Antennas Propagat. Vol.AP-5, pp.176-182, April 1957.

100. Tove Larsen, "A survey of the theory of wire grids", IRE Trans.on Microwave Theory and Techniques, Vol.10, pp.191-201, 1962.

101. M.Takada and M.Shinji, "An application of the diffraction grating to the 11 GHz microwave systems", IEEE Trans. Antennas Propagat. Vol.AP-13, No.4, pp.532-541, July 1965.

102. A.T.Villeneuve, "Propagation of electromagnetic wave through inhomogeneous slabs", IEEE Trans.Antennas Propagat. Vol.AP-13, No.6, pp.926-933, Nov.1965.

103. Rubens A.Sigelmann, "Surface waves on a grounded dielectric slab covered by a periodically slotted conducting plane", IEEE Trans.Antennas Propagat. Vol.AP-15, No.5, pp.672-676, Sept.1967.

104. A.R.Neureuther and K.Zaki, "Numerical solutions of electromagnetic boundary value problems by means of the asymptotic anticipation method", Radio Science, Vol.3, No.12, pp.1158-1167, Dec.1968.

105. Johannes Jacobsen , "Analytical, numerical and experimental investigation of guided waves on periodically strip loaded dielectric slabs", IEEE Trans. Antennas Propagat. Vol.AP-18, No.8, pp.379-388, May 1970.

106. Chao-Chun Chen, "Scattering by a two dimensional periodic array of conducting plates", IEEE Trans.Antennas Propagat. Vol.AP-18, No.6, pp.660-665, Sept.1970.

107. Robert B.Green, "Diffraction efficiencies for infinite perfectly conducting gratings of arbitrary profile", IEEE Trans.Microwave Theory and Technique, Vol.MTT-18, No.6, pp.313-318, June 1970.

108. H.A.Kalhor and A.R.Neureuther, "Numerical method for the analysis of diffraction gratings", J.Opt.Soc.Am. Vol.61, No.1, pp.43-48, Jan.1971.

109. Shung-Wu Lee, "Scattering by dielectric loaded screen", IEEE Trans.Antennas Propagat. AP-19, No.6, pp.656-665, Sept. 1971.

110. V.Jamnejad-Dailami, R.Mittra and T.Itoh, "A comparative study of the Rayleigh hypothesis and analytic continuation methods as applied to sinusoidal gratings", IEEE Trans. Antennas Propagat. Vol.AP-20, No.3, pp.392-394, May 1972.

111. H.Ikuno and K.Yasuura, "Improved point-matching method with application to scattering from a periodic surface", IEEE Trans.Antennas Propagat. Vol.AP-21, No.5, pp.657-662, Sept.1973.

112. J.P.Montgomery , "Scattering by an infinite periodic array of thin conductors on a dielectric sheet", IEEE Trans.Antennas Propagat. Vol.AP-23, No.1, pp.70-75, Jan.1975.

113. H.A.Kalhor and Armand, "Scattering of waves by grating of conducting cylinders", Proc.IEE, Vol.122, No.3, pp.245-248, March 1975.

114. R.A.Hurd and B.K.Sachdeva, "Scattering by a dielectric loaded slit in a conducting plane", Radio Science, Vol.10, No.5, pp.565-572, May 1975.

115. D.R.Wilton and S.Govind, "Incorporation of edge conditions in moment method solutions", IEEE Trans.Antennas Propagat. Vol.AP-25, No.6, pp.845-850, Nov. 1977.

116. J.P.Montgomery, "Scattering by an infinite periodic array of microstrip elements", IEEE Trans.Antennas Propagat. Vol.AP-26, No.6, pp.850-853, Nov.1978.

117. J.P.Montgomery, "Scattering by an infinite array of multiple parallel strips", IEEE Trans.Antennas Propagat. Vol.AP-27, No.6, pp.798-807, Nov.1979.

118. H.A.Kalhor, "Diffraction of electromagnetic wave by plane metallic gratings", J.Opt.Soc.Am. Vol.68, No.9, pp.1202-1205, Sept. 1978.

119. T.Tamir, "Microwave models of blazed dielectric gratings for integrated optics applications", Proc.of IEEE MTT-S International Microwave Symposium, Washington, May 1980.

120. K.C.Chang and T.Tamir, "Simplified approach to surface wave scattering by blazed dielectric gratings", Appl. Opt. Vol.19, pp.282-288, 1980.

121. A.Gruss, K.T.Tam and T.Tamir, "Blazed dielectric gratings with high beam-coupling efficiencies", Appl.Phys.Lett. Vol.36, No.7, pp.523-525, April 1980.

122. K.C.Chang, V.Shah and T.Tamir, "Scattering and guiding of waves by dielectric gratings with arbitrary profiles", J.Opt.Soc.Am. Vol.70, No.7, pp.804-813, July 1980.

123. K.C.Chang and T.Tamir, "Bragg-reflection approach for blazed dielectric gratings", Opt.Comm. (Netherlands), Vol.26, No.3, pp.327-330, Sept. 1978.

124. T.Tamir and K.C.Chang, "Analysis and design of blazed dielectric gratings", Integrated and Guided Wave Optics Technical Digest, Jan. 1980.

125. E.L.Rope and G.Tricoles, "Waves scattered by corrugated dielectric gratings", Proc.of the AP-S International Symposium, June 1980.

126. H.A.Kalhor, "EM scattering by an array of perfectly conducting strips by a physical optics approximation", IEEE Trans.Antennas Propagat. Vol.AP-28, No.2, pp.277-278, March 1980.

127. Jack H.Richmond, "On the edge mode in the theory of TM scattering by a strip or strip grating", IEEE Trans. Antennas Propagat. Vol.AP-28, No.6, pp.883-887, Nov.1980.

128. R.Pauchard, "Scattering by a grating of continuous and discontinuous wires", Ann.Telecommun. Vol.35, pp.303-312, Sept.-Oct. 1980.

129. S.L.Prosvinrnin and I.I.Reznik, "Diffraction of a plane wave beam by a double ribbon grating", Radio Phys. and Quantum Electron. Vol.23, No.7, pp.588-596, July 1980.

130. M.J.Archer, "Periodic multi-element strip gratings", Electron.Lett. Vol.18, No.22, pp.958-959, Oct.1982.

131. N.Marcuvitz, "Waveguide handbook", IEE Electromagnetic Waves Series 21, 1986.

132. R.Petit, "Electromagnetic theory of gratings", Springer Verlag, New York, 1980.

133. H.A.Kalhor and M.Ilyas, "Scattering of plane electro-magnetic waves by a grating of conducting cylinders embedded in a dielectric slab in free space", IEE Proc. Part H, Vol.128, No.3, pp.155-158, June 1981.

134. E.A.Parker and S.M.A.Hamdy, "Rings as elements for fre-quency selective surfaces", Electron.Lett. Vol.17, No.7, pp.612-614, Aug.1981.

135. E.A.Parker, S.M.A.Hamdy and R.J.Langley, "Arrays of con-centric rings as frequency selective surfaces", Electron. Lett. Vol.17, No.23, pp.880-881, Nov.1981.

136. Y.Hayashi and S.Ohro, "Analytical method for the scatter-ing problem of surface waves by a conducting strip", Trans.Inst.Electron and Comm.Engg. Japan, Vol.J 67-B, No.2, pp.230-231, Feb.1984.

137. R.C.Hall and Raj Mittra, "Scattering from a periodic array of resistive strips", IEEE Trans.Antennas Propagat. Vol.AP-33, No.9, pp.1009-1011, Sept.1985.

138. Raj Mittra, R.C.Hall and c.H.Tsao, "Spectral domain analysis of circular patch frequency selective surfaces", IEEE Trans.Antennas Propagat. Vol.AP-32, No.5, pp.533-536, May 1984.

139. Xu-Jeadong, Chen Guorui, "Microwave characteristics and applications of planar metallic grating systems", J.China Inst.Commun. Vol.5, pp.83-87, April 1984.

140. J.G.Gallagher and D.J.Brammer, "Scattering from an infinite array of periodic broken wires buried in a dielectric sheet", Radio Science, Vol.20, No.1, pp.50-62, Jan.Feb. 1985.

141. Tom Cwik and Raj Mittra, "Scattering from general periodic screens", Electromagnetics, Vol.5, pp.263-283, 1985.

142. Tom Cwik, "Scattering from general periodic screens", Ph.D.Dissertation, University of Illinois, Dec.1986.

143. J.D.Kanellopoulos, P.G.Cottis and P.G.Daneil, "Scattering of vertically polarised em wave from infinite dielectric cylinders embedded in a dielectric lossy medium", Inter. Jour.Electronics, Vol.59, No.4, pp.423-433, Oct.1985.

144. G.Bogdanov and G.Sh.Kevanishvili, "Diffraction of plane E-polarised wave from a lattice of coaxial cylinders", Radio Phys. and Quantum Electronics, Vol.28, No.2, pp.157-162, Feb.1985.

145. N.Yamauchi, "Higher order Bragg diffraction by dielectric grating", Trans.Inst.Electron and Commun.Eng. Japan, Vol.J 68-B, No.8, Aug.1985.

146. J.Y.Suratteau and R.Petit, "Numerical study of perfectly conducting wire gratings in the resonance region", International Jour. of IR and MM waves, Vol.6, No.9, pp.831-865, Sept.1985.

147. A.Buyukaksoy and G.Uzgoren, "Scattering of a plane wave by metallic strip grating on the plane interface of two dielectric media", Proc.of MELECON-85, Conference, Spain, Oct. 1985.

148. K.Kobayashi, "Diffraction of a plane wave by a thick strip grating", Proc. of the IEEE AP-S International Symposium, Canada, pp.553-556, 1985.

149. K.Kobayashi, "Diffraction of electromagnetic waves by a parallel plate grating with dielectric loading (1)", The 100th Anniversary Bulletin of Chuo University, pp.473-524, 1985.

150. K.Kobayashi, "Diffraction of a plane electromagnetic wave by a parallel plate grating with dielectric loading: the case of transverse incidence", Canad.Jour.Phys. Vol.63, No.4, pp.453-465, 1985.

151. M.Nishimoto and K.Aoki, "Scattering of plane electromagnetic wave by a semi-infinite strip grating", Trans. on IECE, Japan, Vol.E 69, No.11, pp.161-164, Nov.1986.

152. Te-Kao Wu, "Fast convergent integral equation solution of strip gratings on dielectric substrate", IEEE Trans. Antennas Propagat. Vol.AP-35, No.2, pp.205-207, Feb.1987.

153. R.H.Ott, R.G.Kouyoumjian and L.Peters Jr., "Scattering by a two dimensional periodic array of narrow plates", Radio Science, Vol.2, No.11, pp.1347-1359, Nov.1967.

154. K.V.Seshagiri Rao and Prakash Bhartia, "Analysis of trans-mission structure with periodically loaded elliptical bars between parallel ground planes", Microwaves and Optical Technol.Lett. Vol.1, No.8, pp.282-286, Oct. 1988.

155. T.Yamasaki and T.Hinata, "Scattering of electromagnetic wave by plane grating with reflector", Trans. of Inst. of Electronics and Commun.Japan, Vol.61-B, No.11, pp.52-60, 1978.

156. Kitajima, Itakura and Yesuura, "On the diffraction of a plane wave by planar infinite grating with reflector plates", Trans.IECE Japan, Vol.54-B, No.6, pp.295, June 1971.

157. T.Mashiko and S.Adachi, "Plane wave scattering from an infinite loaded dipole planar array over a lossy half space", Proc. of the IEEE AP-S International Symposium, June 1981.

158. H.A.Kalhor and M.Ilyas, "Scattering of plane electro-magnetic waves by a grating of conducting cylinders embedded in a dielectric slab over a ground plane", IEEE Trans.Antennas Propagat. Vol.AP-30, No.4, pp.576-579, July 1982.

159. P.G.Cottis and J.D.Kanellopoulos, "Scattering from a conducting cylinder above a lossy medium", Int.Jour. Electronics, Vol.65, No.5, pp.1031-1038, 1988.

160. M.Z.El-gamal and L.Shafai, "Scattering of electromagnetic waves by arrays of conducting and dielectric cylinders", Int.Jour.Electronics, Vol.65, No.5, pp.1013-1029, 1988.

161. Hassan A.Kalhor, "Electromagnetic scattering by a dielectric slab loaded with a periodic array of strips over a ground plane", IEEE Trans.Antennas Propagat. Vol.AP-36, No.1, pp.147-151, Jan.1988.

162. H.M.Barlow and A.L.Cullen, "Microwave measurements", Constable and Company, London, 1950.

163. S.Roberts and A.Von Hippel, "New method for measuring dielectric constant and loss in the range of centimeter waves", J.Appl.Phys. Vol.17, No.7, pp.610-616, 1946.

164. T.W.Dakin and C.N.Works, "Microwave dielectric measurements", J.Appl.Phys.Vol.18, No.9, pp.789-796, 1947.

165. H.T.Al-Hafid, B.R.Vishvakarma and H.M.Al-Rizzo, "Complex dielectric constant of sand and dust particles at 11 Ghz as a function of moisture content", Ind.Jour.Radio and Space Phys. Vol.14, No.2, pp.21-24, 1985.

166. P.Venugopalan, K.G.Nair, P.K.Chaturvedi and V.R.Ravindran, "A microwave method for detecting inhomogeneities in cured rocket propellant", NDT International 17, No.5, pp.277-279, Oct.1984.

167. E.F.Buckley, "Outline of evaluation procedure for micro-wave anechoic chambers", Microwave Journal, Vol.6, pp.69-75, Aug.1963.

168. W.H.Emerson, "Electromagnetic wave absorbers and anechoic chambers through the years", IEEE Trans.Antennas Propagat. Vol.AP-21, pp.484-490, July 1973.

169. E.J.Zachariah, K.Vasudevan, P.A.Pravinkumar, P.Mohanan and K.G.Nair, "Design, development and performance eva-luation of an anechoic chamber for microwave antenna studies", Ind.Jour. of Radio and Space Phys. Vol.13, pp.29-31, Feb.1984.

170. W.H.Kummer and E.S.Gillespie, "Antenna measurements-1978", Proc.of IEEE, Vol.66, No.4, pp.483-507, April 1978.

171. J.Appel Hansen, "Reflectivity level of radio anechoic chambers", IEEE Trans.Antennas Propagat. Vol.AP-21, pp.490-498, July 1973.

172. E.F.Buckley, "Design, evaluation and performance of modern microwave anechoic chamber for antenna measurements", Electronic Components, pp.1119-1126, Dec.1965.

LIST OF PUBLICATIONS OF THE AUTHOR

I. Papers published in research journals:

1. "Reflector backed perfectly blazed strip gratings simulate corrugated reflector effects". Electronics Letters, Vol.23, No.2, Jan.1987, pp.86-87.

2. "Low backscattered TM polarised strip gratings". Electronics Letters, Vol.23, No.17, Aug.1987, pp.905-906.

3. "Microwave method for monitoring the curing conditions of a solid rocket propellant", NDT International (U.K.), Vol.19, No.6, Dec.1986, pp.398-400.

4. "Microwave method for locating the inhomogeneities in cured rocket propellant samples". NDT International (U.K.), Vol.19, NO.6, Dec.1986, pp.395-397.

5. "Microwave Non-destructive flaw/defect detection system for non-metallic media backed by a microprocessor based instrumentation". Jour. of Microwave Power and Electro-magnetic Energy (USA), Vol.24, No.2, 1989, pp.74-78.

6. "Development of a Non-Destructive Test Facility for testing curing state and other parameters of solid rocket propellants". ISRO Technical Report, ISRO-RESPOND, TR-64, 1987, pp.1-9.

7. "Microwave techniques for the NDT of solid rocket propellants". Quality Evaluation, Vol.6, No.1, Jan-Mar.1986, pp.1-3.

II. Papers presented in symposium/seminar

1. "Perfectly blazed dual-periodic strip gratings". Proc. of the IEEE AP-S International Symposium, Syracuse,New York, 1988, pp.651-654.

2. "An instrumentation for flaw/defect detection in tyres". Presented in National Symposium on Instrumentation (NSI-13), Mysore, Nov.1988.

3. "Reflector backed perfectly blazed strip gratings". Proc. of the International Symposium on Electronic Devices, Circuits and Systems, ISELDECS-1987, IIT Kharagpur, Dec.1987, pp.457-459.

4. "Electromagnetic scattering by periodic metallic strips on a dielectric sheet". Presented in the National Symposium on Microwave Propagation and Antennas, Cochin University, Dec.1988.

5. "Effect of periodic strip structure on reduction of Radar Cross Section of planar surfaces". Proc. of the 1989 IEEE AP-S International Symposium, California, USA, pp.868-871.

6. "Shunt impedance improves the microstrip antenna performance". Communicated.

7. "Bandwidth enhancement of microstrip antennas using shunt impedance techniques". Communicated.

8. "RCS of a strip loaded dielectric slab". Communicated.

9. "A novel multioctave microstrip antenna". Communicated.